CHEMISTRY OF GASEOUS ORGANOSILICON

REACTIVE INTERMEDIATES

A Thesis presented by:

K.J.Hughes

For the degree of:

Doctor of Philosophy

Department of Chemistry,

University of Leicester.

May 1987.

UMI Number: U002470

UMI

Dissertation Publishing

ProQuest

ACKNOWLEDGEMENTS

CONTENTS

CHAPTER ONE

REVIEW

SILYLENES (R$_2$Si:)

These are the silicon equivalent of carbenes. Experimental and theoretical studies have shown that unlike carbenes, the singlet is usually the ground state for simple silylenes [1,2]. A recent calculation [2] shows that the singlet-triplet separation is dependant on the R-Si-R angle and that above about 129° the triplet state becomes the ground state. This raises the possibility that bulky substituents attached to the silicon may reverse the ordering of states and make the triplet state the ground state.

Silylenes can readily be produced by pyrolysis of an appropriate substrate, the most common method being pyrolysis of a disilane.

$$XYZSi-SiXYZ \longrightarrow XYSi: + SiXYZ_2$$
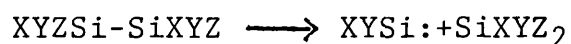
Factors determining whether the disilane produces a silylene or silyl radicals have been discussed by Davidson [3], and can be summarised by the statement that a silylene will be produced in preference to silyl radicals providing the disilane contains a bond into which a silylene can readily insert. In practice, Z can be hydrogen, halogen, or alkoxy. X and Y can be any of these and also alkyl or aryl. This and other methods of silylene production have been extensively reviewed by Gaspar [4].

1

Silylene Reactions

The most important reactions of silylenes can be broadly classified as:

(i) Insertions.

(ii) Additions. (including dimerisation)

(iii) Rearrangements.

(i) Insertions

$$R_2Si: + X-Y \longrightarrow R_2SiXY$$
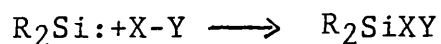
Silylenes are known to insert into a wide variety of σ-bonds [4]. However, quantitative information about such reactions is sparse, due to the experimental difficulties involved in obtaining such information.

Experimental methods of obtaining Arrhenius parameters for silylene insertions can be divided into two categories.

a) From gas kinetic studies of decomposition of organosilicon compounds, combined with a knowledge of heats of formation of reactant and products.

eg. $MeSiH_3 \overset{1}{\underset{-1}{\rightleftharpoons}} CH_4 + :SiH_2$
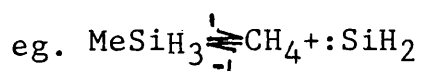
Measure A_1 and E_1 experimentally, which combined with thermodynamic data of reactant and products allows A_{-1}

2

and E_{-1} to be calculated. The combination of experimental error from the kinetic measurement and errors in the heats of formation and entropies can give rise to considerable uncertainty in the derived Arrhenius parameters for silylene insertion.

b) Trapping experiments can be employed. For example, dimethylsilylene has been photochemically generated from $(Me_2Si)_6$ in the presence of trimethylsilane and the following reaction scheme devised.

$(Me_2Si)_6 \xrightarrow{nh\nu} nMe_2Si:$ (1)

$Me_2Si: + Me_3SiH \longrightarrow Me_5Si_2H$ (2)

$Me_2Si: + Me_5Si_2H \longrightarrow Me_7Si_3H$ (3)

$Me_2Si: \longrightarrow$ surface polymer   (4)
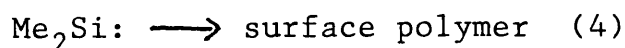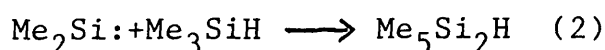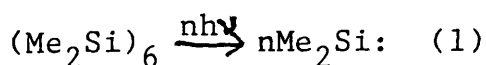
Mixtures of $(Me_2Si)_6$ and Me_3SiH were photolysed for a fixed time between 413-510K. From variation of product yields with temperature, it was determined that $E_2=E_3=E_4$, and from the nature of reaction (4) that these activation energies are all close to zero [5].

A variation of this method can be used to determine relative reactivities of various σ-bonds to silylenes. The silylene is generated in the presence of two different traps, and the relative yields of the products provides a measure of the relative reactivity of the silylene towards each trap. This method has been applied by Gu and Weber [6] to show that

3

silicon-hydrogen and silicon-oxygen bonds in monosilanes have approximately equal reactivity to insertion by dimethylsilylene.

The only quantitative data on silylene insertions into silicon-oxygen bonds has been carried out by Davidson and Maghsoodi [7], who from a kinetic study of thermal decomposition of various methoxydisilanes, allied with thermochemical data arrived at the conclusion that dimethylsilylene insertion into silicon-oxygen σ-bonds has an activation energy very close to zero. Furthermore, by a comparison with kinetic data for other disilane decompositions, activation energies for dimethylsilylene insertion into silicon-hydrogen and silicon-chlorine bonds were estimated relative to insertion into silicon-oxygen.

Theoretical studies have also been used to obtain information regarding the mechanism and energy barrier to silylene insertion reactions. In the case of silylene insertion into X-H(X=N,P,O,S,F,Cl) in which X has a lone pair of electrons. Theoretical calculations [8] show that the mechanism of insertion proceeds via a donor-acceptor complex followed by hydrogen migration.

The most comprehensive theoretical calculations have been performed on $:SiH_2$ insertion into hydrogen [9,10], giving reasonable agreement with experimentally derived values of $5.5kcalmol^{-1}$ [11] and $8.2kcalmol^{-1}$ [12]. Calculations have also been performed on $:SiH_2$ insertion into SiH_4 giving a zero

activation energy [9], in reasonable agreement with experimental results. However, the calculated value of H_2Si: insertion into CH_4 is $27.51 kcalmol^{-1}$, significantly different from the experimentally determined value of approximately $19 kcalmol^{-1}$ [13].

Table 1.1 gives a summary of some experimentally determined activation energies of silylene insertions.

TABLE 1.1

Silylene	Bond	$Ea/kcalmol^{-1}$	reference
H_2Si:	H-H	8.2	12
H_2Si:	C-H	19	13
Me_2Si:	Si-C	19	14
H_2Si:	Si-H	1.3	11
Me_2Si:	Si-H	$\ll 1.2$	5
Me_2Si:	Si-H	2.9 ± 1.5	7
Me_2Si:	Si-O	0	7
Me_2Si:	Si-Cl	5.6 ± 1.5	7

(ii) Addition Reactions

The most important addition reactions of silylenes are to alkenes, which initially form silacyclopropanes.

$$\text{eg. } Me_2Si: + R_2C=CR_2 \rightarrow Me_2Si \underset{CR_2}{\overset{CR_2}{\diagdown | }}$$
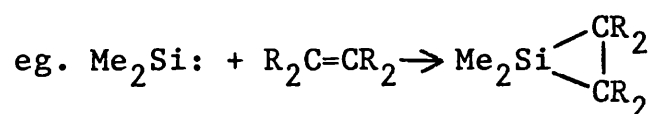
Silacyclopropanes are known to react with methanol to form a ring opened product.

$$\text{eg. Me}_2\text{Si} \diagdown \underset{\diagdown CR_2}{\overset{CR_2}{\diagup}} \quad + \text{ MeOH} \longrightarrow \text{Me}_2\text{Si(OMe)CR}_2\text{CR}_2\text{H}$$
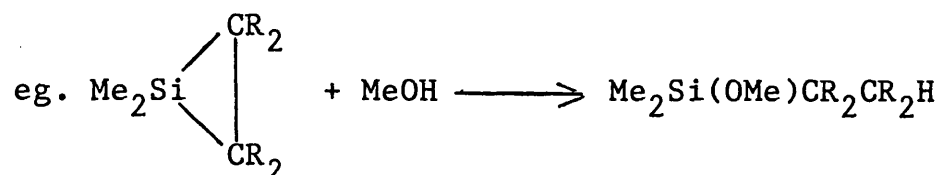
Experimental studies have been carried out to determine the mechanism of silylene addition to alkenes [15,16,17]. They involve generation of a silylene in the presence of a suitably substituted alkene, and the application of nmr to determine the structure of the silirane, and the ring opened product after the addition of methanol. From the nmr data, it is concluded that addition of dimethylsilylene to alkenes is stereospecific, and since dimethylsilylene is a ground state singlet, it suggests the addition is a concerted cis-addition.

Addition of silylenes to conjugated dienes is an interesting reaction since the possibility now exists that the addition will proceed via a concerted 1,4-addition.

Experiments by Chernyshev et al [18] showed that dichlorosilylene and difluorosilylene, generated by pyrolysis of the respective silacyclopent-3-enes, react with 2,3-dimethylbutadiene to produce only the products expected by a concerted 1,4-addition.

A more comprehensive investigation of silylene addition to

substituted butadienes has been performed by Gaspar [19], who found that addition of dimethylsilylene to butadienes unsubstituted at the 1 and 4 positions produced the expected product of 1,4-addition. However, in the case of butadienes with methyl groups at the 1 and/or 4 positions, the observed products could only be explained in terms of 1,2-addition to produce a silacyclopropane which subsequently rearranged.

$Me_2Si: +$ ⟶ Me_2Si

Me_2Si Me_2Si

Me_2Si Me_2Si Me_2Si Et
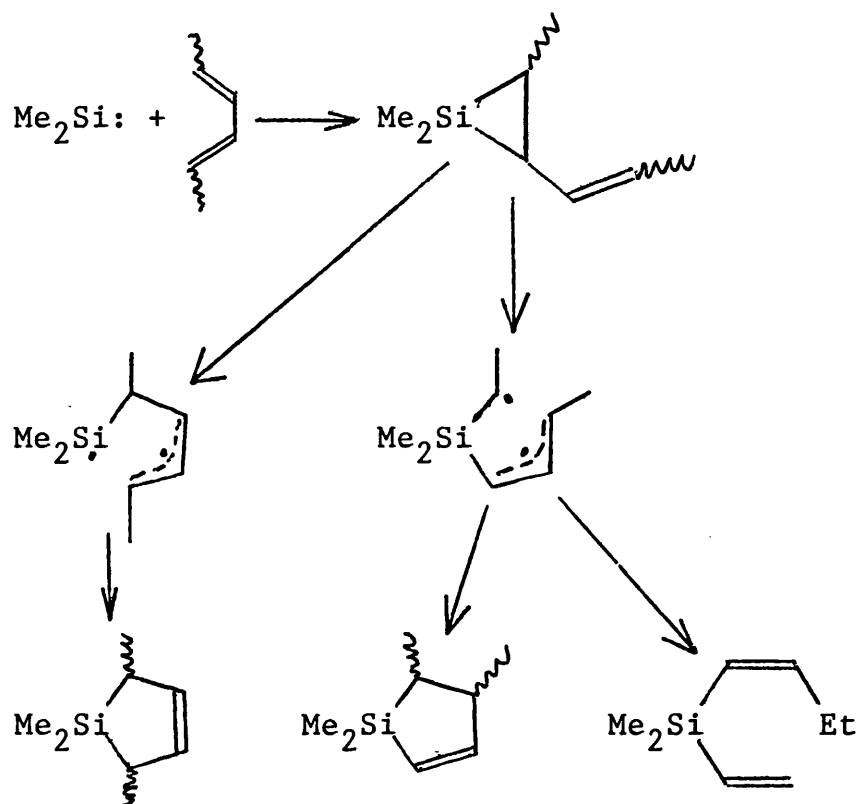
From these results, Gaspar concluded that addition of dimethylsilylene to butadienes proceeded via 1,2-addition to form a silacyclopropane with subsequent rearrangement to form the observed products. But, from this mechanism, it would be expected that butadienes unsubstituted at the 1 and 4 positions would produce some silacyclopent-2-enes, as observed in unpublished results on trapping of $Me_2Si:$ by

butadiene in our laboratory, but apparently not seen by Gaspar or Chernyshev.

Silylene dimerisation to form a disilene is known to occur, and was first observed by Conlin and Gaspar [20], who generated dimethylsilylene in the gas phase and observed formation of 1,1-dimethyl-1,3-disilacyclobutane along with 1,3-dimethyl-1,3-disilacyclobutane. Which had previously been characterised as the major stable products of rearrangement of tetramethyldisilene [21].

$$2Me_2Si: \longrightarrow Me_2Si=SiMe_2 \xrightarrow{\Delta} Me_2Si\overset{\triangle}{\underset{\triangledown}{}}SiH_2 \ + \ HMeSi\overset{\triangle}{\underset{\triangledown}{}}SiHMe$$
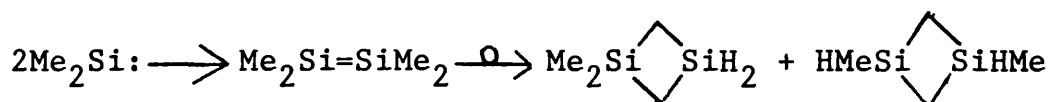
(iii) Rearrangements

This is a fascinating area of silylene chemistry, in which silylenes may undergo a series of intramolecular rearrangements to produce products often quite different from the starting material.

eg. $(Me_3Si)_2Si: \xrightarrow{\Delta}$

$$\begin{array}{c} H_2Si-\!\!\!\backslash \\ | \quad\quad SiMe_2 \\ Me_2Si-\!\!\!/ \end{array}$$ 60% yield
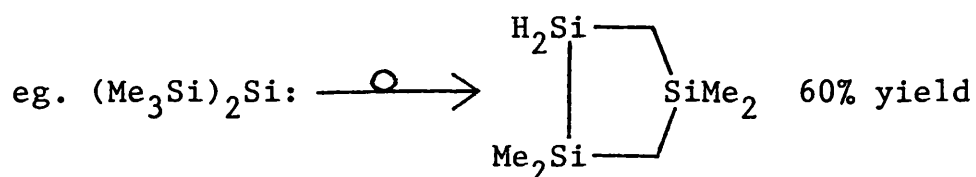
Bis(trimethylsilyl)silylene was generated in the gas phase under low pressure conditions favouring unimolecular reactions, and was found to produce the trisilolane shown above in 60% yield [22].

Plausible mechanisms can be drawn for such reactions which involve silylene to silene, and silylene to disilene isomerisations, along with intramolecular insertion of silylenes into σ-bonds and intramolecular addition to π-bonds. Many examples of these reactions have been neatly summarised by Gaspar [4].

SILENES ($R_2Si=CH_2$)

Silenes are reactive intermediates containing a silicon-carbon $p\pi-p\pi$ bond. The first reliable evidence for the existence of silenes was obtained from kinetic experiments on the thermal decomposition of dimethylsilacyclobutane, which implied the presence of dimethylsilene as a reactive intermediate [23].

$$Me_2Si \quad \longrightarrow \quad Me_2Si \quad \longrightarrow \quad C_2H_4 + Me_2Si=CH_2$$
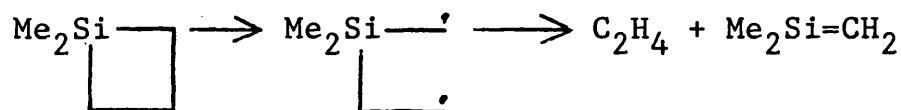
Arrhenius parameters obtained for decomposition of dimethylsilacyclobutane were:

$$\log k/s^{-1} = (15.64 \pm 0.2) - (261.5 \pm 2.1 kJmol^{-1}/2.303RT)$$

These are identical to Arrhenius parameters for cyclobutane decomposition [24], which is known to decompose by a diradical mechanism [25]. This implies that the mechanism of dimethylsilacyclobutane decomposition proceeds via initial diradical formation with subsequent production of

of ethene and dimethylsilene.

Matrix isolation studies have also been of use in confirming the existence of silenes. For example $Me_2Si=CHMe$ has been isolated in an argon matrix at 8K and identified by its infra-red spectrum. Upon warming the matrix, formation of the dimerised silene was observed, while in the presence of methanol, the adduct between the silene and methanol was found [26,27]. With appropriate substitution, it is now possible to produce silenes stable at room temperature in the absence of air.

$$(Me_3Si)_3Si-\overset{\overset{\displaystyle O}{\|}}{\underset{\underset{\displaystyle C_{10}H_{12}}{\diagdown}}{C}} \quad \underset{\longleftarrow}{\overset{h\nu}{\longrightarrow}} \quad (Me_3Si)_2Si=C(OSiMe_3)C_{10}H_{12}$$

$$\text{(1)} \qquad\qquad\qquad\qquad \text{(2)}$$
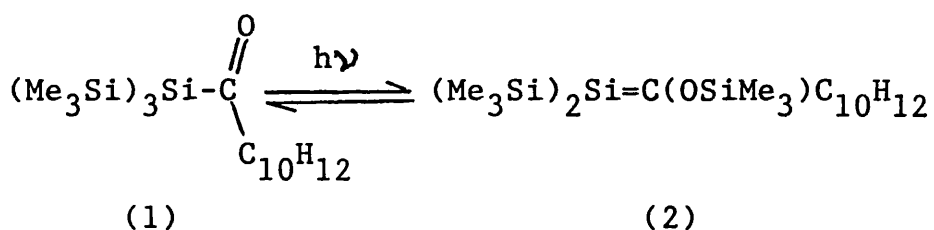
Brook et al [28] photolysed an ether solution of (1), and on removal of solvent and recrystallisation obtained crystals of (2), characterised by I.R. nmr and mass spectrometry.

Thermal Generation of Transient Silenes

The usual method of generation of silenes is by pyrolysis of a silacyclobutane as mentioned previously.

$$R_2Si\overline{}\overset{\Delta}{\longrightarrow} R_2Si=CH_2 + C_2H_4$$
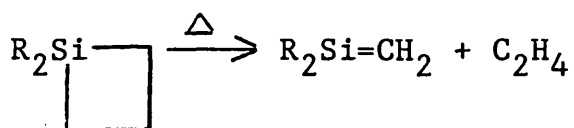
However, in cases where the silacyclobutane contains one or two silicon-hydrogen bonds, there is the added complication of a competing primary decomposition route involving a 1,2-hydrogen shift with ring opening to produce a silylene [29].
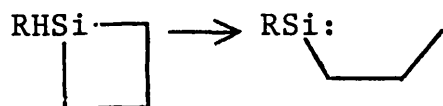
Other silene precursors available include silabicyclo-[2.2.2]octadiene derivatives.
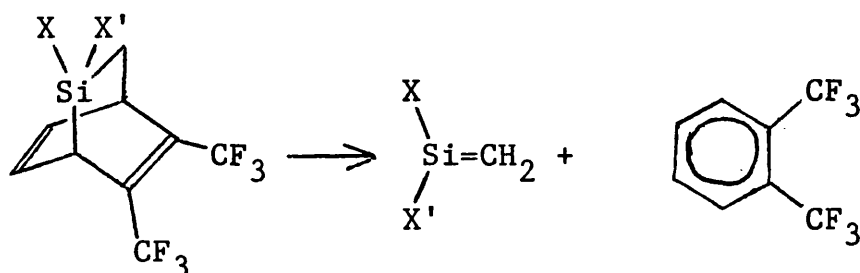
Which have been shown by Maier et al [30,31], to be suitable for generation of a variety of silenes, examples being:

$$X=X'=H,D,Cl \ : \ X=H,X'=Cl \ : \ X=H,X'=D \ : \ X=H,X'=CH_3$$
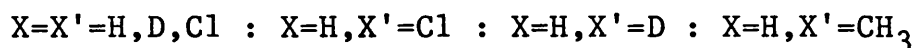
Silene Reactions

The reactivity of silenes arises from a combination of the polarity of silenes and the magnitude of the silicon-carbon π-bond. The results of theoretical calculations on $H_2Si=CH_2$ show that there are charges of +0.55e on silicon and -0.77e on carbon [32]. The π-bond strength of silenes has been

the subject of both theoretical and experimental investigation. For example, a recent theoretical calculation [33] on $H_2Si=CH_2$ gave the π-bond strength to be $37 kcalmol^{-1}$. This is in good agreement with experimental estimates of the π-bond strength in dimethylsilene, obtained from an analysis of kinetic and thermodynamic data which give $37.5\pm6 kcalmol^{-1}$ [34] and $39\pm5 kcalmol^{-1}$ [35].

The important reactions of silenes can be classified as:

a) Dimerisation.

b) Addition.

c) Cycloaddition.

d) Rearrangement.

a) Dimerisation

In the absence of other trapping agents, simple silenes will readily dimerise in a head to tail fashion.

$$2Me_2Si=CH_2 \longrightarrow Me_2Si \diamondsuit SiMe_2$$
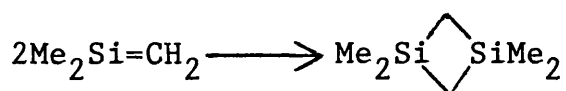
Kinetics of this process have been investigated by Gusel'nikov et al [36] in a flow apparatus in which dimethylsilacyclobutane is pyrolysed to generate dimethylsilene, which then flows through a tube of variable length and temperature (25,150 or 300°C) before detection by mass spectrometry. Analysis of the results indicated that dimerisation has zero activation energy and an

A-factor of $10^{6.55} dm^3 mol^{-1} s^{-1}$

b) Addition

$$R_2Si=CH_2 + X-Y \longrightarrow R_2SiXCH_2Y$$
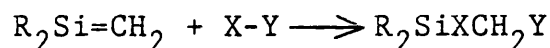
Silenes are able to undergo a very wide variety of additions of this type, with the more nucleophilic of X and Y adding to silicon. Evidence for this comes from a study of addition of tetrahydrofuran (THF) to $Me_2Si=C(SiMe_3)(SiMeBu^t_2)$ from which a crystalline adduct is obtained, and from X-ray diffraction, and nmr of a solution in THF at $30^{\circ}C$, the structure of the adduct was shown to be [37]:

$$Me_2Si\bar{C}(SiMe_3)(SiMeBu^t_2)$$
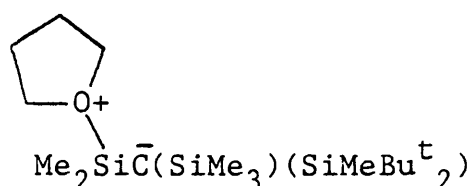
Very few kinetic measurements have been made on these types of reactions. The only data available are for addition of HCl, HBr and Me_3SiOMe to dimethylsilene [38,39]. The experiment involves copyrolysis of dimethylsilacyclobutane with the appropriate reagent. From analysis of the results with a knowledge of the mechanism, it is possible, with the aid of numerical integration, to estimate Arrhenius parameters for addition relative to Arrhenius parameters for silene dimerisation, as measured by Gusel'nikov et al [36]. This technique was also applied to addition of methanol to dimethylsilene, however, this turned out to be too fast to

be measured by this technique. Table 1.2 gives a summary of the estimates for additions to dimethylsilene.

TABLE 1.2

Reactants	$\log_{10}(A/dm^3mol^{-1}s^{-1})$	$Ea/kJmol^{-1}$	Reference
$Me_2Si=CH_2+HCl$	7.5±0.5	10±7	38
$Me_2Si=CH_2+HBr$	7.4±0.5	36±7	38
$Me_2Si=CH_2$ + Me_3SiOMe	5.3±0.2	6.3±0.2	39

c) Cycloaddition reactions

4+2 cycloadditions

The most important reaction of this type is reaction of a silene with a 1,3-diene to produce a silacyclohexene. This has been studied experimentally by Gusel'nikov et al [40] who generated dimethylsilene in the gas phase in the presence of butadiene or 2-methylbutadiene. After identification of products by a combination of chromatography, mass spectrometry and I.R. spectrometry, it was concluded that addition of dienes to silenes is a one step concerted process, and does not involve initial 1,2-addition with subsequent rearrangement.
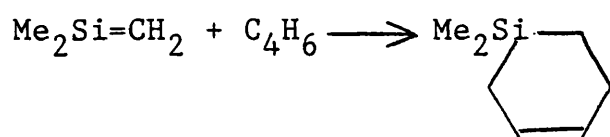
This view is confirmed in later work by Brook and Harris, [41] who produced a THF solution of $(Me_3Si)_2Si=C(Ph)(OSiMe_3)$ which after being refluxed with 2,3-dimethylbutadiene gave only the expected product of Diels-Alder addition, identified by nmr.

$(Me_3Si)_2Si=C(Ph)(OSiMe_3)$ +
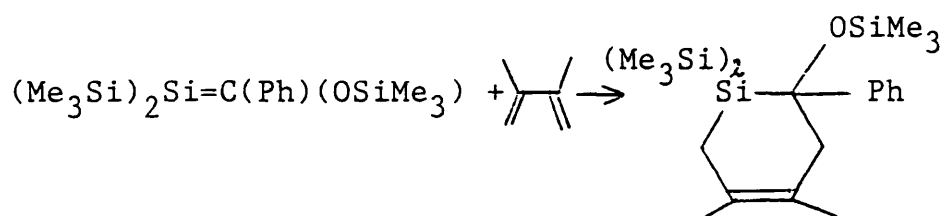
Quantitative information on butadiene addition to silenes is extremely sparse. Information which is available comes from a competitive experiment between silene dimerisation and trapping by butadiene, in which dimethylsilene is produced by I.R. multiphoton induced decomposition of dimethylsilacyclobutane in the presence of butadiene [42]. By analogy with structurally similar processes and transition state theoretical arguments, Arrhenius parameters for silene addition to butadiene have been estimated as [43]:

$$\log k/dm^3mol^{-1}s^{-1} = (7\pm1)-(\sim30kJmol^{-1}/2.303RT)$$

2+2 cycloadditions

$$R_2Si=CH_2 + X=Y \qquad R_2Si—\!—\!\!\underset{\displaystyle X—Y}{\big|\quad\big|}$$
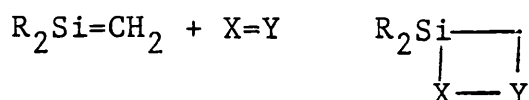
The most common reaction of this type is silene

dimerisation, which was discussed previously. A wide variety of other reactions of this type are known to occur. For example, Gusel'nikov et al [40] generated dimethylsilene from gas-phase pyrolysis of dimethylsilacyclobutane; in the presence of propene, they observed two new products, which were identified as 1,1,3-trimethyl-1-silacyclobutane and allyltrimethylsilane. These were interpreted as arising from addition of propene to dimethylsilene to form a diradical intermediate which could either ring close or undergo an intramolecular rearrangement.

$$Me_2Si=CH_2 + C_3H_6 \longrightarrow Me_2Si\text{---}^{\circ} \longrightarrow Me_2Si$$

$$Me_3Si$$
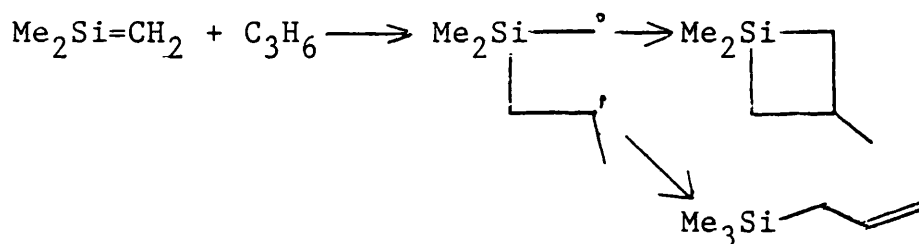
Very little quantitative information is available for this type of reaction. An activation energy of $61\pm17kJmol^{-1}$ has been estimated for addition of ethene to dimethylsilene from a study of the gas phase decomposition of dimethylsilacyclobutane [34].

From copyrolysis experiments on dimethylsilacyclobutane and oxygen [38], with analysis of the products produced and a knowledge of the reaction mechanism; with the aid of numerical integration, Arrhenius parameters for addition of oxygen to dimethylsilene have been estimated to be:

$$\log k/\mathrm{dm^3 mol^{-1} s^{-1}} = (7.6\pm0.3)-(15\pm5\mathrm{kJmol^{-1}}/2.303RT)$$

Also, P.John [44], from conventional sealed tube pyrolyses, has obtained Arrhenius parameters for propene addition to dimethylsilene to be:

$$\log k/\mathrm{dm^3 mol^{-1} s^{-1}} = (5.2\pm0.6)-(35\pm4\mathrm{kJmol^{-1}}/2.303RT)$$

It should be emphasised that these measurements are all relative to Arrhenius parameters for dimerisation of dimethylsilene as measured by Gusel'nikov et al [36].

Ene Reactions

Silenes are known to undergo ene reactions with a variety of compounds. Wiberg [45] has generated $Me_2Si=C(SiMe_3)_2$ in the presence of various alkenes, and observed the formation of products arising from an ene reaction.
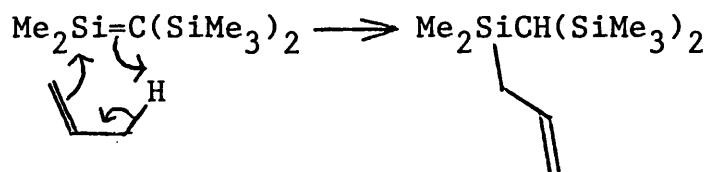
By studying a series of substituted propenes, Wiberg was able to measure the effect of various substituents on the rate of the ene reaction relative to 2+4 cycloaddition of the silene to 2,3-dimethylbutadiene, and so establish that the alkene acts as a nucleophile relative to the silene.

In a separate experiment, Conlin et al [46] generated a silene by flash vacuum pyrolysis of 2,2-dimethyl-3-neopentyl-2-silabicyclo[2.2.1]hept-5-ene. Besides observation of the products expected from silene dimerisation, they also observed products consistent with an intramolecular ene reaction.
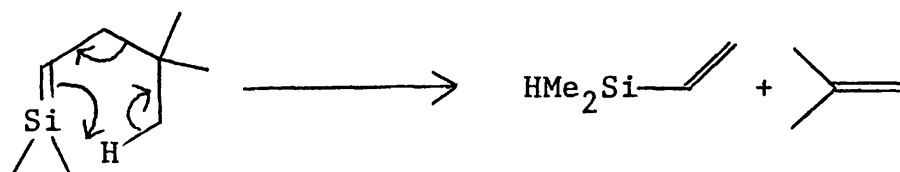
Ene reactions are also known to occur with carbonyl compounds containing hydrogen at the alpha carbon atom.
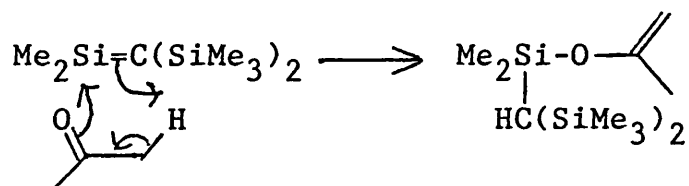
This has been investigated by Wiberg [45] who found this reaction to be faster than the ene reaction of isobutene with the analogous silene by a factor of 180 at 115°C.

d) Rearrangement

In experiments by Conlin and Wood [47], on the pyrolysis of methylsilacyclobutane in the presence of butadiene or trimethylsilane, products were observed that were consistent with formation of dimethylsilylene. The conclusion drawn from this was that methylsilene was initially formed and then rapidly isomerised to dimethylsilylene, which was

trapped by butadiene or trimethylsilane.
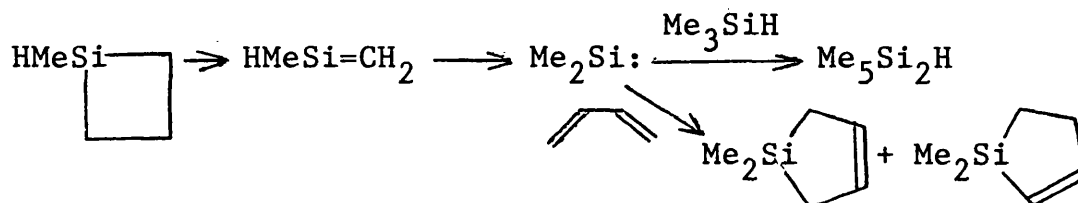
This conclusion was confirmed by later work [48] in which the same experiment was carried out, but three different sources of methylsilene were used.

Evidence has been obtained from copyrolysis of silacyclobutane and butadiene that isomerisation of silene to methylsilylene can occur [49]. Also, a silene to silylene isomerisation involving migration of a silyl group has been observed by Barton et al [50].

The silene to silylene isomerisation via a 1,2-hydrogen shift has been investigated theoretically and shown to be very nearly thermoneutral, with an activation energy of approximately $40 kcalmol^{-1}$ [51,52].

Also, Nagase and Kudo [52] have shown that methyl substitution in silene has very little effect on the silene to silylene isomerisation via a 1,2-hydrogen shift, and in a further study, they calculated activation energies for silene to silylene isomerisation involving migration of various groups, the results of which are summarised below and overleaf in table 1.3.

$$RHSi=CH_2 \rightleftharpoons H\ddot{S}iCH_2R$$
$$(1) \qquad\qquad (2)$$
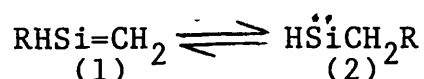
TABLE 1.3

	Activation Energy/kcalmol^{-1}	
	(1) $\rightarrow$ (2)	(2) $\rightarrow$ (1)
R = H	42.2	43
R = Me	54.7	44.4
R = H$_3$Si	26.4	24.8

For isomerisation of methylsilene to dimethylsilylene, Barton and Davidson [54] have estimated ΔS to be approximately zero. Since this isomerisation has been calculated to be approximately thermoneutral, it follows that the methylsilene to dimethylsilylene isomerisations should be a reversible reaction with an equilibrium constant close to one. By carrying out experiments on thermally generated dimethylsilylene with and without added butadiene [54], with a kinetic analysis of the results and previous experimental data, it was concluded that at high temperature, in the absence of butadiene an equimolecular equilibrium mixture of methylsilene and dimethylsilylene was present, and that trapping experiments with butadiene could be misleading due to the significantly greater reactivity of butadiene with dimethylsilylene than with methylsilene.

Davidson and Scampton [55] have successfully applied this

idea of a reversible silene to silylene isomerisation with Arrhenius parameters of:

$$\log \ k/s^{-1} = 13.5 - 170 kJmol^{-1}/2.303RT$$

To explain with the aid of numerical integration, the observed experimental results in which methylsilene or dimethylsilylene were generated over a wide range of conditions with or without added butadiene.

It should be noted that there is still controversy over Arrhenius parameters for methylsilene to dimethylsilene isomerisation. As a recent study [56] involving sealed tube pyrolysis of methylsilacyclobutane and a five fold excess of butadiene, after analysis of the results gave Arrhenius parameters for methylsilene to dimethylsilylene isomerisation of:

$$\log \ k/s^{-1} = (9.6 \pm 0.2) - (30.4 \pm 0.7 kcalmol^{-1}/2.303RT)$$

DISILENES

A disilene is a compound that contains a silicon-silicon $p\pi-p\pi$ bond. The first indirect evidence for existence of disilenes was obtained by Rork and Peddle [57], who prepared three different compounds that would be expected to decompose thermally by retro-Diels-Alder reactions to

produce tetramethyldisilene.
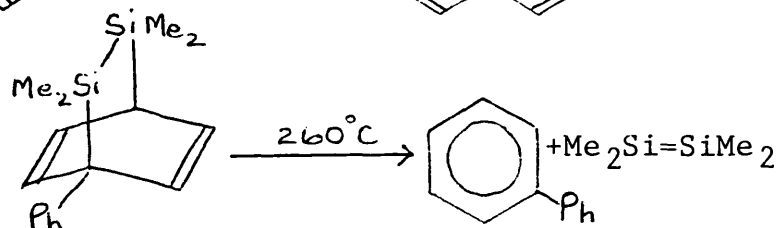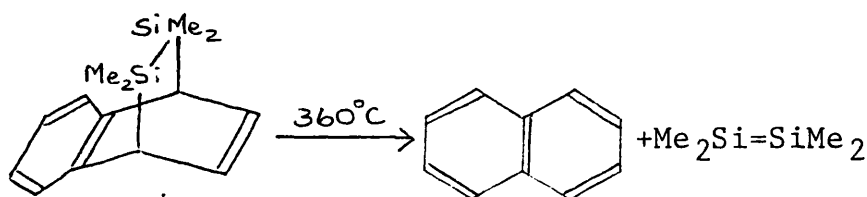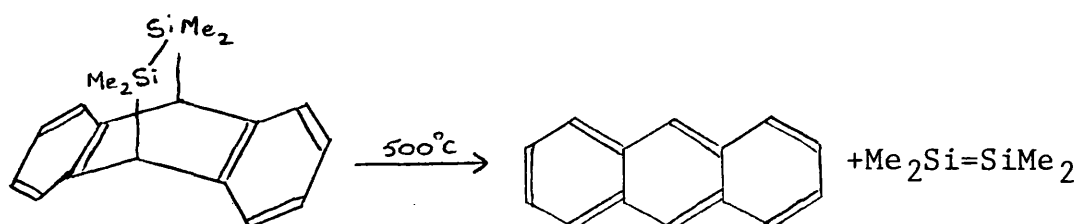
The existence of the disilene was implied by the detection of products that could be produced via intramolecular rearrangement of the disilene, also the disilene could be trapped by Diels-Alder reaction with various dienes.

Recently, stable disilenes containing bulky substituents have been prepared. For example, tetrakis(2,6-diethylphenyl)disilene has been synthesised and its crystal structure determined by x-ray diffraction [58]. This showed that the silicon-silicon double bond is significantly shorter than a silicon-silicon single bond, also, the silicon-silicon double bond in this disilene was twisted by 10°, presumably as a result of steric repulsion between the bulky substituents. Further experimental

evidence for the existence of a silicon-silicon double bond has been obtained from a solid state ^{29}Si nmr study of tetramesityldisilene [59] which showed that the electronic structure of the silicon-silicon double bond bears a close resemblance to that of a carbon-carbon double bond.

Very little experimental information is available concerning the π-bond energy of disilenes. The thermal cis-trans isomerisation of deuterated benzene solutions of 1,2-bis[(trimethylsilyl)amino]-1,2-dimesityldisilene and 1,2-di-tert-butyl-1,2-dimesityldisilene has been studied by variable temperature nmr [60]. From this work, activation energies for cis-trans isomerisation were measured as 25.4 ± 2.2kcalmol^{-1} and 31.3 ± 3.7kcalmol^{-1} respectively. From a kinetic study of the decomposition of chemically activated disilane [61], a π-bond energy of 26 ± 2.6kcalmol^{-1} was estimated for disilene ($H_2Si=SiH_2$). From an analysis of earlier work involving generation and diene trapping of disilenes, these authors estimated the π-bond energy of substituted disilenes to be 25.8 ± 4.8kcalmol^{-1}, finally, from theoretical calculations, they estimated the π-bond energy of disilene to be 22.2 ± 1.9kcalmol^{-1}, Thus it can be seen that further work is necessary to accurately determine the π-bond energy of disilenes.

Several theoretical studies have been undertaken to determine the structure of simple disilenes. These show that disilene is a non-planar trans-bent structure [62,63],

but the barrier to distortion is extremely small with the planar structure being only 1kcalmol^{-1} less stable, and for tetramethyldisilene, the planar structure is calculated to be the more stable structure [63].

There is a possibility that disilenes can isomerise to silylsilylenes via a 1,2-shift as shown in the following equation.

$$RHSi=SiH_2 \rightleftharpoons H\ddot{S}iSiRH_2$$

$$\quad (A) \qquad\qquad (B)$$
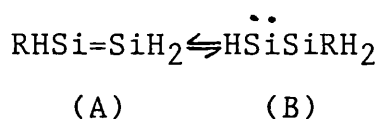
Calculations have been performed for R=H, Me and SiH$_3$. The results of which are summarised in the following table 1.4.

TABLE 1.4

	Activation energy/kcalmol^{-1}		
	(A) → (B)	(B) → (A)	Reference
R = H	15.4	9	64
R = SiH$_3$	17.2	8.4	65
R = Me	34.7	27.8	65

These calculations show that in each case the disilene is the more stable isomer by 5-10kcalmol^{-1}, also methyl migration is a less favoured process than either hydrogen or silyl migration.

Experimental evidence for disilene-silylsilylene isomerisations has been obtained by Barton et al [66] who

generated tetramethyldisilene in the presence of excess trimethylsilane, and detected a product consistent with rearrangement of the disilene via a methyl shift to a silylsilylene which was then trapped by the added trimethylsilane.
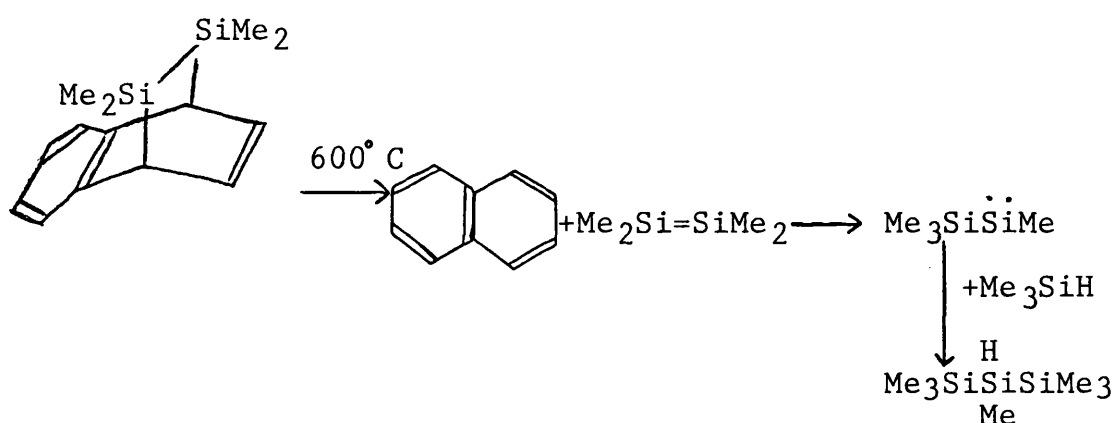
Sealed tube pyrolyses of precursors to $Me_2Si=SiMe(SiMe_3)$ and $(Me_3Si)Me_2SiSiMe$ in the presence of 2,3-dimethylbutadiene have provided convincing evidence of a reversible disilene-silylsilylene isomerisation involving migration of a silyl group [67]. It was also shown that methyl migration is considerably slower than silyl migration, as would be expected from the calculated activation energies [65].

There is a considerable amount of chemistry involving disilenes besides that mentioned here, similar to the chemistry of silenes discussed earlier, and well covered in a recent review by Raabe and Michl [68].

SILYL RADICALS (R₃Si·)

These are the silicon equivalent of alkyl radicals, in which the unpaired electron is located on silicon. These species undergo many typical radical reactions such as hydrogen abstraction [69], addition to double bonds [70], and disproportionation [71]. Gas phase recombination of trimethylsilyl radicals has been investigated by Cadman et al [72] using a rotating sector technique between 317-399K to obtain Arrhenius parameters for recombination of:

$$\log k/dm^3mol^{-1}s^{-1}=11.25$$

Competitive experiments have been performed on chlorine abstraction by trimethylsilyl radicals from alkyl chlorides, from which Arrhenius parameters for abstraction have been measured relative to recombination, hence absolute Arrhenius parameters have been determined for a variety of chlorine abstractions [73]. For example:

$$Me_3Si\cdot +MeCl \longrightarrow Me_3SiCl+Me\cdot$$
$$\log k/dm^3mol^{-1}s^{-1}=8.02-(16.98kJmol^{-1}/2.303RT)$$

This is a very useful reaction, as excess methyl chloride is an efficient trap for silyl radicals, and by monitoring formation of the chlorosilane, Arrhenius parameters for decomposition channels leading to silyl radicals can be obtained [74].

THERMOCHEMISTRY

This is of great value as a knowledge of thermochemical quantities combined with kinetic data allows Arrhenius parameters to be estimated for individual reaction steps that are difficult or impossible to measure experimentally. For example:

$$Me_3SiSiMe_2H \underset{-1}{\overset{1}{\rightleftharpoons}} Me_3SiH + Me_2Si:$$
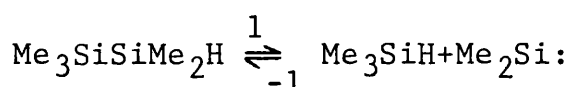
E_1 can be measured experimentally [75]. If the heats of formation of reactant and products are known, or alternatively $D(Me_3Si-SiMe_2H)$ and the silylene stabilisation energy (SSE) [35], then E_1 can be calculated as follows:

$$E_{-1} = E_1 - \Delta H$$

$$\Delta H = \Delta H_f^\circ(Me_3SiH) + \Delta H_f^\circ(Me_2Si:) - \Delta H_f^\circ(Me_3SiSiMe_2H)$$
or
$$\Delta H = D(Me_3Si-SiMe_2H) - SSE$$

Traditional calorimetric methods of determining heats of combustion and hence heats of formation have proved to be unreliable when applied to organosilicon compounds, due to incomplete combustion caused by formation of solid films of silica over uncombusted material [76]. Recently, more accurate calorimetric data have been obtained for several organosilicon compounds, which are listed in the CATCH tables [77], from work largely done by Pedley and

27

co-workers, who employed HF along with O_2 in the calorimeter to convert silica to H_2SiF_6, and thus overcame the problem of incomplete combustion.

Bond dissociation energies may be obtained from a variety of methods. Under electron impact in a mass spectrometer, molecules can dissociate and one of the fragments become ionised.

$$R_1-R_2+e \longrightarrow R_1^+ + R_2\cdot + 2e$$
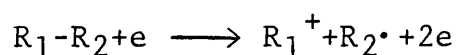
If the ionised fragment and the other fragment are produced in their ground state from a ground state molecule, then the appearance potential of the ion produced is simply related to the ionisation potential of the fragment and the dissociation energy of the bond broken to form it. The appearance potential is given by:

$$A.P.(R_1^+) = D(R_1-R_2) + I.P.(R_1\cdot)$$

To determine bond dissociation energies by this method the ionisation potential of the R_1 radical is required. This is a very difficult quantity to determine directly, therefore to determine bond dissociation energies some additional information is necessary. For example, if $D(R_1-R_2)$ can be obtained by a different method, then $I.P.(R_1\cdot)$ can be determined and can be used to determine other bond dissociation energies involving R_1 [78]. Appearance potentials of a large number of organosilicon ions have been measured by Potzinger et al [79], which combined with

28

heat of combustion measurements, allow bond dissociation
energies to be calculated, which can be used to calculate
heats of formation of all silicon compounds containing
hydrogen, chlorine and alkyl groups.

In assessing the reliability of results from electron impact
studies, it should be noted that in addition to the errors
in the appearance potentials, which may themselves be
considerable due to experimental difficulties or
misinterpretation of the ionisation efficiency curves, there
will be errors in the supporting data, be they bond
dissociation energies or heats of formation.

Kinetic methods are of use in determining bond dissociation
energies. From a kinetic study of the gas phase reaction of
iodine with silanes, Walsh [35] has measured various
silicon-hydrogen bond dissociation energies to an accuracy
of $\leqslant \pm 2\,\text{kcalmol}^{-1}$. A useful by-product of this is that
providing the heats of formation of RX, RH, H· and X· are
known, it enables the derivation of other bond dissociation
energies [D(R-X)] via the following thermodynamic
relationships.

$$D(R-X) = \Delta H_f^o(R\cdot) + \Delta H_f^o(X\cdot) - \Delta H_f^o(RX)$$

$$\Delta H_f^o(R\cdot) = \Delta H_f^o(RH) - \Delta H_f^o(H\cdot) + D(R-H)$$

Pyrolysis techniques can also be used to determine bond
dissociation energies.

$$R_1 - R_2 \xrightarrow{\triangle} R_1 \cdot + R_2 \cdot$$
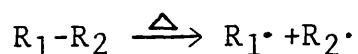
If the reverse reaction is assumed to have zero activation energy, a reasonable assumption for radical recombination, then measurement of the rate of dissociation into radicals yields an activation energy which can be identified with the bond strength. A problem with this is that a radical chain mechanism develops which is kinetically complex. However, for organosilicon compounds, one of the propagating steps, the dissociation of a large radical into a small radical and a silene is of reduced importance due to the weakness of π-bonds to silicon. As a result, the chain lengths of such decompositions are shorter than those in hydrocarbon pyrolyses. This factor can help in overcoming the problem of secondary reactions, enabling Arrhenius parameters for the initial dissociation to be measured. In any chain reaction, initiation is the step of highest activation energy, so the chain length tends to decrease with increasing temperature. If the chain length can be reduced to below unity, the reaction becomes rate determined by the initial dissociation. This was achieved by Davidson et al [69] who pyrolysed tetramethylsilane between 840-1055K and found that formation of methane obeyed first order kinetics over the whole temperature range, but the rate constants fell into two distinct groups with a crossover point at 950K. The high temperature Arrhenius parameters corresponded to a non-chain process rate determined by the initial dissociation into radicals, and gave a lower limit to the activation energy for the

reaction.

$$Me_4Si \xrightarrow{\triangle} Me_3Si\cdot + Me\cdot$$
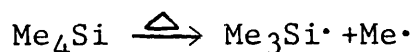
An alternative method of overcoming the problem of secondary reactions is to trap one of the initially formed radicals. For example, one of the primary processes in the pyrolysis of allyltrimethylsilane is allylic bond homolysis.

$$Me_3Si\diagup\diagdown \xrightarrow{\triangle} Me_3Si\cdot + \diagup\diagdown\diagdown$$
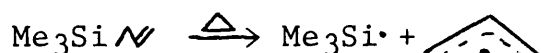
By pyrolysing allyltrimethylsilane with an excess of methylchloride, the trimethylsilyl radical initially produced is efficiently trapped by methylchloride to produce trimethylchlorosilane.

$$Me_3Si\cdot + MeCl \longrightarrow Me_3SiCl + Me\cdot$$
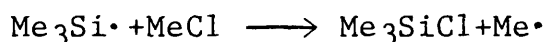
By measuring rate constants for trimethylchlorosilane formation, Arrhenius parameters for the initial dissociation into radicals can be determined [74].

Thus, by a variety of experimental techniques, heats of formation and bond dissociation energies applicable to organosilicon compounds can be obtained. However, it is desirable to produce a group additivity scheme so that thermochemical data can be estimated for organosilicon compounds for which no experimental data are available.

Benson's Electrostatic Model

This was developed by Benson to determine heats of formation of hydrocarbons [80]. It assigns a constant charge of $+y$ to each hydrogen atom and $-ny$ to each carbon atom (n=number of hydrogen atoms bonded to carbon). From this it is possible to calculate an electrostatic energy (E_{el}) for any molecule which arises from the pairwise interaction of all the charges present in it. From the assumption of constant charges on the atoms, E_{el} can be written as:

$$E_{el} = y^2 (\sum_{i<j} n_i n_j / r_{i,j})$$

$n_i = +1$ for H atoms, 0 for quaternary C, -1 for tertiary C, -2 for secondary C and -3 for primary C. The term in the brackets is independant of y and depends only on the geometry of the molecule. It is then shown that the heat of formation of an alkane is given by:

$$\Delta H_f^{\circ}(C_nH_{2n+2}) = -2(n+1) - 0.5 + E_{el}(C_nH_{2n+2})$$

By choosing an appropriate value of y, the calculated heats of formation fit the observed heats of formation for n-alkanes up to C_7H_{16} and branched alkanes to C_5H_{12} to $\pm 0.2 kcalmol^{-1}$.

Davidson [14] applied Benson's electrostatic model to methylsilanes and some disilanes in order to evaluate the

reliability of the CATCH tables [77] and the results of Potzinger et al, with the conclusion that the results of Potzinger et al [79] are to be preferred. More recently, O'Neal and Ring [81] have applied Benson's electrostatic model to silanes, polysilanes and their alkyl derivatives, taking into account recent calorimetric results, and concluded that the CATCH calorimetric heats of formation are to be favoured over the results of Potzinger et al. They also concluded that recent combustion studies with HF are providing reliable heats of formation for organosilicon compounds. From these data they constructed a table of group additivity enthalpies, and also derived group additivity entropies and heat capacities from the results of statistical thermodynamic calculations. Internal consistencies of estimated reaction enthalpy and entropy are thought to be reliable to $\pm 1.5 kcalmol^{-1}$ and ± 1.0 e.u. respectively, although errors in individual heats of formation and entropies could be significantly less accurate due to uncertainties in the experimental heats of formation and estimated parameters for statistical thermodynamic calculations. However, it provides a convenient method of estimating heats of formation and entropies for organosilicon compounds. For example:

$$\Delta H_f^\circ [(CH_3)_3SiCH_2SiH(CH_3)_2]$$
$$=5[C-(Si)(H)_3]+[Si-(C)_4]+[C-(Si)_2(H)_2]+[Si(C)_3(H)]$$
$$=5(-10.2)+(-18.3)+(-9.62)+(-11.3)$$
$$=-90.22 kcalmol^{-1}$$

33

References

1. K. Krogh-Jesperson, J. Am. Chem. Soc., 1985, $\underline{107}$, 537.

2. M. S. Gordon, Chem. Phys. Lett., 1985, $\underline{114}$, 348.

3. I. M. T. Davidson, J. Organomet. Chem., 1970, $\underline{24}$, 97.

4. P. P. Gaspar, React. Intermed., 1985, $\underline{3}$, 333.
    P. P. Gaspar, React. Intermed., 1981, $\underline{2}$, 335.
    P. P. Gaspar, React. Intermed., 1978, $\underline{1}$, 229.

5. I. M. T. Davidson, F. T. Lawrence & N. A. Ostah, J. Chem. Soc. Chem. Comm., 1980, 859.

6. T. Y. Gu, & W. P. Weber, J. Organomet. Chem., 1980, $\underline{195}$, 29.

7. I. M. T. Davidson & S. Ijadi-Maghsoodi, Organometallics, in press.

8. K. Raghavachari, J. Chandrasekhar, M. S. Gordon & K. J. Dykema, J. Am. Chem. Soc., 1984, $\underline{106}$, 5853.

9. D. R. Gano & M. S. Gordon, J. Am. Chem. Soc., 1984, $\underline{106}$, 5421.

10. A. Sax, & G. Olbrich, J. Am. Chem. Soc., 1985, $\underline{107}$, 4868.

11. P. John & J. H. Purnell, J. Chem. Soc. Faraday Trans. I, 1973, $\underline{69}$, 1455.

12. R. T. White, R. C. Espino-Rios, D.S. Rogers, M. A. Ring & H. E. O'Neal, Int. J. Chem. Kinet., 1985, $\underline{17}$, 1029.

13. B. A. Sawray, H. E. O'Neal, M. A. Ring & D. Coffey Jr., Int. J. Chem. Kinet., 1984, $\underline{16}$, 31.

14. I. M. T. Davidson, J. Orgnomet. Chem., 1979, $\underline{170}$, 365.

15. V. J. Tortorelli & M. Jones Jr., J. Am. Chem. Soc., 1980, $\underline{102}$, 1425.

16. D. Seyferth, D. C. Annarelli & D. P. Duncan, Organometallics, 1982, $\underline{1}$, 1288.

17. M. Ishikawa, K. I. Nakagawa & M. Kumada, J. Organomet. Chem., 1979, $\underline{178}$, 105.

18. E. A. Chernyshev, S. A. Bashkirova, N. G. Komalenkova, M. Y. Kel'man & V. N. Bochkarev, Dokl. Akad. Nauk. SSSR, 1984, $\underline{276}$, 1151.

19. D. Lei, R. J. Hwang & P. P. Gaspar, J. Organomet. Chem., 1984, 271, 1.

20. R. T. Conlin & P. P. Gaspar, J. Am. Chem. Soc., 1976, 98, 868.

21. D. N. Roark & G. J. D. Peddle, J. Am. Chem. Soc., 1977, 94, 5837.

22. Y. S. Chen, B. H. Cohen & P. P. Gaspar, J. Organomet. Chem., 1980, 195, C1.

23. M. C. Flowers & L. E. Gusel'nikov, J. Chem. Soc. (B), 1968, 419.

24. R. W. Carr Jr. & W. D. Walters, J. Phys. Chem., 1963, 67, 1370.

25. S. W. Benson, "Thermochemical Kinetics", 2nd Ed., Wiley (1976).

26. O. L. Chapman, C. C. Chang, J. Kolc, M. E. Jung, J. A. Lowe, T. J. Barton & M. L. Tumey, J. Am. Chem. Soc., 1976, 98, 7844.

27. M. R. Chedekel, M. Skoglund, R. L. Kreeger & H. Schecter, J. Am. Chem. Soc., 1976, 98, 7846.

28. A. G. Brook, F. Abdesaken, B. Gutekunst, G. Gutekunst & R. K. Kallury, J. Chem. Soc. Chem. Comm., 1981, 191.

29. I. M. T. Davidson, A. Fenton, S. Ijadi-Maghsoodi, R. J. Scampton, N. Auner, J. Grobe, N. Tillman & T. J. Barton, Organometallics, 1984, 3, 1593.

30. G. Maier, G. Mihm & H. P. Reisenauer, Angew, Chem. Int. Ed. Engl., 1981, 20, 597.

31. G. Maier, G. Mihm & H. P. Reisenauer, Chem. Ber., 1984, 117, 2351.

32. B. T. Luke, J. A. Pople, M. B. Krogh-Jesperson Y. Apeloig, M. Karni, J. Chandrasekhar & P. V. R Scheyer, J. Am. Chem. Soc., 1985, 108, 270.

33. M. W. Schmidt, M. S. Gordon & M. Dupuis, J. Am. Chem. Soc., 1985, 107, 2585.

34. S. Basu, I. M. T. Davidson, R. Laupert & P. Potzinger, Ber. Bunsenges. Phys. Chem., 1979, 83, 1282.

35. R. Walsh, Acc. Chem. Res., 1981, 14, 246.

36. L. E. Gusel'nikov, K. S. Konobeyevsky, V. M. Vdovin & N. S. Nametkin, Dokl. Akad. Nauk. SSSR, 1977, 235, 1086.

37. N. Wiberg, G. Wagner, G. Muller & J. Riede, J. Organomet. Chem., 1984, <u>271</u>, 381.

38. I. M. T. Davidson, C. E. Dean & F. T. Lawrence, J. Chem. Soc. Chem. Comm., 1981, 52.

39. I. M. T. Davidson & I. T. Wood, J. Chem. Soc. Chem. Comm., 1982, 550.

40. N. S. Nametkin, L. E. Gusel'nikov, R. L. Ushakova & V. M. Vdovin, Dokl. Akad. Nauk, SSSR, 1971, <u>201</u>, 1365.

41. A. G. Brook & J. W. Harris, J. Am. Chem. Soc., 1976, <u>98</u>, 3381.

42. H. M. Frey, A. Kashoulis, M.-L. Ling, S. P. Lodge, I. M. Pidgeon & R. Walsh, J. Chem. Soc. Chem. Comm., 1984, 478.

43. R. Walsh, J. Chem. Soc. Chem. Comm., 1982, 1415.

44. P. John, personal communication to I. M. T. Davidson.

45. N. Wiberg, J. Organomet. Chem., 1984, <u>273</u>, 141.

46. R. T. Conlin, M. P. Bescellieu, P. R. Jones & R. A. Pierce, Orgnometallics, 1982, <u>1</u>, 396.

47. R. T. Conlin, D. L. Wood, J. Am. Chem. Soc., 1981, <u>103</u>, 1843.

48. R. T. Conlin, Y. W. Kwak, Organometallics, 1984, <u>3</u>, 918.

49. R. T. Conlin & R. S. Gill, J. Am. Chem. Soc., 1983, <u>105</u>, 618.

50. T. J. Barton, S. A. Burns & G. T. Burns, Organometallics, 1982, <u>1</u>, 210.

51. H. F. Shaefer III & Y. Yoshioka, J. Am. Chem. Soc., 1981, <u>103</u>, 7366.

52. T. Kudo & S. Nagase, J. Chem. Soc. Chem. Comm., 1984, 141.

53. T. Kudo & S. Nagase, J. Chem. Soc. Chem. Comm., 1984, 1392.

54. I. M. T. Davidson, S. I.-Maghsoodi, T. J. Barton & N. Tillman, J. Chem. Soc. Chem. Comm., 1984, 478.

55. I. M. T. Davidson & R. J. Scampton, J. Organomet. Chem., 1984, <u>271</u>, 249.

56. R. J. Conlin & Y.-W. Kwak, J. Am. Chem. Soc., 1986, <u>108</u>, 834.

57. D. N. Roark & G. J. D. Peddle, J. Am. Chem. Soc., 1972, 94, 5837.

58. S. Masamune, S. Murakami, J. T. Snow, H. Tobita & D. J. Williams, Organometallics, 1984, 3, 333.

59. K. W. Zilm, D. M. Grant & J. Michl, Organometallics, 1983, 2, 193.

60. M. J. Michalczyk, R. West & J. Michl, Organometallics, 1985, 4, 826.

61. G. Olbrich, P. Potzinger,B. Reimann & R. Walsh, Organometallics, 1984, 3, 1267.

62. K. Krogh-Jesperson, J. Phys. Chem., 1982, 86, 1492.

63. K. Krogh-Jesperson, J. Am. Chem. Soc., 1985, 107, 537.

64. M. S. Gordon, T. N. Truong & E. K. Bonderson, J. Am. Chem. Soc., 1986, 108, 1421.

65. S. Nagase & T. Kudo, Organometallics, 1984, 3, 1320.

66. W. D. Wulff, W. F. Goure & T. J. Barton, J. Am. Chem. Soc., 1978, 100, 6236.

67. H. Sakurai, Y. Nakadaira & H. Sakaba, Organometallics, 1983, 2, 1484.

68. G. Raabe & J. Michl, Chem. Rev., 1985, 85, 419.

69. A. C. Balwin, I. M. T. Davidson & M. D. Reed, J. Chem. Soc. Faraday Trans. I, 1978, 74, 2171.

70. R. N. Haszeldine, S. Lythgoe & P. J. Robinson, J. Chem. Soc. (B). 1970, 1364.

71. L. Gammie, I. Safarik, O. P. Strausz, R. Roberge & C. Sandorfy, J. Am. Chem. Soc., 1980, 102, 378.

72. P. Cadman, G. M. Tilsey & A. F. Trotman-Dickenson, J. Chem. Soc. Faraday Trans. I, 1972, 68, 1849.

73. P. Cadman, G. M. Tilsey & A. F. Trotman-Dickenson, J. Chem. Soc. Faraday Trans. I, 1973, 69, 914.

74. T. J. Barton, S. A. Burns, I. M. T. Davidson, S. Ijadi-Maghsoodi & I. T. Wood, J. Am. Chem. Soc., 1984, 106, 6367.

75. I. M. T. Davidson and J. I. Matthews, J. Chem. Soc. Faraday Trans. I, 1976, 72, 1403.

76. I. M. T. Davidson, Quart. Rev., 1971, 25, 111.

77. CATCH tables, Univ. of Sussex, 1972; updated 1977.

78. S. J. Band, I. M. T. Davidson and C. A. Lambert, J. Chem. Soc. (A), 1968, 2068.

79. P. Potzinger, A. Ritter and J. Krause, Z. Naturforsch, 30a, 1975, 347.

80. S. W. Benson and M. Luria, J. Am. Chem. Soc., 1975, 97, 704.

81. H. E. O'Neal and M. A. Ring, J. Organomet. Chem., 1981, 213, 419.

CHAPTER TWO

APPARATUS AND EXPERIMENTAL METHOD

INTRODUCTION

Most of the experimental work described in this thesis was carried out using either the low pressure pyrolysis (LPP) apparatus [1], or the stirred flow reactor (SFR) apparatus [2]. Both methods are described in this chapter.

THE LPP APPARATUS

A schematic diagram of the apparatus is shown in figure 2.1. It consists of a vacuum line in which samples could be stored and manipulated. Samples could be introduced into the mass spectrometer either through the reaction vessel, or via a metrosil leak that by-passed the reaction vessel.

The reaction vessel was constructed from quartz, and had a volume of approximately $55cm^3$. The reaction vessel was isolated from the vacuum line by a solenoid valve, that could be operated manually or by a microcomputer. Samples entered the reaction vessel through a tube that ended in a perforated sphere, and thus became evenly distributed. The reaction vessel was situated in a furnace consisting of a steel tube wrapped with heating wire, insulated with fireproof clay and contained in a housing of asbestos board and aluminium. The furnace temperature was controlled by a "variac" variable transformer, the temperature was measured with a single junction chrome-alumel thermocouple inserted into a pocket in the reaction vessel, and connected to a

digital meter with ambient temperature compensation.

The mass spectrometer was a V.G.Micromass Q801 quadrupole mass spectrometer which could operate in two modes. An entire mass spectrum, up to 300 a.m.u. could be viewed on an oscilloscope screen and recorded on chart paper. The second mode in which the mass spectrometer could operate utilised an eight channel peak selector which could follow quantitatively any change in intensity of mass peaks. It scanned the selected mass peaks repeatedly and measured their heights in the form of voltages which were displayed on a digital voltmeter.

A Research Machines 380Z microcomputer was used to collect and process data. Four scans of the selected peaks were made to obtain a background reading before the computer opened the solenoid valve for 3s, thus allowing reactant into the reaction vessel. The computer collected data concerning the peak height from the digital voltmeter, and used its internal clock to time each reading, the maximum possible scan speed was 1s, thus giving a minimum time interval between data points of 0.125s.

DATA PROCESSING

Since the height of a mass peak at any given time is directly proportional to the concentration in the reaction vessel of the species represented by it, observed peak

height-time profiles were effectively concentration-time profiles.

For a first order decay of reactant:

$$d[R]/dt = -k[R]$$

therefore, $\ln[R_t] = -kt + \ln[R_o]$

$[R_t]$ = reactant concentration at time = t

$[R_o]$ = reactant concentration at time = zero

since $[R_t] = cP_t$

c = constant

P_t = peak height at time = t

therefore, $\ln P_t = -kt + \ln P_o$.

Therefore, a plot of $\ln P_t$ vs. t is a straight line with a gradient of -k and an intercept of P_o, the initial peak height of reactant. The value of k so measured needed to be corrected due to a contribution caused by leak-out of reactant from the reaction vessel. This was separately measured by introducing samples of reactant into the reaction vessel at lower temperatures, at which no decomposition of the reactant occurred.

For a first order formation of a product;

$$d[P]/dt = k[R]$$

therefore, $k = \dfrac{d[P]/dt}{[R]}$

Therefore by measuring the initial gradient of the product concentration-time profile, along with the initial concentration of reactant, first order rate constants for product formation could be calculated.

In some cases, the decay of reactant was accompanied by the formation of an isomer of the reactant with a very similar mass spectrum, thus making measurements of rate constants for reactant decomposition more difficult. A method of obtaining more accurate rate constants for reactant decomposition in such a case was to process the original peak height-time profile as described to get an approximate measure of the rate constant for reactant decomposition (k), and also a measure of the minimum peak height (m), obtained after complete decomposition of the reactant. Then use these values of k and m to make a correction to the original peak height-time profile, by subtracting a quantity from each peak height equal to $m(1-\exp(-kt))$. This correction has the effect of subtracting the build up of product from the reactant peak height-time profile. At t = 0, the correction = 0, as $t \rightarrow \infty$, the correction approaches m, thus the corrected peak height-time profile can now be processed to obtain an improved measurement of the rate constant for reactant decomposition.

THE SFR APPARATUS

A schematic diagram of the SFR apparatus is given in figure

2.2. As in the LPP apparatus, samples were stored and manipulated on a vacuum line. $10cm^3$ samples could be injected into a stream of dry deoxygenated nitrogen at a pressure of approximately 2.5 atm., and carried into a quartz reaction vessel through a tube ending in a perforated sphere, thus giving an even distribution of material in the reaction vessel. The reaction vessel had a volume of approximately $10cm^3$, and a pocket into which a thermocouple was inserted to measure the temperature. The reaction vessel was situated inside a furnace of similar design to that used in the LPP apparatus.

Material flowed out of the reaction vessel via a second tube tangential to the wall of the reaction vessel, thus ensuring stirred flow [3], and was carried into a gas chromatograph (gc). The gc used was a Pye-Unicam GCD, temperature programmable between 30 and $400^{o}C$, with detection by FID. It was connected to a conventional chart recorder, and also connected to a digital voltmeter interfaced to a Research Machines 380Z microcomputer, which allowed data to be collected and stored on magnetic disc, and processed by the computer.

The apparatus could be used both to check the purity of samples by setting the furnace temperature at a low value at which no decomposition of the sample would occur. If the furnace temperature was raised, pyrolysis products could be observed and characterised with authentic samples. By

measurement of the reactant and product peak areas, first order rate constants for product formation could be calculated, as discussed by Baldwin, Davidson and Howard [2] and summarised in appendix 1.

MEASUREMENT OF ARRHENIUS PARAMETERS

Having obtained rate constants by the LPP or SFR technique, Arrhenius parameters were obtained from a plot of logk vs. 1000/T, which was analysed by the method of least squares to obtain values of the activation energy and A-factor. In this work, the assumption was made that each value of logk had equal error, and thus no attempt was made to weight the data. Errors in the activation energy and A-factor quoted in this work represent scatter about the best fit line, and are equal to one standard deviation of the sample mean.

Figure 2.1

Schematic Diagram of LPP Apparatus
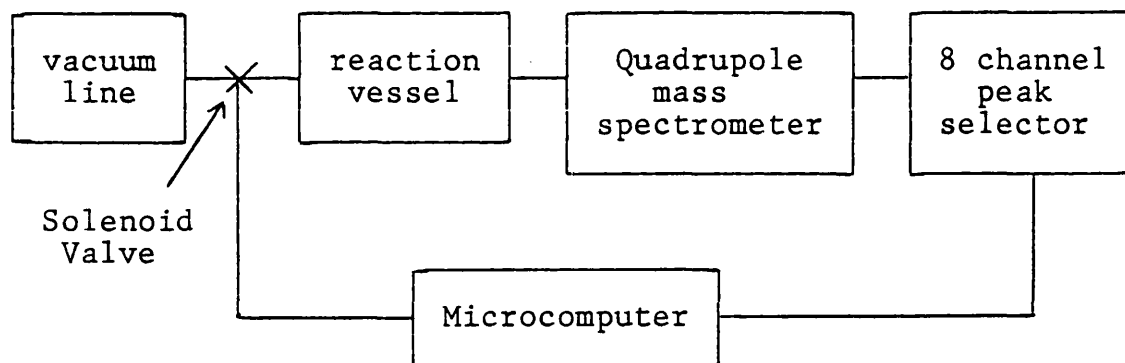
Figure 2.2

Schematic Diagram of SFR Apparatus
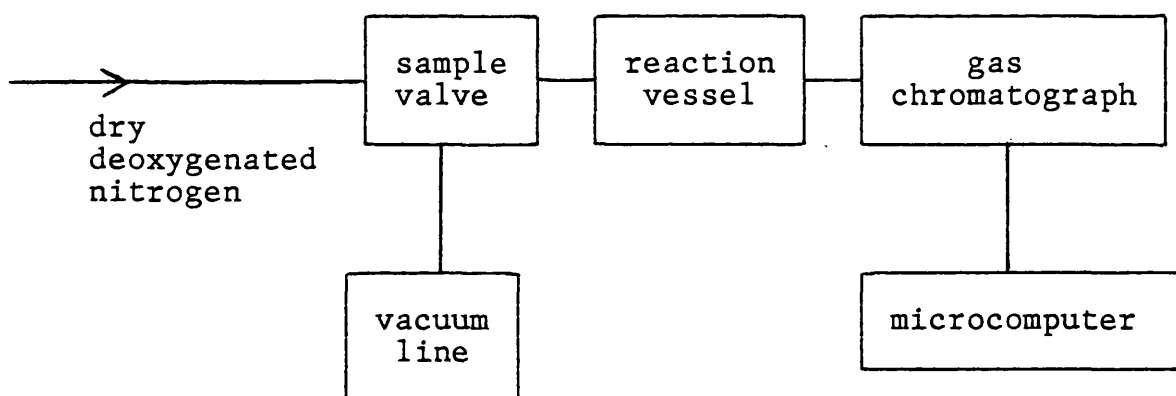
References

1. I. M. T. Davidson, M. A. Ring, J. C. S. Faraday Trans. I, 1980, 76, 1520.

2. A. C. Baldwin, I. M. T. Davidson, A. V. Howard, J. C. S. Faraday Trans. I, 1975, 71, 972.

3. M. F. R. Mulcahy, P. J. Williams, Austral. J. Chem., 1961, 14, 534.

CHAPTER THREE

PYROLYSIS OF ALKENYL SILANES

INTRODUCTION

Previous gas-kinetic studies on the pyrolysis of allyltrimethylsilane [1,2] have shown that there are two concurrent primary reactions, homolysis of the silicon-allyl bond and retroene elimination of dimethylsilene as shown in scheme 3.1.

Scheme 3.1

Primary reactions in the decomposition of allyltrimethylsilane

$$Me_3Si \diagup\diagdown\diagup\diagup \longrightarrow Me_3Si\cdot \ + \ \diagup\diagdown\diagdown$$

$$\searrow Me_2Si=CH_2 \ + \ C_3H_6$$
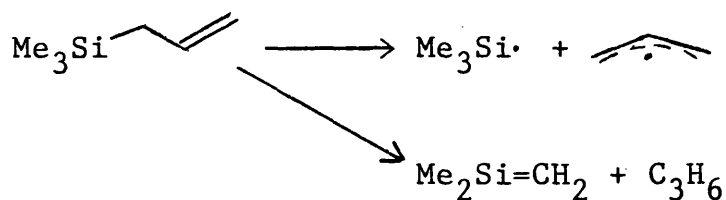
The two concurrent primary reactions in scheme 3.1 were distinguished from each other by the use of excess methylchloride,[2,3] which acted as a selective trap for trimethylsilyl radicals. Thus Arrhenius parameters could be obtained for the formation of trimethylchlorosilane, which related to the silicon-allyl bond homolysis. In addition, by measuring rate constants for the decomposition of allyltrimethylsilane, then subtracting rate constants for trimethylchlorosilane formation, it was possible to obtain rate constants and hence Arrhenius parameters for the retroene reaction in scheme 3.1. In the pyrolysis of

allyltrimethylsilane alone, it was shown that secondary radical addition reactions were important in the production of trimethylvinylsilane, rather than the unimolecular reaction sequences previously suggested.[4,5]

It was therefore decided to investigate the mechanism of pyrolysis of some higher alkenyl silanes, which would be expected to behave in a similar manner with competing retroene and allylic bond homolysis as primary reactions. By obtaining Arrhenius parameters for carbon-allyl bond homolysis, it was hoped to obtain information concerning any alpha-silyl or beta-silyl substituent effect. In addition, computer simulation was used to investigate the isomerisation of $HMe_2Si\overset{.}{C}H_2 \longrightarrow Me_3Si\cdot$.

RESULTS

Pyrolysis of 4-(dimethylsilyl)but-1-ene (1)

Approximately 1.0 torr samples of (1) were pyrolysed using the SFR technique between 800-887K, products were identified by comparison of gc retention time with authentic samples and/or gc/mass spectrometry. Table 3.1 (overleaf) gives the observed product composition at 860K, inequalities in the table represent difficulties in resolving gc peaks.

Rate constants were obtained for the formation of ethene, propene and trimethylsilane and are given in Table 3.2.

48

Table 3.1

Product composition at 860K

product	relative amount
methane	~1
ethene	32
propene	13
butadiene	$\leqslant$3
C_4H_8	$\leqslant$1.5
dimethylsilane	3
trimethylsilane	$\leqslant$19
tetramethylsilane	1
dimethylvinylsilane	$\geqslant$6
trimethylvinylsilane	1.5
dimethylallylsilane	5
trimethylallylsilane	10
DSCB	$\leqslant$1.5
DMSP	$\leqslant$1.5

DSCB : 1,1,3,3-tetramethyl-1,3-disilacyclobutane
DMSP : 1,1-dimethyl-1-silacyclopent-3-ene

Table 3.2

Rate constants for product formation /s^{-1}

T/K	ethene	propene	trimethylsilane
914	0.557	0.251	0.326
887	0.213	0.0775	0.128
871	0.12	0.0368	0.07
860	0.078	0.0213	0.0451
850	0.0443	0.011	0.0243
835	0.0368	0.00813	0.0198
835	0.0403	0.00881	0.0219
810	0.0163	0.00311	0.00878
800	0.0112	0.00197	0.00489
778	0.00473	0.00072	0.00197

Figures 3.1, 3.2 and 3.3 give the resulting Arrhenius plots which were analysed by the method of least squares to give the Arrhenius parameters in Table 3.3.

Table 3.3

product	logA	E/kJmol^{-1}
ethene	11.16±.45	201.2±7.3
propene	13.49±.57	248.5±9.1
trimethylsilane	11.86±.43	216.9±7.0

Pyrolysis of (1) with excess methylchloride

Samples of a 10:1 mixture of methylchloride and (1) with an initial pressure of approximately 0.6 torr were pyrolysed using the LPP technique. Rate constants were obtained for the decomposition of (1) and the formation of trimethylchlorosilane, by monitoring the mass peaks at $86(M^+-C_2H_4)$ and $108(M^+)$ respectively, and are given in Table 3.4 along with rate constants obtained by subtracting the rate constants for formation of trimethylchlorosilane from the rate constants for decomposition of (1). Figures 3.4, 3.5 and 3.6 give the resulting Arrhenius plots which were analysed by the method of least squares to give the following Arrhenius parameters.

Table 3.4

Rate constants for decomposition of (1) (k_1/s^{-1}), formation of trimethylchlorosilane (k_2/s^{-1}) and the result of $k_1-k_2=k_3/s^{-1}$.

T/K	k_1/s^{-1}	k_2/s^{-1}	k_3/s^{-1}
866	0.0289	0.016	0.0129
866	0.0288	0.0157	0.0131
852	0.017	0.0084	0.0086
852	0.0168	0.0078	0.009
843	0.0118	0.0056	0.0065
842	0.0113	0.0051	0.0062
836	0.0091	0.00397	0.00513
835	0.00874	0.00355	0.00519
828	0.00645	0.00285	0.0036
827	0.00632	0.00256	0.00376
819	0.00435	0.00164	0.00271
818	0 00451	0.00167	0.00284
806	0.00252	0.000886	0.00163
805	0.00217	0.0006	0.00157
805	0.00243	0.000865	0.00157

$$\log k_1/s^{-1} = (12.81 \pm .17) - (237.9 \pm 2.7 \text{kJmol}^{-1}/2.303RT)$$

$$\log k_2/s^{-1} = (15.48 \pm .44) - (286.3 \pm 7 \text{kJmol}^{-1}/2.303RT)$$

$$\log k_3/s^{-1} = (10.35 \pm .22) - (202.5 \pm 3.4 \text{kJmol}^{-1}/2.303RT)$$

The effect of a tenfold excess of methylchloride on the product composition was investigated using the SFR technique, the results of which are shown in Table 3.5 which gives the approximate relative changes in product yields.

Table 3.5

product	change
methane	x2
C4 hydrocarbons [a]	x4
dimethylvinylsilane	x1/2
trimethylvinylsilane	x1/4
dimethylallylsilane	x1/7
trimethylallylsilane	x1/5

[a] mostly but-1-ene, with a smaller increase in butadiene.

Using the SFR technique, it was not possible to obtain accurate rate constants for the formation of trimethylchlorosilane due to an overlap between the gc peaks from trimethylchlorosilane and trimethylvinylsilane.

Pyrolysis of 5-(dimethylsilyl)pent-1-ene (2)

Approximately 0.45 torr samples of (2) were pyrolysed using

<u>Table 3.6</u>
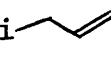
Product composition at 853K.

product	relative amount
methane	~1
ethene	25
propene	32
butadiene	1
C_4H_8	1
dimethylsilane	3
trimethylsilane	1
tetramethylsilane	<1
dimethylvinylsilane	28
trimethylvinylsilane	~1
dimethylallylsilane	7
trimethylallylsilane	~1
DSCB	<1
DMSH	~1

DSCB : 1,1,3,3-tetramethyl-1,3-disilacyclobutane
DMSH : 1,1-dimethyl-1-silacyclohex-3-ene

Table 3.7
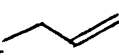
Rate constants for product formation $/s^{-1}$

T/K	C_2H_4	C_3H_6	$HMe_2Si\!-\!\!\diagup\!\!\diagup$	$HMe_2Si\!-\!\!\diagdown\!\!\diagup\!\!\diagup$
855	0.0958	0.127	0.103	0.0278
853	0.0901	0.117	0.0977	0.0254
844	0.0625	0.0788	0.0668	0.0171
844	0.0663	0.0824	0.0698	0.0164
832	0.0399	0.051	0.0459	0.0101
830	0.0372	0.0471	0.0437	0.0105
829	0.0355	0.045	0.0429	0.00999
823	0.0283	0.0345	0.0326	0.00812
819	0.0244	0.0287	0.0277	0.00673
819	0.0241	0.0294	0.0289	0.00639
811	0.018	0.0223	0.0217	0.00466
810	0.0191	0.0221	0.0204	0.00473
809	0.0167	0.0208	0.0195	-
798	0.0114	0.0122	0.0119	0.00296
798	0.00965	0.0125	0.0121	0.00243
788	0.00678	0.00868	0.00831	0.00186
787	0.00622	0.00819	0.00849	0.00164
785	0.00591	0.00751	0.00702	0.00181
778	0.00523	0.00531	0.00508	-
777	0.00432	0.00494	0.00485	-

the SFR technique between 777-855K, and the products identified by comparison of gc retention time with that of authentic samples and/or gc/mass spectrometry. Table 3.6 gives the observed product composition at 853K.

Rate constants were obtained for the formation of ethene, propene, dimethylvinylsilane and dimethylallylsilane, and are given in Table 3.7. Figures 3.7, 3.8, 3.9 and 3.10 give the resulting Arrhenius plots which were analysed by the method of least squares to give the Arrhenius parameters in Table 3.8.

<p align="center">Table 3.8</p>

product	logA	$E/kJmol^{-1}$
C_2H_4	12.3±.18	218.1±2.9
C_3H_6	12.85±.11	225.2±1.7
HMe_2Si⟍⟋	12.1±.13	214.1±2
HMe_2Si⟍⟋⟍⟋	12.04±.26	222.9±4

Pyrolysis of (2) with excess methylchloride

Samples of a 10:1 mixture of methylchloride and (2) with an initial pressure of approximately 0.6 torr, were pyrolysed using the LPP technique between 773-848K. Rate constants for the decomposition of (2) and the formation of dimethylchlorosilane were obtained by monitoring the mass

Table 3.9

Rate constants for the decomposition of (2) (k_4/s^{-1}), formation of dimethylchlorosilane (k_5/s^{-1}) and the result of $k_4-k_5=k_6/s^{-1}$

T/K	$\cdot k_4/s^{-1}$	k_5/s^{-1}	k_6/s^{-1}
848	0.0445	0.00982	0.0347
845	0.0402	0.00748	0.0327
831	0.0237	0.00359	0.0201
831	0.0249	–	0.0213
821	0.0168	0.00303	0.0135
820	0.0165	0.00287	0.0136
813	0.0123	–	–
811	0.0109	–	–
806	0.00972	0.00105	0.00867
806	0.00952	–	0.00847
796	0.00599	0.000688	0.0053
794	0.00596	0.000608	0.00535
787	0.00454	0.000399	0.00414
786	0.00445	–	–
775	0.00258	–	–
773	0.00274	–	–

peaks at $87(M^+-C_3H_5)$ and $79(M^+-Me)$ respectively, and are given in Table 3.9 along with rate constants obtained by subtracting the rate constants for formation of dimethylchlorosilane from those for the decomposition of (2).

Figures 3.11, 3.12 and 3.13 give the resulting Arrhenius plots, which were analysed by the method of least squares to give the following Arrhenius parameters.

$$\log k_4/s^{-1}=(11.47\pm.16)-(208.1\pm2.4kJmol^{-1}/2.303RT)$$
$$\log k_5/s^{-1}=(15.4\pm.4)-(283.1\pm6.2kJmol^{-1}/2.303RT)$$
$$\log k_6/s^{-1}=(10.75\pm.21)-(198\pm3.3kJmol^{-1}/2.303RT)$$

An effect of methylchloride on the product composition as measured from the SFR technique was to cause a fourfold reduction in the formation of allyldimethylsilane, while leaving vinyldimethylsilane relatively unaffected.

DISCUSSION

From the observed range of products it is obvious that the mechanisms of decomposition of (1) and (2) are complex. In each case there is the possibility of a retroene reaction as shown in scheme 3.2.

Scheme 3.2

$$Me_2\overset{\displaystyle |}{\underset{\displaystyle H}{Si}}\diagup\diagdown \longrightarrow Me_2Si{=}CH_2{+}C_3H_6$$

$$HMe_2Si\diagup\diagdown\underset{\displaystyle H}{} \longrightarrow HMe_2Si{-}\diagup\diagup + C_3H_6$$
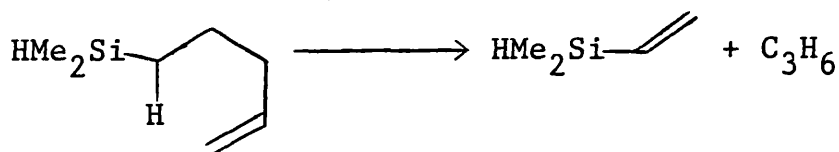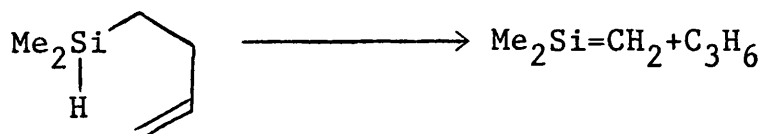
In addition there are a wide range of radical reactions possible, initiated by allylic bond homolysis. Schemes 3.3 and 3.4 give some of the possible radical reactions for (1) and (2) respectively. From the product composition as given in Table 3.3, the following conclusions regarding the mechanism of pyrolysis of (1) can be formed, with a similar set of conclusions applicable to the pyrolysis of (2). DSCB, the product of dimerisation of the dimethylsilene produced in the concurrent retroene reaction was a minor product because the silene would mainly undergo radical addition reactions. Both $HMe_2Si\overset{\displaystyle \cdot}{C}H_2$ and $Me_3Si\cdot$ can give methyl radicals by dissociation, but this process is minor, as indicated by the small amount of methane. Formation of butadiene and dimethylsilacyclopentene suggests that abstraction reactions occur from both the allylic carbon and from silicon; the silicon centred radical so formed

Scheme 3.3

Homolysis

$$HMe_2Si\diagdown\diagup \longrightarrow C_3H_5^\cdot + HMe_2Si\dot{C}H_2 \longrightarrow Me_3Si^\cdot$$

Abstraction

$$HMe_2Si\diagdown\diagup + R^\circ \longrightarrow RH + HMe_2Si^\cdot$$

$$\longrightarrow C_4H_6 + HMe_2Si^\cdot$$

$$RH + Me_2\dot{S}i\diagdown\diagup \longrightarrow Me_2Si \longrightarrow Me_2Si + H'$$

$$HMe_2Si\dot{C}H_2 + Me_3Si\diagdown\diagup$$

Addition

$$HMe_2Si\diagdown\diagup + Me_3Si^\cdot \longrightarrow HMe_2Si \diagup\diagdown \dot{} \diagup SiMe_3$$

$$HMe_2Si \diagdown\diagup\diagdown \underset{SiMe_3}{\dot{}} \longrightarrow Me_3Si\diagup\diagdown + HMe_2Si^\cdot$$

chain sequence

$$HMe_2Si\diagdown\diagdown\diagup + HMe_2Si^\cdot \longrightarrow HMe_2Si\diagdown\diagup SiMe_2H \longrightarrow HMe_2Si\diagdown\diagup\diagdown SiMe_2H$$

chain sequence

$$HMe_2Si\diagdown\diagup\dot{} + HMe_2Si\diagup \xrightarrow{-C_2H_4}$$

$$HMe_2Si\diagdown\diagup + Me^\cdot \longrightarrow C_3H_6 + HMe_2Si\diagdown\diagup \longrightarrow HMe_2Si^\cdot + C_2H_4$$

$$HMe_2Si\diagdown\diagup\diagdown\dot{} \longrightarrow \diagup\diagup + HMe_2Si\dot{C}H_2 \longrightarrow Me_3Si^\cdot$$

$$HMe_2Si\diagup\dot{}\diagdown \longrightarrow HMe_2Si^\cdot + C_2H_4$$

59

Scheme 3.4

Homolysis

Abstraction

Addition

chain sequence

chain sequence

cyclises in the endo-fashion, as found by Barton and Revis.[6] Radical addition reactions were important in the pyrolysis of (1), as expected from the work on allyltrimethylsilane,[1.2], but there are some quite subtle factors at play in determining the distribution of products from these reactions. These depend not only on the balance between terminal and internal addition, but on whether a chain sequence can develop or not. Thus quantitative conclusions regarding the outcome of these radical addition reactions would require further work, such as computer simulation of the reaction mechanism. As a result of the complexity of these pyrolysis mechanisms, the Arrhenius parameters obtained from experiments without excess methylchloride do not relate to elementary reactions, and are only of use in determining the relative product yields.

In the presence of excess methylchloride, silicon centred radicals are selectively trapped thus simplifying the pyrolysis mechanisms with respect to the radical reactions, as shown in schemes 3.5 and 3.6 overleaf. Arrhenius parameters for the allylic bond homolysis in (1) can be obtained by measuring the kinetics of formation of trimethylchlorosilane, assuming that the isomerisation of $HMe_2Si\overset{\bullet}{C}H_2$ to $Me_3Si\cdot$ is fast. Arrhenius parameters for the allylic bond homolysis in (2) can be obtained by measuring the kinetics of formation of dimethylchlorosilane over the initial stages of the reaction, during which there will be a negligible contribution from secondary reactions to the

Scheme 3.5

$$HMe_2Si\diagdown \longrightarrow C_3H_5^{\cdot} + HMe_2Si\overset{\bullet}{C}H_2 \xrightarrow{\text{MeCl}} Me_3Si^{\cdot} \longrightarrow Me_3SiCl + Me^{\cdot}$$

$$HMe_2Si\diagdown + R^{\cdot} \longrightarrow RH + Me_2\overset{\bullet}{Si}\diagdown \longrightarrow Me_2Si \longrightarrow Me_2Si + H^{\cdot}$$

$$RH + HMe_2Si^{\cdot} \xrightarrow{\text{MeCl}} HMe_2SiCl + Me^{\cdot}$$

$$RH + HMe_2Si\diagdown \longrightarrow C_4H_6 + HMe_2Si^{\cdot}$$

$$HMe_2Si\diagdown + Me^{\cdot} \longrightarrow HMe_2Si\diagdown \longrightarrow C_3H_6 + HMe_2Si^{\cdot}$$

$$HMe_2Si\diagdown \quad \downarrow {-C_2H_4}$$

$$HMe_2Si^{\cdot} \xrightarrow{\text{MeCl}} HMe_2SiCl + Me^{\cdot}$$

Scheme 3.6
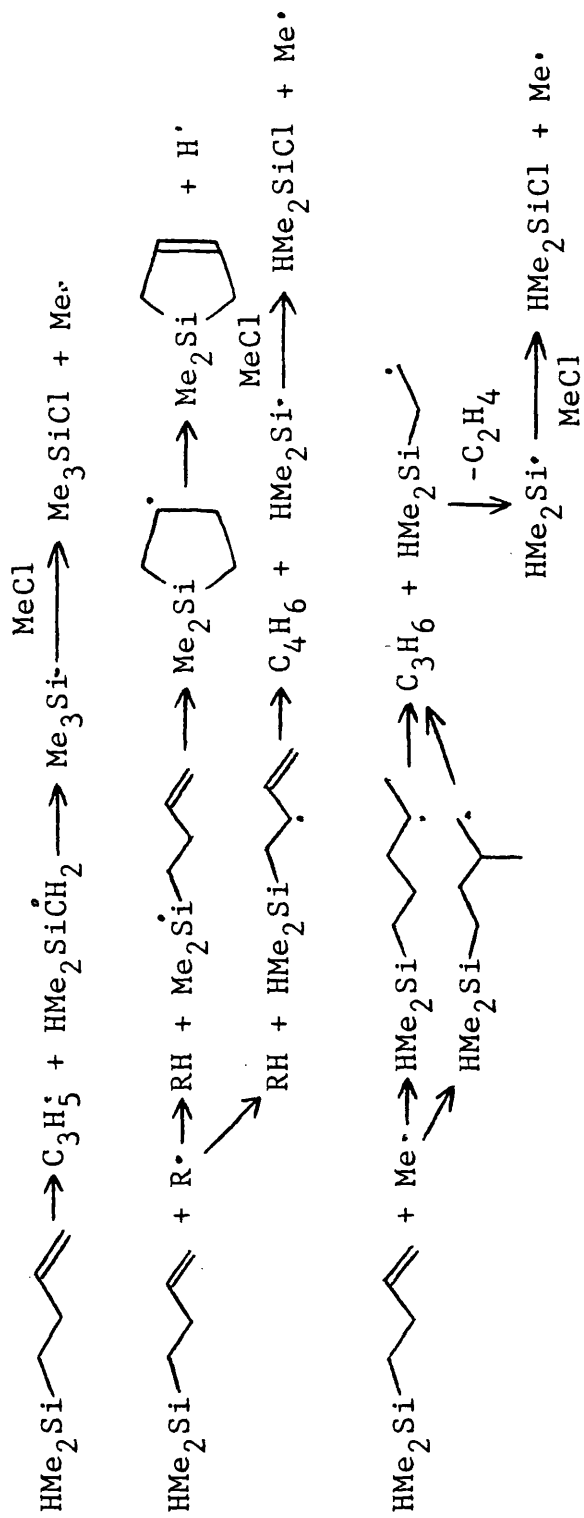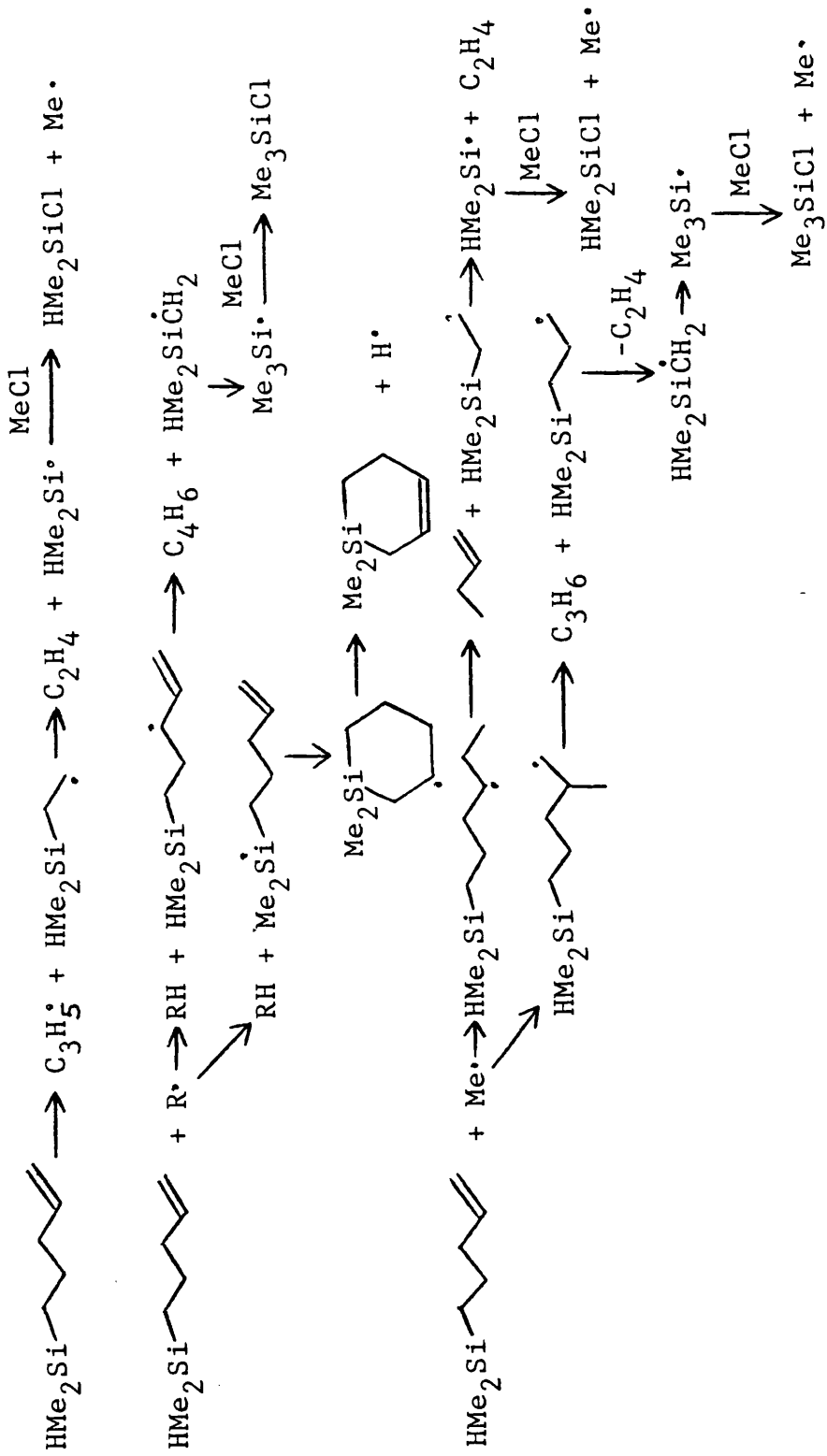
formation of dimethylchlorosilane, assuming that loss of ethene from HMe_2Si—— is fast. Table 3.10 summarises the measured Arrhenius parameters for these processes.

Table 3.10

	logA	$E/kJmol^{-1}$
allylic bond homolysis in (1)	15.48±.44	286.3±7
allylic bond homolysis in (2)	15.4±.4	283.1±6.2

These Arrhenius parameters are reasonable for the homolysis of a carbon-allyl bond. The A-factor for such a process is expected to be $<10^{16}s^{-1}$ because of stiffening in the transition state.[7] As the allylic stabilisation energy is ca. 14kcal/mol, the activation energies obtained for homolysis in (1) and (2) correspond to 'normal' alkyl-alkyl bond dissociation energies of 344.9±7 and 341.7±6.2kJ/mol respectively. However, due to uncertainties in the experimental measurements, the allylic stabilisation energy, and alkyl-alkyl bond dissociation energies,[8] it is not possible to draw any conclusions regarding the stabilisation effect of alpha-silyl or beta-silyl substituents on alkyl radicals, apart from the observation that if any such stabilisation exists then it is a small effect. More accurate measurements of the alpha-silyl and beta-silyl stabilisation effects have been obtained from a kinetic study of the pyrolysis of 2,2-

dimethyl-3-trimethylsilylpropane and 2,2-dimethyl-4-trimethylsilylbutane with 2,2-dimethylbutane as a reference compound. For these compounds, homolysis of the t-butyl-carbon bond is the only primary reaction, thus allowing better quality kinetic data to be obtained which suggest that alpha-silyl and beta-silyl substituents each stabilise alkyl radicals by 2.6±1kcal/mol.[9]

Several other workers have published results relevant to the alpha and beta-silyl stabilisation effects. Ingold et al [10] observed a stabilisation effect with both alpha and beta-silyl substituted radicals from the results of hydrogen abstraction reactions by Bu^tO radicals. From esr studies, Krusic and Kochi [11] concluded that both alpha and beta-silyl substituted radicals were more stable than their alkyl counterparts, although their explanation of the alpha-silyl stabilisation effect in terms of p_π -d_π electron delocalisation has been challenged.[12] Lilt et al [13] found that alpha-halosilanes were more reactive than haloalkanes in free radical reduction by organotin hydrides; their preferred explanation was stabilisation of the transition state for halogen abstraction by a polar effect, although alpha-silyl radical stabilisation could have been a contributory factor. Walsh et al have measured the alpha and beta-silyl stabilisation effects to be ca. 0.4 and 3kcal/mol respectively.[14,15] Clearly, both the alpha and beta-silyl stabilisation effects are small and elusive, the agreement over the beta-silyl stabilisation is pleasing, but

there is still some uncertainty over the extent of the alpha-silyl stabilisation effect.

For each compound there are retroene reactions that are alternative primary decomposition pathways to the carbon-allyl bond homolysis. Arrhenius parameters can be obtained for these retroene pathways by subtraction of the rate constants obtained for the carbon-allyl bond homolysis from the rate constants for the total decomposition. However, kinetic experiments on 4-(trimethylsilyl)but-1-ene with excess methylchloride, for which there is no reasonable retroene reaction, show that secondary radical reactions were not completely suppresssed by methylchloride.[9] Therefore the Arrhenius parameters so obtained will be underestimates of the true Arrhenius parameters for the retroene reactions.

Investigation of $HMe_2Si\dot{C}H_2 \longrightarrow Me_3Si\cdot$ by computer simulation

The mechanism of pyrolysis of (1) is interesting in that it involves the isomerisation of $HMe_2Si\dot{C}H_2$ to $Me_3Si\cdot$ via a hydrogen shift. Only two examples of this type of rearrangement have previously been reported, both involving silicon as the migrating group.[16,17] For the isomerisation reaction $HMe_2Si\dot{C}H_2 \longrightarrow Me_3Si\cdot$ ΔH is simply D(Si-H)-D(C-H)=90.3-99.2=-8.9kcal/mol.[18,14] The analogous 1,2-H shift in $CH_3\dot{C}H_2$ has been calculated to have an activation energy of 46kcal/mol.[19] To the extent that

this is an appropriate analogy, the activation energy for the isomerisation of $HMe_2Si\overset{\bullet}{C}H_2$ to $Me_3Si\cdot$ would be less than 46kcal/mol by up to 9kcal/mol. It was therefore decided to investigate the isomerisation of $HMe_2Si\overset{\bullet}{C}H_2$ to $Me_3Si\cdot$ by computer simulation.

The experimental data that was simulated was the ratio (R) of Me_3SiCl formed to (1) decomposed in pyrolyses of (1) with excess methylchloride. The Arrhenius parameters obtained for the formation of Me_3SiCl and the decomposition of (1) give values of (R) ranging from R=0.34 at 805K to R=0.56 at 866K. Scheme 3.7 overleaf gives the reaction mechanism used for the computer simulation. Table 3.11 gives the Arrhenius parameters for the individual reactions in Scheme 3.7, along with the relative rates of each reaction at 866K calculated after a reaction time of 3s with an initial reactant concentration of $2 \times 10^{-7} mol/dm^3$ and a tenfold excess of methylchloride.

In principle, Me_3SiCl is not a unique measure of reaction 4 and hence of $Me_3Si\cdot$ radicals, because Me_3SiCl is also known to be formed by the radical induced rearrangement of HMe_2SiCH_2Cl,[20] therefore reactions 12 to 17 were included to ensure that this rearrangement did not invalidate the conclusions concerning the isomerisation of $HMe_2Si\overset{\bullet}{C}H_2$ to $Me_3Si\cdot$. As can be seen from the relative rates given in Table 3.11, these reactions proved to be negligible as ca. 99% of the Me_3SiCl came from reaction 4.

Scheme 3.7

$$\text{ClMe}_2\text{Si}\overset{\bullet}{\text{C}}\text{H}_2 \xrightarrow[\text{MeCl}]{17} \text{Me}_3\text{SiCl}$$

$$\text{Me}_3\text{SiCl} + \text{HMe}_2\text{Si}\overset{\bullet}{\text{C}}\text{H}_2$$

$$\text{Me}_3\text{SiCl} + \text{Me}_2\overset{\bullet}{\text{Si}}\text{CH}_2\text{Cl} \xrightarrow{16}$$

$$\overset{13}{\diagup}\ \text{Me}_3\text{Si}\bullet$$

$$\text{HMe}_2\text{Si}\overset{\bullet}{\text{C}}\text{H}_2$$

$$\overset{\text{O}}{\text{HMe}_2\text{SiCH}_2\text{Cl}} \xrightarrow{14} \text{Me}_3\text{SiCl}$$

$$\text{Me}_3\text{SiH} + \text{Me}_2\overset{\bullet}{\text{Si}}\text{CH}_2\text{Cl} \xleftarrow{15}$$

$$\text{HMe}_2\text{Si}\overset{\bullet}{\text{C}}\text{H}_2$$

$$\xleftarrow{12}\ \text{HMe}_2\text{Si}\overset{\bullet}{\text{C}}\text{H}_2 + \text{Cl}\bullet$$

$$\overset{8}{}\quad \text{MeCl}$$

$$\text{Me}_3\text{SiH} \overset{7}{}$$

$$\xrightarrow{1}\ \text{HMe}_2\text{Si}\overset{\bullet}{\text{C}}\text{H}_2 \underset{3}{\overset{2}{\rightleftharpoons}} \text{Me}_3\text{Si}\bullet$$

$$\text{MeCl}$$

$$\overset{4}{\diagup}\ \text{Me}_3\text{SiCl}$$

$$\overset{9}{\diagup}\ \text{Me}_3\text{SiH}$$

$$\xleftarrow{6}\ \text{HMe}_2\text{Si}$$

$$\text{Me}_3\text{SiH} + \text{Me}_2\overset{\bullet}{\text{Si}} \overset{5}{}$$

$$\text{HMe}_2\text{Si} \xrightarrow{11} \text{other products}$$

$$\xrightarrow[\text{MeCl}]{10}\ \text{ClMe}_2\text{Si}$$
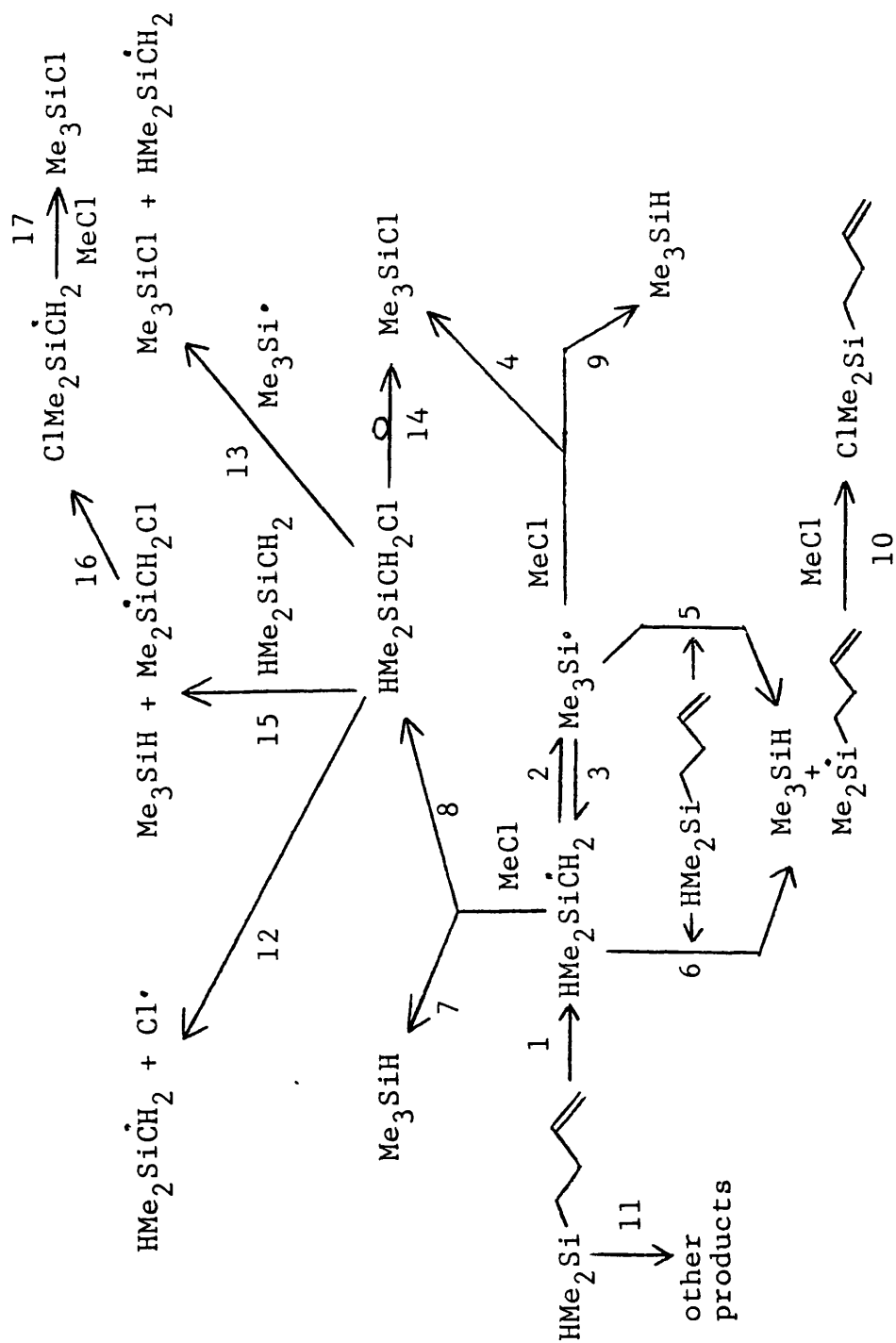
Table 3.11

reaction	logA	E/kcalmol^{-1}	comment	relative rate[a]
1	15.5	68.4	this work	1.046
2	13.5	varied	this work	3.014
3	13.5	E(2)+8.9	see text	1.973
4	7.6	4.1	see ref.22	1.0
5	9.5	14.3	see ref.16	0.019
6	8.1	7.2	see ref.23	0.0004
7	8.5	9.6	see ref.7	0.0028
8	8.0	9.1	see ref.24	0.0012
9	9.5	17.9	see ref.16	0.026
10	7.6	4.1	see ref.22	0.02
11	10.35	48.4	this work	0.826
12	15.0	81	see ref.7	4×10^{-9}
13	7.6	4.1	see ref.22	1.7×10^{-1}
14	12.5	49.5	see ref.25	0.0012
15	8.1	7.2	see ref.23	8×10^{-9}
16	-	-	fast	-
17	8.5	9.6	see ref.7	8×10^{-9}

[a] see text, E(2)=40

Figures 3.14 and 3.15 show the dependence of (R) on E(2) at 866 and 806K respectively, from which it can be seen that the best agreement between the experimental and calculated results is obtained with E(2)<44kcal/mol. The calculated value of (R) was found to be insensitive to any further decrease in E(2) below 40kcal/mol. Therefore from these results alone it is impossible to be any more specific about the value of E(2), however, these results are in agreement with theoretical calculations concerning this isomerisation which give a value for E(2) of 42.6kcal/mol, and $\Delta H = ^-10.8$kcal/mol.[21]

Figure 3.1 : Arrhenius plot for formation of ethene from (1).
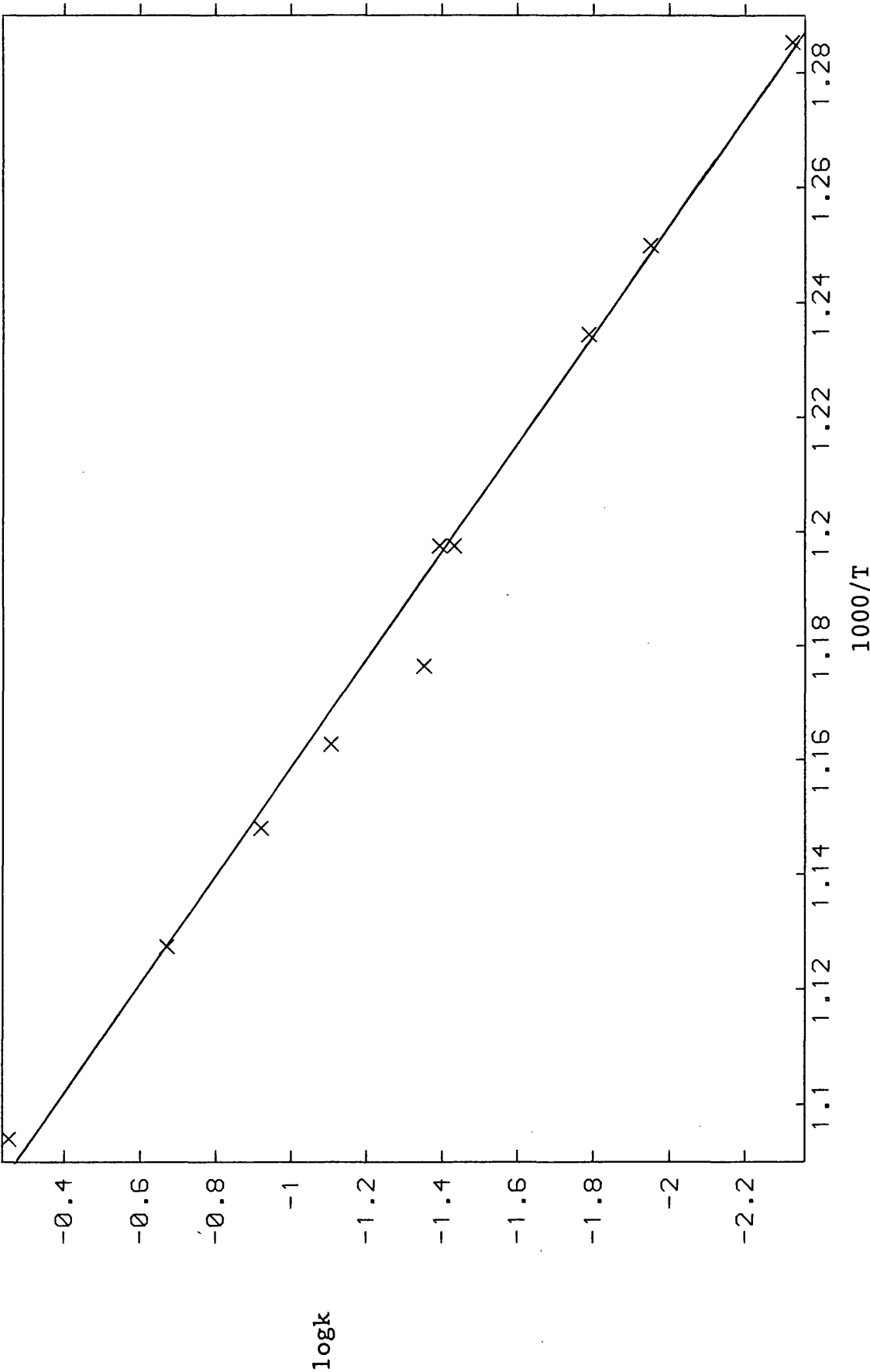
Figure 3.2 : Arrhenius plot for formation of propene from (1).
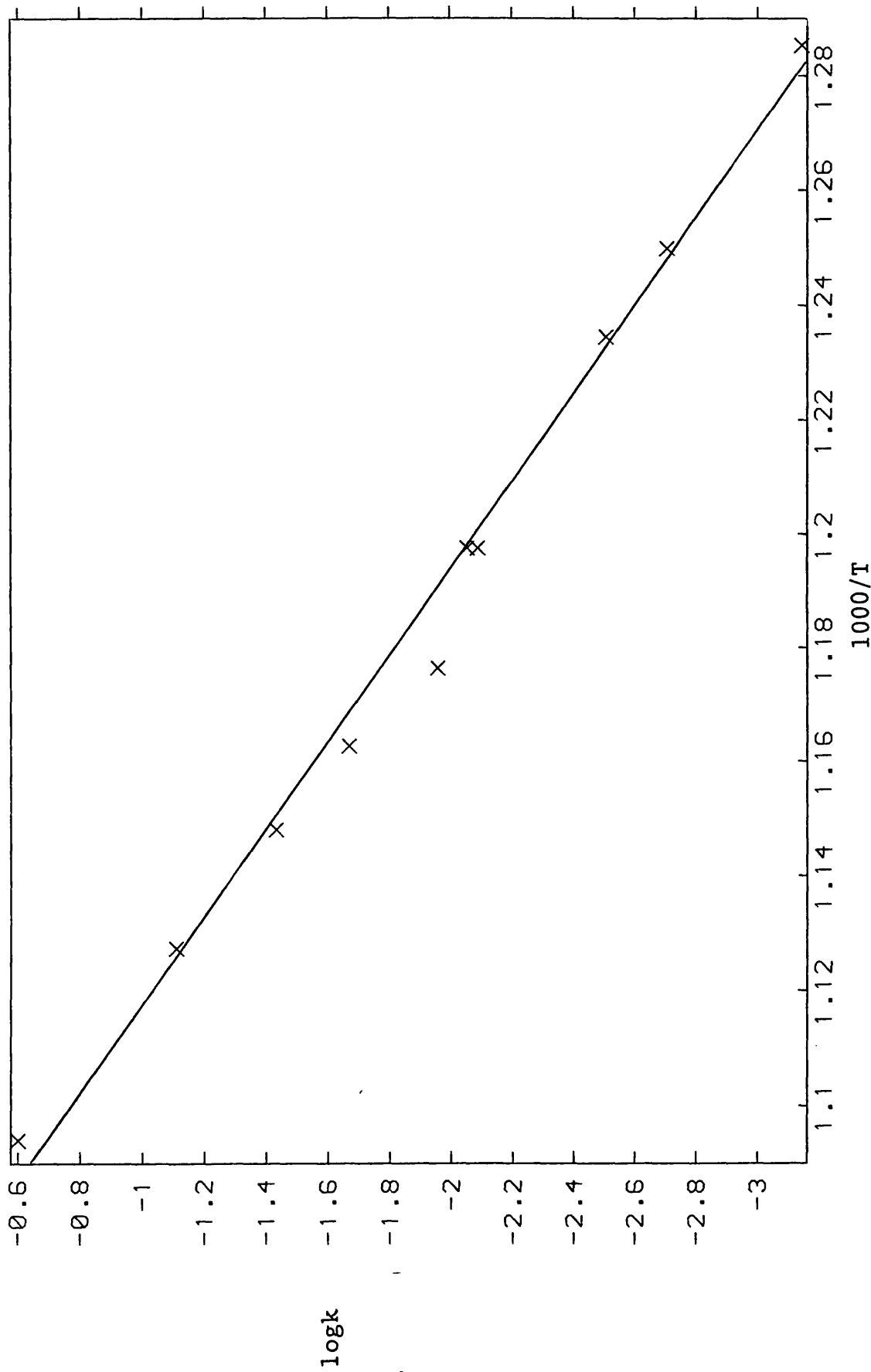
Figure 3.3 : Arrhenius plot for formation of trimethylsilane from (1).

73
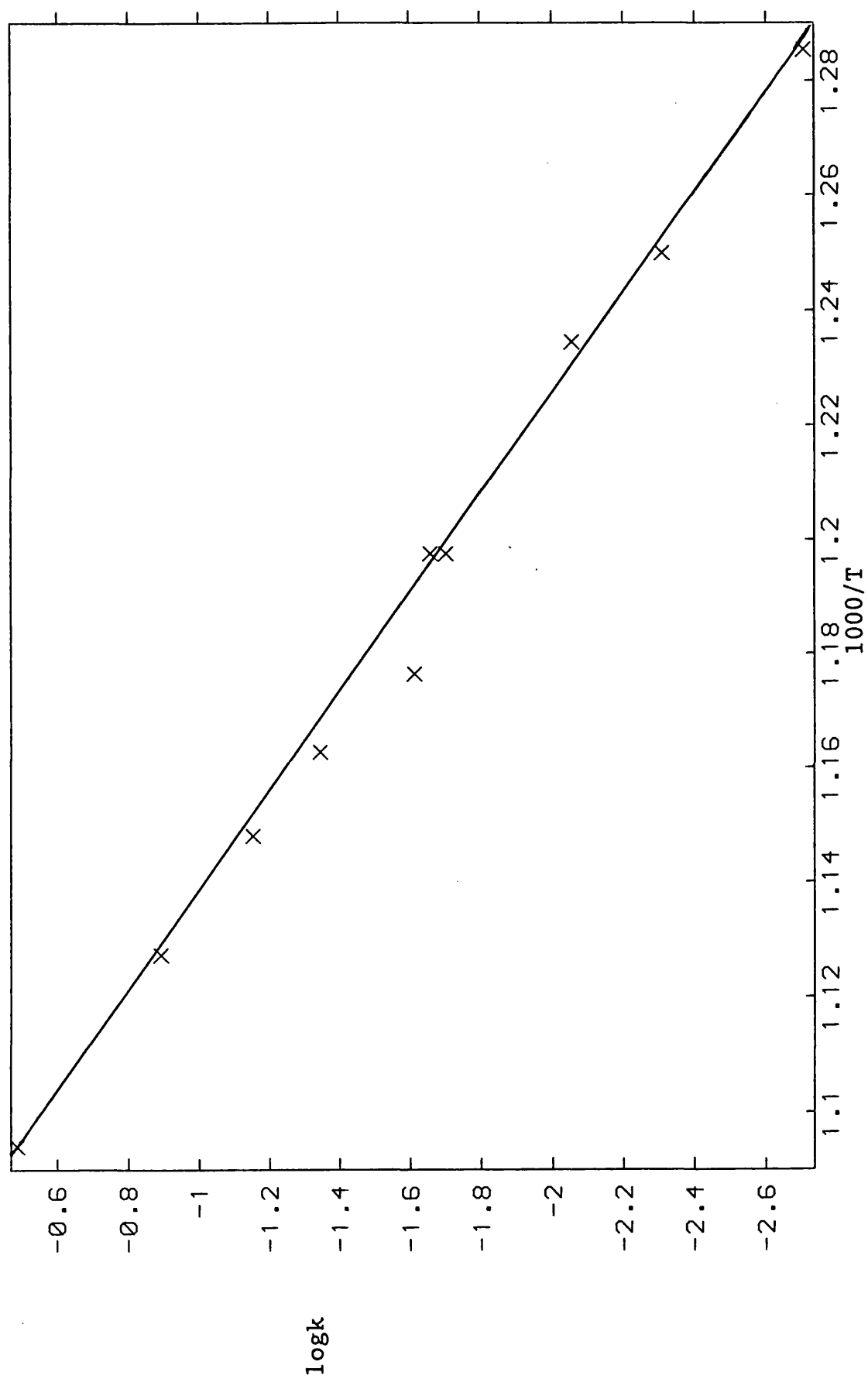
Figure 3.4 : Arrhenius plot for decay of (1) in excess MeCl.
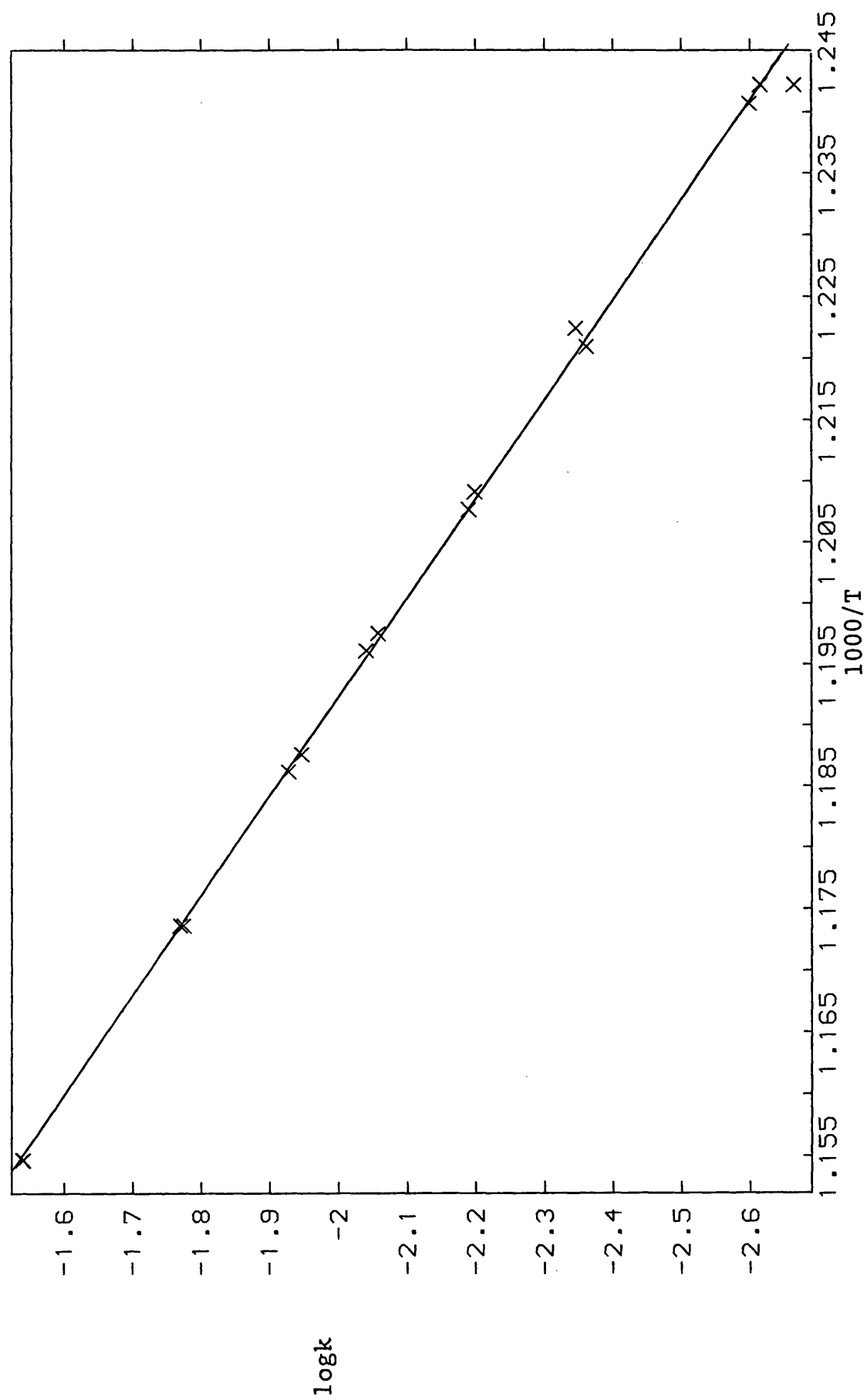
Figure 3.5 : Arrhenius plot for trimethylchlorosilane formation from (1) + excess MeCl.

logk
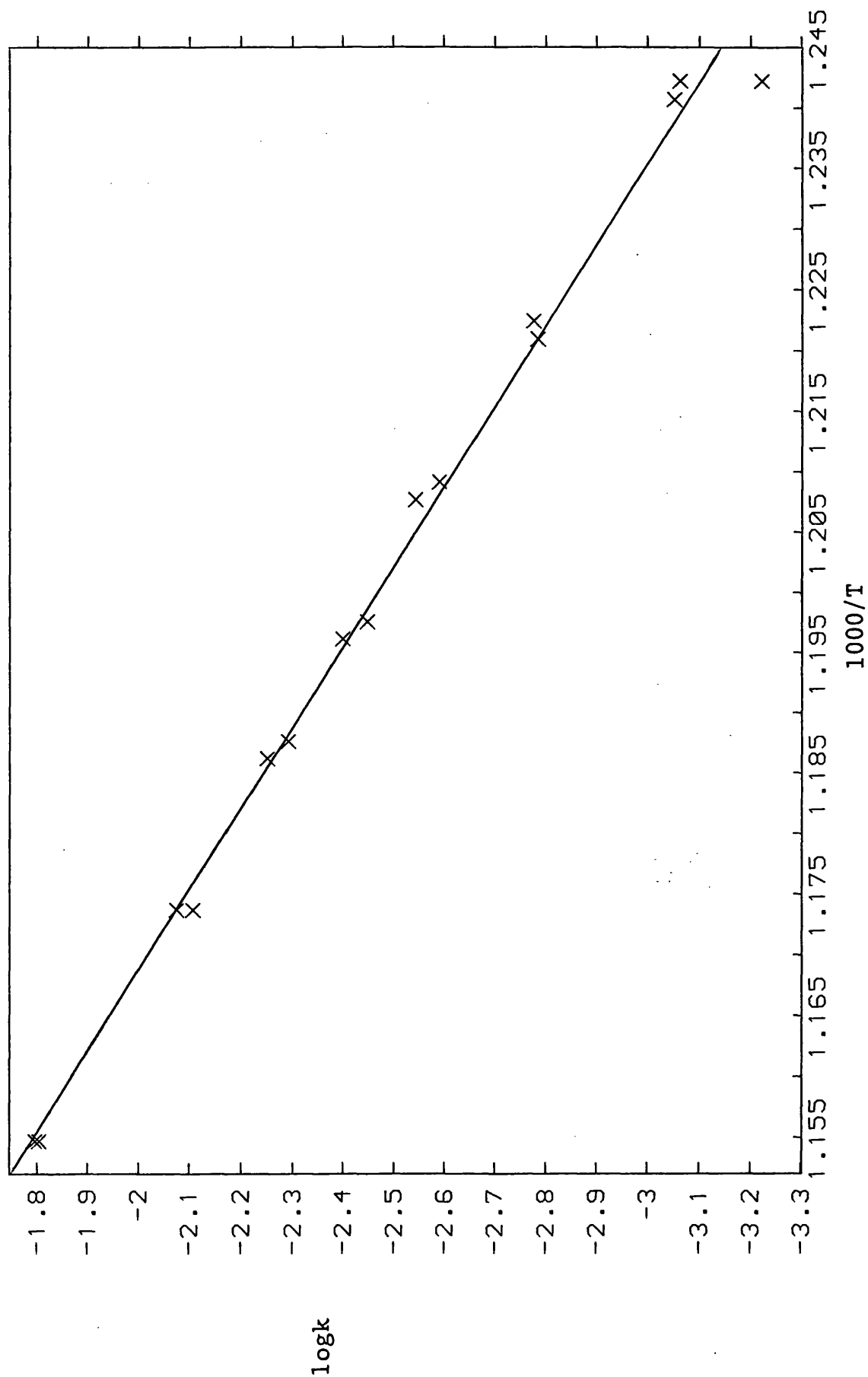
1000/T

Figure 3.6 : Plot of log $k_3(=k_1-k_2)$vs.1000/T.
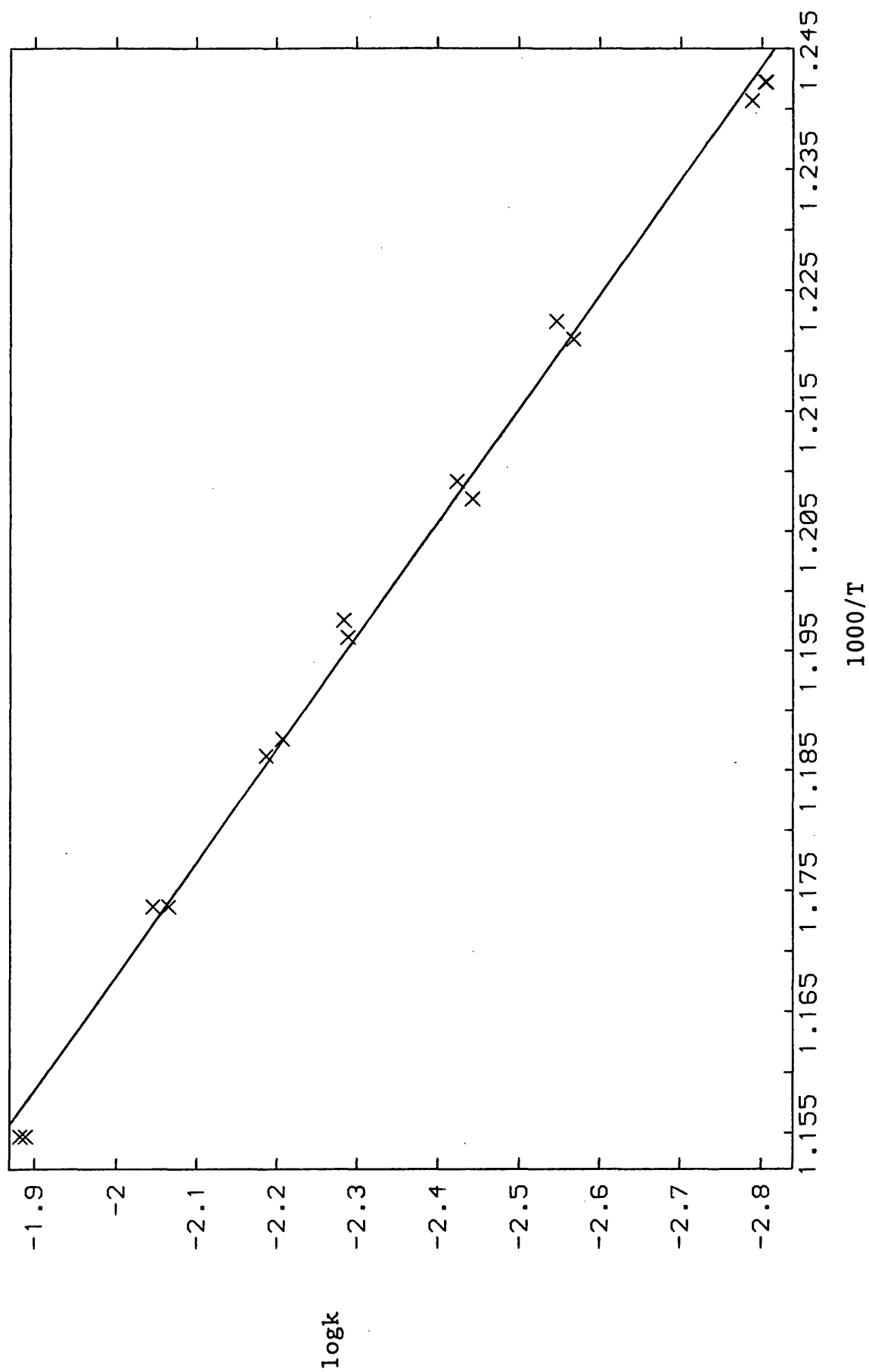
Figure 3.7 : Arrhenius plot for formation of ethene from (2).
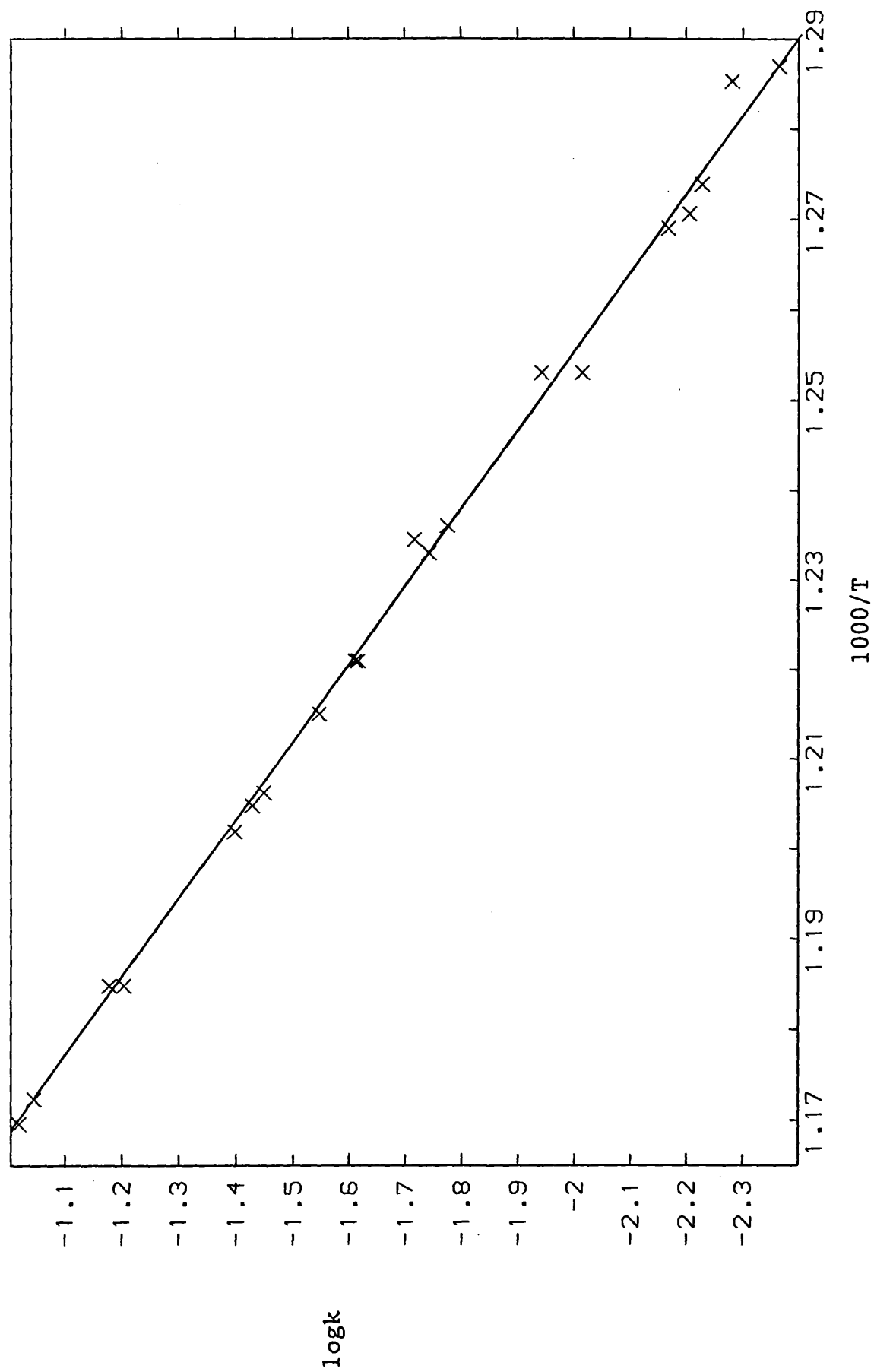
Figure 3.8 : Arrhenius plot for formation of propene from
(2).

logk
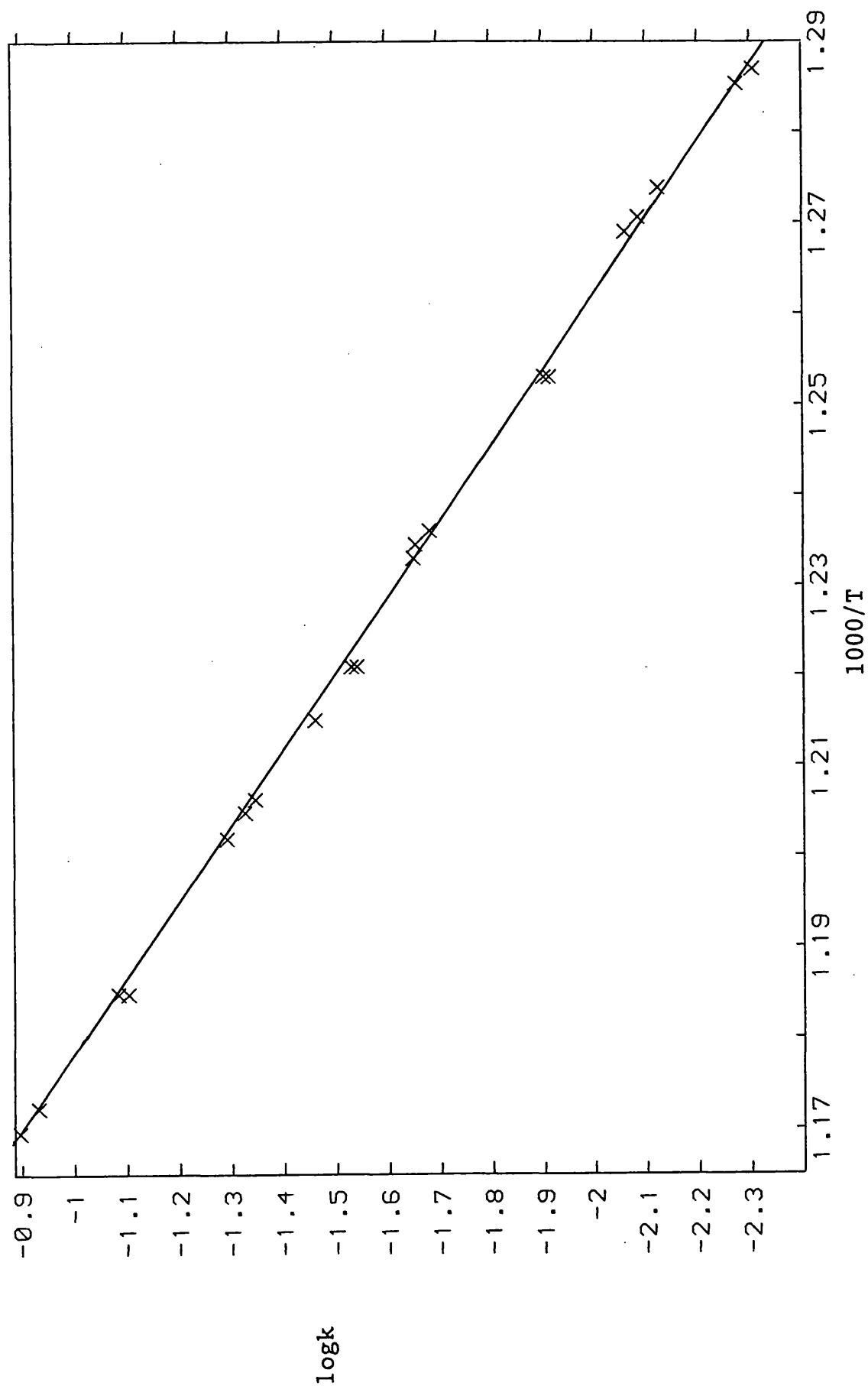
Figure 3.9 : Arrhenius plot for formation of
dimethylvinylsilane from (2).
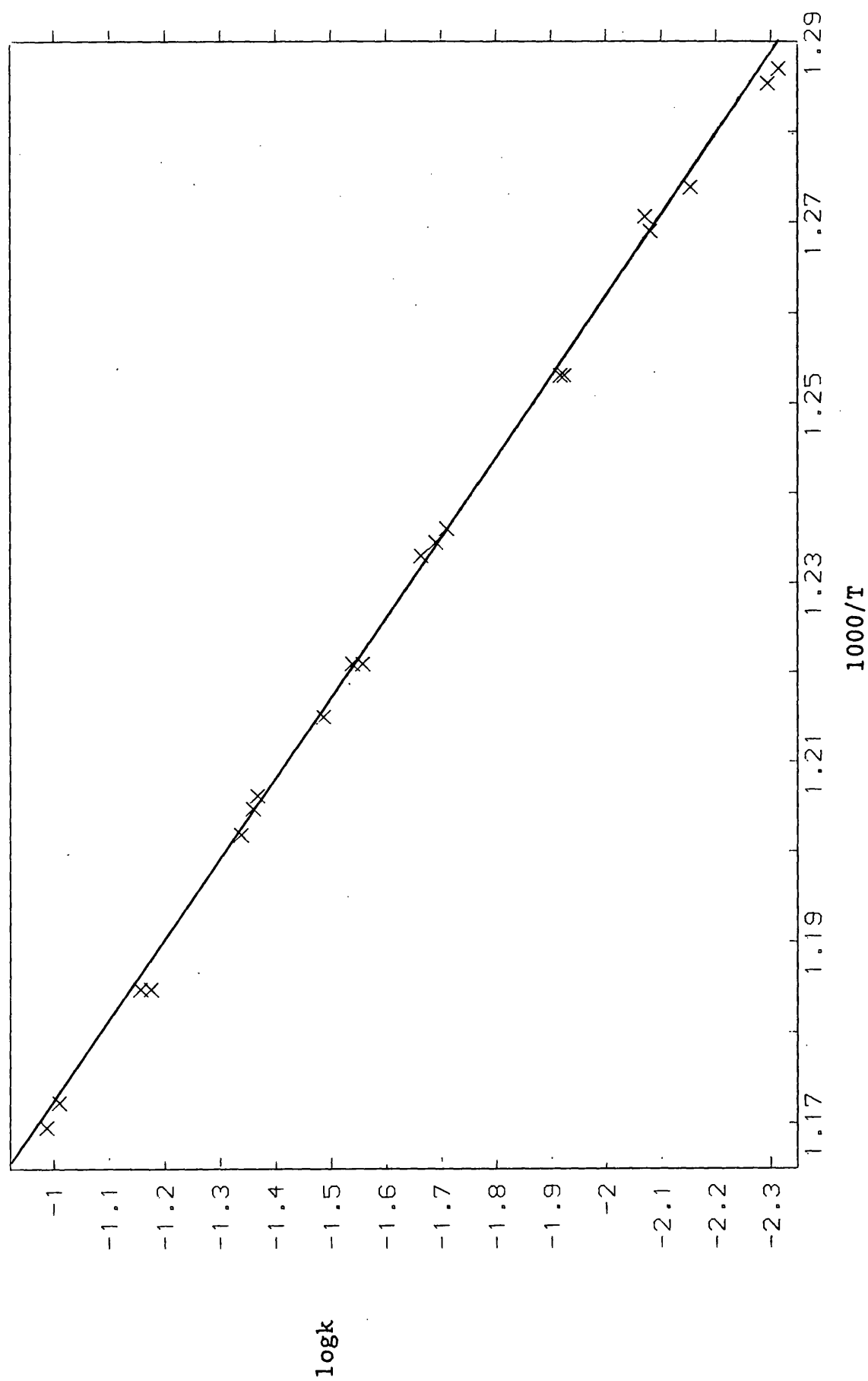
Figure 3.10 : Arrhenius plot for formation of
allyldimethylsilane from (2).
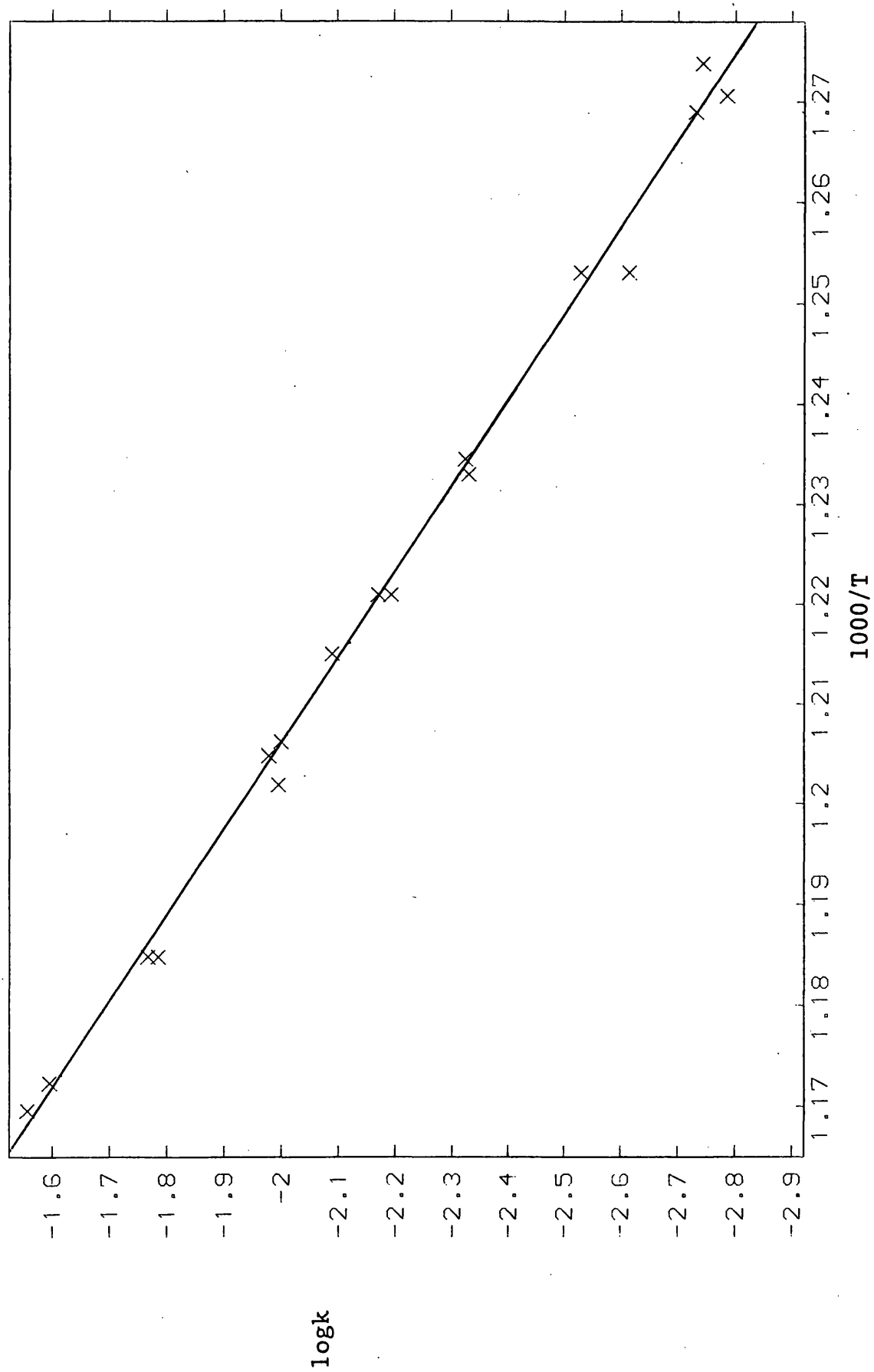
Figure 3.11 : Arrhenius plot for decay of (2) in excess
MeCl.
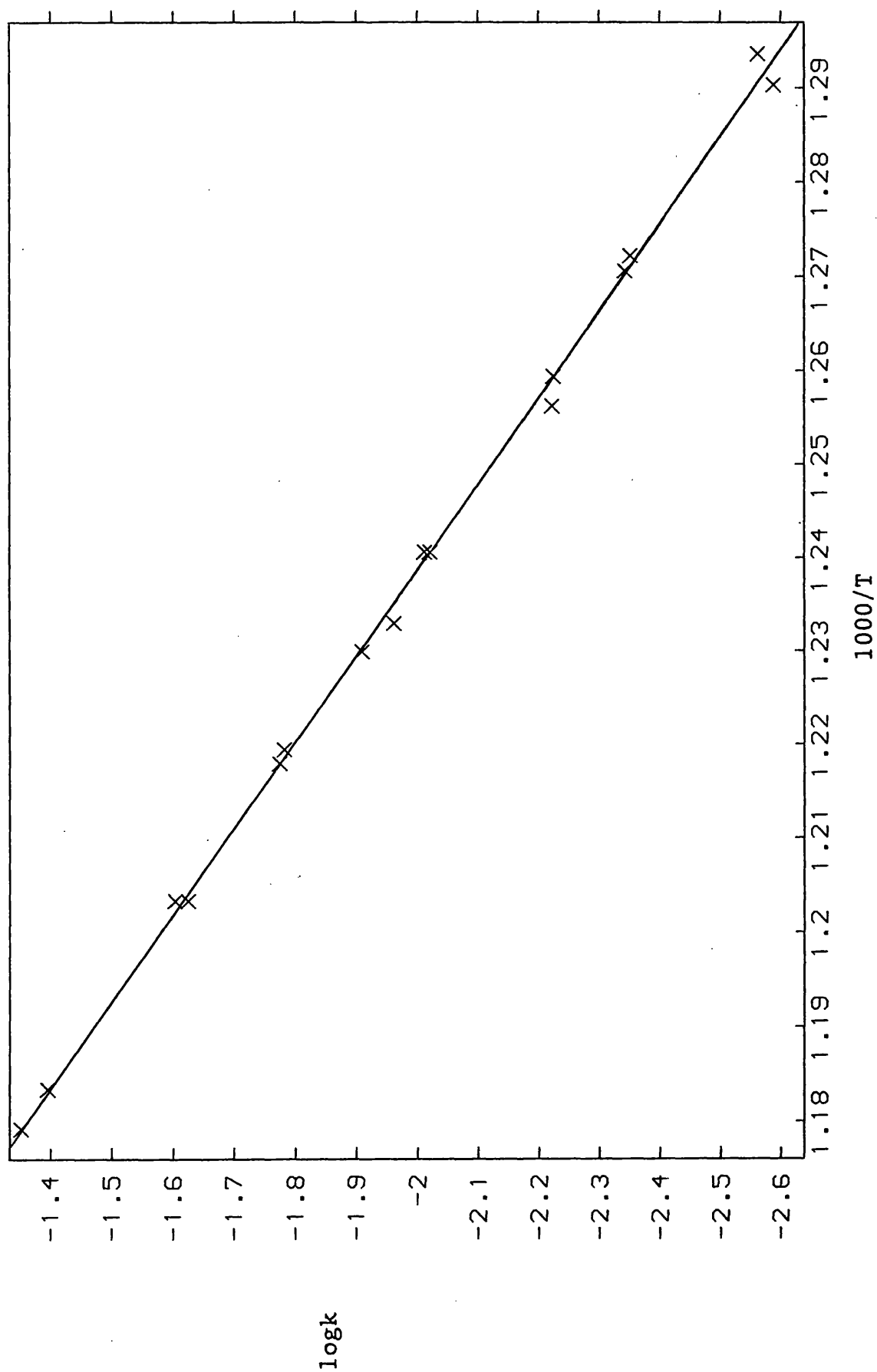
Figure 3.12 : Arrhenius plot for formation of
dimethylchlorosilane from (2) + excess MeCl.
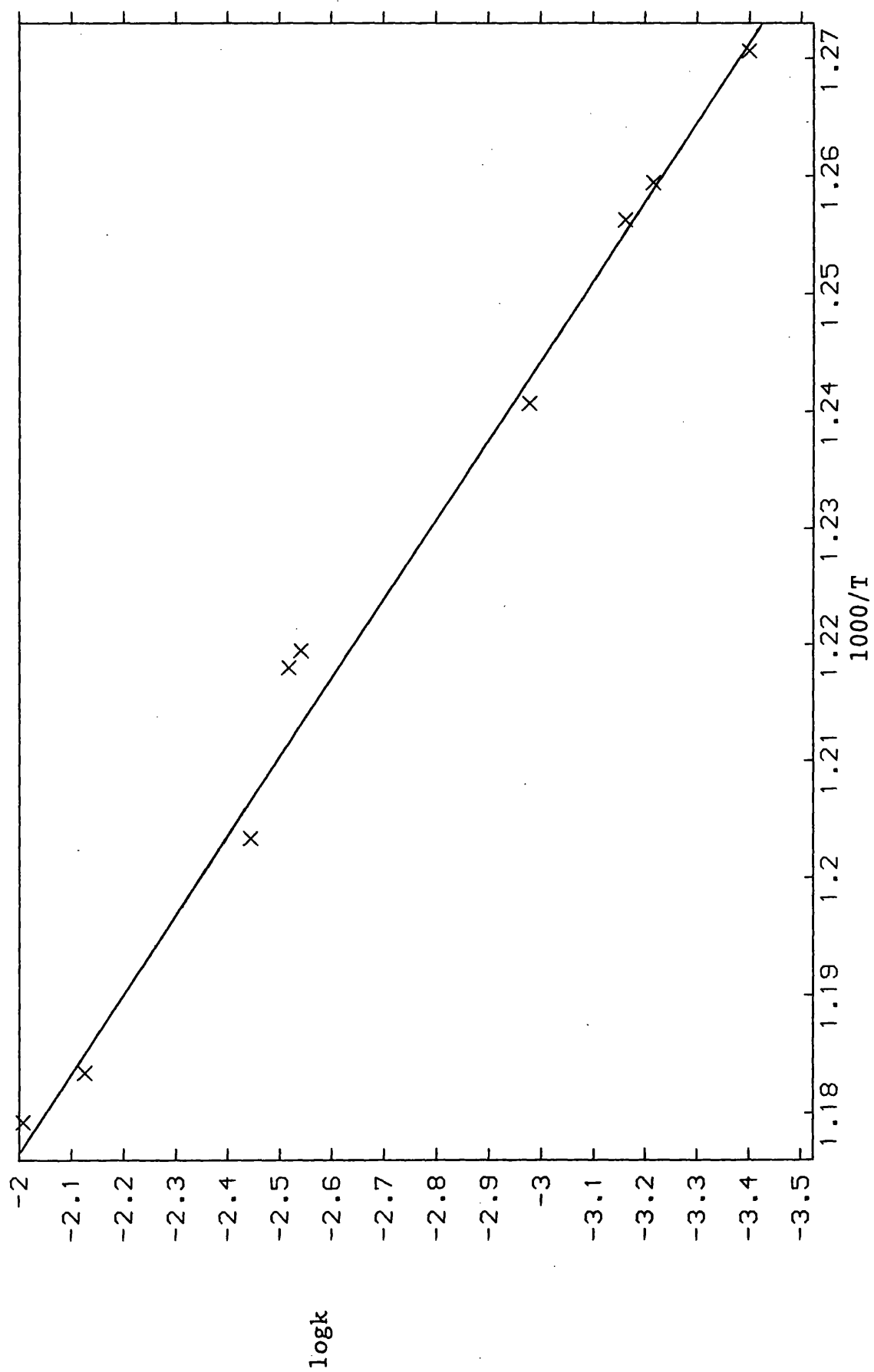
Figure 3.13 : Plot of $\log k_6 (=k_4 - k_5)$ vs. 1000/T.

83
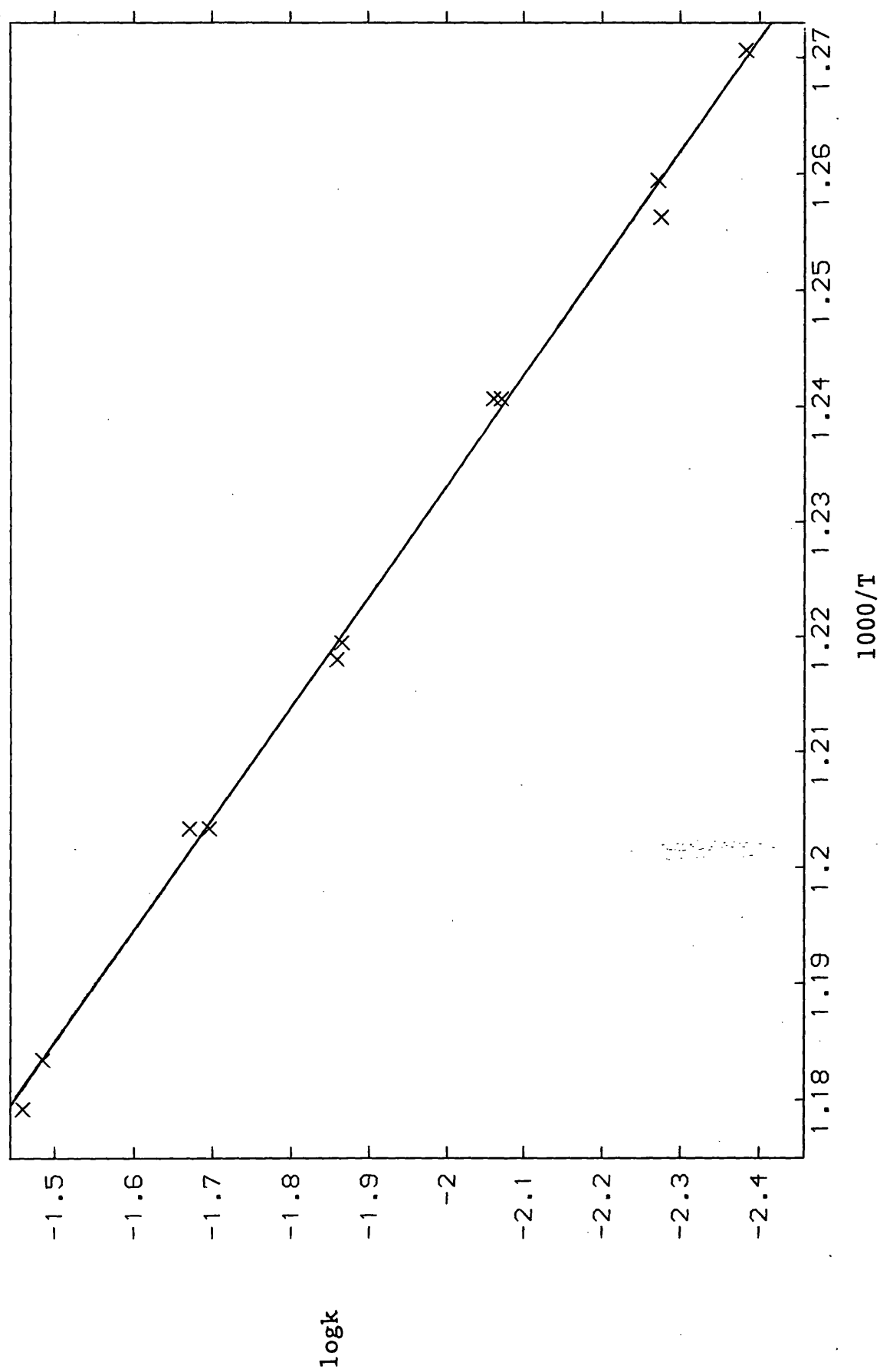
Figure 3.14 : Plot of (R) at 866K vs. E(2).
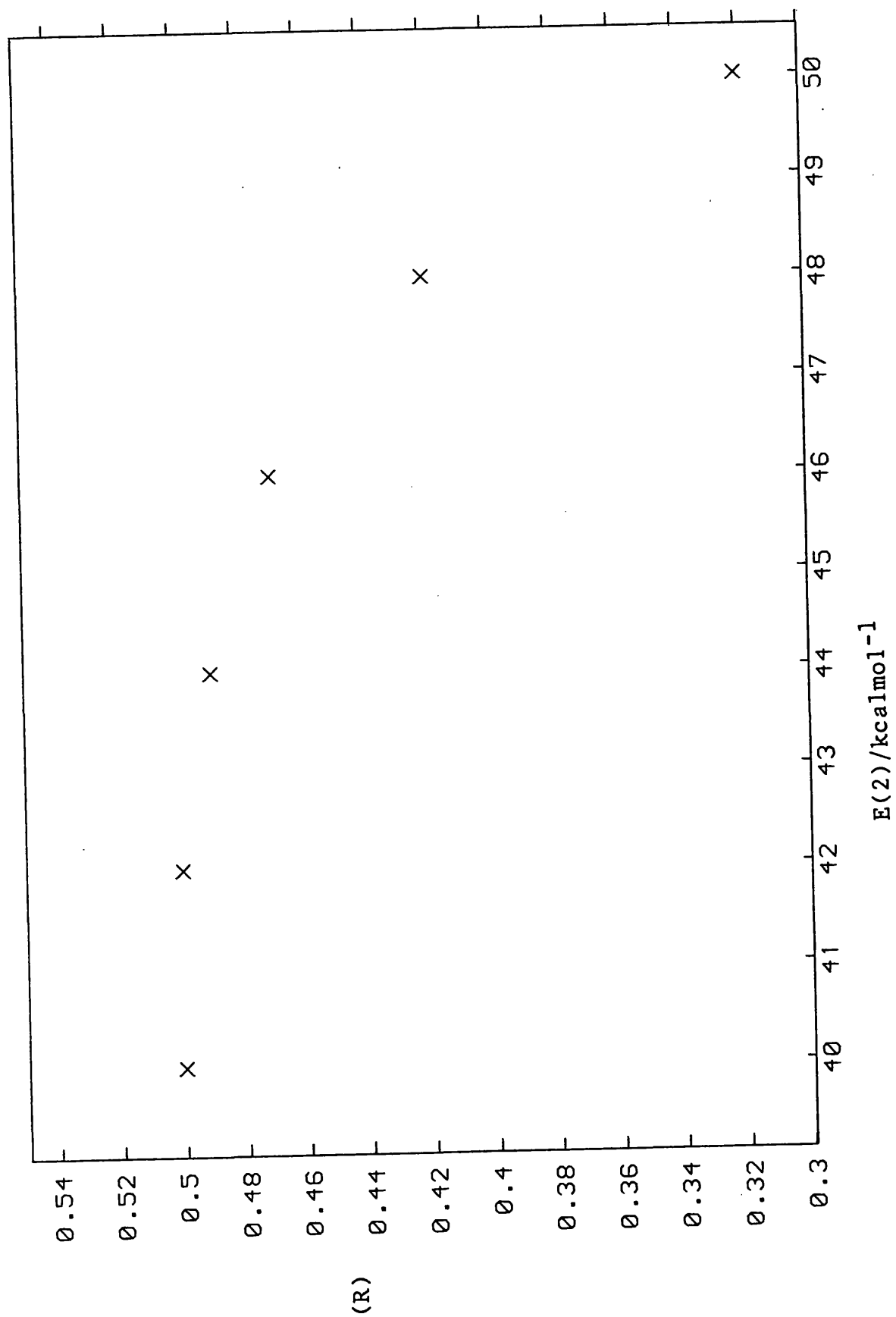
Figure 3.15 : Plot of (R) at 806K vs. E(2).
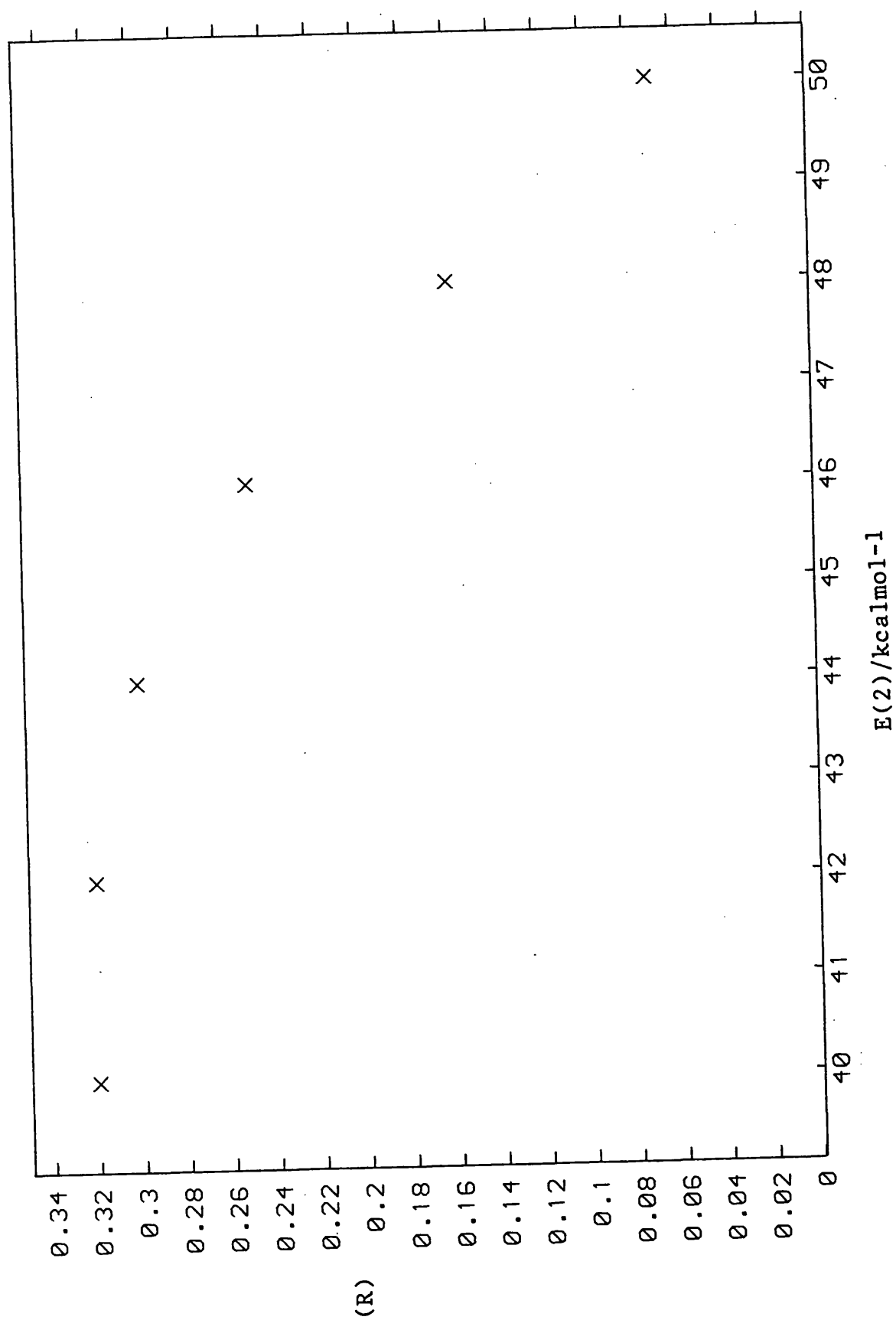
References

1. I. M. T. Davidson and I. T. Wood, J. Organomet. Chem., 1980, 187, 665.

2. T. J. Barton, S. A. Burns, S. Ijadi-Maghsoodi and I. T. Wood, J. Amer. Chem. Soc., 1984, 106, 6397.

3. See chapter one.

4. H. Sakurai, A. Hosomi and M. Kumada, J. C. S. Chem. Comm., 1970, 767.

5. S. M. Neider, G. R. Chambers and M. Jones Jr., Tetrahedron Lett., 1979, 40, 3793.

6. T. J. Barton and A. Revis, J. Amer. Chem. Soc., 1984, 106, 3802.

7. S. W. Benson, "Thermochemical Kinetics", 2nd Ed., Wiley (1976).

8. W. Tsang, J. Amer. Chem. Soc., 1985, 107, 2872.

9. I. M. T. Davidson, T. J. Barton, K. J. Hughes, S. Ijadi-Maghsoodi, A. Revis and G. C. Paul, Organometallics, in press.

10. R. A. Jackson, K. V. Ingold, D. Griller and A. S. Nazran, J. Amer. Chem. Soc., 1985, 107, 208.

11. P. J. Krusic and J. Kochi, J. Amer. Chem. Soc., 1969, 91, 6161.

12. A. R. Lyons, G. W. Neilson and M. C. R. Symons, J. C. S. Faraday Trans. II. 1972, 68, 807.

13. J. W. Lilt, F. G. Belmonte and P. A. Zieske, J. Amer. Chem. Soc., 1983, 105, 5665.

14. A. M. Doncaster and R. Walsh, J. C. S. Faraday Trans. I, 1976, 72, 2908.

15. N. Auner, R. Walsh and J. Westrup, J. C. S. Chem. Comm., 1986, 207.

16. I. M. T. Davidson, P. Potzinger and B. Reimann, Ber. Bunsenges Phys. Chem., 1982, 86, 13, and references therein.

17. I. M. T. Davidson, G. Fritz, F. T. Lawrence and E. Matern, Organometallics, 1982, 1, 1453.

18. R. Walsh, Accts. Chem. Res., 1981, 14, 246.

19. L. B. Harding, J. Amer. Chem. Soc., 1981, 103, 7469.

20. I. N. Jung and W. P. Weber, J. Org. Chem., 1976, 41, 946.

21. T. J. Barton, A. Revis, I. M. T. Davidson, S. Ijadi-Maghsoodi, K. J. Hughes and M. S. Gordon, J. Amer. Chem. Soc., 1986, 108, 4022.

22. P. Cadman, G. M. Tilsley and A. F. Trotman-Dickenson, J. C. S. Faraday Trans. I, 1973, 69, 914.

    I. M. T. Davidson and J. I. Matthews, J. C. S. Faraday Trans. I, 1981, 77, 2277.

23. N. Arthur and T. N. Bell, Rev. Chem. Intermed., 1978, 2, 37.

24. J. Currie, H. W. Sidebottom and J. M. Tedder, Int. J. Chem. Kinet., 1974, 6, 481.

25. I. M. T. Davidson and S. Ijadi-Maghsoodi, Organometallics, 1985. 5, 2086.

CHAPTER FOUR

ION-MOLECULE REACTIONS OF DIMETHYLSILENE AND

DIMETHYLSILYLENE

GAS PHASE ION CHEMISTRY OF DIMETHYLSILENE

Introduction

Since the initial discovery of dimethylsilene as a reactive intermediate in the pyrolysis of dimethylsilacyclobutane [1], there has been interest in the structure and reactivity of silenes from both theoretical and experimental viewpoints, most recently summarised by Raabe and Michl [2]. However, nothing has previously been published involving ion-molecule reactions of silenes, therefore, it was decided to undertake an investigation of the reactions of dimethylsilene with anionic reagents in the gas phase.

The Flowing Afterglow Technique

The experiments were performed in a flowing afterglow system at 298K as previously described [3] with one modification. A port 90cm from the sampling orifice was added, to allow the introduction of neutral species through a 9.5mm i.d. quartz tube wrapped with 8 turns of 26 gauge nichrome wire. A variable transformer controls the voltage across the wire and the approximate temperature is measured using a chromel-alumel thermocouple inserted in a small indentation at the end of the quartz tube. A diagram of the apparatus is shown in figure 4.1 (overleaf).

figure 4.1

electron
multiplier

Quadrupole
mass filter

fixed
inlets

He

NF₃
NH₃
CH₄
N₂O

Diffusion
pumps

Roots
pump

sampling
orifice

pyrolysis
port

electron
gun
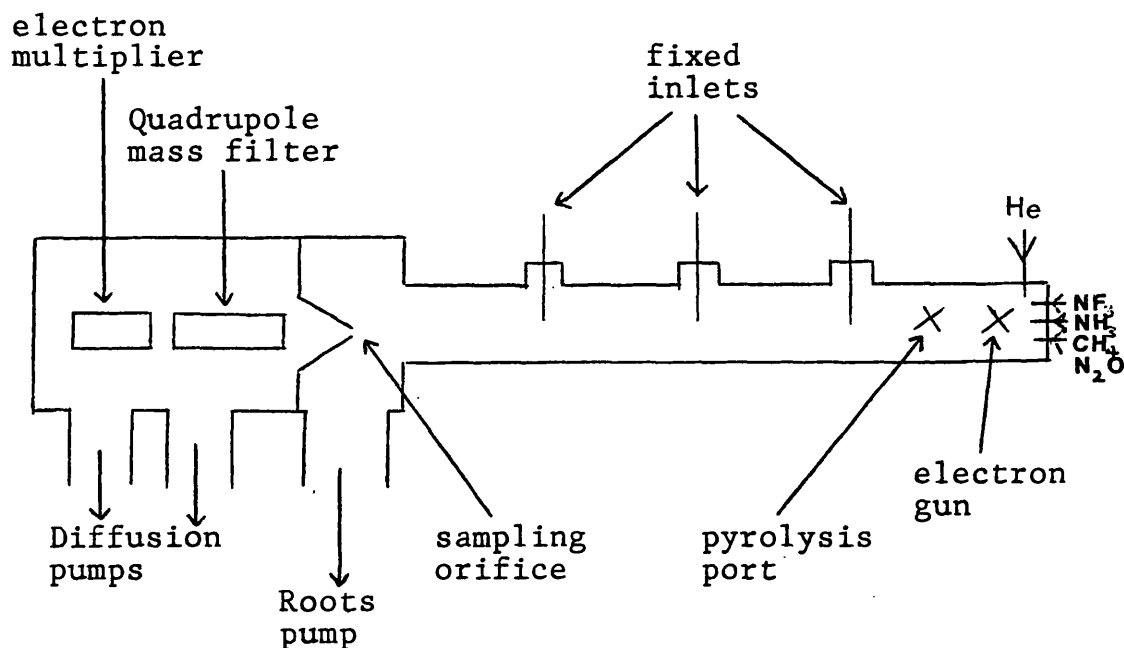
The instrument consists of a flow tube (100x7.6cm i.d.) in
which anions are generated and allowed to react, and a
differentially pumped mass spectrometer system for mass
analysis and detection of the ions.

In a typical experiment, a large flow $(\sim 140STPcm^3s^{-1})$ of
purified helium buffer gas is continuously pumped through
the flow tube establishing a pressure of ~0.4torr and an
average flow velocity of $\sim 70ms^{-1}$. Ions are generated by the
introduction into the flow tube of small flows $(<1STPcm^3s^{-1})$
of the appropriate gas at the upstream end of the flow tube,
which is ionised by electron impact from a thoriated iridium
filament. For the majority of experiments, amide, hydroxide
or flouride are the ions initially produced as shown in the

following equations.

$$NH_3 \xrightarrow{e} {}^-NH_2 + H$$

$$N_2O \xrightarrow{e} O^- + N_2$$

$$O^- + CH_4 \longrightarrow {}^-OH + CH_3$$

$$NF_3 \xrightarrow{e} F^- + NF_2$$
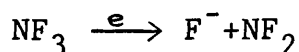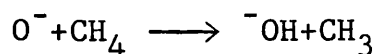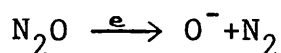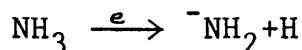
Amide and hydroxide are two of the strongest bases available in the gas phase [4], capable of abstracting a proton from most organic molecules. Only the vinyl anion (CH_2CH^-) and unactivated aliphatic anions $(CH_3^-$ etcetera) cannot be prepared in the flowing afterglow [5]. Therefore, by addition of the appropriate reagents through the inlets, it is possible to generate virtually any organic anion whose reactions with any molecule can be studied.

Since the flowing afterglow technique only gives the charge to mass ratio of the anions, it is necessary to have chemical methods to determine the structure of isomeric anions, in particular, silyl anions and alpha-silyl carbanions. Several reagents are available to do this. Nitrous oxide has been shown [6] to be a useful reagent in distinguishing between various types of carbanion, therefore Depuy and Damrauer [7] investigated the reactions of silyl anions and alpha-silyl carbanions with nitrous oxide and concluded that silyl anions react by oxygen transfer, and alpha-silyl carbanions react by oxygen transfer with loss of CR_2 as shown overleaf.

$$R_3Si^- + N_2O \longrightarrow R_3Si\diagdown_{N=N}\diagup^-O \longrightarrow R_3SiO^- + N_2$$

$$R_3SiCR_2^- + N_2O \longrightarrow R_3Si\diagdown_{CR_2-N}\diagup^{^-O}N \longrightarrow R_3SiO^- + R_2CN_2$$
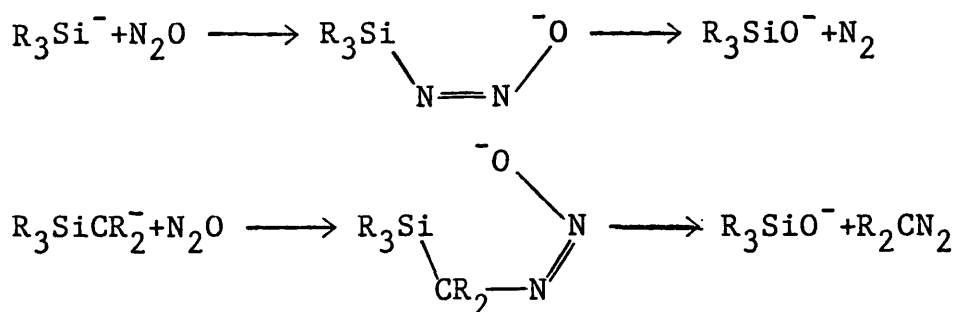
It has also been shown that CO_2, OCS and CS_2 are of use in distinguishing between silyl anions and alpha-silyl carbanions as shown in the following equations. [8]

$$R_3Si^- + CO_2 \longrightarrow R_3SiO^- + CO$$

$$R_3SiCR_2^- + CO2 \longrightarrow R_3SiO^- + R_2CCO$$

$$R_3Si^- + CS_2(OCS) \longrightarrow R_3SiS^- + CS(CO)$$

$$R_3SiCR_2^- + CS_2(OCS) \longrightarrow R_3SiS^- + R_2CCS(R_2CCO)$$
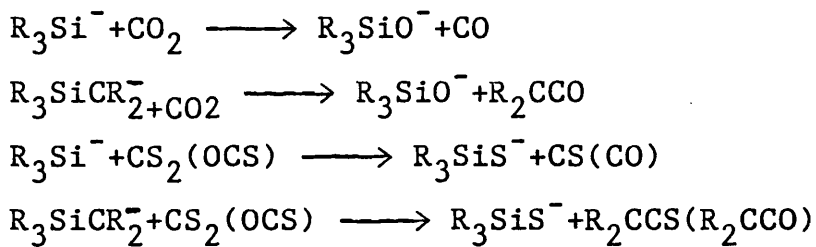
Therefore, it is possible to deduce the structure of an anion both from its charge to mass ratio (m/e), and also its reaction with N_2O, CO_2, OCS and CS_2.

Results and Discussion

Amide + Dimethylsilacyclobutane (DMSCB)

By introducing DMSCB through the pyrolyser at room temperature, peaks were observed at m/e values of 99, 116 and 117, consistent with deprotonation of DMSCB and adduct formation between amide+DMSCB, and hydrooxide+DMSCB.

Hydroxide arises as an impurity in the generation of amide due to the presence of small amounts of water in the apparatus.

Amide + 1,1,3,3-tetramethyl-1,3-disilacyclobutane (TMDSCB)

The behaviour of this mixture was very similar to that of DMSCB+amide, with peaks observed at m/e values of 143, 160 and 161, consistent with deprotonation of the disilacyclobutane, and adduct formation with amide and hydroxide.

The reaction mechanism for decomposition of DMSCB is as follows:

$$Me_2Si\text{----} \longrightarrow C_2H_4 + Me_2Si=CH_2$$

$$2Me_2Si=CH_2 \longrightarrow Me_2Si\diamondsuit SiMe_2$$
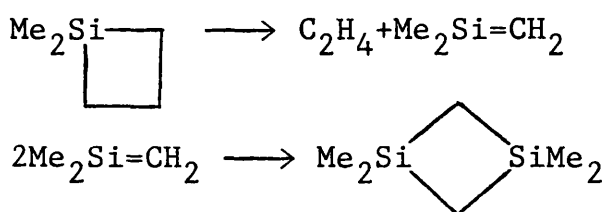
The reason for investigation of the room temperature reaction of DMSCB and TMDSCB is to enable any ions produced from reaction of dimethylsilene and amide to be unambiguously identified.

Amide + Dimethylsilene

Upon introduction of DMSCB through the pyrolyser in the presence of amide, as the pyrolyser temperature is

increased, the major new product has a m/e value of 71, and there is also a minor product with a m/e value of 143. This is consistent with formation and deprotonation of dimethylsilene, but also shows that some dimerisation of dimethylsilene occurs before deprotonation as shown below.

$$Me_2Si \square \longrightarrow C_2H_4 + Me_2Si=CH_2 \xrightarrow{Me_2Si=CH_2} Me_2Si \diamondsuit SiMe_2$$

$$\Big\downarrow {}^-NH_2 \qquad\qquad\qquad \Big\downarrow {}^-NH_2$$

$$M-1 \qquad\qquad\qquad\qquad M-1$$

$$m/e=71 \qquad\qquad\qquad m/e=143$$
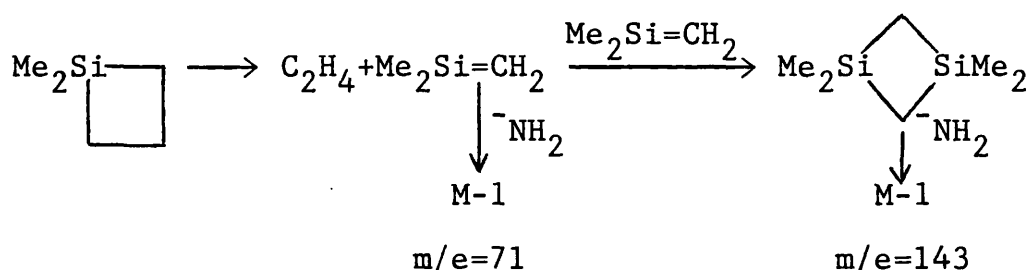
Structure of Deprotonated Dimethylsilene

Having shown that it is possible to generate deprotonated dimethylsilene, it is necessary to employ chemical methods to determine its structure, as there are the two possibilities shown below:

$$Me_2Si=CH_2 \xrightarrow{H_2N-} MeSi \overset{CH_2}{\underset{CH_2}{\diagdown}}{}^- \quad \text{or} \quad Me_2Si=\bar{C}H \longleftrightarrow Me_2\bar{S}i\equiv CH$$

$$\qquad\qquad\qquad\qquad (1) \qquad\qquad\qquad\qquad\qquad (2)$$
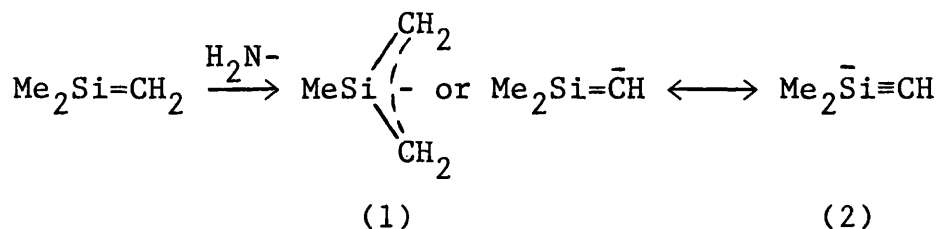
Having produced deprotonated dimethylsilene its reactions with N_2O, CO_2, CS_2 and OCS were studied by introducing the appropriated neutral further down the flow tube.

It has previously been noted that the order of reactivity of

these neutrals is $N_2O < CO_2 < OCS \approx CS_2$, and that delocalised anions and/or ones with lower basicity are less reactive with these neutrals.[8]

The deprotonated dimethylsilene did not react with N_2O but reacted with CO_2, OCS and CS_2, as shown in the equation below.

$$
\underset{m/e=71}{\begin{array}{c}\text{MeSi}\big\langle\!\!\!\begin{smallmatrix}\text{CH}_2\\[2pt]\end{smallmatrix}\!\!\!\big\rangle^- \\ \text{CH}_2\end{array}} + CO_2 \longrightarrow \underset{m/e=73}{\begin{array}{c}\text{MeSi}\big\langle\!\!\!\begin{smallmatrix}\text{CH}_2\\[2pt]\end{smallmatrix}\!\!\!\big\rangle^- \\ \text{O}\end{array}} + CH_2CO
$$

$$
\underset{m/e=71}{\begin{array}{c}\text{MeSi}\big\langle\!\!\!\begin{smallmatrix}\text{CH}_2\\[2pt]\end{smallmatrix}\!\!\!\big\rangle^- \\ \text{CH}_2\end{array}} + CS_2 \longrightarrow \underset{m/e=89}{\begin{array}{c}\text{MeSi}\big\langle\!\!\!\begin{smallmatrix}\text{CH}_2\\[2pt]\end{smallmatrix}\!\!\!\big\rangle^- \\ \text{S}\end{array}} + CH_2CS
$$

$$
\underset{m/e=71}{\begin{array}{c}\text{MeSi}\big\langle\!\!\!\begin{smallmatrix}\text{CH}_2\\[2pt]\end{smallmatrix}\!\!\!\big\rangle^- \\ \text{CH}_2\end{array}} + OCS \longrightarrow \underset{m/e=89}{\begin{array}{c}\text{MeSi}\big\langle\!\!\!\begin{smallmatrix}\text{CH}_2\\[2pt]\end{smallmatrix}\!\!\!\big\rangle^- \\ \text{S}\end{array}} + CH_2CO
$$

It was concluded that (1) was the structure of deprotonated dimethylsilene as its reaction with these neutral reagents involved either oxygen or sulphur transfer with loss of CH_2 as expected from alpha-silyl carbanions. The possibility that (1) rearranged to $Et\ddot{S}iCH_2^-$ was discounted

by the results of ion-molecule reactions of deprotonated dimethylsilylene to be discussed later in this chapter.

Acidity of Dimethylsilene

The gas phase acidity of a compound RH is defined as the enthalpy change for the reaction.

$$RH \longrightarrow R^- + H^+$$
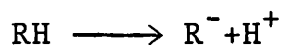
The flowing afterglow technique can be used to obtain an approximate measure of the acidity of a compound by the following method. The compound is introduced into the flowing afterglow in the presence of bases of varying strengths to see if proton abstraction occurs. Then the process is reversed and various neutral reagents are introduced into the flowing afterglow, in the presence of the deprotonated compound, to see if proton abstraction occurs. For example, if RH has an acidity between $NH_3(404 kcalmol^{-1})$ and $H_2O(391 kcalmol^{-1})$, then $^-NH_2$ will abstract a proton from RH but ^-OH will not, and R^- will abstract a proton from H_2O, but will not abstract a proton from NH_3.

Amide and hydroxide both abstract a proton from dimethylsilene, also upon addition of D_2O downstream of deprotonated dimethylsilene, it was observed that this had very little effect on deprotonated dimethylsilene, and no

H-D exchange was observed. These results show that dimethylsilene is a stronger acid than water.

Addition of $Bu^tOH(373 kcalmol^{-1})$ downstream of deprotonated dimethylsilene eliminated deprotonated dimethylsilene and produced a similar amount of Bu^tO^-, indicating that dimethylsilene is a weaker acid than Bu^tOH.

However, experiments with $MeOH(379 kcalmol^{-1})$ were ambiguous, as MeO^- (generated from $^-NH_2 + (MeOCH_2)_2$) was observed to deprotonate dimethylsilene, but MeOH added downstream of deprotonated dimethylsilene was observed to react with deprotonated dimethylsilene and produce methoxide, but in much larger quantities than the original amount of deprotonated dimethylsilene present. This shows a difficulty in these experiments, in that with the current experimental set-up, a variety of neutral and anionic species are present in the flow tube, which can lead to complications in determining the acidity of neutral species.

Nevertheless, these results show that the gas phase acidity of dimethylsilene is between $H_2O(\Delta H° = 391 kcalmol^{-1})$ and $Bu^tOH(\Delta H° = 373 kcalmol^{-1})$.

Reactions of Anions with Dimethylsilene

Dimethylsilene undergoes addition reactions with a variety of neutral polar reactants (X-Y), with the more nucleophilic

of X and Y adding to silicon [9,10]. The reactions of allyl and cyanide anion with dimethylsilene were investigated in the flowing afterglow to explore the ion-molecule analog of such reactions, and to look for any evidence of addition to the carbon end of the double bond of dimethylsilene.

Allyl anion + Dimethylsilene

Allyl anions were generated by reaction of amide with propene.

$$^-NH_2 + \quad \diagup\!\!\diagdown\!\!\diagdown \quad \longrightarrow \quad NH_3 + \quad \diagup\!\!\diagup\!\!\diagdown$$

Upon reaction with dimethylsilene, a peak with a m/e value=113, corresponding to addition of allyl anion to dimethylsilene was observed, which was expected to be either the silyl anion or alpha-silyl carbanion as shown below.

$$Me_2Si=CH_2 + \quad \diagup\!\!\diagup\!\!\diagdown \quad \longrightarrow \quad Me_2SiCH_2^- \quad or \quad Me_2\overline{Si}CH_2\diagdown\!\!\diagdown$$

$$\qquad\qquad\qquad\qquad\qquad\qquad (3) \qquad\qquad (4)$$

$$m/e=113$$
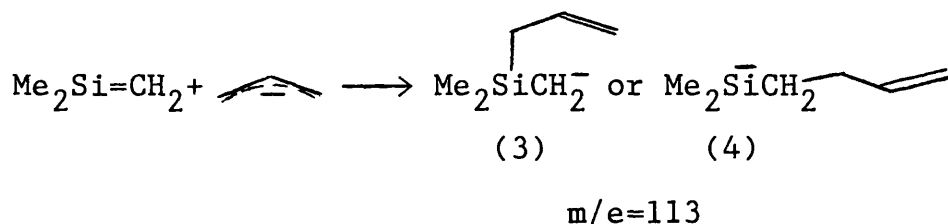
However, subsequent reaction with nitrous oxide added downstream produced peaks at m/e values of 111 and 139, consistent with reaction of an allylic anion with nitrous oxide. [11]

$$HMe_2SiCH_2\overline{CHCH_2}\overline{CH_2} \xrightarrow{N_2O} HMe_2SiCH=\overline{C}CH=CH_2 + H_2O + N_2$$

$$m/e=113 \qquad\qquad m/e=111$$

(5)

$$HMe_2SiCH_2CH=CH\overline{C}N_2 + H_2O$$

$$m/e=139$$
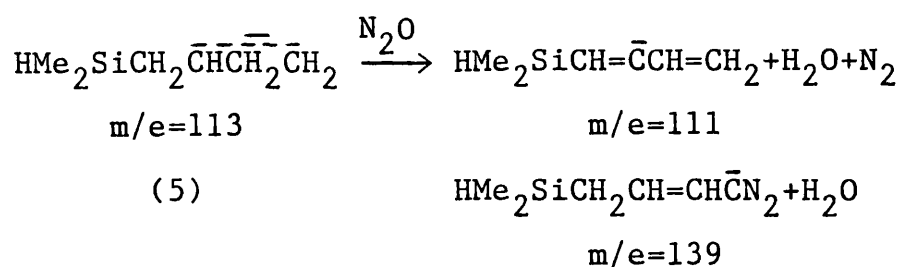
(5) could arise from (4) by proton migration, and (3) could rearrange to (4) by migration of the allyl group from silicon to carbon.
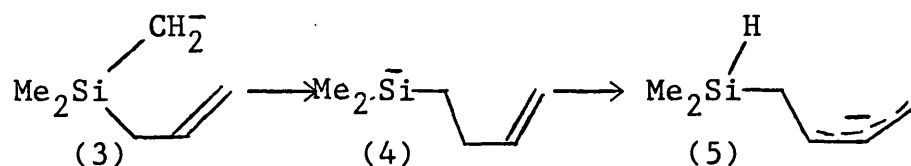
Thus from this experiment, it is impossible to tell if the initial addition of allyl anion to dimethylsilene occurred at silicon or carbon.

Cyanide Anion + Dimethylsilene

Cyanide anions were generated by electron impact on BrCN.

$$BrCN \xrightarrow{e} Br + {}^-CN$$
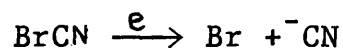
Upon reaction with dimethylsilene, a peak at m/e=98 is produced, as expected for addition of ^-CN to dimethylsilene. This adduct was found to be unreactive towards N_2O, but reacted with CO_2 giving oxygen transfer with loss of CH_2, and CS_2 giving sulphur transfer with loss

of CH_2. This is consistent with addition of ^-CN to silicon, and not carbon.

$$Me_2Si=CH_2 + {}^-CN \longrightarrow Me_2SiCH_2^-$$

$$\begin{array}{c} | \\ CN \\ m/e=98 \end{array}$$

with branches: CO$_2$ to left, CS$_2$ to right

$$\underset{m/e=100}{Me_2SiO^-} \qquad (6) \qquad \underset{m/e=116}{Me_2SiS^-}$$

$$CH_2CO + \underset{}{CN} \qquad\qquad CN + CH_2CS$$
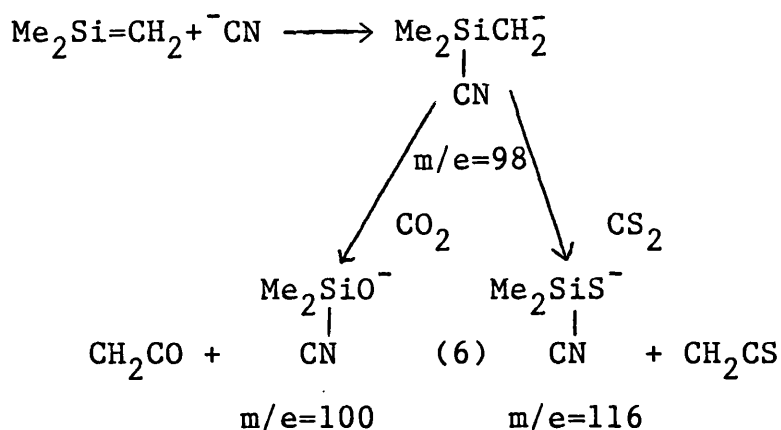
An added complication with addition of CO_2, is that if the amount of CO_2 is increased, the (6) undergoes further reaction with CO_2, a common reaction of siloxides.[7]

$$Me_2SiO^- \xrightarrow{CO_2} Me_2SiOCO_2^-$$
$$\underset{m/e=100}{} \underset{CN}{|} \qquad \underset{m/e=144}{} \underset{CN}{|}$$
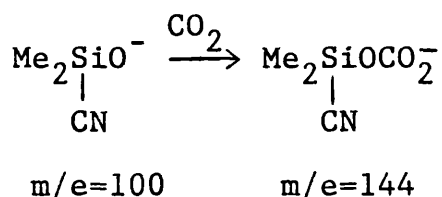
Cycloaddition Reactions of Dimethylsilene

As discussed in chapter one, dimethylsilene undergoes a variety of cycloaddition reactions, such as dimerisation, reaction with butadiene, etcetera. It was therefore decided to explore the occurrence or otherwise, of various cycloaddition reactions with the flowing afterglow technique.

Dimethylsilene Dimerisation

As mentioned earlier, upon generation of dimethylsilene in the presence of amide, there is evidence for some dimerisation of dimethylsilene before reaction with amide, as a small peak at m/e=143 corresponding to deprotonation of 1,1,3,3-tetramethyl-1,3-disilacyclobutane is observed.

$$Me_2Si \longrightarrow C_2H_4 + Me_2Si=CH_2 \xrightarrow{Me_2Si=CH_2} Me_2Si \diamond SiMe_2$$

$$\downarrow{}^-NH_2 \qquad\qquad\qquad \downarrow{}^-NH_2$$

$$M-1 \qquad\qquad\qquad\qquad M-1$$

$$m/e = 71 \qquad\qquad\qquad m/e = 143$$
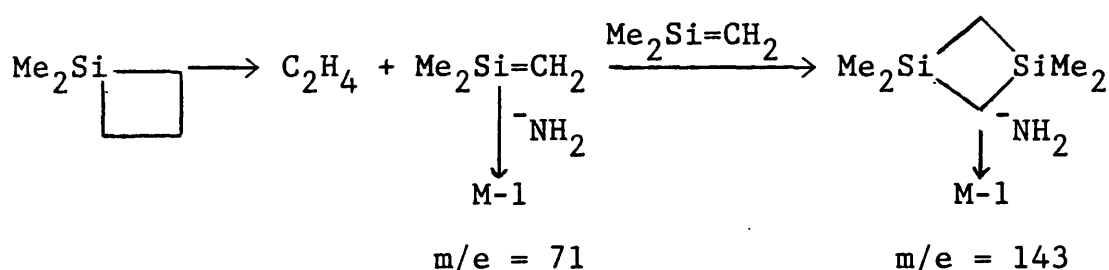
In addition in the presence of fluoride, a peak at m/e=163 corresponding to an adduct of fluoride + TMDSCB is observed.

Dimethylsilene + Butadiene

This experiment was carried out by introducing both DMSCB and varying quantities of butadiene together, through the pyrolysis port into the flowing afterglow, in the presence of amide, hydroxide, or fluoride.

It was expected that dimethylsilene would undergo a 4+2 cycloaddition with butadiene, as shown overleaf, and that the silacyclohexene so formed would react with amide, flouride, and hydroxide.

$$Me_2Si=CH_2 + \text{(butadiene)} \longrightarrow Me_2Si\text{(silacyclohexene ring)}$$
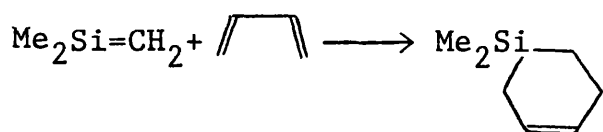
Neither amide nor hydroxide gave any evidence that cycloaddition had occurred, with no sign of deprotonation of the silacyclohexene, or adduct formation.

Reaction with fluoride appeared to indicate that cycloaddition had occurred, as a small amount of a peak at $m/e=145$ was produced, corresponding to a fluoride adduct of the silacyclohexene. However, this result must be treated with caution, as a small peak at $m/e=145$ was already present before the introduction of butadiene.

Dimethylsilene + Oxygen

It was expected [12] that dimethylsilene would react with oxygen as shown.

$$Me_2Si=CH_2 + O_2 \longrightarrow Me_2Si\overset{\displaystyle|\quad|}{\underset{O-O}{}} \longrightarrow Me_2Si=O + CH_2O$$
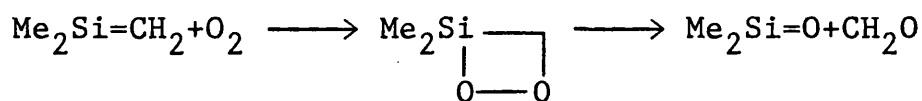
This would lead to production of dimethylsilanone, a reactive intermediate containing a silicon-oxygen π-bond, which in the absence of trapping agents would produce cyclic compounds, made up of three or more dimethylsilanone molecules.

Upon reaction of dimethylsilene with oxygen, in the presence of amide, no evidence of the four-membered ring was obtained, and only a minor peak corresponding to deprotonated dimethylsilanone was observed.

However, recent theoretical calculations on a related system [13], the reaction of $H_2C=O$ with dimethylsilene, propose a mechanism leading to cyclic $(Me_2SiO)_3$ which does not involve formation of dimethylsilanone, and the possibility of a similar mechanism occurring here cannot be ruled out without further investigation.

GAS PHASE ION CHEMISTRY OF DIMETHYLSILYLENE

Introduction

In common with silenes, there has been much interest in the structure and reactivity of silylenes in recent years, as was discussed in chapter one and was recently reviewed by Gaspar [14]. However, nothing has previously been published involving ion-molecule reactions of silylenes. Therefore, it was decided to undertake an investigation of the reactions of dimethylsilylene with anionic reagents in the gas phase, using the flowing afterglow technique, as described earlier.

Results and Discussion

The source of dimethylsilylene was 1,2-dimethoxytetramethyldisilane, which upon heating decomposes to produce initially, dimethyldimethoxysilane and dimethylsilylene.

$$(MeO)Me_2SiSiMe_2(OMe) \longrightarrow Me_2Si(OMe)_2 + Me_2Si:$$
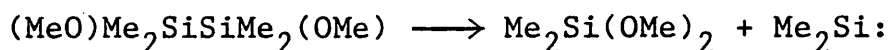
As discussed in chapter one, various experimental and theoretical work has shown that, at high temperature, an equilibrium exists between dimethylsilylene and methylsilene, as shown below.

$$Me_2Si: \rightleftharpoons HMeSi=CH_2$$

It was therefore decided to use the flowing afterglow technique to investigate this equilibrium by reaction with fluoride anion, with structure determination by subsequent reaction with N_2O and CO_2.

1,2-dimethoxytetramethyldisilane + Fluoride

The aim of this experiment was to see if the precursor to dimethylsilylene underwent any reactions with fluoride and subsequent reactions with N_2O or CO_2, that might interfere with the expected reactions of dimethylsilylene or methylsilene with these reagents.

Upon introduction of 1,2-dimethoxytetramethyldisilane into the flowing afterglow in the presence of fluoride, a minor product was observed at m/e=77, as would be expected for addition of fluoride to dimethylsilylene or methylsilene. This was eliminated by subsequent addition of N_2O or CO_2, which produced a peak at m/e=93, consistent with conversion of $Me_2\bar{S}iF$(m/e=77) by N_2O or CO_2 to FMe_2SiO^- (m/e=93). A plausible mechanism for this is shown below.

$$(MeO)Me_2SiSiMe_2(OMe) \xrightarrow{\text{F}^-} \left[\underset{\underset{OMe}{|}}{(MeO)Me_2Si-\underline{S}iMe_2} \overset{F}{} \right] \longrightarrow (MeO)_2SiMe_2 + Me_2\bar{S}iF \underset{\underset{Me_2\overset{O^-}{\underset{||}{S}}iF}{N_2O\downarrow CO_2}}{}$$
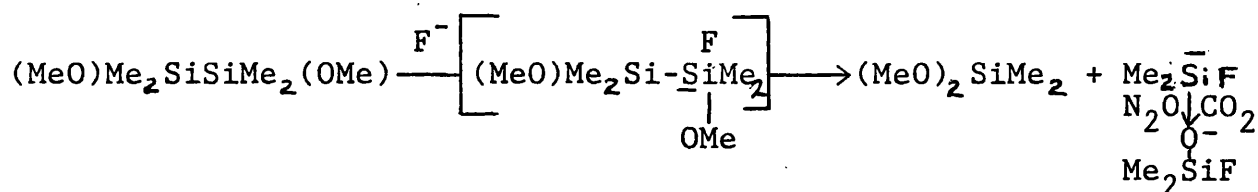
Supporting evidence for this mechanism, comes from the observation of small quantities of the fluoride adduct of $Me_2Si(OMe)_2$, which would be produced along with $Me_2\bar{S}iF$.

Dimethyldimethoxysilane + Fluoride

The aim of this experiment was to see if dimethyldimethoxysilane, the major stable product of 1,2-dimethoxytetramethyldisilane pyrolysis, underwent any reaction with fluoride and subsequent reaction with N_2O or CO_2, that might interfere with the expected reactions of dimethylsilylene or methylsilene with these reagents.

Pyrolysis of 1,2-dimethoxytetramethyldisilane in the presence of Fluoride

The conclusion, of the room temperature reactions of 1,2-dimethoxytetramethyldisilane and dimethyldimethoxysilane with fluoride, is that while $Me_2\bar{S}iF$ is a minor product of room temperature reaction of fluoride with 1,2-dimethoxytetramethyldisilane, it is possible by using N_2O and CO_2 to unambiguously detect any $HMeFSiCH_2^-$ arising from isomerisation of dimethylsilylene to methylsilene.

1,2-dimethoxytetramethyldisilane was introduced through the pyrolyser into the flowing afterglow in the presence of fluoride, with the temperature of the pyrolyser being increased in steps, and at each temperature the presence of $Me_2\bar{S}iF$ and $HFMeSiCH_2^-$ was investigated by reaction with N_2O and CO_2.

As the temperature was increased, until pyrolysis occurred ($\sim320^\circ C$), there was an increase in the intensity of the peaks at m/e=77 and 139, consistent with decomposition of 1,2-dimethoxytetramethyldisilene to dimethylsilylene and dimethyldimethoxysilane. Subsequent addition of N_2O and CO_2 eliminated the peak at m/e=77 and produced a new peak at m/e=93, consistent with the following equation.

$(MeO)Me_2SiSiMe_2(OMe) \longrightarrow Me_2Si(OMe)_2 + Me_2Si:$

$$Me_2Si: \xrightarrow{F^-} Me_2\bar{S}iF \xrightarrow[N_2O]{CO_2} Me_2\overset{O^-}{\underset{}{\bar{S}}}iF$$

$m/e=77 \qquad m/e=93$
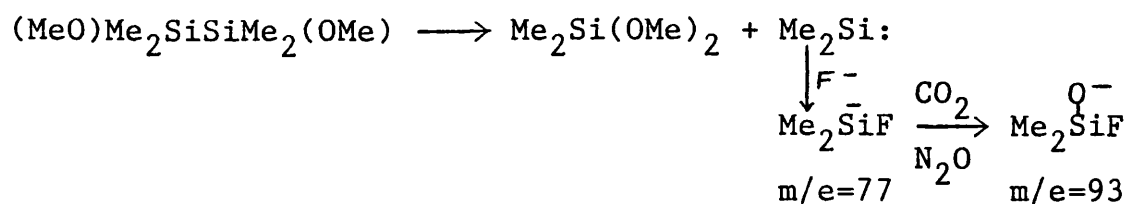
As the temperature was increased further, the intensity of product peaks increased also, but upon reaction with N_2O or CO_2 in the approximate temperature range 320-370°C, there was no indication of any isomerisation of dimethylsilylene.

However, at temperatures above approximately 370°C, upon reaction with N_2O or CO_2, a new peak at $m/e=79$ as well as at $m/e=93$ was observed, and at the highest temperature reached (approx. 470°C), somewhat greater quantities of the peak at $m/e=79$ resulted.

These results indicate that as the temperature is increased, the rate of isomerisation of dimethylsilylene is increased, to such an extent that significant quantities of methylsilene can be produced before reaction of dimethylsilylene with fluoride, as shown below.

$$Me_2Si: \rightleftharpoons HMeSi=CH_2$$

$$\downarrow F^- \qquad F^{\searrow}{}_F$$

$$Me_2\bar{S}iF \; m/e=77 \quad HMe\bar{S}iCH_2^- \; m/e=77$$

$$CO_2 \Big| N_2O \qquad CO_2 \Big| N_2O$$

$$Me_2FSiO^- \qquad HMeFSiO^-$$

$$m/e=93 \qquad m/e=79$$
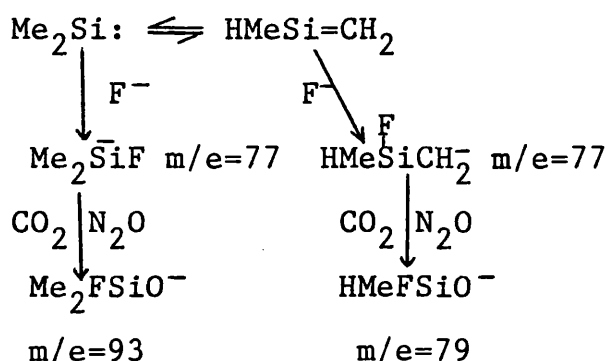
In the absence of trapping agents, various dimeric products arising from dimethylsilylene and methylsilene are observed [15]. In these experiments, employing the flowing afterglow technique, products that could be identified as arising from dimeric products of dimethylsilylene and methylsilene, were minor compared to $Me_2\bar{S}iF$ and $HMeFSiCH_2^-$, produced directly from dimethylsilylene and methylsilene. Therefore, in this work no conclusions could be drawn on the nature of these dimeric products.

Dimethylsilylene + Butadiene

This experiment was carried out by introducing 1,2-dimethoxytetramethyldisilane, along with butadiene, through the pyrolyser at various temperatures, into the flowing afterglow, in the presence of fluoride.

At all temperatures at which pyrolysis occurred, a new peak was observed at m/e=131, corresponding to a fluoride adduct of dimethylsilacyclopentene, indicating that cycloaddition of dimethylsilylene with butadiene occurred.

$$(MeO)Me_2SiSiMe_2(OMe) \longrightarrow Me_2Si(OMe)_2 + Me_2Si:$$
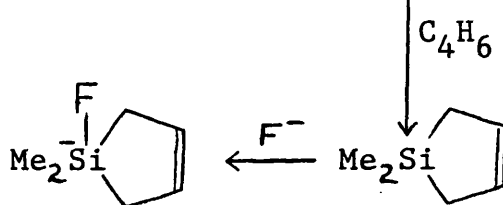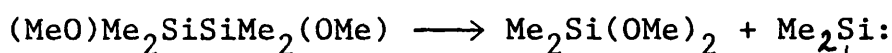
m/e=131

Due to the greater reactivity of silylenes compared to silenes with butadiene [15,16], and the lack of evidence from work discussed earlier in this chapter concerning cycloaddition of dimethylsilylene with butadiene, even if any isomerisation of dimethylsilylene to methylsilene occurred, it will not alter the conclusion that cycloaddition of dimethylsilylene with butadiene can be detected with the flowing afterglow technique.

Dimethylsilylene + Amide

Upon pyrolisis of 1,2-dimethoxytetramethyldisilane at a temperature at which dimethylsilylene undergoes ion-molecule reactions faster than isomerisation to methylsilene, as shown by previous experiments with fluoride+ dimethylsilylene, reaction with amide produces a peak at m/e=57, as expected for deprotonated dimethylsilylene.

$$Me_2Si: + H_2N^- \longrightarrow Me\ddot{S}iCH_2^- \longleftrightarrow Me\bar{S}i=CH_2$$
$$m/e=57$$
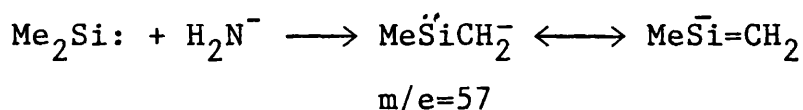
Subsequent addition of N_2O, CO_2 or OCS gave no reaction with deprotonated dimethylsilylene. However, subsequent addition of CS_2 gave a new peak at m/e=75, corresponding to addition of S and loss of CH_2, indicating that deprotonated dimethylsilylene reacts as though the negative charge is located on carbon.

$$\text{Me}\overset{\cdot\cdot}{\text{Si}}\text{CH}_2^- + \text{CS}_2 \longrightarrow \text{Me}\overset{\cdot\cdot}{\text{Si}}\text{S}^- + \text{CH}_2\text{CS}$$

m/e=57   m/e=75
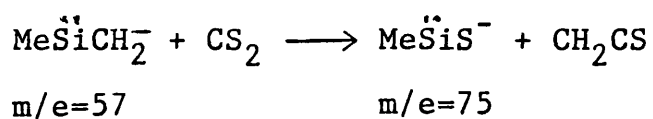
Gas-phase acidity measurements were also carried out on dimethylsilylene generated in the flowing afterglow. It was clearly shown that dimethylsilylene is a stronger acid than $H_2O(391 \text{kcalmol}^{-1})$, as deprotonated dimethylsilylene did not react with D_2O added downstream. However, experiments with methanol were subject to the same ambiguity as found in acidity measurements with dimethylsilylene.

Thus the only conclusion regarding the acidity of dimethylsilylene is that it is a stronger acid than water.

References

1. M. C. Flowers & L. E. Gusel'nikov, J. Chem. Soc. (B), 1968, 419.

2. G. Raabe & J. Michl, Chem. Rev., 1985, 85, 419.

3. V. M. Bierbaum. C. H. Depuy, R. H. Shapiro and J. H. Stewart, J. Am. Chem. Soc., 1976, 98, 4229.

4. J. E. Bartness, R. T. McIver Jr., in "Gas Phase Ion Chemistry"; Bowers, M. T., Ed.; Academic Press, New York, 1979, Vol.2, pp.87-121.

5. C. H. Depuy and V. M. Bierbaum, Accts. Chem. Res., 1981, 14, 146.

6. V. M. Bierbaum, C. H. Depuy and R. H. Shapiro, J. Am. Chem. Soc., 1977, 99, 5800.

7. C. H. Depuy and R. Damrauer, Organometallics, 1984, 3, 362.

8. C. H. Depuy and R. Damrauer, unpublished work.

9. See chapter one.

10. G. Raabe & J. Michl, Chem. Rev., 1985, 85, 419.

11. S. R. Kaas, J. Filey, J. M. Van Doren and C. H. Depuy, J. Am. Chem. Soc., accepted for publication.

12. I. M. T. Davidson, C. E. Dean & F. T. Lawrence, J. Chem. Soc. Chem. Comm., 1981, 52.

13. S. M. Bachrack and A. Streitweiser Jr., J. Am. Chem. Soc., 1985, 107, 1186.

14. P. P. Gaspar, React. Intermed., 1985, 3, 333.
    P. P. Gaspar, React. Intermed., 1981, 2, 335.
    P. P. Gaspar, React. Intermed., 1978, 1, 229.

15. I. M. T. Davidson and R. J. Scampton, J. Organomet. Chem., 1984, 271, 249.

16. I. M. T. Davidson, S. I.-Maghsoodi, T. J. Barton and N. Tillman, J. Chem. Soc. Chem. Comm., 1984, 478.

QUANTITATIVE ASPECTS OF GAS PHASE UNIMOLECULAR ISOMERISATION REACTIONS OF ORGANOSILICON REACTIVE INTERMEDIATES

Introduction

In recent years there have been reports in the literature of mechanisms involving unimolecular isomerisation reactions of reactive intermediates [1]. Therefore, it was decided to investigate the validity of some of these mechanisms by computer modelling. Any reaction mechanism can be written as a set of differential equations, one for each species involved, the solution of which gives the reaction profile of each species. A NAG library file was available which could solve simultaneous differential equations by 'Gears' method. A computer program written by A. C. Baldwin [2] used this subroutine to calculate the reaction profile of each species in a proposed reaction mechanism. It required the initial reactant concentration, temperature, reaction time and reaction mechanism expressed as a series of differential equations, and Arrhenius parameters for each individual step in the proposed mechanism.

For many of the individual reaction steps proposed, no direct experimental measurements are available, but Arrhenius parameters can be estimated from thermodynamic calculations, theoretical calculations, or educated guesses.

CHAPTER FIVE

COMPUTER MODELLING OF PYROLYSIS MECHANISMS

Estimation of individual Arrhenius parameters

i) Kinetic measurements

Kinetic measurements have been carried out on the thermal decomposition of various silanes and disilanes, and Arrhenius parameters obtained for primary decomposition routes, which involve silylene generation by 1,2-migration of hydrogen, methyl, or silyl groups. These kinetic measurements can be used as a basis for estimating Arrhenius parameters for analogous reactions for which no direct measurements are available. For example, the reaction below is a 1,2-hydrogen shift to form a silylene.

$$Me_2Si \overset{\wedge}{-\!\!-}SiMeH \xrightarrow{\ 1\ } HMe_2Si \overset{\wedge}{\ } \ddot{S}iMe$$
$$(1) \qquad\qquad (2)$$
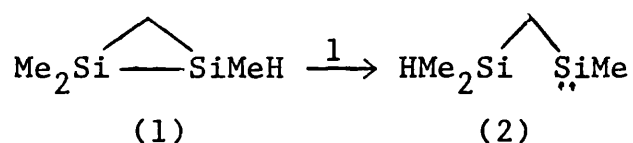
A close analogy to this is the thermal decomposition of pentamethyldisilane, which proceeds via a 1,2-hydrogen shift from silicon to silicon with silylene formation.

$$Me_3SiSiMe_2H \xrightarrow{\ 2\ } Me_3SiH + Me_2Si:$$
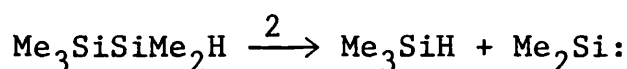
Arrhenius parameters for this reaction have been experimentally measured to give; [3]

$$\log k_2/s^{-1} = 12.93 - (198kJmol^{-1}/2.303RT)$$

From this, log A(1) can be estimated to be 12.93. The activation energy for step 1 can be estimated to be $(198-E03)kJmol^{-1}$, where E03 is the element of ring strain released on passing from (1) to the transition state between (1) and (2).

ii) <u>Thermodynamic calculations</u>

For a reversible reaction,

$$X \underset{2}{\overset{1}{\rightleftharpoons}} Y$$

If the activation energy for step 1 is known, along with the heats of formation of X and Y, then the activation energy for step 2 can be calculated as follows:

$$E(2) = \Delta H_f^o(X) - \Delta H_f^o(Y) + E(1)$$

This method has been used by Davidson and Scampton, [4] who combined kinetic measurements and thermodynamic data to estimate activation energies for bimolecular insertion reactions of simple silylenes into silicon-hydrogen, silicon-carbon, and carbon-hydrogen bonds to be 0-12, 62, and $82kJmol^{-1}$ respectively. If the relevant heats of formation are unknown, then it is possible to estimate them using the additivity scheme devised by O'Neal and Ring [5] as discussed in

chapter one.

iii) Entropy calculations

From transition state theory, the rate constant for a reaction of order m can be written as: [6]

$$k = \frac{e^m kT}{h} \exp(\Delta S^{\ddagger}/R) \exp(-E/RT) (c^{\ominus})^{(1-m)}$$

For a unimolecular reaction, this expression becomes.

$$k = \frac{ekT}{h} \exp(\Delta S^{\ddagger}/R) \exp(-E/RT)$$

From this, the A-factor can be written as:

$$A = \frac{ekT}{h} \exp(\Delta S^{\ddagger}/R)$$

Where $\Delta S^{\ddagger}$ is the entropy change on passing from the reactant to the transition state. For a reversible reaction.

$$X \underset{2}{\overset{1}{\rightleftharpoons}} Y$$
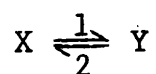
It follows that:

$$\frac{A(1)}{A(2)} = \exp((\Delta S_1^{\ddagger} - \Delta S_2^{\ddagger})/R) = \exp(\Delta S/R)$$

where ΔS is the entropy change on passing from X to Y. If A(1) is known, along with ΔS, then A(2) can be calculated. Even if neither A-factor is known, a knowledge of ΔS still allows the difference between the A-factors to be calculated. Therefore, a method of estimating entropies of compounds would be very useful.

Using the additivity tables devised by O'Neal and Ring [5], it is possible to derive the intrinsic entropy of any silane, polysilane, and their alkyl derivatives. Corrections can be made to take into account the effect of hindered rotation about each carbon-silicon and silicon-silicon bond, which have been estimated [5] to reduce the entropy by 0.7 and 0.3 e.u./mole respectively. In addition, as described by Benson [7], a symmetry correction of $R\ln\sigma$ needs to be subtracted, where σ is the symmetry number, and is defined as the total number of independent permutations of identical atoms (or groups) in a molecule that can be arrived at by simple rigid rotations of the entire molecule. σ can be calculated from the following equation.

$$\sigma = \sigma_{ext} \times \sigma_{int}$$

σ_{ext} depends on the point group of the molecule, σ_{int}

arises from molecules with internal rotations, such as a CH_3 group or SiR_3 group. For example to calculate the entropy of $Me_3SiSiMe_2H$.

$$\sigma_{ext} = 1 \qquad \sigma_{int} = 3^6$$
$$\text{therefore } \sigma = 3^6$$

Groups: $[Si-(Si)(C)_3]+[Si-(Si)(C)_2(H)]+5[C-(Si)(H)_3]$

$S^\circ = ^-20.48+(^-0.86)+(5\times30.41)-(5\times0.7)-0.3-R\ln3^6$

$S^\circ = 113.8$ e.u.

A problem arises in that O'Neal and Ring's additivity tables do not apply to reactive intermediates, such as silenes and silylenes, in which case, analogies have to be made with stable compounds for which entropies are known or can be readily calculated. An example being the isomerisation of methylsilene-dimethylsilylene investigated by Davidson and Scampton. [4]

$$Me_2Si: \rightleftharpoons HMeSi=CH_2$$
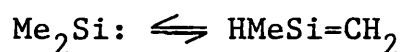
The entropy of dimethylsilylene can be estimated by a comparison with the entropy of a related compound, such as dimethylsilane by making a symmetry and spin correction. As the symmetry and spin are unchanged:

$S^o(Me_2Si:) = S^o(Me_2SiH_2)$

$\sigma_{ext} = 2 \qquad \sigma_{int} = 3^2$

therefore $\sigma = 18$

Groups: $[Si-(C)_2(H)_2] + 2[C-(Si)(H)_3]$

$S^o = 17.6 + (2 \times 30.41) - (2 \times 0.7) - R\ln 18$

$\quad = 71.27$ e.u.

In the case of methylsilene, an estimate of its entropy can be made from the entropy of propene, with a correction for the effect of replacing carbon with silicon. For propene, $\sigma_{ext}=1$, $\sigma_{int}=3$, therefore $\sigma=3$. The rotational barrier in propene is 1.9kcalmol^{-1} [8] which leads to a reduction in the entropy of 0.8 e.u. [5].

Groups: $[C_d-(H)_2]+[C_d(H)(C)]+[C-(H)_3(C)]$

$S^o = 27.61 + 7.97 + 30.41 - R\ln 3 - 0.8$

$\quad = 63.01$ e.u.

An approximation for the difference in entropy upon substitution of silicon for carbon, can be obtained by comparing the entropies of analogous compounds, such as Me_2SiH_2 and Me_2CH_2, which are 71.27 and 62.9 e.u. respectively. This gives a difference in entropy upon substitution of silicon for carbon of 8.37 e.u.

$S^o(HMeSi=CH_2) = 63.01+8.37 = 71.38$ e.u.

Thus, for the following reaction:

$$Me_2Si: \underset{2}{\overset{1}{\rightleftharpoons}} HMeSi=CH_2$$

$S°$ 71.27   71.38
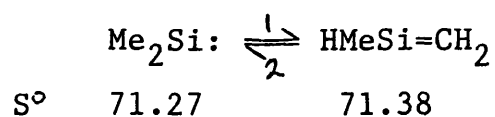
$\Delta S = 0.11$ e.u.

Since $\dfrac{A(1)}{A(2)} = e^{\Delta S/R}$

Therefore: $\dfrac{A(1)}{A(2)} = e^{0.06} = 1.06$

$\log(A(1)) - \log(A(2)) = 0.02$

The result of this is that the difference in A-factors for the dimethylsilylene-methylsilene isomerisation is negligible.

PRELIMINARY RESULTS ON THE REARRANGEMENT OF BIS(TRIMETHYLSILYL)SILYLENE

Introduction

In experiments carried out on the gas phase flow pyrolysis of methoxytris(trimethylsilyl)silane or chlorotris (trimethylsilyl)silane, [9] which both initially produce bis(trimethylsilyl)silylene. The dominant reaction is rearrangement to produce in ca.60% yield 1,1,4,4-tetramethyl -1,2,4-trisilacyclopentane, as shown overleaf:

$$(Me_3Si)_2Si: \xrightarrow{\Delta}$$

(60%)
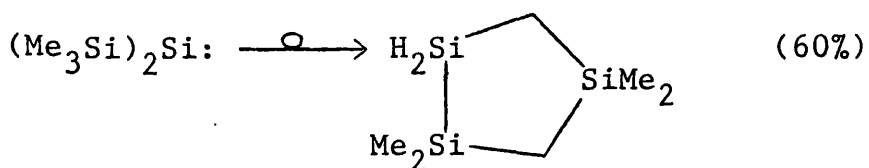
In addition, at least eight other unidentified products were observed, all with yields of <10%.

To account for the formation of the trisilacyclopentane, a mechanism was proposed consisting of a sequence of silylene to silylene rearrangements, also involving disilirane (disilacyclopropane) intermediates as shown in scheme 5.1.

There are many similarities between scheme 5.1 and the model developed for the methylsilene - dimethylsilylene system,[4] as shown in scheme 5.2. It was therefore decided to extend this model to account for the predominant formation of the trisilacyclopentane from bis(trimethylsilyl)silylene.

Results and Discussion

As a starting point, scheme 5.3 was devised. The initial step in the rearrangement of bis(trimethylsilyl)silylene is silylene insertion to form disilirane (2). Disilirane (2) can then undergo hydrogen, methyl and trimethylsilyl shifts from silicon to silicon, or silicon to carbon.

Scheme 5.3 takes into account some of the possible

119

Scheme 5.1

(Me$_3$Si)$_3$Si-X (X=OMe, Cl)

$\downarrow \Delta$

Me$_3$Si$\ddot{\text{Si}}$SiMe$_3$

$\downarrow$ C-H insertion

Me-shift $\longleftarrow$ H(Me$_3$Si)Si—SiMe$_2$ $\xrightarrow{\text{Me}_3\text{Si-shift}}$

Si-H insertion $\uparrow$ $\downarrow$ H-shift

Me$_3$SiSi $\overset{\frown}{}$ SiMe$_2$H $\xrightarrow[\text{insertion}]{\text{C-H}}$ H(Me$_3$Si)Si $\diamondsuit$ SiHMe ?

$\downarrow$ C-H insertion

H-shift $\longleftarrow$ Me$_2$Si—SiH(CH$_2$SiHMe$_2$) $\xrightarrow{\text{Me-shift}}$

$\downarrow$ CH$_2$SiHMe$_2$ shift

Me$_2$Si $\overset{\frown}{}$ SiH $\xrightarrow[\text{insertion}]{\text{C-H}}$ Me$_2$Si $\diamondsuit$SiH$_2$? (with SiHMe$_2$)
     SiH
     Me$_2$

Si-H insertion $\swarrow$ $\downarrow$ C-H insertion $\searrow$ C-H insertion

H$_2$Si $\overset{\frown}{}$ SiMe$_2$ (Me$_2$Si ring)

(Me$_2$SiHCH$_2$)MeSi $\diamondsuit$ SiH$_2$?

Me$_2$Si $\overset{\frown}{}$ SiH$_2$?
     Si
   H   Me

120

Scheme 5.2

HMeSi=CH$_2$ Me$_2$Si:
precursor   precursor

HMeSi=CH$_2$ $\xrightleftharpoons[3]{4}$ Me$_2$Si: (10)
(9)

HMeSi⟨⟩SiHMe (6)   Me$_2$Si=SiMe$_2$ (1)

6   21   5   7

Me$_3$SiSiMe $\xrightleftharpoons[19]{18}$ (Me$_3$Si)HSi=CH$_2$
(2)   (8)

16 | 28   8   22   20

HMe$_2$Si⟨⟩SiMe $\xrightleftharpoons[13]{12}$ Me$_2$Si—SiMeH $\xrightleftharpoons[15]{14}$ Me$_3$Si⟨⟩SiH (5)
(4)   (3)   17 | 29

Me$_2$Si⟨⟩SiH$_2$ (7)

121

Scheme 5.3

122

consequences of decomposition of disilirane (2) by hydrogen
shift from silicon to silicon, and trimethylsilyl shift from
silicon to carbon, because the hydrogen shift will be the
most important decomposition route of disilirane (2),
and the trimethylsilyl shift provides an alternative route
to 1,1,4,4-tetramethyl-1,2,4-trisilacyclopentane, not
considered in scheme 5.1.

The initial set of parameters for scheme 5.3 are shown in
table 5.1. The Arrhenius parameters were estimated by
comparison with analogous reactions in scheme 5.2, [4] with
the following modifications and additions.

The A-factor for reaction 9 was increased from $10^{13.5}$ to
$10^{13.68}$ to take into account the increase in the reaction
path degeneracy (ie. an increase from 6 to 9 in the number
of carbon-hydrogen bonds into which the silylene can
insert).

The A-factors for reactions involving closing of 5 and 6
membered rings, were estimated from the A-factors for
reactions involving closing of 3 and 4 membered rings. No
great variation was expected since any increase in the
A-factor for the closing of 5 and 6 membered rings due to
the transition state being less constrained would be
countered to some extent by the loss of more free rotations.
Arrhenius parameters for step 21 were based on
experimentally measured Arrhenius parameters for

Table 5.1

Reaction	log A	$E/kJmol^{-1}$	Comments
1	12.6	165	E = 82+EC3
2	14	218	E = 301-EO3
3	13	115	E = 198-EO3
4	12.6	95	E = 12+EC3
5	13.5	136	E = 82+EC4
6	13.5	170	
7	13.5	170	
8	12.3	120	
9	13.68	136	E = 82+EC3
10	13.5	255	E = 301-EO4
11	13.5	255	E = 301-EO4
12	13	20	E = 12+EC5
13	12.6	95	E = 12+EC3
14	13	115	E = 198-EO3
15	13.5	136	E = 82+EC4
16	13.5	255	E = 301-EO4
17	13.5	255	E = 301-EO4
18	13.5	255	E = 301-EO4
19	13	100	E = 82+EC6
20	13	100	E = 82+EC6
21	13.7	199	E = 282-EO3
22	12.6	145	E = 62+EC3
23	13	90	E = 82+EC5
24	13.5	255	E = 301-EO4

Initial concentration of species (1) = 1×10^{-5} mol/dm^3
Temperature = 773K
Reaction time = 0.01s

dimethylsilylene extrusion from hexamethyldisilane, [10] which can be thought of either as a methyl shift from silicon to silicon, or as a trimethylsilyl shift from silicon to carbon.

From the work of Davidson and Scampton [4] on scheme 5.2, EC3 and EC4 were estimated to be 83 and $54kJmol^{-1}$ respectively. EC5 is unknown, but was arbitrarily set at $8kJmol^{-1}$, in view of the lower strain energy in a five membered ring.

The calculated yield of 1,1,4,4-tetramethyl-1,2,4-trisilacyclopentane (species (9)), from the reactions in scheme 5.3 with the parameters in table 5.1 was 0.08%, since the experimental observation was a 60% yield of (9), then obviously either scheme 5.3 is incomplete and/or some of the estimated Arrhenius parameters are incorrect.

However, this result is useful in that an analysis of the calculated product yields, and relative rates (table 5.2) of each reaction gives an indication of why the yield of (9) is so low, and the relative importance of each step in the reaction mechanism.

This shows that by far the major product is (4), produced in 95% yield, in addition, decomposition steps for disilacyclobutanes have negligible effect, with the implication that the inclusion of species (8), (12), (13)

Table 5.2

Reaction	Relative Rate[a,b]
1	1251
2	0.1
3	94674
4	93409
5	1259
6	6.34
7	0.04
8	6.31
9	3.81
10	1×10^{-6}
11	8×10^{-6}
12	8×10^{-6}
13	187
14	187
15	2.52
16	1×10^{-6}
17	1×10^{-6}
18	1×10^{-6}
19	1×10^{-6}
20	1×10^{-6}
21	1.0
22	8×10^{-5}
23	1.0
24	6×10^{-4}

a) The rate of a reaction is calculated from the rate constant and the concentration of the appropriate species after 0.003s

b) The rate of step 23 was arbitrarily set at 1.0

and (14) is unnecessary, and that step 23 is the sole route to production of (9).

Therefore, it is necessary either to alter various Arrhenius parameters for scheme 5.3, and/or introduce extra reactions, primarily, in order to decrease the yield of (4) and increase the yield of .(9).

Whenever any Arrhenius parameters in scheme 5.3 were altered, to be consistent it was necessary to make similar alterations to analogous reactions in scheme 5.2. Therefore, the aim was not only to produce a model to reproduce the experimental results of Gaspar, [9] but, at the same time, ensure that computer simulation of scheme 5.2 still gave results in reasonable agreement with the experimentally determined ratios of (7)/(6) as shown in table 5.3.

<div align="center">

Table 5.3

Temperature/K	(7)/(6)
850	0.6
760	1.4

(initial intermediate = $Me_2Si:$)

</div>

EFFECT OF VARIATION OF ARRHENIUS PARAMETERS ON SCHEMES 5.2 AND 5.3

Disilirane ring strain energy

A major contribution to the energetics of reactions involving disiliranes is the element of ring strain overcome on closing the three membered ring (EC3), or released on opening it (EO3). EC3+EO3=ES3, the total ring strain, the value of which is unknown for disiliranes.

The results of computer modelling on scheme 5.2 showed that the calculated ratio of (7)/(6) was very sensitive to the value of EC3, which had to be 83kJ/mol, but very insensitive to the value of EO3 which was varied between 83-166kJ/mol with a negligible effect on the calculated ratio of (7)/(6).

Variation of EO3 in scheme 5.3 had a beneficial effect in that increasing the value of EO3 led to an increased yield of (9), re-investigation of scheme 5.2 showed that it was possible to increase EO3 up to 198kJ/mol (giving zero activation energy for step 12 scheme 5.2) without destroying the agreement between calculation and experiment.

Formation and Decomposition of 1,3-disilacyclobutanes

Arrhenius parameters for decomposition of 1,3-disilacyclobutanes were based on experimental measurements

of the decomposition of 1,3-dimethyl-1,3-disilacyclobutane [11] from which the following Arrhenius parameters were obtained.

$$\log k/s^{-1} = (13.5 \pm 0.2) - (255 \pm 3 kJmol^{-1}/2.303RT)$$

Experimental measurements of the decomposition of 1,3-disilacyclobutane gave the following Arrhenius parameters. [11]

$$\log k/s^{-1} = (13.3 \pm 0.3) - (230 \pm 4 kJmol^{-1}/2.303RT)$$

These results show a reduction in activation energy on replacing methyl groups with hydrogen of 25kJ/mol. A similar reduction in activation energy for step 24 of scheme 5.3 was tried, and found to have a negligible effect on the yield of (4).

Therefore the problem of overproduction of (4) was approached by reduction in the rate constants for formation of 1,3-disilacyclobutanes. From group additivity values and a measured heat of formation, the ring strain in a 1,3-disilacyclobutane has been estimated [5] to be 100kJ/mol. In combination with the experimental measurement of decomposition of 1,3-dimethyl-1,3-disilacyclobutane, [11] and the computer model of scheme 5.2, [4] EO4 and EC4 were set at 46 and 54kJ/mol respectively. The effect of increasing EC4 up to 60kJ/mol was beneficial to scheme 5.3

in that it led to an increase in the yield of (9). However, scheme 5.2 proved to be sensitive to an increase in EC4, leading to a decrease in the ratio of (7)/(6). Variation of the A-factor for ring closing reactions leading to the production of four membered rings had a similar effect, in that reduction of logA from 13.5 down to 12.9 gave a decrease in the ratio of (7)/(6) in scheme 5.2, but increased the yield of (9) in scheme 5.3.

Silylene Insertion into silicon-hydrogen bonds

As mentioned previously, the activation energy for the insertion of a silylene into a silicon-hydrogen bond is 0-12kJ/mol. By reduction of the activation energy from 12 to zero in scheme 5.3, this had a beneficial effect in that the yield of (9) was increased. The same change in scheme 5.2 led to an increase in the ratio of (7)/(6).

The effect on the computer model of scheme 5.3 of increasing EO3 to 198kJ/mol, decreasing the A-factor for reactions forming four membered rings to logA = 12.9 with corrections for the reaction path degeneracy, and decreasing the activation energy for silylene insertion reactions into silicon-hydrogen bonds from 12kJ/mol to zero, is shown in tables 5.4 and 5.5, which give the relative rates and product yields respectively. It can be seen that the yield of (9) is 54.8%, as compared to 0.08% before these changes were made.

Table 5.4

Reaction	Relative Rate
1	1.9
2	0.1
3	2261
4	2261
5	0.78
6	0.02
7	1.6×10^{-4}
8	0.02
9	0.01
10	3.6×10^{-7}
11	1.7×10^{-6}
12	1.7×10^{-6}
13	27.3
14	27.3
15	9.4×10^{-3}
16	2×10^{-7}
17	1×10^{-6}
18	5×10^{-9}
19	5×10^{-9}
20	1×10^{-5}
21	1.0
22	8×10^{-5}
23	1.0
24	1×10^{-4}

Table 5.5

Species	Yield (%)
9	54.8
4	42.8
3	1.12
6	0.77
11	0.51

The effect of making analogous changes to the computer model of scheme 5.2 was minor, in that the calculated ratios of (7)/(6), starting from a dimethylsilylene precursor at 850K and 760K were 0.7 and 1.26 respectively, in satisfactory agreement with the experimentally determined ratios of (7)/(6) shown in table 5.3.

From kinetic measurements, the silicon-allyl bond dissociation energies, in allyltrimethylsilane [12] and allylpentamethyldisilane,[13] are 305$\pm$8 and 287$\pm$6kJ/mol respectively, corresponding to a stabilisation energy of ~18kJ/mol in the pentamethyldisilanyl radical. A very similar effect has also been noted by Walsh [14] in the unsubstituted disilanyl radical. In reaction 21 of scheme 5.3, both of the bonds broken would be weakened by such an effect, but the bond formed would not. Therefore, the activation energy of reaction 21 was arbitrarily decreased by 10kJ/mol. The computer model of scheme 5.3 was very sensitive to this, the yield of (9) increasing from 55% to 85%.

Having shown that computer simulation of scheme 5.3 can lead to predominant formation of (9), to get a more realistic model, additional reactions of intermediates (2) and (3) were considered, along with any other possible decomposition routes for species (4), which was still being produced in too high a yield.

This led to the addition of reactions 25 to 39 to scheme 5.3, as shown in scheme 5.4, for which Arrhenius parameters could be estimated from analogous reactions already present in scheme 5.3. Two pathways considered, but not included in scheme 5.4 are as follows:

a) The route to (9) originally suggested by Gaspar,[9] as shown in scheme 5.1, this was discounted as it involves species (3) as shown below.

$$Me_3SiSi \overset{\triangle}{\underset{(3)}{\quad}} SiMe_2H \xrightarrow{40} Me_2Si \overset{\triangle}{\quad} SiH(CH_2SiMe_2H)$$
$$\downarrow$$
$$(9)$$
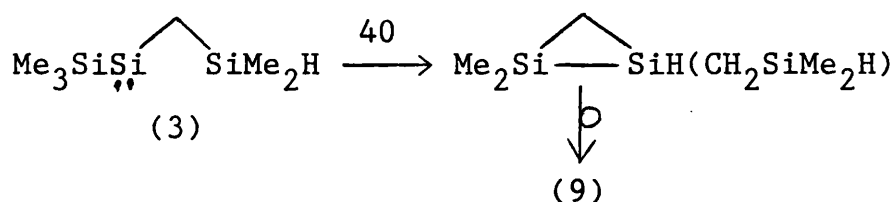
The rate constant for reaction 40 would be identical to reaction 1, which is smaller than the rate constant for reaction 5 by a factor of 120, thus indicating that this would be an extremely minor route for species (3) to follow.

b) Trimethylsilyl shift from silicon to silicon in species (2) as shown below.

$$\underset{Me_3Si}{\overset{H}{\underset{|}{Si}} \overset{\triangle}{\quad} SiMe_2} \underset{42}{\overset{41}{\rightleftharpoons}} HSi: \overset{SiMe_2}{\underset{SiMe_3}{|}} \longrightarrow H_2Si \overset{SiMe_2}{\underset{SiMe_2}{|}}$$
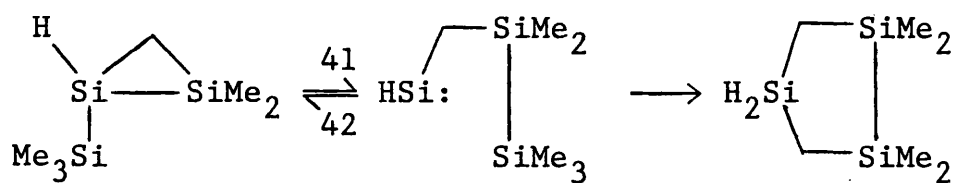
Compared to reaction 21, reaction 41 would be a minor

Scheme 5.4

Me$_3$SiSiSiMe$_3$ (1)

$\underset{2}{\overset{1}{\rightleftharpoons}}$

H(Me$_3$Si)Si—SiMe$_2$ (2)

$\underset{22\ \text{Me}_2\text{Si}}{\overset{21}{\rightleftharpoons}}$ HSi: SiMe$_3$ | SiMe$_2$ (15)

$\xrightarrow{23}$ H$_2$Si SiMe$_2$ | Me$_2$Si (9)

$\underset{4}{\overset{3}{\rightleftharpoons}}$

Me$_3$SiSiSi: SiMe$_2$H (3)

$\underset{7}{\overset{6}{\rightleftharpoons}}$

H(Me$_3$Si)Si=CH(SiHMe$_2$) (5)

$\xrightarrow{8}$ Steps 8 to 20 as in scheme 5.3

$\underset{26}{\overset{25}{\rightleftharpoons}}$ (4) (12)

$\xrightarrow{36}$ (10)—(15)

(See scheme 5.3)

HMeSi SiHMe (17) | Me$_2$Si

$\xleftarrow{29}$

(Me$_3$Si)MeHSi SiMe (16)

$\underset{33}{\overset{32}{\rightleftharpoons}}$

$\underset{28}{\overset{27}{\rightleftharpoons}}$

H(Me$_3$Si)Si SiHMe (4)

$\underset{35}{\overset{30}{\rightleftharpoons}}$ $\underset{5}{\overset{24}{\rightleftharpoons}}$

H(Me$_3$Si)SiMe(SiMe$_3$)

$\underset{34}{\overset{31}{\rightleftharpoons}}$

HMeSi—SiMe(SiMe$_3$) (18)

$\underset{38}{\overset{37}{\rightleftharpoons}}$

MeSi: HMeSi SiMe$_3$ (19)

$\xrightarrow{39}$ HMeSi SiMe$_2$ | HMeSi (20)

134
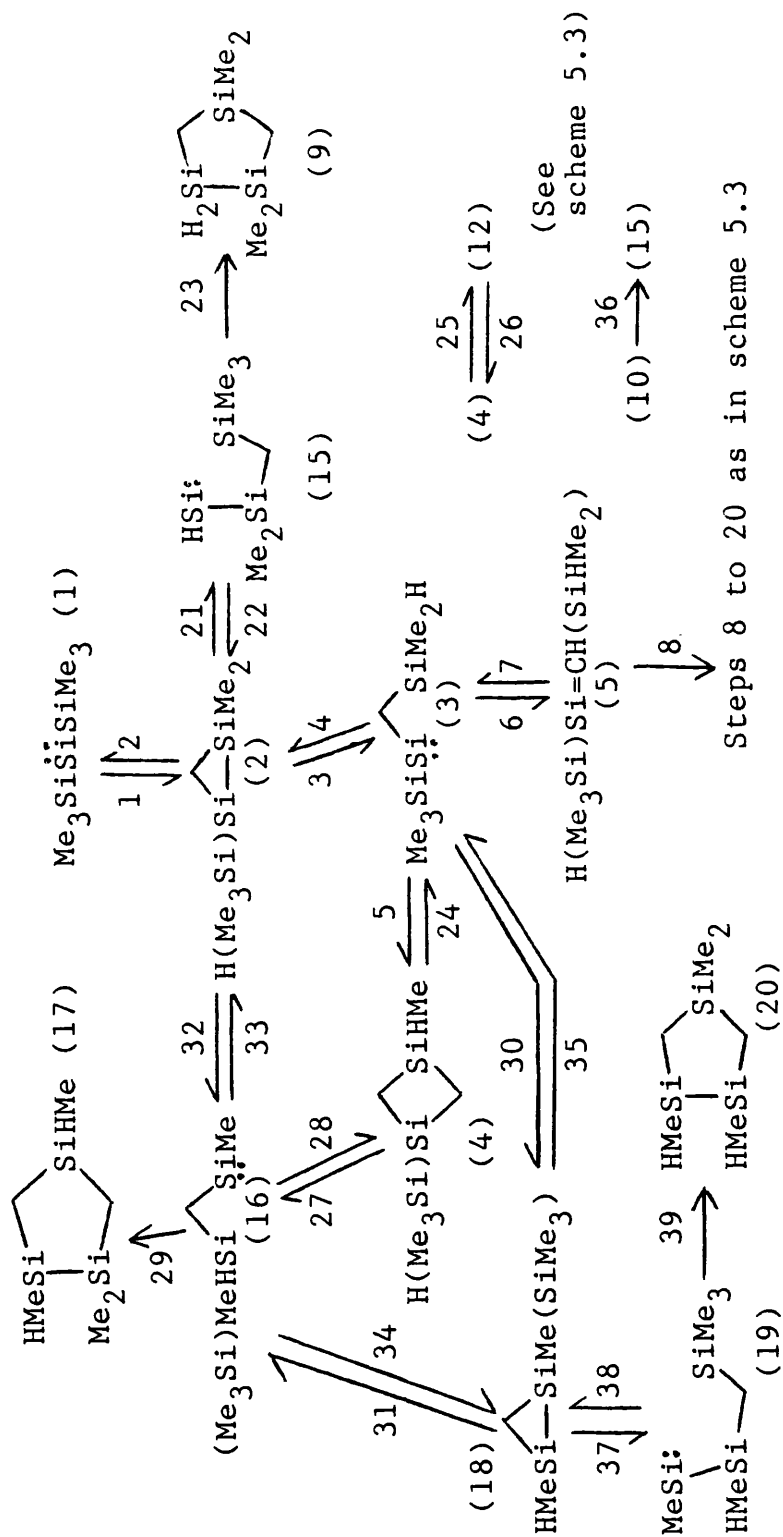
pathway, since there would be more strain energy to be overcome in forming a cyclic transition state involving three silicon atoms. Also, the reverse reaction, step 42 would be more important than reaction 22, since silylene insertion into a silicon-silicon bond has a lower activation energy than silylene insertion into a silicon-carbon bond.

Table 5.6 gives a list of Arrhenius parameters for scheme 5.4. To reduce "stiffness" in the numerical integration, it was necessary to increase $E(3)$ from 4 to 24kJ/mol, this had no adverse effect, since $k(3)$ and $k(4)$ were still by far the largest rate constants in the model. Tables 5.7 and 5.8 give the relative rates and product yields respectively, from which it can be seen that the yield of (9) is 60.6%.

This work shows that it is possible to extend the model developed by Davidson and Scampton [4] to include the rearrangement of bis(trimethylsilyl)silylene, the major modification being an increase in E03 from 83 to 194kJ/mol, giving a total disilirane ring strain energy of 277kJ/mol. This value is reasonable, since the strain energy in a substituted silirane has been estimated to be 226kJ/mol,[15] while it is known that further silicon substitution in a ring increases the strain.[5,16]

From an analysis of the relative rates in table 5.7, it is possible to produce a simplified reaction mechanism as shown

<u>Table   5.6</u>

Reaction	log A	E/kJmol^{-1}	Comments
1	12.6	165	E = 82+EC3
2	14	107	E = 301-EO3
3	13	24	see text
4	12.6	83	E = O+EC3
5	12.72	136	E = 82+EC4
6	13.5	170	
7	.13.5	170	
8	12.3	120	
9	12.9	136	E = 82+EC4
10	13.5	230	see ref 11
11	13.5	230	see ref 11
12	13	8	E = O+EC5
13	12.6	83	E = O+EC3
14	13	4	E = 198-EO3
15	12.72	136	E = 82+EC4
16	13.5	230	see 10 above
17	13.5	230	see 10 above
18	13.5	255	see 10 above
19	13	100	
20	13	100	
21	13.7	78	E = 282-EO3-10
22	12.6	145	E = 62+EC3
23	13	90	E = 82+EC5
24	13.5	230	see 10 above
25	13.7	236	E = 282-EO4
26	12.9	116	E = 62+EC4
27	13.5	230	see 10 above
28	12.42	136	E = 82+EC4
29	13	90	E = 82+EC5
30	12.9	145	E = 62+EC3
31	13	4	E = 198-EO3
32	13.7	88	E = 282-EO3
33	12.6	145	E = 62+EC3
34	12.6	83	E = O+EC3
35	13.4	88	E = 282-EO3
36	14	97	E = 301-EO3
37	13.7	88	E = 282-EO3
38	12.6	145	E = 62+EC3
39	13	90	E = 82+EC5

Table 5.7

Reaction	Relative Rate (reaction 5 = 1.0)
1	5.7
2	0.3
3	2895
4	2893
5	1.0
6	0.03
7	2×10^{-4}
8	0.03
9	0.02
10	5×10^{-7}
11	2×10^{-6}
12	2×10^{-6}
13	34.7
14	34.7
15	0.01
16	3×10^{-7}
17	1.5×10^{-6}
18	6×10^{-9}
19	6×10^{-9}
20	6×10^{-5}
21	3.26
22	2×10^{-4}
23	3.26
24	1×10^{-4}
25	8×10^{-5}
26	2×10^{-5}
27	3×10^{-5}
28	2×10^{-4}
29	1.06
30	0.37
31	1.63
32	0.7
33	8×10^{-5}
34	1.25
35	8×10^{-6}
36	2×10^{-4}
37	8×10^{-5}
38	6×10^{-9}
39	8×10^{-5}

Table 5.8

Species	Yield (%)
9	60.6
4	18.6
17	19.7

in scheme 5.5, which shows only the reactions of any consequence.

This model is still incomplete, since it does not account for the minor products, however, it should be possible to extend this scheme when information about the nature and yields of these products becomes available.

Scheme 5.5

Me₃Si$\ddot{\text{S}}$iSiMe₃ (1)

$\xrightarrow{1}$

$\underset{(2)}{\text{H(Me}_3\text{Si)Si}-\text{SiMe}_2}$

$\xrightarrow{21}$ $\underset{(15)}{\text{Me}_2\text{Si}}\overset{\text{HSi:}\quad \text{SiMe}_3}{}$

$\xrightarrow{23}$ $\underset{(9)}{\text{Me}_2\text{Si}}\overset{\text{H}_2\text{Si}\quad \text{SiMe}_2}{}$

$\overset{3}{\underset{4}{\rightleftarrows}}$

$\underset{(3)}{\text{Me}_3\text{Si}\ddot{\text{S}}\text{i}\quad \text{SiMe}_2\text{H}}$

$\xrightarrow{5}$ $\underset{(4)}{\text{H(Me}_3\text{Si)Si}\quad \text{SiHMe}}$

$\xrightarrow{32}$

$\underset{(16)}{\text{HMe(Me}_3\text{Si)Si}\quad \overset{\cdot\cdot}{\text{S}}\text{iMe}}$

$\xrightarrow{29}$ $\underset{(17)}{\text{HMeSi}\quad \text{SiHMe} \atop \text{Me}_2\text{Si}}$

$\overset{34}{\underset{31}{\rightleftarrows}}$

$\xrightarrow{30}$ $\underset{(18)}{\text{(Me}_3\text{Si)MeSi}-\text{SiMeH}}$

139
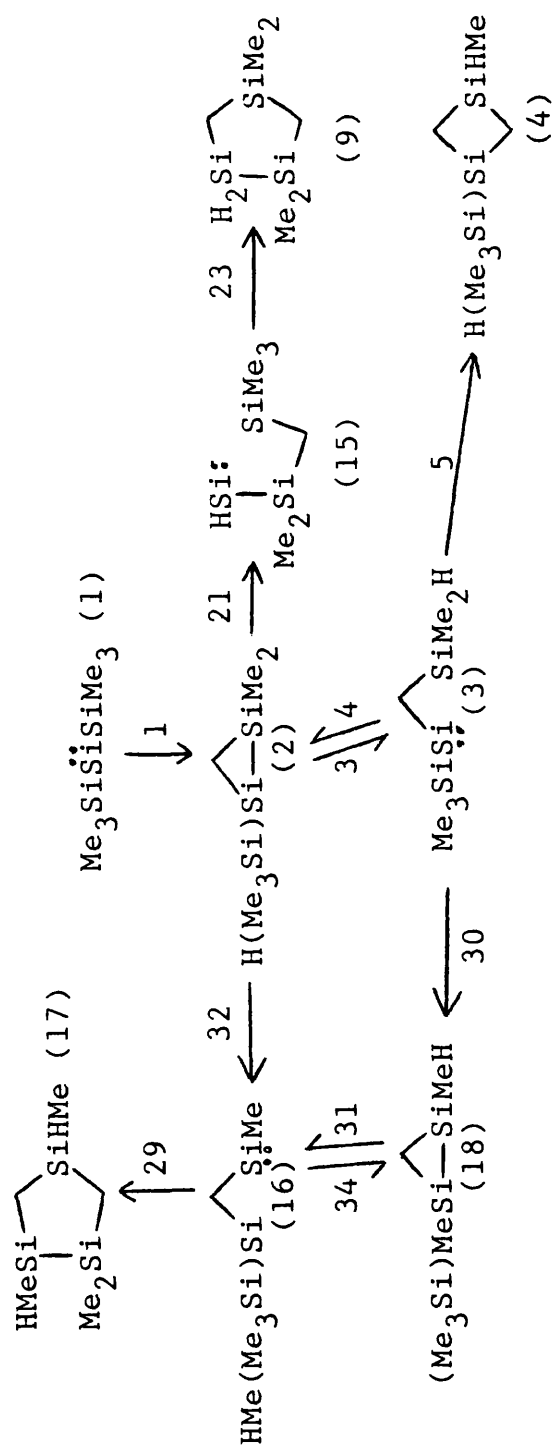
References

1. P. P. Gaspar, React. Intermed., 1985, 3, 333.
    P. P. Gaspar, React. Intermed., 1981, 2, 335.
    P. P. Gaspar, React. Intermed., 1978, I, 229.

2. A. C. Baldwin, Ph.D. thesis, Leicester, 1976.

3. I. M. T. Davidson and J. I. Matthews, J. Chem. Soc.
    Faraday Trans. I, 1976, 72, 1403.

4. I. M. T. Davidson & R. J. Scampton, J. Organomet. Chem.,
    1984, 271, 249.

5. H. E. O'Neal and M. A. Ring, J. Organomet. Chem., 1981,
    213, 419.

6. P. J. Robinson, J. Chem. Ed., 1978, 55, 509.

7. S. W. Benson, "Thermochemical Kinetics", 2nd Ed., Wiley
    (1976).

8. A. D. English and W. E. Palke, J. Am. Chem. Soc., 1973,
    95, 8536.

9. Y. S. Chen, B. H. Cohen & P. P. Gaspar, J. Organomet.
    Chem., 1980, 195, Cl.

10. I. M. T. Davidson and A. V. Howard, J. Chem. Soc.
    Faraday Trans. I, 1975, 71, 69.

11. N. Auner, I. M. T. Davidson, S. Ijadi-Maghsoodi and F.
    T. Lawrence, Organometallics, 1986, 5, 431.

12. T. J. Barton, S. A. Burns, I. M. T. Davidson, S. Ijadi-
    Maghsoodi & I. T. Wood, J. Am. Chem. Soc., 1984, 106,
    6367.

13. I. M. T. Davidson and S. Ijadi-Maghsoodi, unpublished
    work.

14. R. Walsh, Acc. Chem. Res., 1981, 14, 246.

15. D. Seyferth, D. C. Annarelli, S. C. Vick and D. P.
    Duncan, J. Organomet. Chem., 1980, 201, 179.

16. M. S. Gordon, J. Am. Chem. Soc., 1980, 102, 7419.

CHAPTER SIX

FURTHER COMPUTER MODELLING OF PYROLYSIS MECHANISMS

INTRODUCTION

This chapter describes the results of the computer modelling of three silylene reaction mechanisms. It is an extension of the previous chapter, in that it involves a reinvestigation of the methylsilene-dimethylsilylene isomerisation, and the rearrangement of bis(trimethylsilyl)silylene, incorporating further information concerning the identity and yields of some of the minor products.[1]

Where possible, Arrhenius parameters for individual reactions were calculated from a combination of estimated thermodynamic data for each species, and a set of rules provided by O'Neal,[2] summarised below. They are closely modelled on the "thermochemical kinetics" rules devised by Benson,[3] which have been successfully applied to hydrocarbon chemistry.

O'Neal's 'rules'

For a reversible unimolecular reaction:

$$\frac{A_f}{A_r} = \exp(\Delta S/R)$$

A-factor estimates for ring closing reactions

$$A = \frac{ekT}{h} \times rpd \times \exp(\Delta n^{\ddagger}irot \times 3.5/R)$$

rpd = reaction path degeneracy

$\Delta n^{\ddagger}irot$ = change in the number of internal rotors on passing

to the transition state

= (1-ring size)

A-factor estimates for silylene $\longrightarrow$ silene(disilene) isomerisation

hydrogen shifts: $A = \dfrac{ekT}{h}$ x rpd x $\exp(^-1.4/R)$

methyl and silyl shifts: $A = \dfrac{ekT}{h}$ x rpd x $\exp(^-3.6/R)$

A-factor estimates for disilane and trisilane decompositions forming silylenes by hydrogen shifts

All activation energies = 49kcal/mol

i. H_2Si: or HMeSi: elimination

hydrogen migration to SiH_3: $A = rpd \times 10^{13.6}$

hydrogen migration to silicon with R substitution:
$A = rpd \times 10^{14.2}$

ii. Me_2Si: elimination

hydrogen migration to SiH_3: $A = rpd \times 10^{13.0}$

hydrogen migration to silicon with R substitution:
$A = rpd \times 10^{13.6}$

Hydrogen elimination from disilanes and trisilanes

1,1-elimination: $A = rpd \times 10^{14.35}$

$E_a = 55.3 kcal/mol$

1,2-elimination: $A = rpd \times 10^{13.45}$

$E_a = 52.9 kcal/mol$

Silylene insertion into carbon-hydrogen bonds

	$Ea/kcalmol^{-1}$
$H_2Si:$	19
$R_3Si\ddot{S}iH$	19
$(R_3Si)_2Si:$	19
$HMeSi:$	24
$R_3Si\ddot{S}iMe$	24
$Me_2Si:$	29

Activation energies for three membered ring openings

Reaction type	$E_a/kcalmol^{-1}$
1,2-hydrogen shift from silicon to silicon	49 - E03
1,2-methyl shift from silicon to silicon	67 - E03
1,2-trimethylsilyl shift from silicon to carbon	61.9 - E03

<u>Ring strain corrections for ring opening and ring closing reactions(kcal/mol)</u>
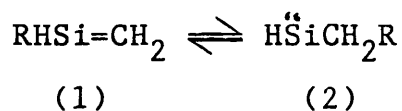
EO3 = 38

EC3 = 12

EO4 = 20

EC4 = 6

EO5 = 2

EC5 = 4

EC6 = 2

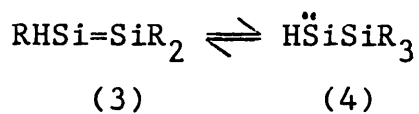<u>Activation energies (kcal/mol) for silylene - silene (disilene) isomerisations</u>

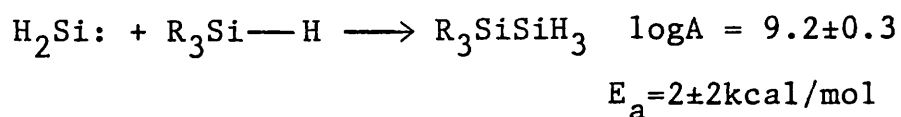$$RHSi=CH_2 \rightleftharpoons H\ddot{S}iCH_2R$$
$$\quad (1) \qquad\qquad (2)$$

reaction	R = SiH$_3$	R = H	R = Me
(1)→(2)	26.2	42.2	54.7
(2)→(1)	24.8	43	44.7

from theorectical calculations by Nagase and Kudo [4]

$$RHSi=SiR_2 \rightleftharpoons H\ddot{S}iSiR_3$$
$$\quad (3) \qquad\qquad (4)$$

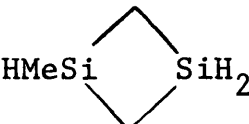| reaction	R = SiH	R = H	R = Me
(3)→(4)	14	30	43
(4)→(3)	7	23	33

144
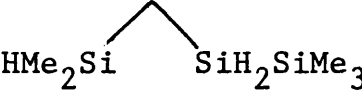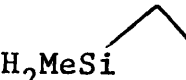
from calculations by O'Neal [2] on experimental results
obtained by Sakurai [5]

$$H_2Si: + R_3Si—H \longrightarrow R_3SiSiH_3 \quad logA = 9.2\pm0.3$$
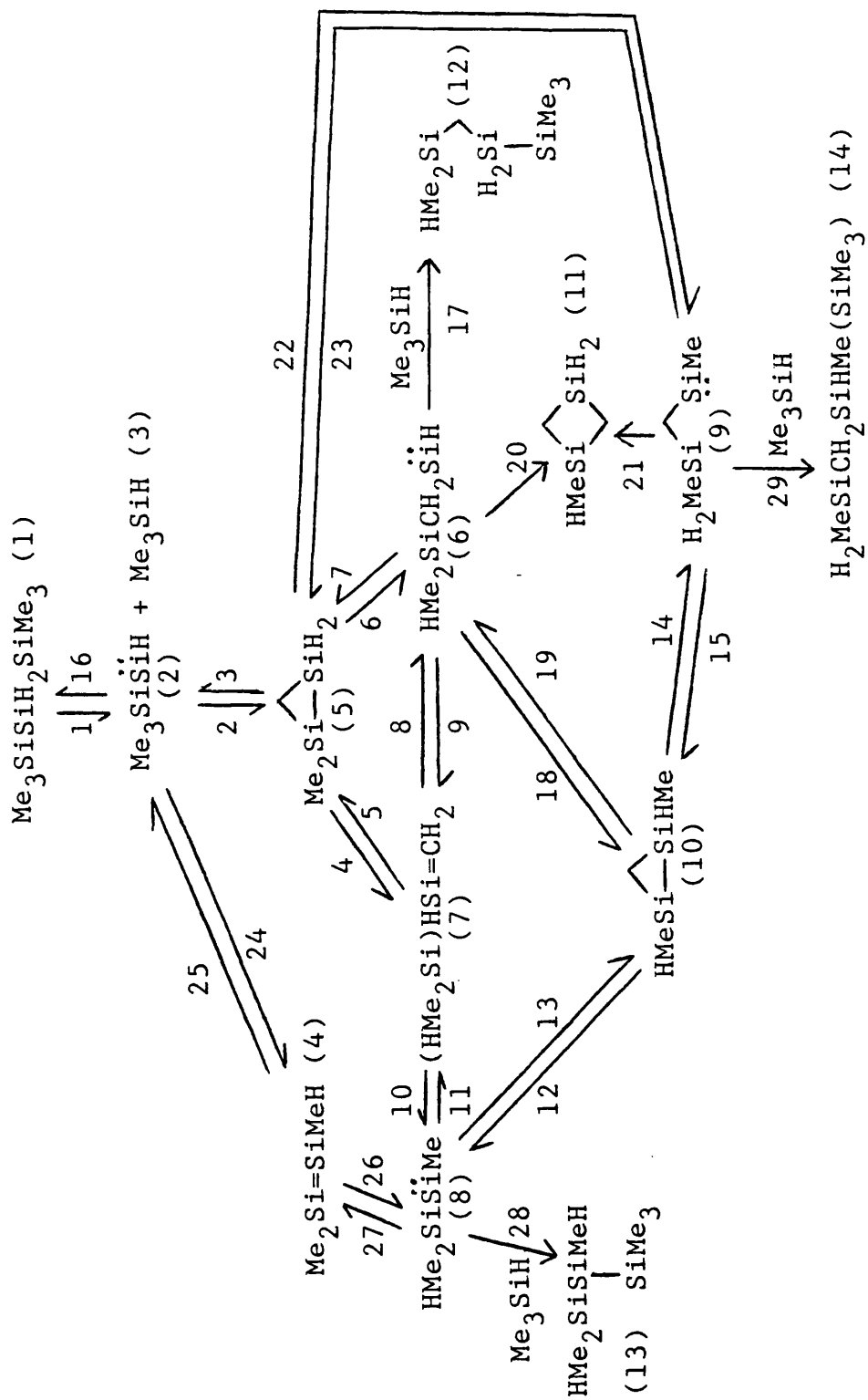$$E_a=2\pm2kcal/mol$$

RESULTS AND DISCUSSION

The first reaction mechanism to be investigated is shown in
scheme 6.1. This is based on experimental work by Gaspar
and Boo,[6] in which 1,1,1,3,3,3-hexamethyltrisilane was
subjected to gas phase flow pyrolysis at 510°C, in the
presence of a thirty-ninefold excess of trimethylsilane, and
a residence time of ca. 0.01s. Four products were isolated
in a combined yield of 26%, as shown below in Table 6.1.

Table 6.1

product	% yield	Product ratio
HMeSi⟨△⟩SiH$_2$ (11)	4	1
HMe$_2$Si⟨^⟩SiH$_2$SiMe$_3$ (12)	11	2.75
HMe$_2$SiSiHMeSiMe$_3$ (13)	7	1.75
H$_2$MeSi⟨^⟩SiMeHSiMe$_3$ (14)	4	1

145

Scheme 6.1

Me$_3$SiSiH$_2$SiMe$_3$ (1)

Me$_3$SiSiH + Me$_3$SiH (3)

Me$_3$SiSiH (2)

Me$_2$Si—SiH$_2$ (5)

(HMe$_2$Si)HSi=CH$_2$ (7)

HMe$_2$SiCH$_2$SiH (6)

Me$_3$SiH

HMe$_2$Si $\rangle$ (12)
H$_2$Si | SiMe$_3$

HMeSi SiH$_2$ (11)

H$_2$MeSi SiMe (9)

H$_2$MeSiCH$_2$SiHMe(SiMe$_3$) (14)

Me$_3$SiH

HMeSi—SiHMe (10)

Me$_2$Si=SiMeH (4)

HMe$_2$SiSiMe (8)

Me$_3$SiH

HMe$_2$SiSiMeH | SiMe$_3$ (13)

1 16 2 3 4 5 6 7 8 9 10 11 12 13 14 15 17 18 19 20 21 22 23 24 25 26 27 28 29

In addition, extra evidence was obtained for the presence of intermediates (2), (4), (6), (8) and (9), from the observed products in the presence of excess dimethylethylsilane or butadiene.

Besides providing the set of rules for estimating Arrhenius parameters for individual reactions, O'Neal also provided estimates of thermodynamic data for the species in scheme 6.1, based on Ring and O'Neal's additivity scheme [7], as shown in Table 6.2.

From the thermodynamic data in Table 6.2, along with the rules for estimation of Arrhenius parameters given earlier, it was possible to calculate Arrhenius parameters for each reaction in scheme 6.1, the results of which are given in Table 6.3.

Computer simulation of scheme 6.1, using the Arrhenius parameters in Table 6.3, gives the relative rate of each reaction, also shown in Table 6.3, and the relative yields of the four experimentally observed products, shown in Table 6.4.

It was decided to try and simulate the relative yields of the products, rather than absolute yields, because the absolute yields would be affected by loss of reactive intermediates to the walls of the reaction vessel, and it was possible, just, by the inclusion of 'wall loss

Table 6.2

Species	ΔH_f°/kcalmol^{-1}	S°/calmol^{-1}K^{-1}
Me$_3$Si$\ddot{S}$iH	17.9	93.2
Me$_2$Si$\overset{\triangle}{\frown}SiH_2$	12.4	90.2
HMe$_2$Si$\diagdown$ Si=CH$_2$ $\diagup$ H	12.8	97.9
HMe$_2$Si$\overset{\frown}{\quad}$S$\ddot{\text{i}}$H	10.5	99.2
Me$_2$Si=SiMeH	7.9	94.3
HMe$_2$Si$\ddot{S}$iMe	14.8	97.1
HMeSi$\overset{\frown}{\quad}$SiHMe	12.6	90.3
H$_2$MeSi$\overset{\frown}{\quad}$S$\ddot{\text{i}}$Me	10.5	99.4

Table 6.3

Arrhenius parameters and relative rates for the reactions in scheme 6.1.

Reaction	logA	Ea/kcalmol^{-1}	Relative rate	Comments
1	14.8	49	6.21	
2	13.07	31	3.47	E = 19+EC3
3	13.77	36.5	2.2×10^{-3}	
4	13.8	14	4432	
5	12.12	13.6	4569	
6	14.08	11	58072	E = 49-EO3
7	12.12	12.9	57931	
8	13.14	26.2	14.55	
9	12.86	24.8	151.8	
10	13.64	42.2	1.6×10^{-3}	
11	13.82	43	1.73×10^{-3}	
12	12.9	36	0.019	E = 24+EC3
13	14.38	38.2	1.3×10^{-3}	
14	14.41	11	54312.8	E = 49-EO3
15	12.42	13.1	54312.3	
16	9.2	3	1.14	
17	9.2	3	1.61	
18	12.42	31.1	0.96	
19	14.36	29	0.46	E = 67-EO3
20	12.13	30	1.00	E = 24+EC4
21	11.83	35	0.01	E = 29+EC4
22	14.12	29	0.602	E = 67-EO3
23	12.11	31.1	0.25	
24	13.34	33	1.67	
25	13.1	43	0.06	
26	13.06	30	219.3	
27	13.34	23	219	
28	9.2	3	0.24	
29	9.2	3	0.86	

Table 6.4

Product	Relative yield
(11)	1
(12)	1.6
(13)	0.36
(14)	0.85

reactions' of reactive intermediates, to produce a wide range of product yields by arbitrary variation of the rate of such reactions, for which no data are available.

The main errors between the calculated relative yields (Table 6.4) and the experimentally observed relative yields (Table 6.1), are in the quantities of species (12) and (13) produced. From the relative rate data given in Table 6.3, it can be seen that species (13) is produced almost entirely via the disilene intermediate, species (4). Therefore, in an attempt to increase the relative yield of species (13), the activation energies for silylsilylene-disilene isomerisation reactions were arbitrarily decreased by 2kcal/mol. This was reasonable, since the values given in O'Neal's rules were the result of calculations by O'Neal,[2] based on non-kinetic experimental results obtained from sealed tube pyrolyses of disilene and silylsilylene precursors, in the presence of a diene trap,[5] these give the possibility of significant errors being present in the calculated results. The effect on the relative yields of making this change is shown in Table 6.5 below.

Table 6.5

product	relative yield
(11)	1
(12)	1.6
(13)	1.14
(14)	0.86

150

Table 6.6

Revised Arrhenius parameters, and relative rates for scheme 6.1.

Reaction	logA	Ea/kcalmol^{-1}	Relative rate	Comments
1	14.8	49	13.86	
2	13.07	31	4.53	E = 19+EC3
3	13.77	36.5	2.2×10^{-3}	
4	13.8	14	4432	
5	12.12	13.6	4569	
6	14.08	11	58073	E = 49-EO3
7	12.12	12.9	57931	
8	13.14	26.2	14.57	
9	12.86	24.8	151.8	
10	13.64	42.2	1.6×10^{-3}	
11	13.82	43	7.3×10^{-3}	
12	12.9	36	0.08	E = 24+EC3
13	14.38	38.2	1×10^{-3}	
14	14.41	11	43018.3	E = 49-EO3
15	12.42	13.1	43017.6	
16	9.2	2.3	2.33	see text
17	9.2	2.3	2.53	see text
18	12.42	31.1	0.96	
19	14.36	29	0.36	E = 67-EO3
20	12.13	30	1.00	E = 24+EC4
21	11.83	35	8.5×10^{-3}	E = 29+EC4
22	14.12	29	0.6	E = 67-EO3
23	12.11	31.1	0.2	
24	13.34	31	7.87	see text
25	13.1	41	0.86	see text
26	13.06	28	3352	see text
27	13.34	21	3350.8	see text
28	9.2	2.3	1.61	see text
29	9.2	2.3	1.07	see text

The only change is an increase in the relative yield of species (13) as desired. However, the relative yields of species (12), (13), and (14) are all too low. Since species (12), (13) and (14) are all produced by silylene insertion into a silicon-hydrogen bond, increasing the rate of silylene insertion into silicon-hydrogen bonds was found to improve the calculated product ratios. Thus by reducing the activation energy for silylene insertion into silicon-hydrogen bonds from 3.0 to 2.3kcal/mol, a set of Arrhenius parameters for scheme 6.1 shown in Table 6.6 was obtained, which led to the relative rates, also given in Table 6.6, and the relative product yields in Table 6.7 below.

Table 6.7

product	relative yield
(11)	1
(12)	2.51
(13)	2.19
(14)	1.08

This shows that with a ⹁ minor alteration to the silylsilylene-disilene activation energies, along with a slight adjustment of the rate of silylene insertion into silicon-hydrogen bonds, it was possible from scheme 6.1 to reasonably reproduce the experimentally observed results, which provides additional evidence for the intermediacy of $Me_2Si=SiHMe$ in the transposition of Me_3SiSiH to $HMe_2SiSiMe$.[6]

Bis(trimethylsilyl)silylene isomerisation

It was decided to reinvestigate [8,9,10] the bis(trimethylsilyl)silylene isomerisation, taking into account additional information concerning the yield and identity of some of the minor products.[1] Table 6.8 summarises all of the presently available experimental results.

Table 6.8

product	yield	relative yield
H_2Si—$SiMe_2$—Me_2Si (5)	60%	1.0
H—Si—Me, Me_2Si, SiH_2 (15)	5%	0.083
$HMeSi$—SiH_2, $SiMe_3$ (18)	⩽5%	⩽0.083
Me_2Si—SiH_2, $SiHMe_2$ (19)	5%	0.083

Following on from the work in the previous chapter, scheme 6.2 was devised, which provides a mechanism to account for the production of all the observed products.

Estimated thermodynamic data for individual species in scheme 6.2 were again provided by O'Neal,[2] and are given in Table 6.9.

Table 6.9

species	$\Delta H_f^{\circ}/kcalmol^{-1}$	$S^{\circ}/calmol^{-1}K^{-1}$
(2)	-34.6	133.3
(3)	-33.5	132
(4)	-33.1	140
(6)	-32.6	140.5
(8)	-32	141.4
(10)	-34.3	132.2
(13)	-37.9	134
(14)	-37.8	143.3
(16)	-37.7	131.8
(17)	-37.6	142.3

By application of the rules for estimating Arrhenius parameters, along with the thermodynamic data in Table 6.9, a set of Arrhenius parameters for the reactions in scheme 6.2 was obtained, as given in Table 6.10. From the computer modelling, the relative rates given in Table 6.10 were obtained, along with the relative product yields given in Table 6.11.

Scheme 6.2

R (1)

$Me_3SiSiSiMe_3$ (2)

$HSi:$ (4)

1

2 3

2/3

4

5

6

7

8

9

10 11

12

13 14

15 16

17 18

19 20

21

22

23

24

25 26

27

28

(Me$_3$Si)HMeSiCH$_2$SiMe (6)

Me(Me$_3$Si)Si—SiHMe (10)

H(Me$_3$Si)Si—SiHMe (9)

Me$_3$SiSi: (8)

HMeSi—SiHMe$_2$

HMeSi / Me$_2$Si SiHMe (7)

H$_2$Si / Me$_2$Si SiMe$_2$ (5)

Me$_2$Si—SiMe$_3$ (3)

H$_2$Si—Si—SiMe$_3$, Me (13)

H—Si(Me)—SiMe$_3$, HSi: SiMe$_3$ (14)

H—Si(Me) / H$_2$Si SiMe$_2$ (15)

Me$_2$Si—SiH$_2$ SiMe$_3$ (16)

HMe$_2$Si—SiH: SiMe$_3$ (17)

H$_2$Si / SiMe$_2$ SiMe$_2$H (19)

HMeSi / SiH$_2$ SiMe$_3$ (18)

Me$_3$SiH + :Si SiHMe (12)

Me$_3$SiH + :Si SiHMe (11)

155

Table 6.10

Initial set of Arrhenius parameters applicable to scheme 6.2.

Reaction	logA	Ea/kcalmol^{-1}	Relative rate	Comments
1	14.68	49	0.32	
2	13.37	31	0.33	E = 19+EC3
3	13.65	29.9	0.012	
4	13.86	23.9	1.0	E = 61.9-EO3
5	12.11	23.5	0.7	
6	11.54	23	0.26	E = 19+EC5
7	13.97	29	0.047	E = 67-EO3
8	12.11	28.1	0.046	
9	11.54	33	5×10^{-4}	E = 29+EC5
10	14.16	11	8855	E = 49-EO3
11	12.11	9.5	8855	
12	12.12	30	0.014	E = 24+EC4
13	12.41	26.7	0.242	
14	14.42	29	0.243	E = 67-EO3
15	13.92	11	9424	E = 49-EO3
16	12.11	9.3	9424	
17	12.41	31	0.011	E = 19+EC3
18	14.2	35.6	7×10^{-5}	
19	14.4	11	1016	E = 49-EO3
20	12.11	10.9	1016	
21	12.13	30	4×10^{-3}	E = 24+EC4
22	12.3	30	6×10^{-3}	E = 24+EC4
23	12.89	31	0.032	E = 19+EC3
24	14.2	35.8	1.4×10^{-3}	
25	14 14	11	12435	E = 49-EO3
26	12.11	10.9	12435	
27	10.77	26	0.031	E = 24+EC6
28	13.6	49	2×10^{-5}	

Initial reactant concentration = 2×10^{-5} moldm^{-3}

Reaction time = 0.01s

Reaction temperature = 773K

Rates calculated at 0.003s

Table 6.11

product	relative yield
(5)	1.0
(7)	0.002
(9)	0.056
(15)	0.113
(18)	0.016
(19)	0.024

Discrepancies between the calculated relative product yields in Table 6.11, and the experimentally observed relative product yields in Table 6.8, are an excess of species (15), and a lack of species (18) and (19).

After further examination of scheme 6.2, it was apparent that to produce a more realistic model, several more reactions of species (14) should be included, which would have the effect of reducing the quantity of species (15) produced. Thus, four extra reactions of species (14) were added, as shown in scheme 6.3. The rules for the estimation of Arrhenius parameters, given earlier in this chapter, were used to calculate Arrhenius parameters for reactions 29 and 32, and A-factors for reactions 30 and 31. The activation energy for reaction 30 was calculated by using Ring and O'Neal's additivity tables,[7] to estimate the heat of formation of species (7), and hence allow ΔH for reaction 30 to be estimated, which along with application of O'Neal's rules to the reverse of reaction 30, allows the activation energy of reaction 30 to be calculated. The activation

Scheme 6.3
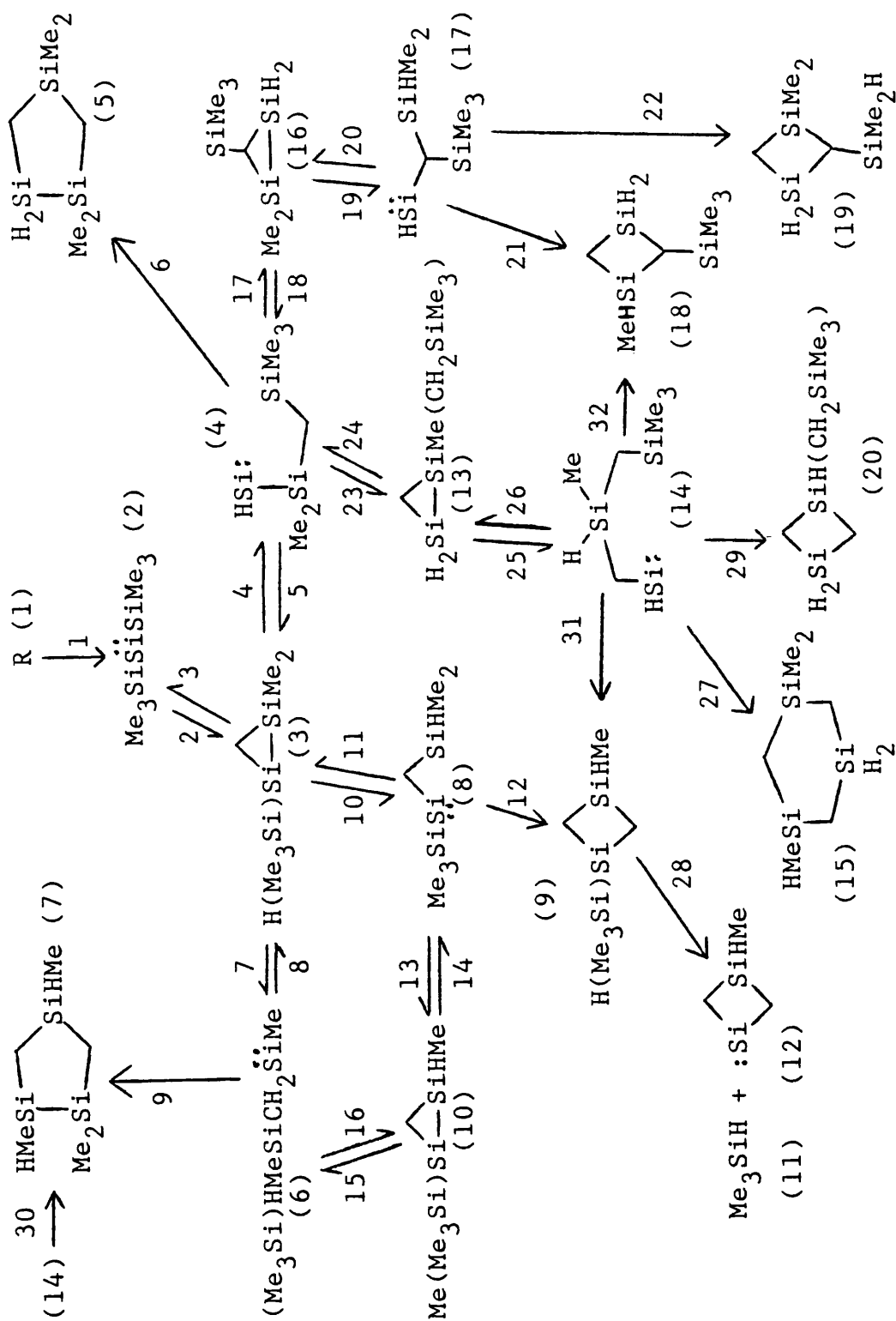
energy of reaction 31, was based on the activation energy for reaction 5, since they are similar types of reaction, with a correction for the different size of ring produced. Table 6.12 gives a list of the Arrhenius parameters for the additional reactions added to scheme 6.2, as shown in scheme 6.3.

<div align="center">Table 6.12</div>

reaction	logA	$E_a/kcalmol^{-1}$
29	11.82	30
30	11.06	20.6
31	11.35	17.5
32	11.65	30

The results of the computer simulation of scheme 6.3 are shown in Tables 6.13 and 6.14 which give the relative rates and relative product yields respectively.

Tables 6.13 and 6.14 show that the major effects of the additional reactions in scheme 6.3, are a reduction in the relative yield of species (15) to the point where it is a negligible product, the main cause of this change being the fact that the rate of reaction 31 is approximately 1000x greater than the rate of reaction 27. An additional consequence of this is the prominence of species (9), whereas it was not a product identified from the experimental work.[1]

Table 6.13

Relative rates of each reaction in scheme 6.3 using the Arrhenius parameters from tables 6.10 and 6.12.

Reaction	Relative rate
1	0.317
2	0.33
3	0.0124
4	1.0
5	0.698
6	0.26
7	0.0466
8	0.0456
9	5×10^{-4}
10	8855
11	8855
12	0.0145
13	0.242
14	0.243
15	9424
16	9424
17	0.0105
18	7.1×10^{-5}
19	1014.7
20	1014.7
21	0.0042
22	0.0063
23	0.0319
24	1.4×10^{-6}
25	12.61
26	12.58
27	3.1×10^{-5}
28	7.3×10^{-5}
29	2.6×10^{-5}
30	0.0203
31	0.0298
32	1.74×10^{-5}

Table 6.14

Relative product yields for scheme 6.3, using Arrhenius
parameters in Tables 6.10 and 6.12.

product	relative yield
(5)	1
(7)	0.0097
(9)	0.169
(15)	1×10^{-4}
(18)	0.016
(19)	0.024
(20)	9×10^{-5}

This highlights a problem with the rules for the estimation
of Arrhenius parameters, because there was no other obvious
route to species (15). Thus to make reaction 27 competitive
with reaction 31 would require a reduction in the rate of
reaction 31 by a factor of approximately 1000, or a
corresponding increase in the rate of reaction 27. This
requires an alteration in the A-factor by a factor of 1000,
or an activation energy change of 10.6kcal/mol. The most
reasonable parameters to change in order to achieve this,
are the A-factors for ring closure. These were obtained
from the following equation.

$$A = \frac{ekT}{h} \times rpd \times \exp(\Delta S^{\ddagger}/R)$$

$\Delta S^{\ddagger}$ is the change in entropy on passing from the open chain
to the transition state on the way to ring formation, the

value of which, was estimated from the change in the number of internal rotors, on passing to the transition state, with a decrease in entropy of 3.5 e.u./rotor. The change in the number of internal rotors on passing to the transition state, is related to the ring size by the following equation.

$$\Delta n^{\ddagger}irot = 1\text{-ring size}$$

Hence the A-factor for ring closing is given by:

$$A = \frac{ekT}{h} \times rpd \times \exp(3.5 \times (1\text{-ring size})/R)$$

However, as the size of the ring produced increases, it may no longer be valid to assume an entropy decrease of 3.5 e.u./rotor. This would have the effect of increasing the A-factor for formation of a six-membered ring, which would be a desired effect. In addition, the activation energies for reactions 27 and 31 could be in error, especially for reaction 31, which was based on the estimated heats of formation of species (3) and (4), along with the estimated activation energy of reaction 4. Thus, further investigation may resolve the problem of insufficient formation of species (15).

Another observation from the calculated product yields in

Table 6.15

Reaction	logA	Ea/kcalmol^{-1}	Relative Rate	Comments
1	14.68	49	0.336	
2	13.36	31	0.349	E = 19+EC3
3	13.65	29.9	0.0124	
4	13.86	23.9	1.0	E = 61.9-EO3
5	12.11	23.5	0.679	
6	11.54	23	0.253	E = 19+EC5
7	13.97	29	0.0466	E = 67-EO3
8	12.11	28.1	0.0456	
9	11.54	33	5.1×10^{-4}	E = 29+EC5
10	14.16	11	8855	E = 49-EO3
11	12.11	9.5	8855	
12	12.12	30	0.0145	E = 24+EC4
13	12.41	26.7	0.242	
14	14.42	29	0.243	E = 67-EO3
15	13.92	11	9424	E = 49-EO3
16	12.11	10.9	9424	
17	12.41	29	0.0377	E = 19-2+EC3 a
18	14.2	35.6	2.5×10^{-4}	
19	14.4	11	3629	E = 49-EO3
20	12.11	10.9	3629	
21	12.13	30	0.0151	E = 24+EC4
22	12.3	30	0.0224	E = 24+EC4
23	12.89	31	0.031	E = 19+EC3
24	14.2	35.8	1.4×10^{-6}	
25	14.14	11	12.25	E = 49-EO3
26	12.11	10.9	12.21	
27	10.77	26	3×10^{-5}	E = 24+EC6
28	13.6	49	7.2×10^{-5}	
29	11.82	30	2.5×10^{-5}	E = 24+EC4
30	11.06	20.6	0.00197	E = 16.6+EC5
31	11.35	17.5	0.0289	
32	11.65	28	6×10^{-5}	E = 24-2+EC4 a

a : insertion into 2° C-H

Table 6.14, was that species (18) and (19) were produced in insufficient quantity. However, this problem was easily overcome, by reducing the activation energy for reaction 17 by 2kcal/mol. This may be justified, since the reaction involves silylene insertion into a secondary carbon-hydrogen bond, which may be expected to be an easier process than silylene insertion into a primary carbon-hydrogen bond.

Tables 6.15 and 6.16 give the final set of Arrhenius parameters, relative rates, and relative product yields, applicable to scheme 6.3.

Table 6.16

product	relative yields
(5)	1
(7)	0.0097
(9)	0.17
(15)	1.5×10^{-4}
(18)	0.059
(19)	0.0876
(20)	9×10^{-5}

The results in Tables 6.15 and 6.16, show that application of O'Neal's rules for estimating Arrhenius parameters, with only a minor modification discussed earlier, give calculated results for the relative yields of species (5), (18) and (19) in good agreement with the experimental results. However, as discussed earlier, the rules in their present form do not account for the production of species (15), and

they also predict that species (9) is a significant product. .
However, this may not be a problem, as the original
experimental work gave at least nine products [8] of which
only four have been identified at present.

Methylsilene-dimethylsilylene isomerisation

The next reaction mechanism to which the rules for the
estimation of Arrhenius parameters were applied, was the
methylsilene-dimethylsilylene isomerisation, as investigated
by Davidson and Scampton.[11]

The initial reaction mechanism is given in scheme 6.4.
Thermodynamic data for individual species in scheme 6.4
given in Table 6.17, were provided by O'Neal,[2] or
calculated from the thermodynamic data in Table 6.2,
modified by the use of Ring and O'Neal's additivity
Tables.[7]

From a combination of experimental measurements, the
thermodynamic data in Table 6.17, and O'Neal's rules for the
estimation of Arrhenius parameters an initial set of
Arrhenius parameters for the reactions in scheme 6.4 were
obtained, and shown in Table 6.18.

Scheme 6.4

HMeSi⊐ (12)

Me$_3$SiSi(OMe)Me$_2$ (1)

$\downarrow$ 22

$\downarrow$ 1

HMeSi=CH$_2$ (3) $\underset{3}{\overset{2}{\rightleftarrows}}$ Me$_2$Si: (2)

HMeSi=CH$_2$ ⟋ 4

Me$_2$Si: $\underset{6}{\overset{}{\rightleftarrows}}$ 20

HMeSi△SiHMe (4)

Me$_2$Si=SiMe$_2$ (6)

7 ⫽ 23

16 ‖ 17

Me$_3$SiṠiMe $\underset{9}{\overset{8}{\rightleftharpoons}}$ (Me$_3$Si)HSi=CH$_2$ (7) (8)

5

10 ⫽ 11

21 ‖ 24

HMe$_2$Si△SiMe (10) $\underset{13}{\overset{12}{\rightleftarrows}}$ Me$_2$Si—SiMeH (5) $\underset{15}{\overset{14}{\rightleftarrows}}$ Me$_3$Si△SiH (9)

18 ‖ 19

Me$_2$Si◇SiH$_2$ (11)
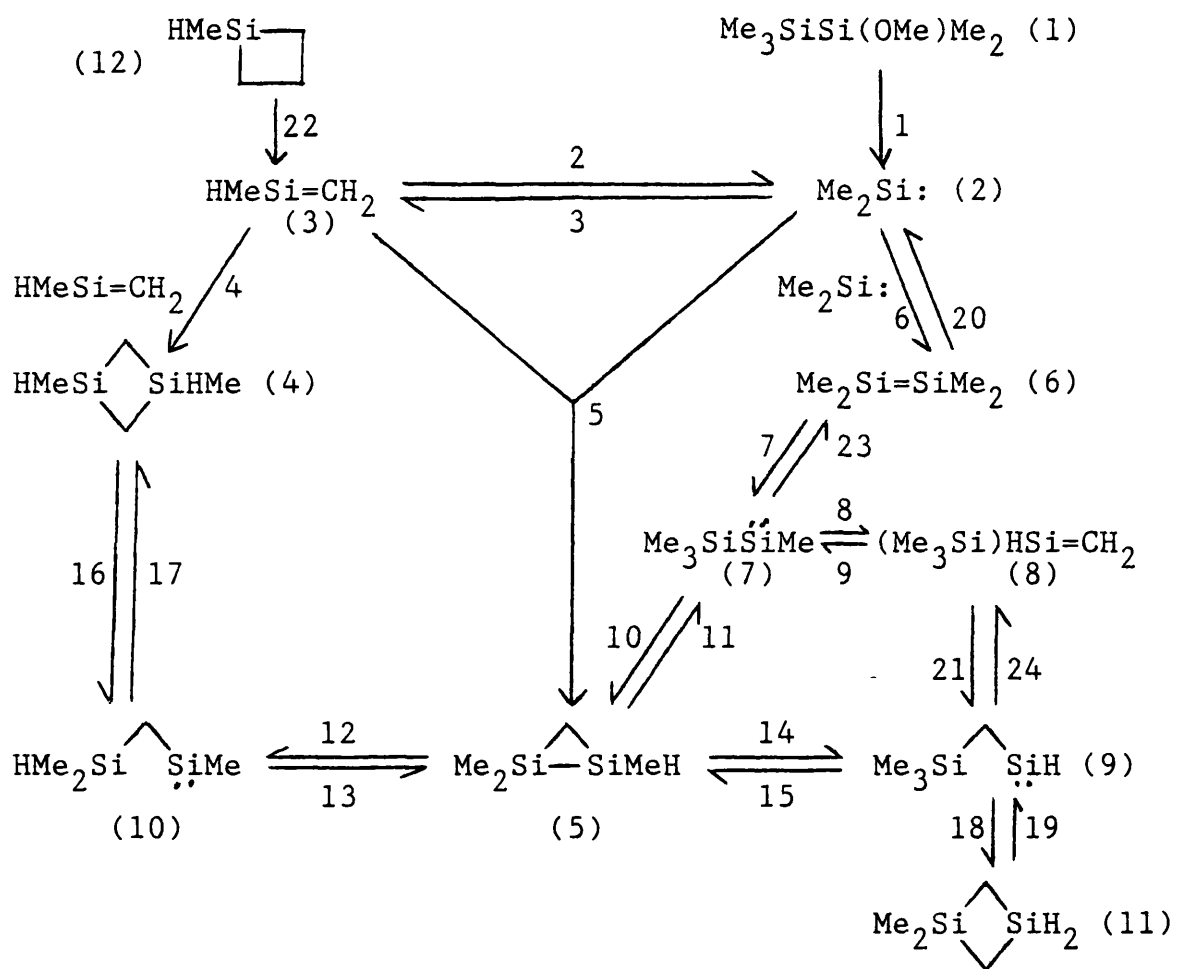
Table 6.18

Initial Arrhenius parameters for scheme 6.4.

Reaction	logA	Ea/kcalmol^{-1}	Comments
1	13.5	52	see reference 11
2	14.04	42.2	
3	14.13	43	
4	6.6	0	see reference 12
5	10	0	see reference 10
6	10	0	see reference 10
7	13.39	41	a
8	13.83	43	
9	14.11	42.2	
10	13.08	36	E = 24+EC3
11	14.49	39.05	
12	14.2	11	E = 49-EO3
13	12.13	12.55	
14	13.82	29	E = 67-EO3
15	12.61	30.65	
16	13.5	61	see reference 13
17	12.14	35	E = 24+EC4
18	12.32	30	E = 24+EC4
19	13.3	55	see reference 13
20	16.2	63	
21	12.96	26.2	
22	15.4	62.5	see reference 14
23	13.35	31	a
24	12.87	24.8	

a : activation energy 2kcalmol^{-1} less than value given in

O'Neal's rules, in order to be consistent with

earlier results from scheme 6.1.

Initial reactant concentration = 2×10^{-5}moldm^{-3}

Reaction time = 9s

Table 6.17

species	$\Delta H_f^o/\text{kcalmol}^{-1}$	$S^o/\text{calmol}^{-1}\text{K}^{-1}$
(2)	24.5	70.4
(3)	24.5	70
(5) *	-5.05	99.34
(6)	-14.2	105.6
(7)	-2	105.8
(8)	-6	104.5
(9) *	-6.7	104.89
(10) *	-6.6	108.22

* : thermodynamic data obtained from Table 6.2, with modifications using additivity tables.

Experimental measurements of the ratio of species (11)/species (4), were originally reported by Davidson and Scampton. [11] However, more recent measurements have been performed,[12] and are given below in Table 6.19

Table 6.19

Temperature/K	Precursor	Ratio of (11)/(4)
760	(1)	1.5
850	(1)	0.7 - 1.0
760	(12)	0.4
850	(12)	0.4

Computer simulation of scheme 6.4, using the parameters in Table 6.18, gave the results shown overleaf in Table 6.20.

Table 6.20

Temperature/K	Precursor	Ratio of (11)/(4)
760	(1)	3.41
850	(1)	1.43
760	(12)	3.38
850	(12)	1.64

The calculated results in Table 6.20 disagree with the experimental results in two respects. The calculated ratio is too high overall, and there is no significant difference in the results from either precursor.

The calculated results are useful however, in that an analysis of the rate of each reaction highlights the important areas of the mechanism, from which an obvious conclusion was that reaction 4 was a trivial source of species (4).

The greatest uncertainty in the Arrhenius parameters in Table 6.18, was for reaction 5, which was an estimated value based on a comparison with carbene chemistry,[11] and reaction 6, which was based on estimated Arrhenius parameters for the dimerisation of $H_2Si:$ and $HMeSi:$.[16]

Since reaction 4 was trivial, it follows that any difference in the calculated ratio, which is dependent on the choice of precursor, will be controlled by differences in the rate of reactions 5 and 6, from each precursor.

However, with the Arrhenius parameters in table 6.18, the calculated ratio of (11)/(4) was found to be insensitive to large variations of Arrhenius parameters for reactions 5 and 6. This indicated that, to make any progress, changes would have to be made to reactions involving species (5), (7), (8) and (9).

From the cycle of reactions involving species (5), (9), (8) and (7), it was apparent that there was a large difference between the heat of formation of species (7), as given in table 6.17, and the heat of formation of species (7), as calculated from the activation energies of reactions 24, 21, 9 and 8. Thus it was decided to leave the heats of formation of species (5) and (9) unchanged, and use the activation energies for reactions 24, 21, 9 and 8, to give the heats of formation of species (8) and (7), and make an alteration to the activation energy of reaction 11, in light of the new value of the heat of formation of species (7).

This gave new values of the heat of formation for species (8) and (7), of -8.1 and -8.9kcal/mol respectively; and a new activation energy for step 11 of 32.15kcal/mol. This by itself had a negligible effect on the calculated ratio of (11)/(4). Further analysis of the calculated rates of reaction indicated that progress might be made if interconversion of species (5) and (7), and (5) and (9), was made more difficult. An obvious way of going about this was to increase the value of EC3, and reduce the value of EO3.

Thus EC3 was increased by 2kcal/mol to 14kcal/mol, and EO3 reduced by 2kcal/mol to 36kcal/mol. These changes increased the activation energies of reactions 10 to 15 by 2kcal/mol, which had a beneficial effect on the calculated ratios of (11)/(4). However, the values of EC3 and EO3 were left unchanged, since to be consistent, any changes to EC3 and EO3 would also have to be made in schemes 6.1 and 6.3, and the relative product yields in scheme 6.1 were found to be very sensitive to small variations in EC3 and EO3.

Therefore, a different approach was adopted, and it was decided to arbitrarily introduce an extra substituent effect to the insertion of silylenes into carbon-hydrogen bonds. For a silylene $R_1R_2Si:$, if R_1 was a silyl group, then the activation energy for insertion of the silylene into a carbon-hydrogen bond was increased by 2kcal/mol, and if R_2 was also a silyl group, then the increase in activation energy was 4kcal/mol. This led to a new set of activation energies for silylene insertion into carbon-hydrogen bonds, as shown in table 6.21.

These changes do not affect scheme 6.1, however they do alter activation energies for some reactions in scheme 6.3, but they make no significant change to the calculated product yields for scheme 6.3 discussed earlier.

In scheme 6.4, only reactions 10 and 11 are affected by this change, both being increased by 2kcal/mol to 38 and

171

34.15kcal/mol respectively. Thus with the Arrhenius parameters as given in table 6.18, with the exception of reactions 10 and 11 as discussed above, the calculated ratios of (11)/(4) are shown in table 6.22.

Table 6.21

Revised activation energies for the insertion of silylenes into carbon-hydrogen bonds.

Silylene	$Ea/kcalmol^{-1}$
$H_2Si:$	19
R_3SiSiH	21
$(R_3Si)_2Si:$	23
$HMeSi:$	24
$R_3SiSiMe$	26
$Me_2Si:$	29

Table 6.22

Temperature/K	Precursor	Ratio of (11)/(4)
760	(1)	3.61
850	(1)	1.57
760	(12)	3.5
850	(12)	1.79

By comparison with the calculated results in table 6.20,

this can be seen to still have a negligible effect. So the next change that was implemented was an arbitrary increase in the activation energy of reaction 14 by 1.5kcal/mol. This led to a dramatic reduction in the calculated ratios of (11)/(4), as shown in table 6.23.

Table 6.23

Temperature/K	Precursor	Ratio of (11)/(4)
760	(1)	1.41
850	(1)	0.68
760	(12)	1.36
850	(12)	0.79

This represents a big improvement, the calculated ratios of (11)/(4) from precursor (1) being now in good agreement with the experimental results, but there is still very little differentiation between the calculated ratios from either species (1) or (12). In order to try and rectify this, the effect of varying Arrhenius parameters for reactions 5 and 6 was reinvestigated, along with the effect of changes to Arrhenius parameters for the silene-silylene isomerisation.

The calculated ratios still proved to be insensitive to changes in Arrhenius parameters for reactions 5 and 6, but it was noticed that a greater difference in the calculated ratios, which was dependent on the choice of precursor,

173

could be achieved to some extent by increasing the A-factors for both reactions 5 and 6.

An alternative method of achieving the same effect would be to slow down the interconversion of silenes and silylenes. This can be achieved by a reduction of the A-factors for silene-silylene isomerisation, which is reasonable, since these are based on an estimate by Walsh [16] from structurally similar processes and transition state theoretical arguments, and thus subject to some error. Therefore, the A-factors for reactions 2, 3, 8 and 9, involving silene-silylene isomerisation via hydrogen migration, were reduced by $10^{0.5}$, the new calculated ratios being given in table 6.24.

Table 6.24

Temperature/K	Precursor	Ratio of (11)/(4)
760	(1)	1.36
850	(1)	0.66
760	(12)	1.3
850	(12)	0.75

The effect of making similar changes to silene-silylene isomerisation reactions in scheme 6.1 was investigated, and was found to have a negligible effect.

The effect of varying Arrhenius parameters for reactions 5 and 6 was then reinvestigated, and found to have little effect, the best calculated results being obtained when logA(5) was increased to 12, and logA(6) increased to 11, as shown below in table 6.25.

Table 6.25

Temperature/K	Precursor	Ratio of (11)/(4)
760	(1)	1.38
850	(1)	0.65
760	(12)	1.28
850	(12)	0.72

Table 6.26 lists the Arrhenius parameters for each reaction in scheme 6.4, that gave the calculated ratios in table 6.25.

Then, to be consistent with scheme 6.1, reactions 25 to 28 as shown below, were added to scheme 6.4.

$$(5) \; \underset{26}{\overset{25}{\rightleftharpoons}} \; HMe_2SiSi{=}CH_2 \; \underset{28}{\overset{27}{\rightleftharpoons}} \; (10)$$
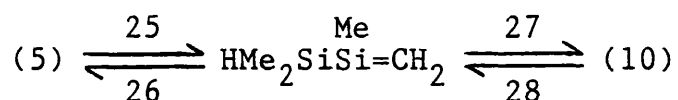
These extra reactions were found to have no effect on the calculated product ratios of (11)/(4).

Table 6.26

Reaction	logA	Ea/kcalmol^{-1}	Comments
1	13.5	52	see reference 11
2	13.54	42.2	see text
3	13.63	43	see text
4	6.6	0	see reference 12
5	12	0	see text
6	11	0	see text
7	13.39	41	a
8	13.53	43	see text
9	13.61	42.2	see text
10	13.08	38	E = 26+EC3
11	14.49	34.15	
12	14.2	11	E = 49-E03
13	12.13	12.55	
14	13.82	30.5	see text
15	12.61	30.65	
16	13.5	61	see reference 13
17	12.14	35	E = 29+EC4
18	12.32	30	E = 24+EC4
19	13.3	55	see reference 13
20	16.2	63	
21	12.96	26.2	
22	15.4	62.5	see reference 14
23	13.35	31	a
24	12.87	24.8	

a : to be consistent with scheme 6.1, activation energy
    reduced by 2kcal/mol from the value quoted in
    O'Neal's rules.

Initial reactant concentration = 2×10^{-5} moldm^{-3}
Reaction time = 9s.

Finally, variation of Arrhenius parameters for reaction 1 was carried out, in order to take into account the reversibility of reaction 1, and again, these changes had a negligible effect on the calculated product ratios of (11)/(4).

From these results, it can be seen that further refinement to scheme 6.4, or the rules for estimation of Arrhenius parameters, will have to be made in order to reproduce more accurately the experimental results.

However, this exercise has been of use, in that it shows that it is possible by computer simulation, to predict experimentally observed results, and gain a better understanding of proposed reaction mechanisms.

References

1. P. P. Gaspar, personal communication to I. M. T. Davidson.

2. H. E. O'Neal, personal communication to I. M. T. Davidson.

3. S. W. Benson, "Thermochemical Kinetics", 2nd Ed., Wiley (1976).

4. T. Kudo & S. Nagase, J. Chem. Soc. Chem. Comm., 1984, 1392.

5. H. Sakurai, Y. Nakadaira & H. Sakaba, Organometallics, 1983, 2, 1484.

6. B. H. Boo and P. P. Gaspar, Organometallics, 1986, 5, 698.

7. H. E. O'Neal and M. A. Ring, J. Organomet. Chem., 1981, 213, 419.

8. Y. S. Chen, B. H. Cohen & P. P. Gaspar, J. Organomet. Chem., 1980, 195, C1.

9. See chapter five.

10. I. M. T. Davidson, K. J. Hughes and R. J. Scampton, Organometallics, 1984, 272, 11.

11. I. M. T. Davidson & R. J. Scampton, J. Organomet. Chem., 1984, 271, 249.

12. I. M. T. Davidson and S. Ijadi-Maghsoodi, unpublished work.

13. L. E. Gusel'nikov, K. S. Konobeyevsky, V. M. Vdovin & N. S. Nametkin, Dokl. Akad. Nauk. SSSR, 1977, 235, 1086.

14. N. Auner, I. M. T. Davidson, S. Ijadi-Maghsoodi and F. T. Lawrence, Organometallics, 1986, 5, 431.

15. M. C. Flowers & L. E. Gusel'nikov, J. Chem. Soc. (B), 1968, 419.

16. B. A. Sawrey, H. E. O'Neal, M. A. Ring and D. Coffey Jr., Int. J. Chem. Kinet., 1984, 16, 7.

17. R. Walsh, J. Chem. Soc. Chem. Comm., 1982, 1415.

CHAPTER SEVEN

KINETICS OF THE ADDITION OF BUTADIENE TO DIMETHYLSILENE,
AND THE PYROLYSIS OF BUTADIENE ADDUCTS OF METHYLSILENE,
DIMETHYLSILENE AND DIMETHYLSILYLENE

INTRODUCTION

In recent years a considerable amount of work has been carried out concerning the interconversion of silenes and silylenes, which involved the use of butadiene as a trap for the reactive intermediates present.[1-7] In the case of silenes, trapping with butadiene produces a silacyclohexene, for silylenes, trapping with butadiene produces a silacyclopentene. The interpretation of results employing butadiene as a silene and silylene trap may be complicated by subsequent decomposition of the adducts, and will also be complicated by the different reactivities of silenes and silylenes towards butadiene. Very little quantitative information regarding these reactions is available, Arrhenius parameters for silene addition to butadiene have been estimated as:[8]

$$\log k / dm^3 mol^{-1} s^{-1} = (7 \pm 1) - (\sim 30 kJmol^{-1} / 2.303RT)$$

and Arrhenius parameters for silylene addition to butadiene have been estimated to be:[9]

$$\log k / dm^3 mol^{-1} s^{-1} = 9.2 - \sim 2kJmol^{-1} / 2.303RT$$

The only kinetic data concerning the decomposition of silacyclohexenes and silacyclopentenes are Arrhenius parameters for the decomposition of 1,1-dimethyl-1-silacyclohex-3-ene (1) and 1,1-dimethyl-1-silacyclopent-3-ene (2),[10] which show that at 900K, (1) decomposes six

times faster than (2). However, apart from the observation that above 600°C 1-methyl-1-silacyclohex-3-ene (3) isomerises to (2), no details of the reaction mechanism and products were given.

It was therefore decided to experimentally measure Arrhenius parameters for the addition of butadiene to dimethylsilene, and also investigate the kinetics and mechanism of pyrolysis of (1), (2) and (3).

RESULTS AND DISCUSSION

Kinetics of the addition of butadiene to dimethylsilene

Samples of a 15:1 mixture of butadiene and dimethylsilacyclobutane with an initial pressure of approximately 0.6 torr were pyrolysed using the LPP technique between 771-831K. The variation of concentration with time of (1), 1,1,3,3-tetramethyl-1,3-disilacyclobutane (4), and butadiene were obtained by monitoring the mass peaks at 126(M$^+$), 129(M$^+$-Me) and 51(M$^+$-3H) respectively. The reaction mechanism is given in scheme 7.1.

Scheme 7.1
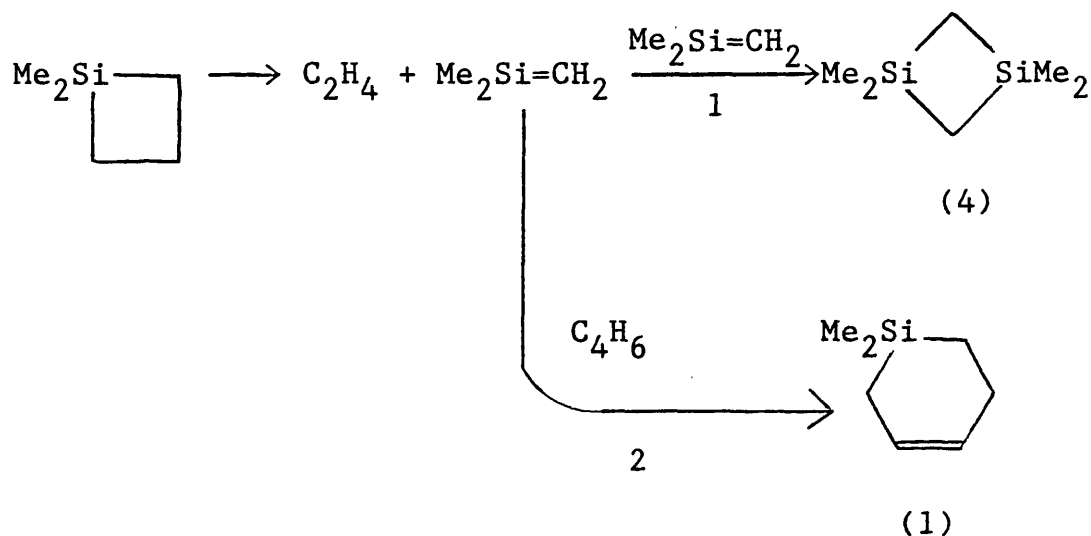
$$\frac{d[(4)]}{dt} = k_1 [Me_2Si=CH_2]^2$$

$$\frac{d[(1)]}{dt} = k_2 [Me_2Si=CH_2][C_4H_6]$$

therefore $\dfrac{\dfrac{d[(1)]}{dt}}{\left(\dfrac{d[(4)]}{dt}\right)^{1/2}} = \dfrac{k_2[C_4H_6]}{(k_1)^{1/2}}$

therefore $k_2 = \dfrac{\dfrac{d[(1)]}{dt} \times (k_1)^{1/2}}{\left(\dfrac{d[(4)]}{dt}\right)^{1/2} \times [C_4H_6]}$

Therefore by measuring the rate of change of the concentrations of species (1) and (4), along with the concentration of butadiene, it is possible to measure k_2. This technique depends on knowing k_1, the rate constant for dimerisation of dimethylsilene which has been experimentally

measured by Gusel'nikov et al [11] to be independent of temperature, and have an A-factor of $10^{6.55} dm^3 mol^{-1} s^{-1}$. An added complication is that the LPP technique provides the variation of peak heights with time, therefore calibration experiments have to be performed to convert the observed peak heights into concentrations. The sensitivity of the mass spectrometer to a particular compound is determined by allowing a known pressure of the compound into the reaction vessel at such a temperature that no decomposition occurs, and measuring the height of the relevant peak in the mass spectrum. The ratio of (peak height)/(sample pressure) gives the sensitivity of the mass spectrometer to the compound in question, by repeating this procedure several times at various sample pressures the average sensitivity (AS) of the compound is obtained. Thus, the pressure of a compound in the reaction vessel is given by:

P(torr) = peak height/AS

From the ideal gas equation, the pressure can be related to the concentration as follow:

$$concentration (mol dm^{-3}) = \frac{P \times 133.3}{1000RT}$$

Therefore, by substitution, the concentration can be expressed in terms of the peak height:

concentration$(mol dm^{-3})$ = $\dfrac{\text{peak height} \times 133.3}{1000RT \times AS}$

Therefore, the expression for k_2 becomes:

$$k_2 = \frac{\frac{d(1)}{dt} \times (k_1)^{1/2} \times AS(C_4H_6)}{\left(\frac{d(4)}{dt}\right)^{1/2} \times AS(1) \times Y \times Z^{1/2}}$$

where $\dfrac{d(1)}{dt}$ and $\dfrac{d(4)}{dt}$ are the initial gradients of the plots of

the peak heights of (1) and (4) against time.

  Y = maximum peak height of 51 (from butadiene)

  $Z = \dfrac{133.3}{1000RT \times AS(4)}$

By measuring $\dfrac{d(1)}{dt}$, $\dfrac{d(4)}{dt}$, the maximum peak height of

butadiene and the average sensitivities of (1), (4) and

butadiene, rate constants for the trapping of dimethylsilene

by butadiene were obtained, and are given in Table 7.1.

Figure 7.1 gives the resulting Arrhenius plot which was

analysed by the method of least squares to give the

following Arrhenius parameters for the addition of butadiene

to dimethylsilene.

  $\log k/dm^3 mol^{-1}s^{-1}$ = $(6.71\pm0.13)-(30.4\pm2.0 kJmol^{-1}/2.303RT)$

These are the first experimentally measured Arrhenius

parameters for this reaction, it is pleasing that the

estimated values quoted previously in this chapter are in

Table 7.1

Rate constants for the trapping of dimethylsilene by butadiene.

T/K	$k/dm^3mol^{-1}s^{-1}$	T/K	$k/dm^3mol^{-1}s^{-1}$
831	62053	791	50595
830	65046	791	53377
824	60620	785	49150
823	58826	784	50704
820	60203	783	52000
820	58128	783	47214
819	58856	783	52279
814	60868	782	49014
813	58851	775	46816
813	58165	774	48551
803	55954	774	45112
802	52682	773	44665
802	52332	772	42427
792	53773	771	41697
792	49749		

good agreement with these measured values. This technique of obtaining Arrhenius parameters for a reaction of dimethylsilene, relative to dimethylsilene dimerisation, has been employed previously to investigate the addition of C_3H_6, [12] HCl,[13] HBr,[13] O_2[13] and Me_3SiOMe[14] to dimethylsilene. It should be stressed that if any subsequent experiments lead to different Arrhenius parameters for dimethylsilene dimerisation, then the measured Arrhenius parameters quoted in this work will have to be revised to take this into account.

Kinetics and Mechanism of the Pyrolysis of 1,1-dimethyl-1-silacyclopent-3-ene (2)

Approximately 0.5 torr samples of (2) were pyrolysed using the SFR technique between 867-925K, the products were identified by comparison of gc retention time with authentic samples and/or gc/mass spectrometry. The major products were butadiene, 1,1-dimethyl-1-silacyclopenta-2,4-diene and 1,1-dimethyl-1-silacyclopent-2-ene. In addition, methane, ethene, propene, dimethylsilane, cyclopentadiene and 1-methyl-1-silacyclopent-3-ene were observed, along with hydrogen observed from LPP experiments. Rate constants for the formation of butadiene, 1,1-dimethyl-1-silacyclopenta-2,4-diene and 1-methyl-1-silacyclopent-3-ene were measured between 883-925K and are given in Table 7.2. Table 7.3 gives the relative product yields for the major products, and some of the minor products at 900K. Figures

Table 7.2

Rate constants for product formation $/s^{-1}$.

T/K	C_4H_6	$Me_2Si\langle\text{ring}\rangle$	$HMeSi\langle\text{ring}\rangle$
925	0.0880	0.0419	0.00312
924	0.0725	0.0387	0.00623
922	0.0887	0.0411	0.00331
913	0.0509	0.0281	0.00229
912	0.0448	0.0251	0.00259
911	0.0414	0.0239	0.00287
902	0.0333	0.0198	0.00301
901	0.0316	0.0193	0.0014
900	0.0292	0.0186	0.00135
894	0.0270	0.0158	———
893	0.0232	0.0167	0.00189
893	0.0221	0.0150	0.00156
884	0.0161	0.011	0.000949
883	0.0164	0.0122	0.00178
883	0.0158	0.0116	0.00172
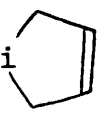
Table 7.3

Relative product yields at 900K.

Product	Relative yield
C_1, C_2 and C_3 hydrocarbons	28
C_4H_6	31
$HMeSi\langle\text{ring}\rangle$	1.5
$Me_2Si\langle\text{ring}\rangle$	20
$Me_2Si\langle\text{ring}\rangle$	~18

7.2, 7.3 and 7.4 give the resulting Arrhenius plots which were analysed by the method of least squares to give the Arrhenius parameters given in Table 7.4.

Table 7.4

product	logA	E/kJmol^{-1}
C_4H_6	14.04±0.64	268±11.1
Me$_2$Si	10.16±0.45	204.7±7.8
HMeSi	8.3±1.5	190±25

Samples of a 10:1 mixture of methanol and (2) with an initial pressure of approximately 0.38 torr were pyrolysed using the LPP technique between 846-925K. Methanol was present to act as a trap for silylenes and silenes, thus minimising any reverse reactions and secondary decomposition of reactant. Rate constants were obtained for the decomposition of (2) and the formation of butadiene by monitoring the mass peaks at 112(M^+) and 50(M^+-4H) respectively, and are given in Table 7.5. Figures 7.5 and 7.6 give the resulting Arrhenius plots which were analysed by the method of least squares to give the Arrhenius parameters in Table 7.6.

Approximately 0.5 torr samples of a 10:1 mixture of methanol

Table 7.5

Rate constants /s^{-1} for the decomposition of (2) and formation of butadiene.

T/K	Decomposition of (2)	Formation of C_4H_6
925	0.0963	0.0998
925	0.0949	0.0996
916	0.0693	0.0672
915	0.0687	0.0681
906	0.0472	0.0474
905	0.0446	0.0476
897	0.0322	0.0368
897	0.0318	0.036
884	0.0207	0.0219
884	0.0199	0.0213
884	0.0197	0.021
877	0.0145	0.0154
875	0.014	0.015
864	0.00907	0.0105
864	0.00872	0.00906
857	0.00629	0.00644
846	0.00376	0.00475

Table 7.6

	logA	E/kJmol^{-1}
decomposition of (2)	13.76±0.13	261.7±2.2
formation of C_4H_6	13.49±0.23	256.7±3.9

and (2) were pyrolysed using the LPP technique between 867-925K. Rate constants for the decomposition of (2) were obtained by monitoring the mass peak at $112(M^+)$, which was corrected to take into account the concurrent formation of 1,1-dimethyl-1-silacyclopent-2-ene, and are given in Table 7.7. Figure 7.7 gives the resulting Arrhenius plot which was analysed by the method of least squares to give Arrhenius parameters for decomposition of:

$$logk/s^{-1}=(14.44\pm0.11)-(272.8\pm1.9kJmol^{-1}/2.303RT)$$

Thus by taking into account the contribution from reactant isomer formation to the decay of the reactant, the Arrhenius parameters for the decay of reactant show a slight increase in both the A-factor and activation energy.

Scheme 7.2 was proposed to account for the observed products of pyrolysis of (2), accounting for the formation of all the major products in Table 7.3 with the exception of C_1, C_2 and C_3 hydrocarbons (predominantly ethene), which were probably formed in secondary reactions. The initial step in the decomposition of (2) is the homolysis of the silicon-carbon bond which will be weakened by allylic stabilisation in the resulting diradical. Silacyclopropane intermediates have previously been proposed as intermediates in the addition of silylenes to butadienes,[15,16,17] and the pyrolysis of dimethyl(cis-propenyl)vinylsilane.[18] The presence of a

Table 7.7

Rate constants for the decomposition of (2).

T/K	k/s^{-1}		T/K	k/s^{-1}
925	0.108		888	0.0253
924	0.105		882	0.0187
915	0.0746		882	0.0187
915	0.0737		875	0.0139
905	0.0492		874	0.0140
904	0.0488		868	0.0103
899	0.0391		867	0.0104
899	0.0375		867	0.0102
889	0.0261			

Scheme 7.2

HMeSi—

HMeSi—

HMeSi·

Me$_2$Si: + C$_4$H$_6$

Me$_2$Si

Me$_2$Si·

Me$_2$Si

Me$_2$Si

Me$_2$Si → Me$_2$Si + H$_2$

silacyclopropane intermediate in scheme 7.2 is consistent with these suggestions, and the observation of 1,1-dimethyl-1-silacyclopent-2-ene as a product. The isomerisation of the initially produced diradical intermediate via a 1,2-hydrogen shift is consistent with the results discussed in chapter 3, and provides a route to 1-methyl-1-silacyclohex-3-ene, the decomposition of which is discussed later in this chapter, and could provide a route to cyclopentadiene and 1-methyl-1-silacyclopentene, observed as minor products in the pyrolysis of (2).

Trapping Experiments

Experiments were also performed using the SFR technique, in which the effect of tenfold excesses of methanol and methylchloride on the product composition was determined. The effect of excess methanol was to increase the amount of butadiene produced, decrease the amount of 1,1-dimethyl-1-silacyclopent-2-ene produced, and have little effect on the production of 1,1-dimethyl-1-silacyclopenta-2,4-diene. These effects are consistent with scheme 7.2 as the methanol reacts with dimethylsilylene, thus reducing the amount of butadiene consumed by recombination of butadiene with dimethylsilylene, and therefore reducing the amount of 1,1-dimethyl-1-silacyclopent-2-ene produced. Since 1,1-dimethyl-1-silacyclopenta-2,4-diene production does not involve dimethylsilylene, methanol would not be expected to

interfere with it production.

The effect of excess methylchloride was similar in that it also reacts with dimethylsilylene, to produce trimethylchlorosilane and therefore suppresses the formation of 1,1-dimethyl-1-silacyclopent-2-ene. In addition to producing trimethylchlorosilane, dimethyldichlorosilane and dimethylchlorosilane were also produced along with two other unidentified products. The most important of these unexpected products was dimethyldichlorosilane, for which two possible mechanisms could be envisaged, as shown in schemes 7.3 and 7.4.

<u>Scheme 7.3</u>

<u>Scheme 7.4</u>

$$Me_2Si: + MeCl \longrightarrow Me_2\overset{\bullet}{Si}Cl + Me\cdot$$
$$\downarrow MeCl$$
$$Me_2SiCl_2 + Me\cdot$$
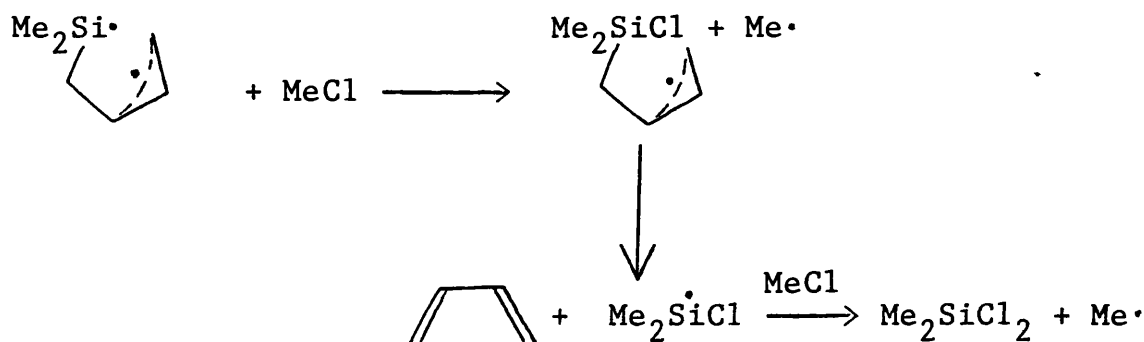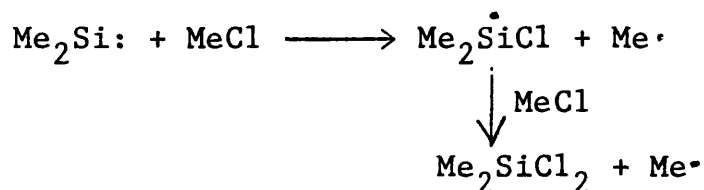
There are problems associated with both of these mechanisms,

for the reaction of the diradical with methylchloride in scheme 7.3, it is not known if this reaction can compete with the ring closing reactions that the diradical can undergo. The reaction of dimethylsilylene with methylchloride to form $Me_2\overset{\bullet}{Si}Cl$ in scheme 7.4 is unusual as it implies that in this case dimethylsilylene is behaving as though it is in a triplet state, at variance with the generally accepted fact that simple silylenes are ground state singlet species.[19,20] However, this is not entirely unprecedented as a similar reaction involving chlorine abstraction by photochemically generated dimethylsilylene has recently been reported.[21] No experimental measurements of the singlet-triplet energy gap in dimethylsilylene are available, however, the possibility of promotion of singlet dimethylsilylene to triplet dimethylsilylene cannot be ruled out, as the singlet-triplet energy gap has been calculated to be 22.9kcal/mole.[19] Also, the production of both singlet and triplet dimethylsilylene from pyrolysis experiments has previously been suggested.[22]

The presence of radicals in the trapping experiments with excess methylchloride is substantiated by the observation of an increase in the amount of 1,1-dimethyl-1-silacyclopenta-2,4-diene produced, which could be formed via hydrogen abstraction reactions from (2) by radicals. Additional evidence for the presence of $Me_2\overset{\bullet}{Si}Cl$ as predicted from schemes 7.3 and 7.4 is given by the observation of

dimethylchlorosilane, which would be produced as a result

of hydrogen abstraction by Me$_2$ṠiCl.

Arrhenius Parameters

It is difficult, given the unknown aspects of the mechanism

of decomposition of (2) and the fact that a significant

product is an isomer of (2), to draw any definite

conclusions from the measured Arrhenius parameters.

However, an important reason for investigating the pyrolysis

of (2) was that it is the major butadiene adduct of

dimethylsilylene, and as such it has been of use in

addressing the question of silylene-silene isomerisation

reactions. While the Arrhenius parameters for the overall

decomposition of (2) obtained in this work are similar to

those used by Davidson and Scampton [5] in their computer

modelling studies, this work shows that the thermal

decomposition of (2) is more complex than just a straight-

forward elimination of dimethylsilylene and butadiene. It

would therefore be desirable to conduct experiments using

butadiene as a trap for dimethylsilylene at temperatures

where (2) is thermally stable.   Thus in the SFR experiments

carried out by Davidson and Scampton,[5] this would be the

case at the temperatures up to and including 873K, at which

the half life of (2) is 53s.   However, at 924K, the half

life of (2) is 6.7s, which given the half life of material

in the reaction vessel of ∼8s, would allow some

decomposition of (2) to occur which could interfere with the

interpretation of the results.

Kinetics and Mechanism of the Pyrolysis of 1,1-dimethyl-1-silacyclohex-3-ene (1)

Approximately 0.15 torr samples of (1) were pyrolysed using the SFR technique between 851-921K, the products, identified by comparison of gc retention time with authentic samples and/or gc/mass spectrometry were:

ethene, trimethylsilane, butadiene, cyclopentadiene, 1,1-dimethyl-1-silacyclobut-2-ene, 1-methyl-1-silacyclopent-3-ene, 1,1-dimethyl-1-silacyclopenta-2,4-diene, 1,1-dimethyl-1-silacyclopent-2-ene, 1,1-dimethyl-1-silacyclopent-3-ene, 1,1,3-trimethyl-1,3-disilacyclobutane, 1,1,3,3-tetramethyl-1,3-disilacyclobutane, 1,1-dimethyl-1-silacyclohexadienes, 1,1-dimethyl-1-silacyclohex-2-ene, and hydrogen identified from LPP experiments.

Rate constants were obtained for the formation of cyclopentadiene, 1,1,3,3-tetramethyl-1,3-disilacyclobutane, 1,1-dimethyl-1-silacyclopent-3-ene, 1,1-dimethyl-1-silacyclobut-2-ene, 1,1-dimethyl-1-silacyclopenta-2,4-diene and 1-methyl-1-silacyclopent-3-ene, and are given in Table 7.8. Table 7.9 gives the relative product yields for the major products and some of the minor products at 900K. Figures 7.8 - 7.13 give the resulting Arrhenius plots, which were analysed by the method of least squares to give the Arrhenius parameters in Table 7.10.

Table 7.8

Rate constants for product formation $/s^{-1}$.

T/K	C_5H_6	Me_2Si⟡$SiMe_2$	Me_2Si⬠	Me_2Si◻	Me_2Si⬠	$HMeSi$⬠
921	0.189	0.0312	——	0.0809	——	——
920	0.147	0.0515	0.0465	0.0856	0.0288	0.058
919	0.138	0.0552	0.0459	0.076	0.022	0.0429
913	0.104	0.0485	0.0386	0.0589	0.0159	0.0328
910	0.0858	0.0343	0.0312	0.0555	0.0128	0.0308
909	0.0855	0.0328	0.0318	0.054	0.0128	0.0324
902	0.0614	0.0282	0.025	0.0375	0.00963	0.0193
900	0.0563	0.0196	0.022	0.0351	0.00885	0.024
900	0.0554	0.0106	0.0188	0.0241	0.007	0.0211
893	0.0403	0.0156	0.0166	0.0267	0.00647	0.0144
891	0.0402	0.0126	0.0147	0.0248	0.00528	0.0148
891	0.0387	0.00656	0.0129	0.0177	0.00505	0.0147
883	0.0249	0.0092	0.0104	0.0161	0.00407	0.00999
881	0.0237	0.00916	0.00993	0.0155	0.00408	0.00881
881	0.0234	0.00858	0.00961	0.0148	0.00383	0.00803
873	0.0162	0.00567	0.00628	0.0114	0.00286	0.00617
872	0.0164	0.00482	0.0062	0.0113	0.00268	0.00631
871	0.0148	0.00445	0.00596	0.0111	0.00269	0.00679
862	0.00999	0.00267	0.00355	0.00663	0.00196	0.00417
861	0.00983	0.00101	0.00282	0.00494	0.0016	0.00368
860	0.0093	0.00184	0.00296	0.00654	0.00164	0.00391
852	0.00611	0.00135	0.00185	0.00401	0.00106	0.00255
852	0.00589	0.00116	0.00182	0.00378	0.00102	0.00228
851	0.00602	0.000578	0.00156	0.00218	0.00107	0.00258

Table 7.9

Relative product yields at 900K from the pyrolysis of (1).
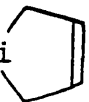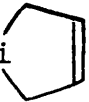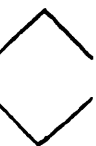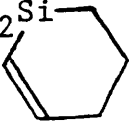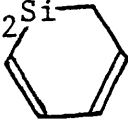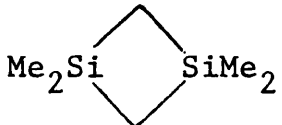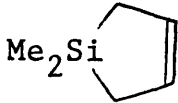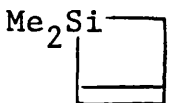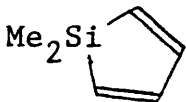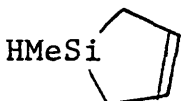
Product	Relative yield
C_4H_6	11.8
C_5H_6	10
Me$_2$Si (four-membered ring with double bond)	6.1
HMeSi (five-membered ring with double bond)	2.2
Me$_2$Si (five-membered ring with two double bonds)	1.6
Me$_2$Si (five-membered ring with double bond)	1.0
Me$_2$Si (five-membered ring with double bond)	4
Me$_2$Si ◇ SiHMe	2
Me$_2$Si (six-membered ring) + Me$_2$Si (six-membered ring with two double bonds)	4

Table 7.10

product	logA	$E/kJmol^{-1}$
C_5H_6	16.43 ± 0.23	304.2 ± 4
Me_2Si ⬦ $SiMe_2$	18.93 ± 1.19	355.9 ± 20
Me_2Si (silacyclopentene)	16.56 ± 0.37	314.1 ± 6.3
Me_2Si (silacyclobutane)	15.7 ± 0.57	295.8 ± 9.7
Me_2Si (silacyclopentadiene)	14.46 ± 0.44	284.4 ± 7.4
$HMeSi$ (silacyclopentadiene)	14.68 ± 0.34	281.8 ± 5.7

Samples of a 10:1 mixture of methanol and (1) with an initial pressure of approximately 0.5 torr were pyrolysed using the LPP technique between 841-925K. Rate constants for the decomposition of (1) were obtained by monitoring the mass peak at $126(M^+)$, which was corrected to take into account the concurrent formation of 1,1-dimethyl-1-silacyclohex-2-ene, and are given in Table 7.11 along with rate constants for the formation of butadiene, obtained by monitoring the mass peak at $54(M^+)$. Figures 7.14 and 7.15 give the resulting Arrhenius plots which were analysed by the method of least squares to give the Arrhenius parameters in Table 7.12.

Table 7.11

Rate constants (s^{-1}) for the decomposition of (1) and formation of butadiene.

T/K	Decomposition of (1)	Formation of butadiene
925	——	0.345
925	——	0.31
924	——	0.307
914	0.209	0.198
913	0.195	0.191
913	0.178	0.186
903	0.132	0.124
902	0.130	0.108
894	0.0896	0.0884
893	0.0877	0.0832
884	0.0607	0.0594
884	0.0588	——
883	0.0553	0.0612
872	0.0362	0.039
863	0.026	0.025
862	0.0241	——
860	0.0242	0.0244
851	0.016	0.0145
850	0.015	0.0143
841	0.00969	0.0103
841	0.00969	——

Table 7.12

	logA	$E/kJmol^{-1}$
decomposition of (1)	14.27±0.15	262.1±2.4
formation of C_4H_6	14.42±0.22	264.6±3.7

Scheme 7.5 was proposed as the mechanism of pyrolysis of (1) as it accounts for the formation of all the major products. From scheme 7.5 it can be seen that silacyclobutanes with vinyl substituents on the ring are involved in the pyrolysis of (1), thus the question arises as to why these species were not observed as products. As discussed in chapter 1, Arrhenius parameters for the decomposition of 1,1-dimethyl-1-silacyclobutane are identical to Arrhenius parameters for cyclobutane decomposition, as the decomposition mechanism involves carbon-carbon bond homolysis in each case. Therefore, Arrhenius parameters for the decomposition of vinyl substituted silacyclobutanes can be estimated by comparison with the measured Arrhenius parameters for vinylcyclobutane decomposition, which also decomposes via carbon-carbon bond homolysis.[23] The Arrhenius parameters obtained for vinylcyclobutane decomposition are:

$$logk/s^{-1} = 14.72-(208.3kJmol^{-1}/2.303RT)$$

At 840K, the lowest temperature used in these experiments, these Arrhenius parameters give a rate constant of $58.4s^{-1}$ which corresponds to a half life of 0.01s. Since in the SFR experiments, the half life of material in the reaction

Scheme 7.5
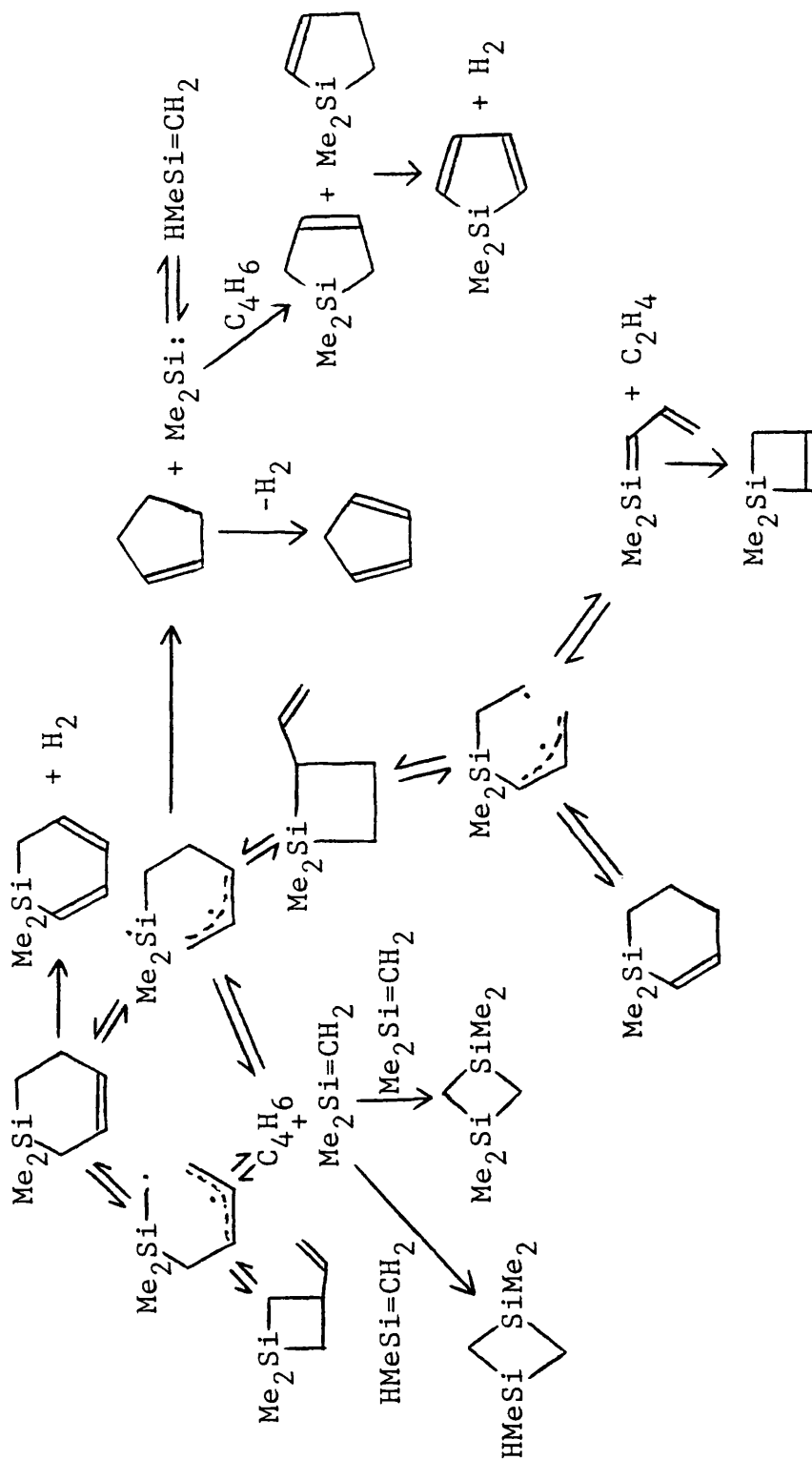
vessel is ~8s, then it is reasonable that no vinyl substituted silacyclobutanes were observed as products.

The most surprising aspect of the pyrolysis mechanism is the formation of cyclopentadiene, with no evidence from gc/mass spectrometry of any other C_5 hydrocarbon being present. The only method of producing cyclopentadiene appears to be via the diradical intermediate produced by silicon-carbon bond homolysis in the reactant, breaking up to give cyclopentene and dimethylsilylene. This is interesting as it gives rise to the possibility of the dimethylsilylene so produced being in the triplet state. As discussed earlier in this chapter, this would not be unprecedented, as the production of triplet dimethylsilylene from pyrolysis experiments has previously been suggested,[22] and chlorine abstraction reactions, consistent with the presence of triplet dimethylsilylene have been reported.[21]

Trapping Experiments

The mechanism of pyrolysis was further investigated by the use of trapping agents. Excess methanol was found to suppress the formation of all the four and five membered cyclic organosilicon products. In addition, three new products were identified by gc/mass spectrometry, which were as expected for the trapping of dimethylsilylene, dimethylsilene and $Me_2Si=$ with methanol. This is consistent with scheme 7.5, as it indicates that the

204

observed four and five membered cyclic organosilicon products are indeed produced via these silenes and silylene.

Excess butadiene was found to suppress the formation of the 1,3-disilacyclobutanes and 1,1-dimethyl-1-silacyclobut-2-ene, consistent with butadiene trapping of the silene precursors to these products. Also, the amounts of 1,1-dimethyl-1-silacyclopent-2-ene and 1,1-dimethyl-1-silacyclopent-3-ene were increased, consistent with a more efficient trapping of dimethylsilylene by butadiene.

Kinetics and Mechanism of the Pyrolysis of 1-methyl-1-silacyclohex-3-ene (3)

Approximately 0.17 torr samples of (3) were pyrolysed using the SFR technique between 832-925K. The products, identified by comparison of gc retention time with authentic samples and/or gc/mass spectrometry were:
ethene, propene, butadiene, cyclopentadiene, 1-methyl-1-silacyclobut-2-ene, 1-methyl-1-silacylopent-3-ene, 1,1-dimethyl-1-silacyclopenta-2,4-diene, 1,1-dimethyl-1-silacyclopent-2-ene, 1,1-dimethyl-1-silacyclopent-3-ene, 1-methyl-1-silacyclohex-2-ene, 1-methyl-1-silacyclohexa-2,4(5)-diene, 1,1-dimethyl-1-silacyclohexa-2,4(5)-diene, and hydrogen, identified from LPP experiments.

Rate constants were obtained for the formation of ethene, propene, butadiene, cyclopentadiene, 1,1-dimethyl-1-

Table 7.13

Rate constants (s^{-1}) for product formation.

T/K	ethene	propene	butadiene
921	0.271	0.0107	0.210
915	0.320	0.0135	0.260
915	0.243	0.00838	0.192
913	0.276	0.010	0.207
905	0.165	0.00628	0.134
904	0.146	0.00549	0.121
902	0.132	0.00522	0.106
895	0.109	0.00481	0.0971
894	0.088	0.00298	0.0752
893	0.0747	0.00291	0.0637
882	0.0523	0.00184	0.0477
882	0.0405	0.00156	0.0364
875	0.0318	0.0012	0.0302
874	0.0332	0.00144	0.0293
863	0.0152	0.000576	0.0160
862	0.0180	0.000645	0.0191
862	0.0173	0.000587	0.0184
854	0.0109	0.000837	0.0129
853	0.0104	0.000553	0.0111
853	0.00993	0.000421	0.0120
844	0.00636	0.000237	0.00763
841	0.00577	0.000283	0.00716
837	0.00412	0.000153	0.00625
835	0.00419	0.000203	0.00599
832	0.00368	0.000197	0.0050

Table 7.14

Rate constants (s^{-1}) for product formation.
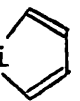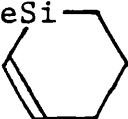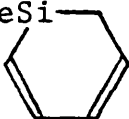
T/K	C_5H_6	Me$_2$Si	Me$_2$Si	HMeSi
925	0.162	0.108	0.0859	0.118
924	0.143	0.0987	0.0743	0.105
923	0.153	0.0923	0.0688	0.101
914	0.0939	0.073	0.0545	0.0811
913	0.0864	0.0678	0.0486	0.0747
913	0.0842	0.0646	0.0494	0.0749
905	0.059	0.0446	0.0376	0.0511
904	0.0546	0.0471	0.0348	0.0526
902	0.0508	0.0423	0.0327	0.0483
895	0.0438	0.0305	0.024	0.0362
895	0.0403	0.0325	0.0252	0.0385
895	0.0359	0.032	0.024	0.0355
885	0.0275	0.0189	0.0199	0.0224
883	0.024	0.0157	0.0178	0.0195
881	0.0241	0.0157	0.0175	0.0188
875	0.0153	0.0124	0.0113	0.0151
874	0.0148	0.0125	0.0116	0.0139
873	0.0134	0.0118	0.0108	0.013
864	0.0103	0.00768	0.00801	0.00814
863	0.00876	0.00703	0.00757	0.0080
862	0.00991	0.00629	0.00837	0.00739
854	0.00591	0.00449	0.00516	0.00486
853	————	0.00417	0.00518	0.00409
852	0.00498	0.00388	0.00494	0.00455
843	0.00337	0.00248	0.00377	0.00284
843	0.00337	0.00249	0.00370	0.00283
841	0.00294	0.00219	0.00336	0.00249
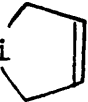
Table 7.15

Relative product yields at 900K from the pyrolysis of (3).

Product	Relative yield
C_2H_4	162
C_3H_6	6.4
C_4H_6	124
Me_2SiH_2	37
C_5H_6	58
HMeSi (cyclobutene ring)	1.0
HMeSi (cyclopentene ring)	44
Me_2Si (cyclopentene ring)	38
Me_2Si (cyclopentene ring)	22
Me_2Si (cyclopentene ring)	49
HMeSi (cyclohexene ring) + HMeSi (cyclohexadiene ring)	37

silacyclopent-3-ene, 1,1-dimethyl-1-silacyclopenta-2,4-diene and 1-methyl-1-silacyclopent-3-ene, and are given in Tables 7.13 and 7.14. Table 7.15 gives the relative product yields for the major products and some of the minor products at 900K. Figures 7.16 - 7.22 give the resulting Arrhenius plots which were analysed by the method of least squares to give the Arrhenius parameters in Table 7.16.

Table 7.16

product	logA	E/kJmol-1
C_2H_4	18.34±0.31	331.7±5.2
C_3H_6	15.86±0.6	313.5±10.1
C_4H_6	15.66±0.36	287±6.1
C_5H_6	16.1±0.21	299.8±3.6
Me_2Si (silacyclopent-3-ene)	15.83±0.15	297.4±2.5
Me_2Si (silacyclopentadiene)	12.42±0.18	241.9±3.1
$HMeSi$ (silacyclopent-3-ene)	15.88±0.18	297.2±3.1

Scheme 7.6 was proposed for the mechanism of pyrolysis of (3). It has many similar features to scheme 7.5, such as the presence of vinyl substituted silacyclobutanes as reactive intermediates, and the production of cyclopentene

Scheme 7.6
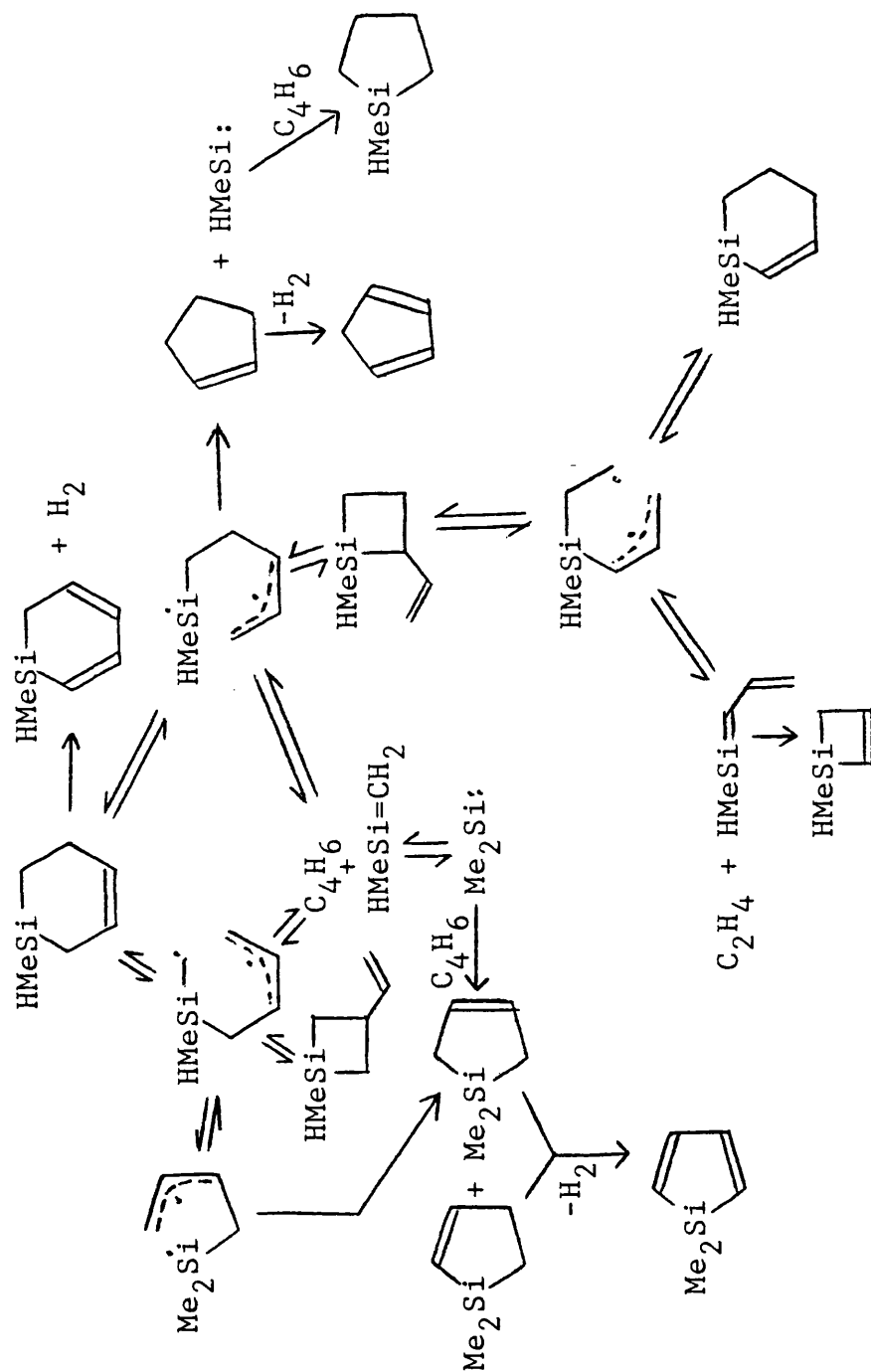
and a silylene from a diradical intermediate. From the work concerning the pyrolysis of hydridosilacyclobutanes,[24] a possible decomposition mechanism of (3) would be a 1,2-hydrogen shift from silicon to carbon to form a silylene, the consequences of which are shown in scheme 7.7. However, the observed products gave no evidence of the occurrence of this decomposition mechanism as there was no evidence of any C_5 hydrocarbon other than cyclopentadiene, or any of the two possible silacyclopentenes predicted by scheme 7.7. Isomerisation of the carbon centred radical formed by carbon-carbon bond homolysis in (3) provides a link to (2), and as discussed earlier in this chapter, gives a possible explanation for the observation of cyclopentadiene and 1-methyl-1-silacyclopentene as minor products in the pyrolysis of (2).

Trapping Experiments

The mechanism of pyrolysis was further investigated by the use of trapping agents. Excess methanol suppressed the formation of 1-methyl-1-silacyclopent-3-ene, 1,1-dimethyl-1-silacyclopent-2-ene, 1,1-dimethyl-1-silacyclopent-3-ene and 1-methyl-1-silacyclohex-2-ene. The new products that were identified by gc/mass spectrometry were methylmethoxysilane and dimethylmethoxysilane, consistent with the presence of methylsilylene and dimethylsilylene as intermediates involved in the production of the silacyclopentenes. In addition, there may have been a small

Scheme 7.7
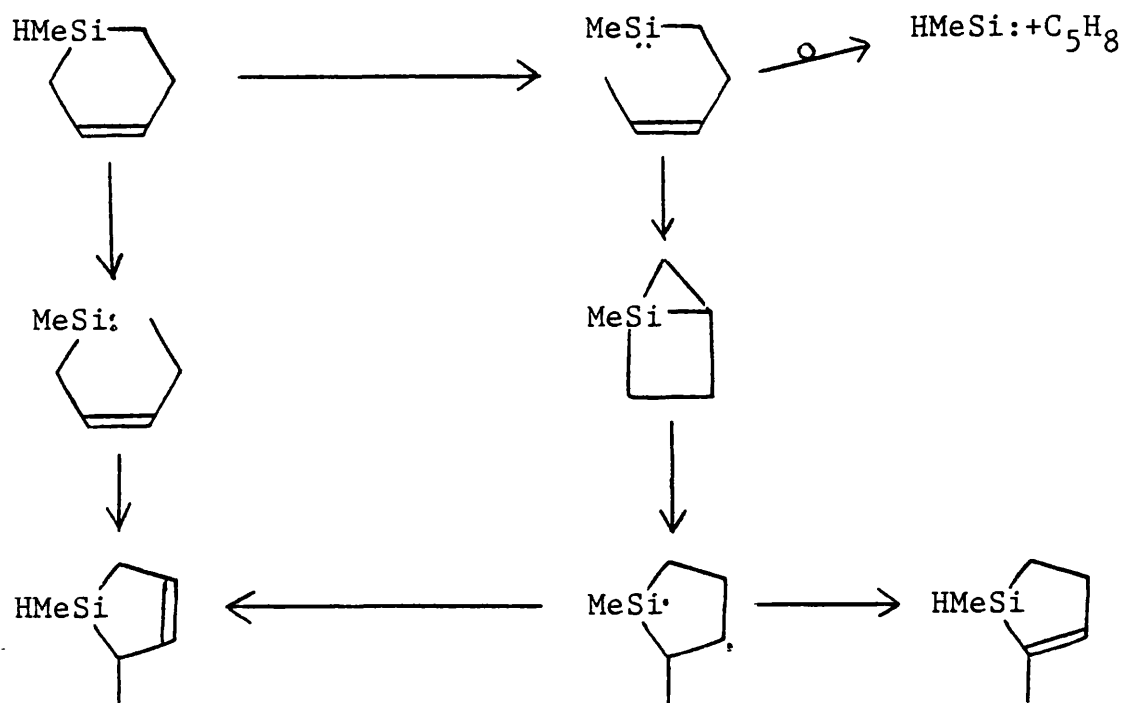
quantity of dimethoxymethylsilane produced; if so, the
mechanism of its production is unclear.

Excess butadiene caused a partial suppression of 1-methyl-
1-silacyclohex-2-ene, and increased the amounts of 1-
methyl-1-silacyclopent-3-ene, 1,1-dimethyl-1-silacyclopent-
2-ene and 1,1-dimethyl-1-silacyclopent-3-ene, again
consistent with methylsilylene and dimethylsilylene as
intermediates involved in the production of the
silacyclopentenes.

These trapping experiments are consistent with
methylsilylene and dimethylsilylene being precursors to the
silacyclopentenes. However, they highlight other
uncertainties about scheme 7.6, specifically, why excess
methanol suppresses the silacyclopentenes but leaves 1,1-
dimethyl-1-silacyclopenta-2,4-diene unaffected. A possible
explanation of this is the isomerisation of the carbon
centred radical formed by carbon-carbon bond homolysis in
(3) leading to the production of (2) without the need of
silylene intermediates, however, if this is the case, under
the conditions employed in the trapping experiment there is
a complete conversion of (2) to 1,1-dimethyl-1-
silacyclopenta-2,4-diene.

Arrhenius Parameters

The main use of the measured Arrhenius parameters for

product formation from the pyrolysis of (1) and (3) is to obtain a measure of the relative importance of the products as a function of temperature.

(3) is the major product of trapping of methylsilene by butadiene, and as such has been of use in addressing the question of silylene-silene isomerisation reactions.[5] Arrhenius parameters for the overall decomposition of (3) in the presence of methanol are identical within experimental error to the measured Arrhenius parameters for the decompostion of (1) obtained in this work.[25] Since this work has shown that the mechanism of decomposition of (3) is extremely complex, it would be desirable to conduct experiments using butadiene as a trap for methylsilene under conditions in which (3) is thermally stable. In the SFR experiments carried out by Davidson and Scampton,[5] this would be the case at the temperatures up to and including 829K, at which the half life of (3) is 122s, but not at 873K or above as the half life at 873K is 18s, giving significant decomposition of (3).

Figure 7.1 : Arrhenius plot for the reaction of butadiene
with dimethylsilene.

215
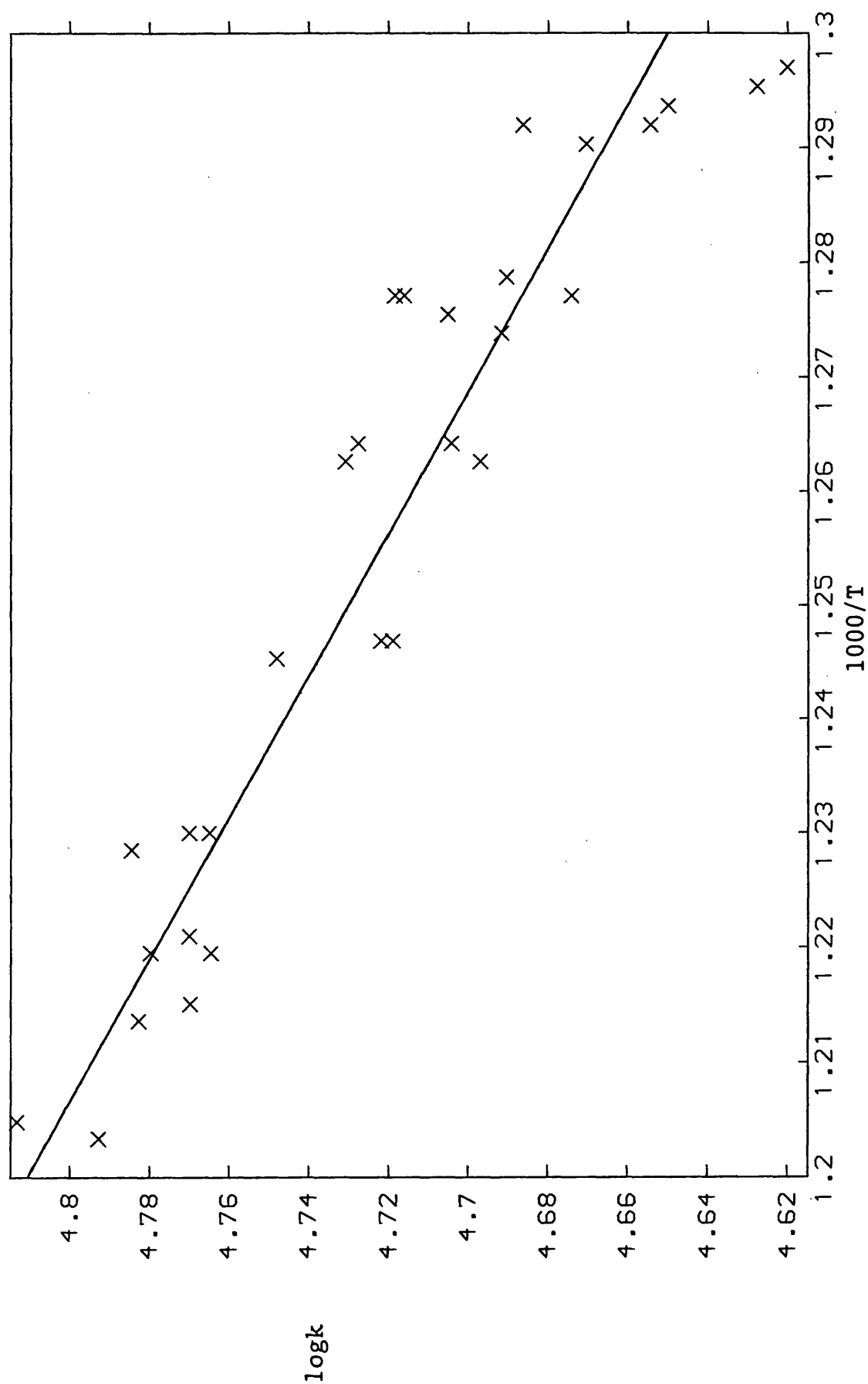
Figure 7.2 : Arrhenius plot for formation of butadiene from (2).
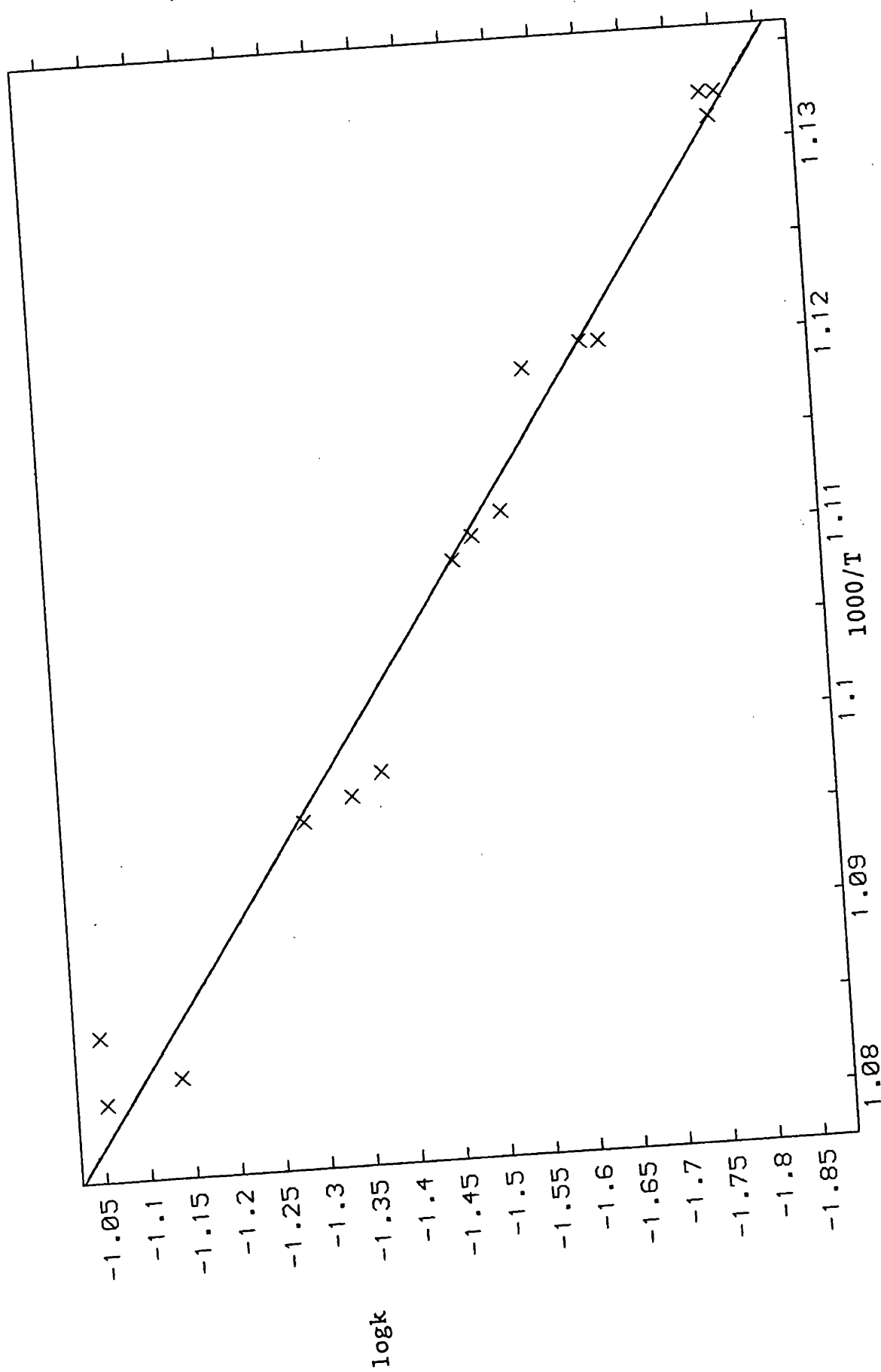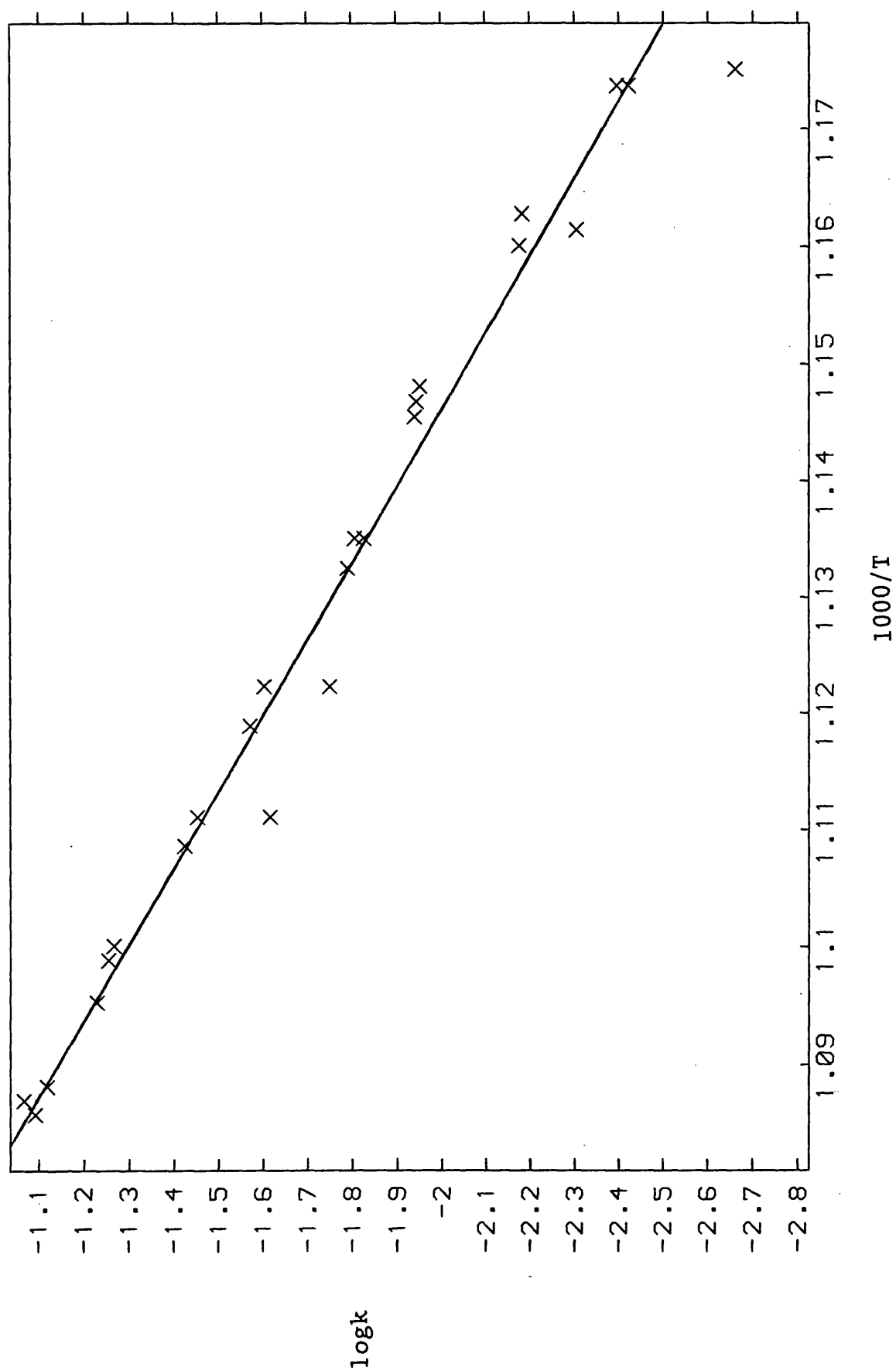
Figure 7.3 : Arrhenius plot for formation of 1,1-dimethyl-1-
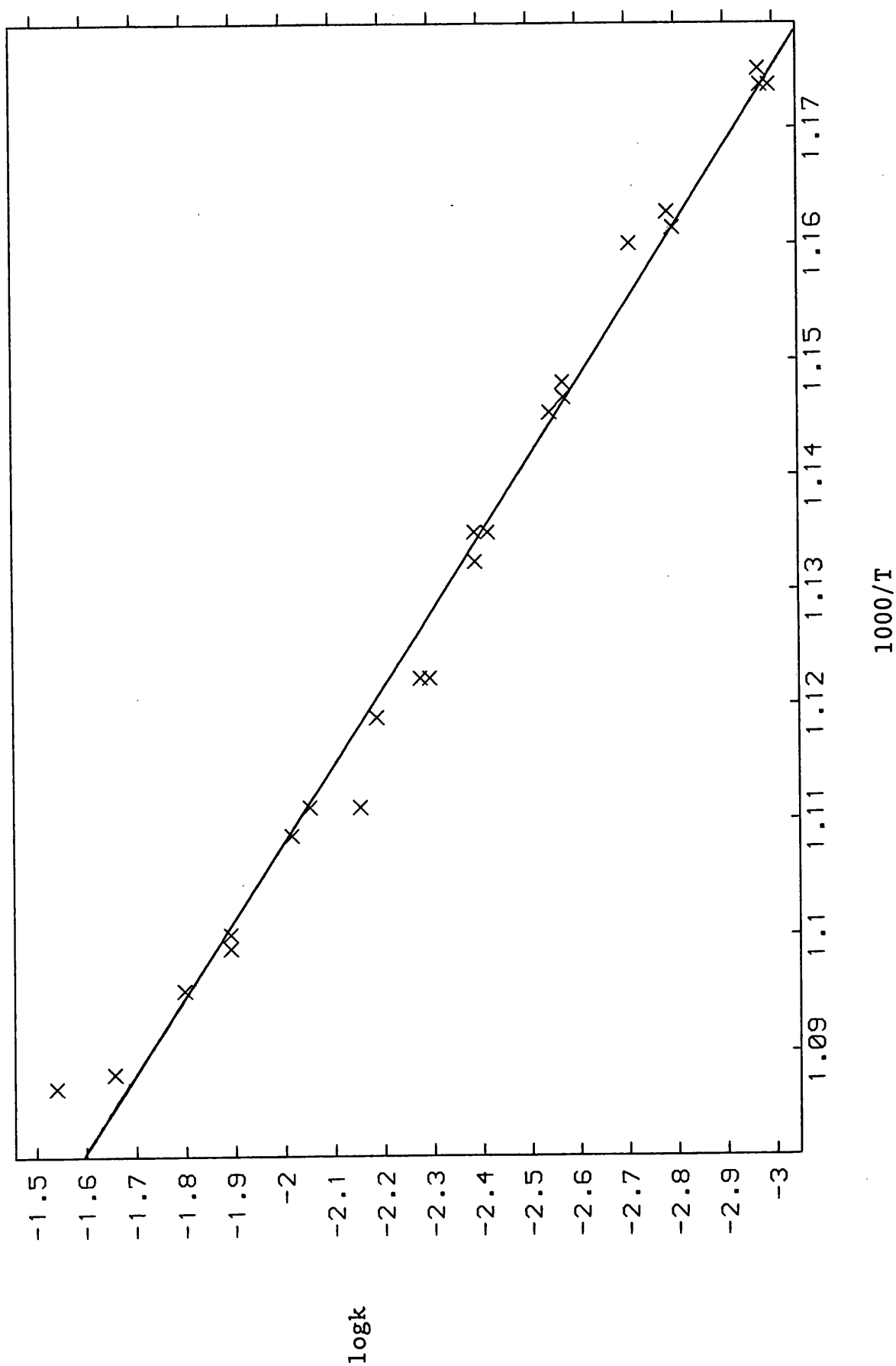silacyclopenta-2,4-diene from (2).

217
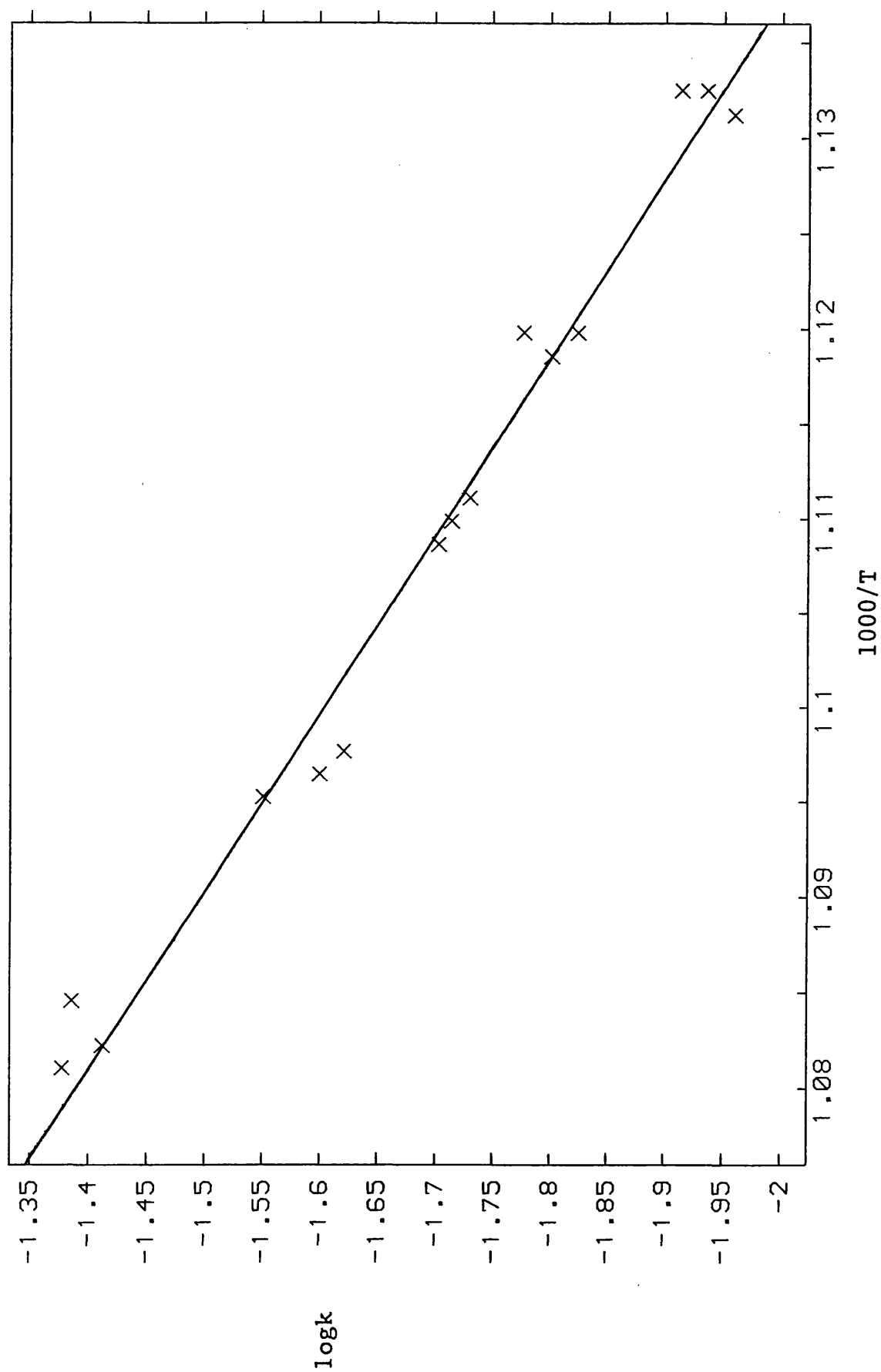
Figure 7.4 : Arrhenius plot for formation of 1-methyl-1-
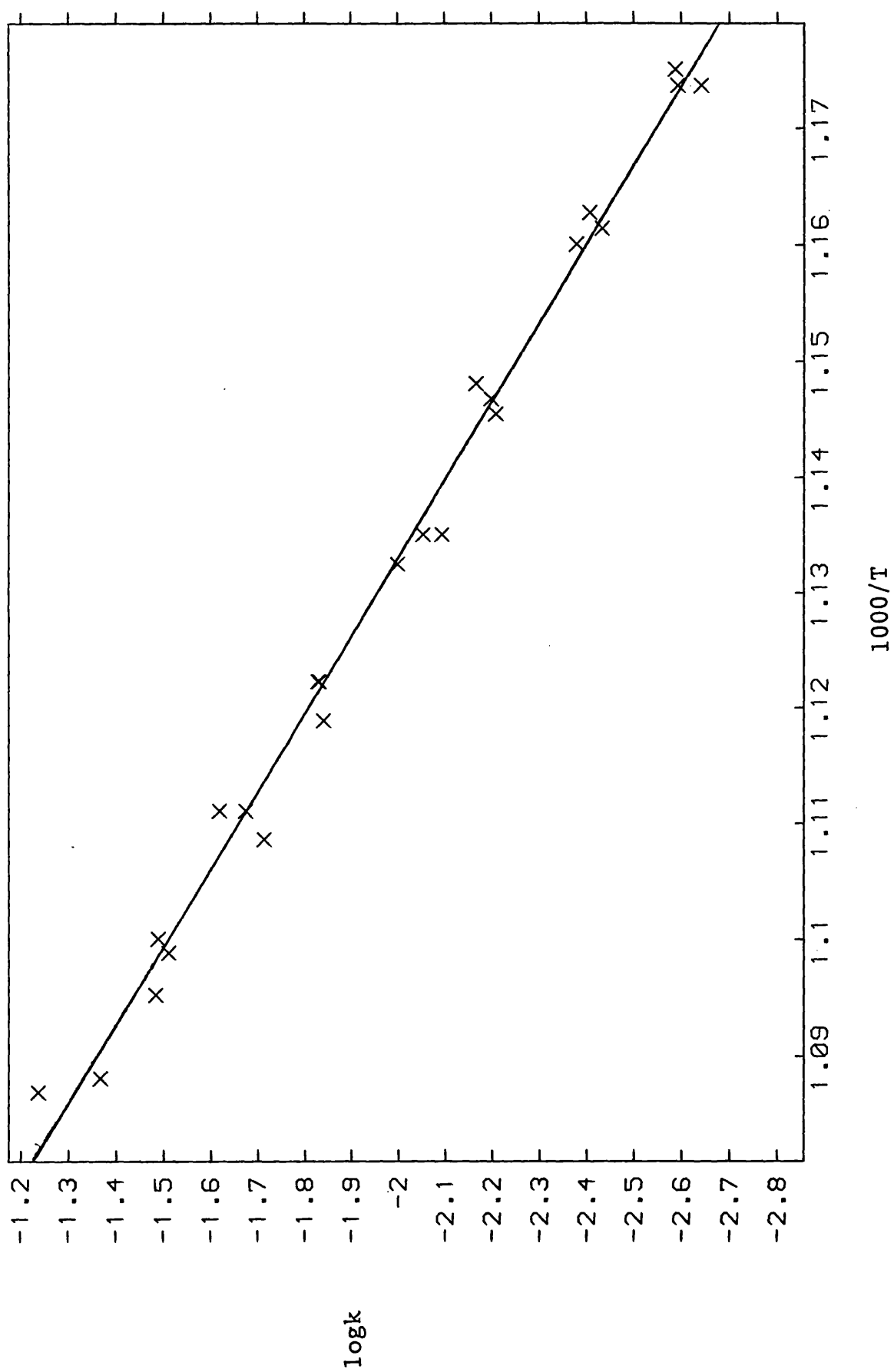silacyclopent-3-ene from (2).
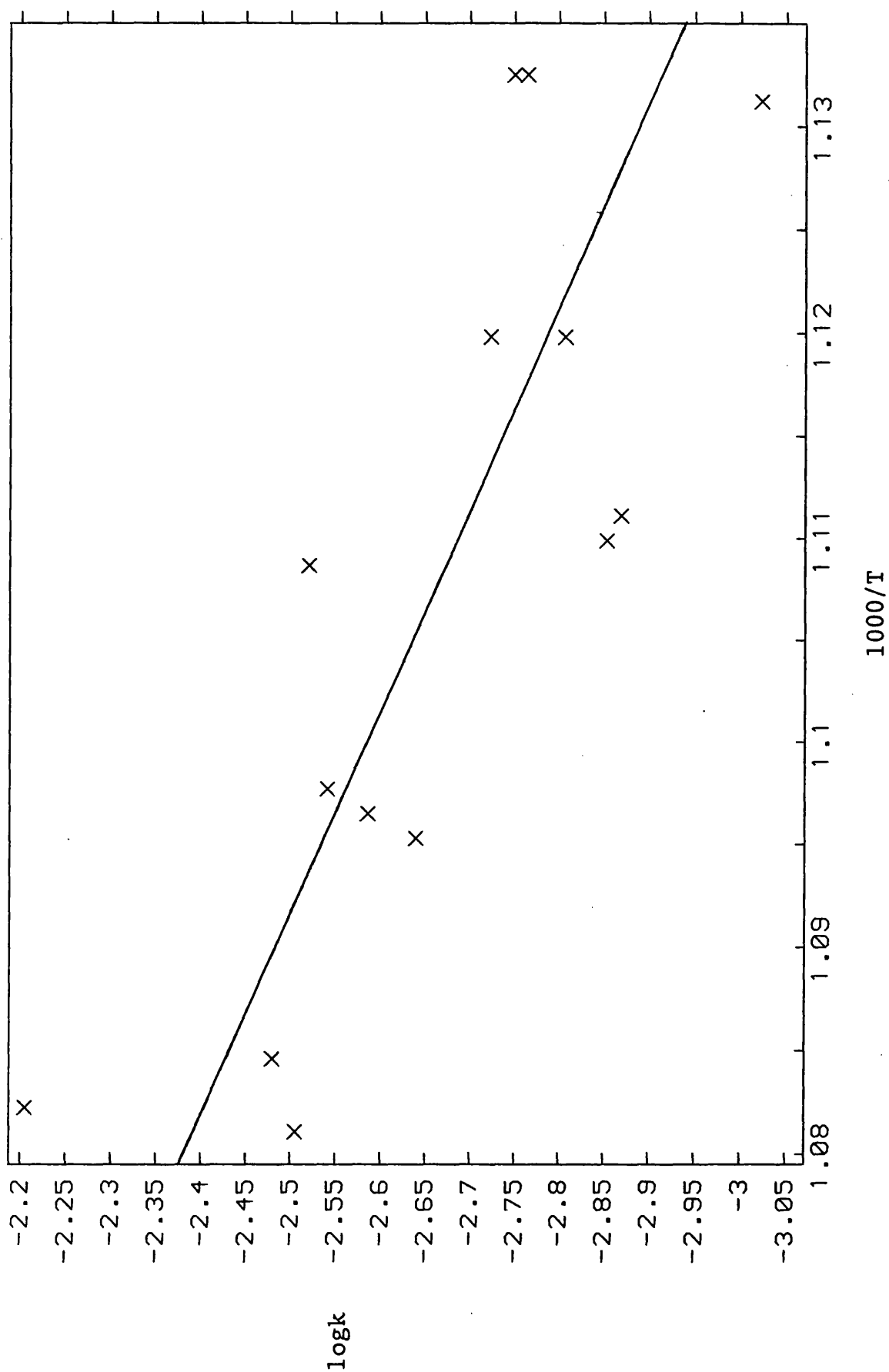
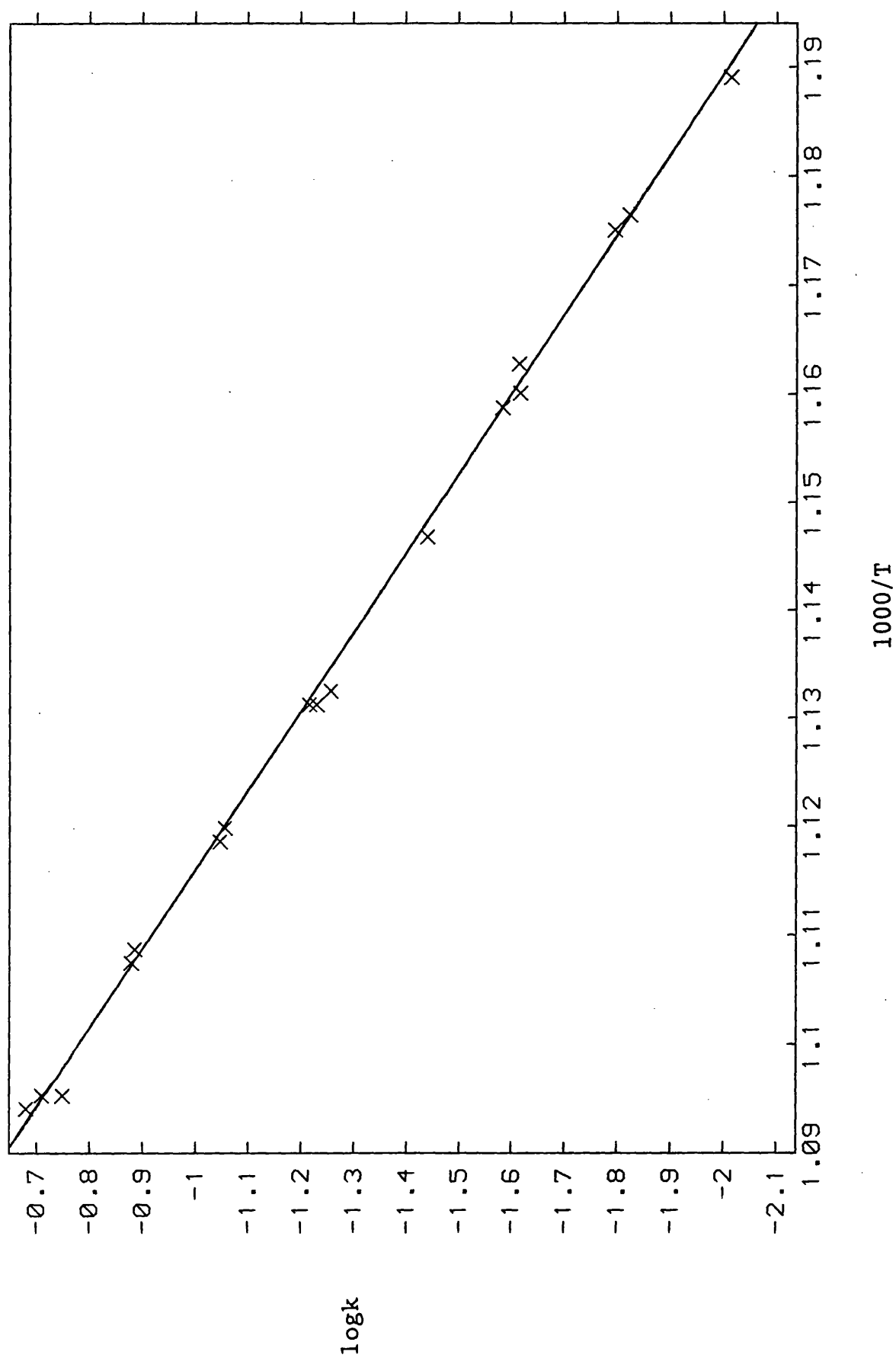Figure 7.5 : Arrhenius plot for decay of (2) in excess
methanol.
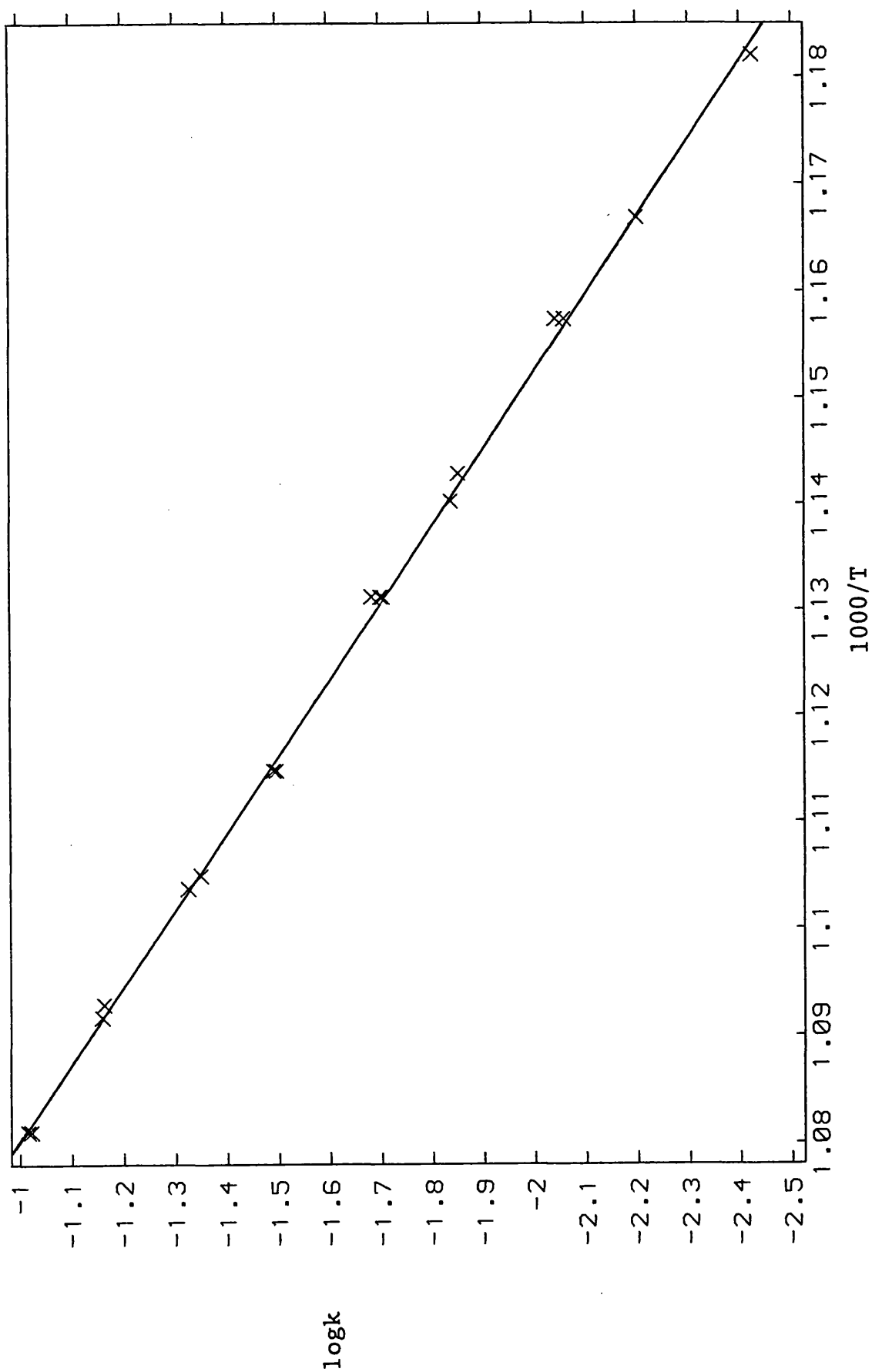
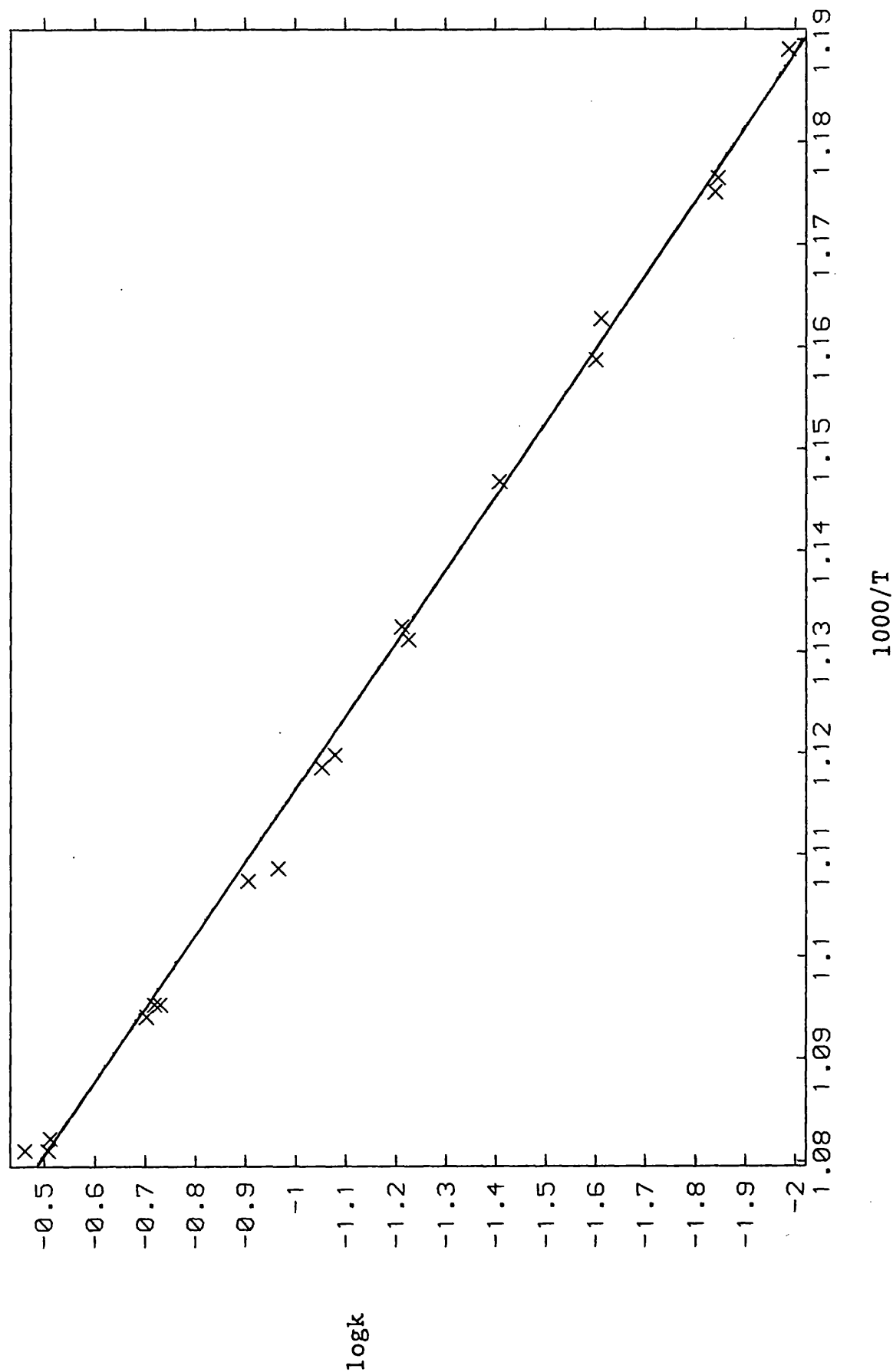Figure 7.6 : Arrhenius plot for formation of butadiene from (2) + excess methanol.
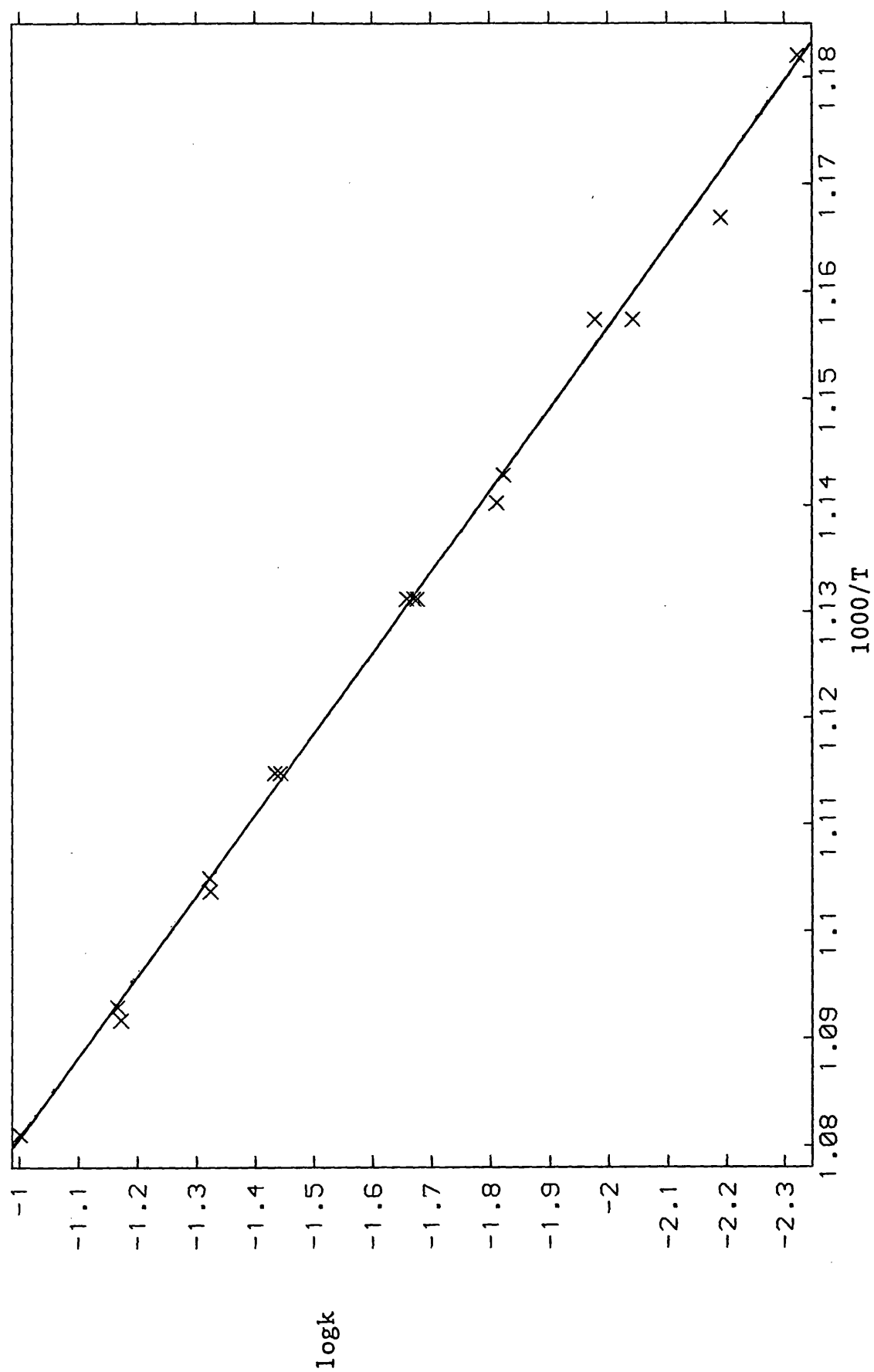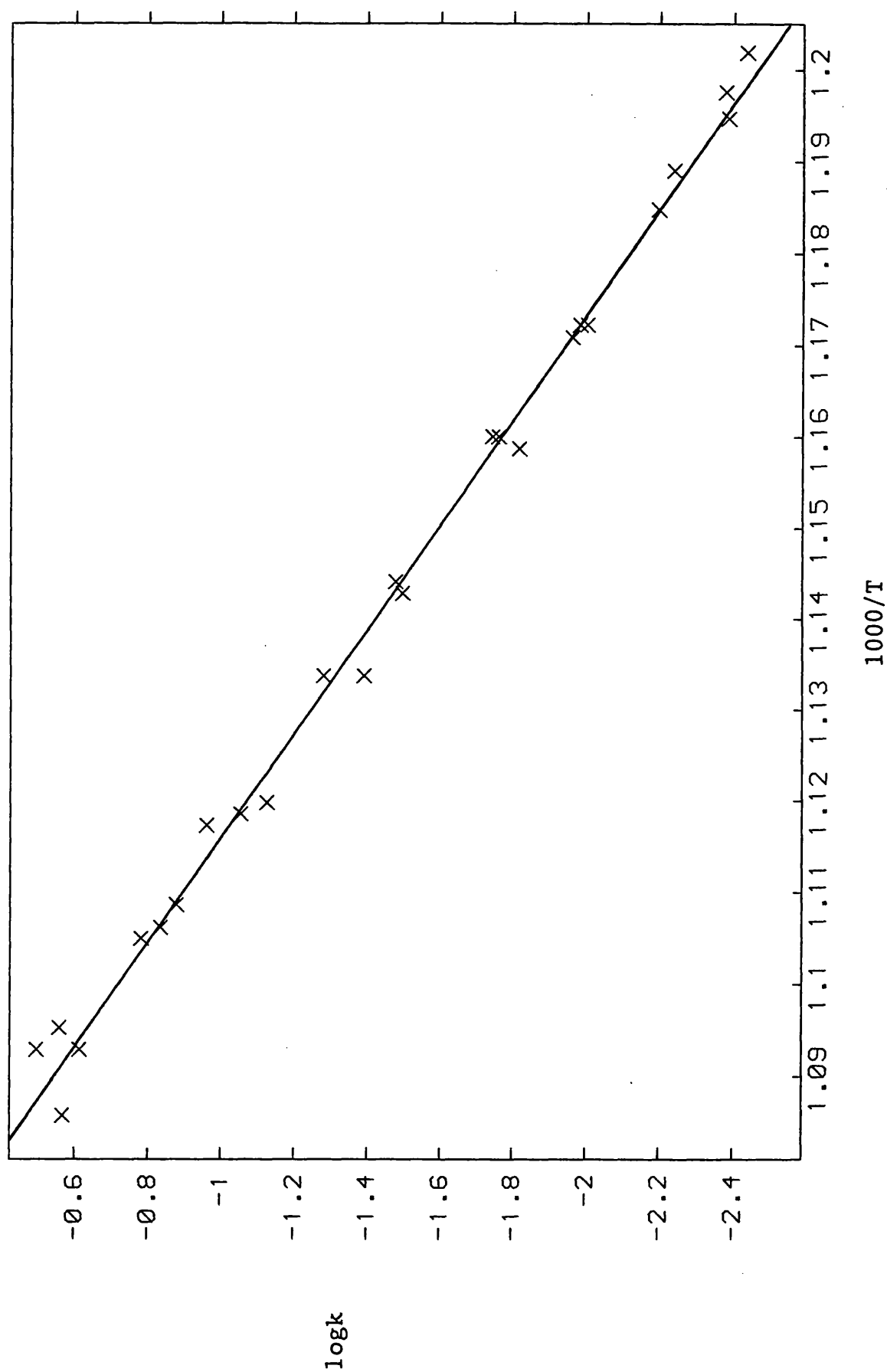
Figure 7.7 : Arrhenius plot for the corrected decay of (2) in excess methanol.
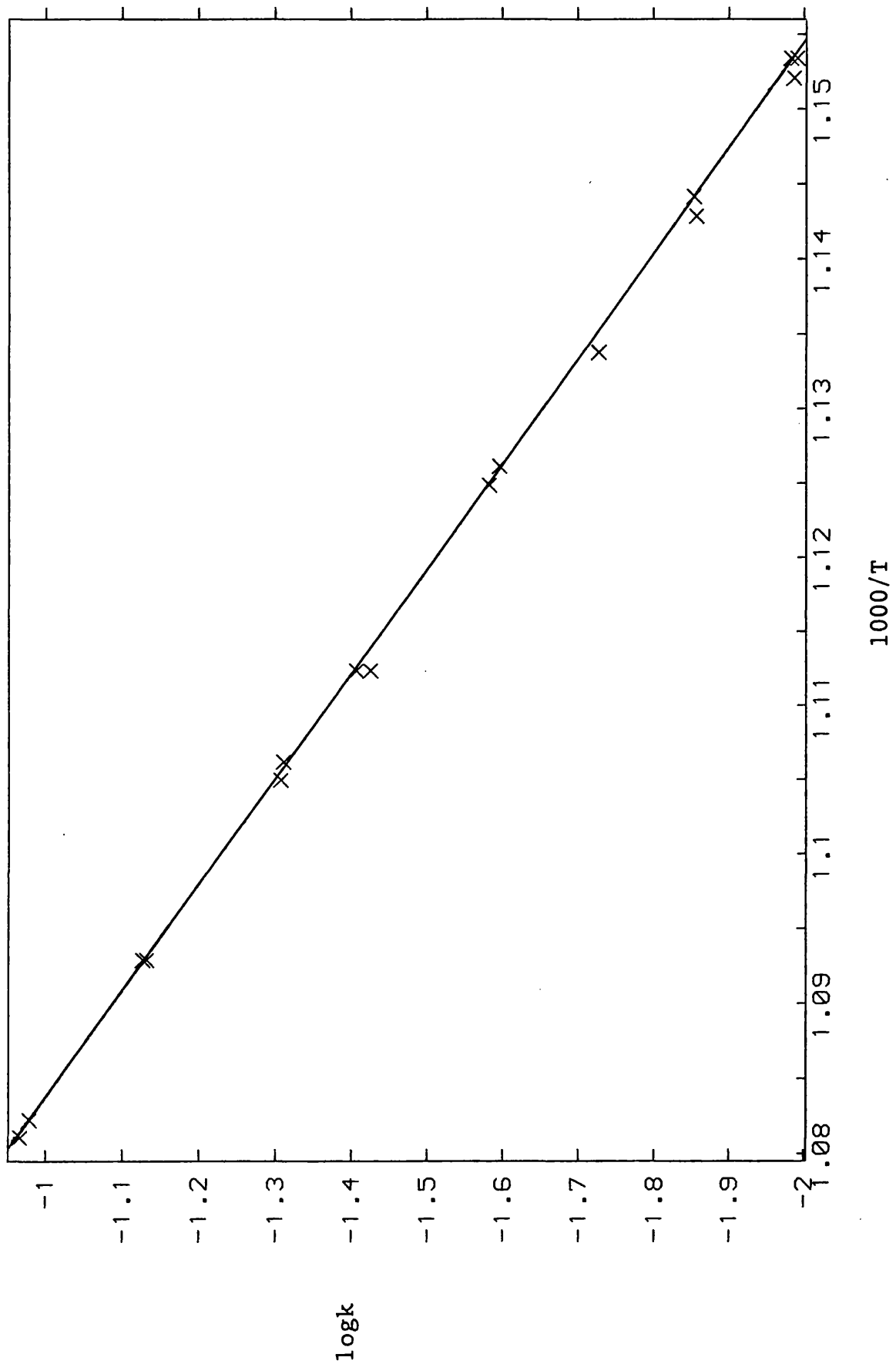
Figure 7.8 : Arrhenius plot for formation of cyclopentadiene from (1).
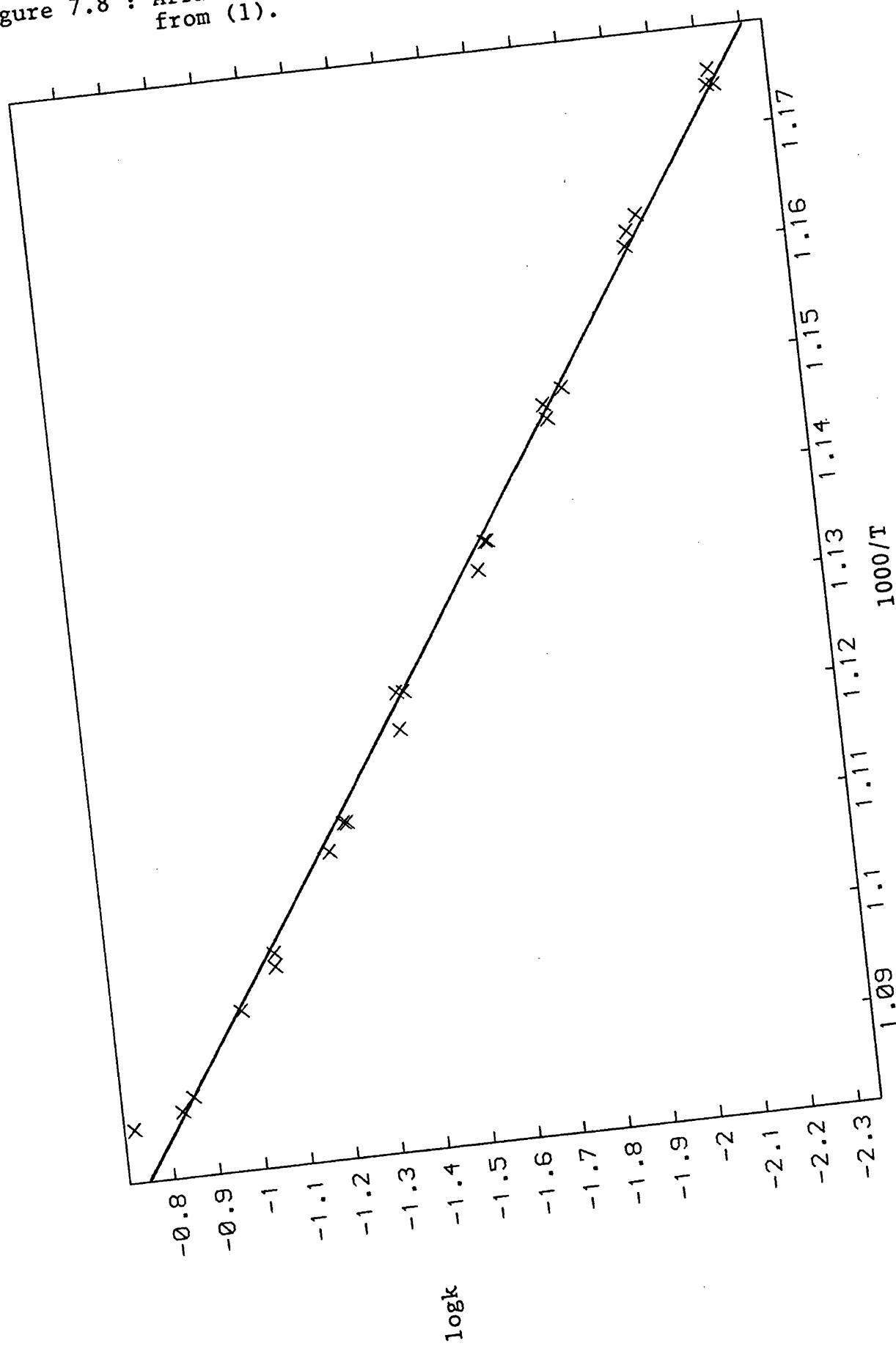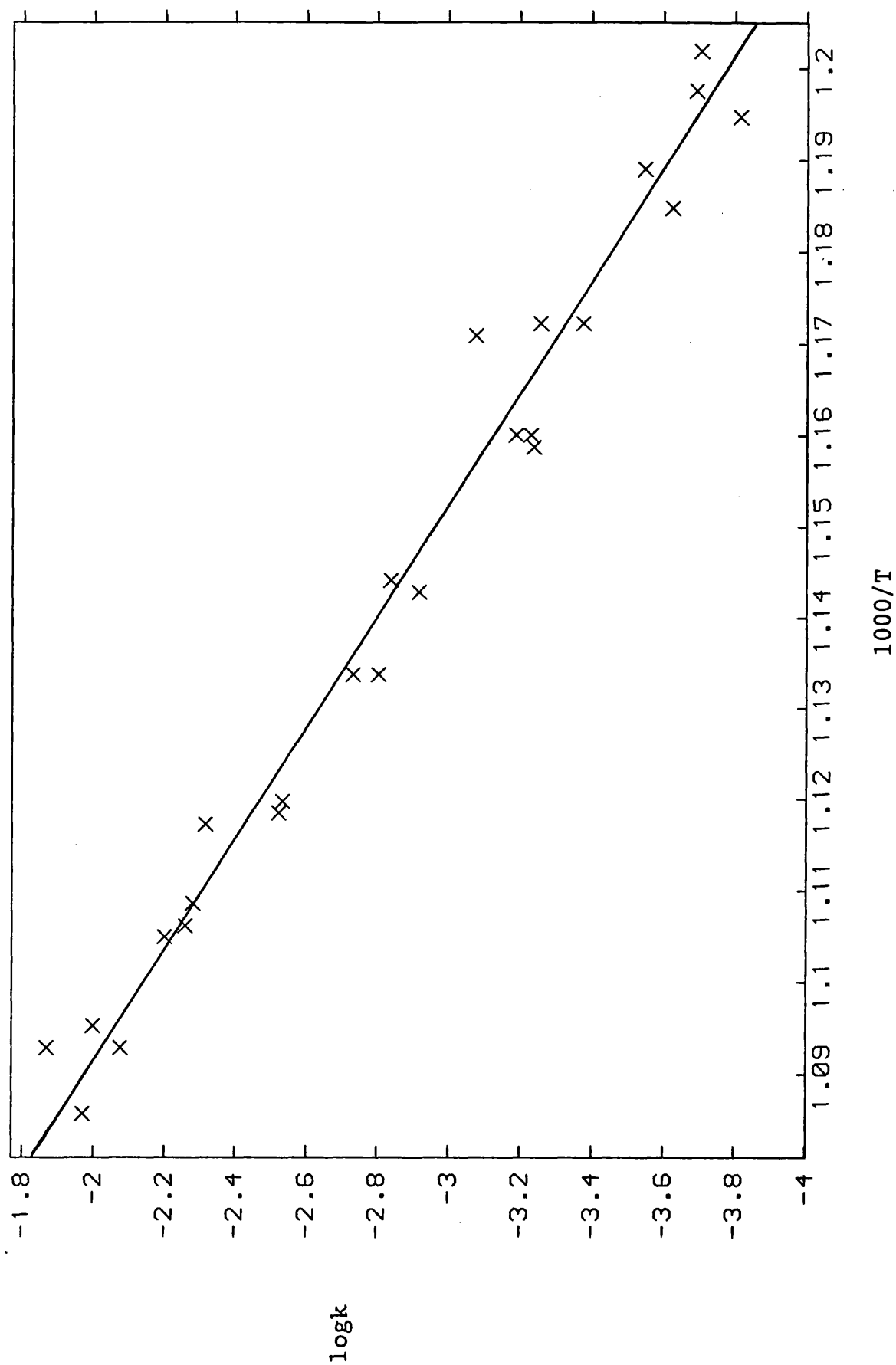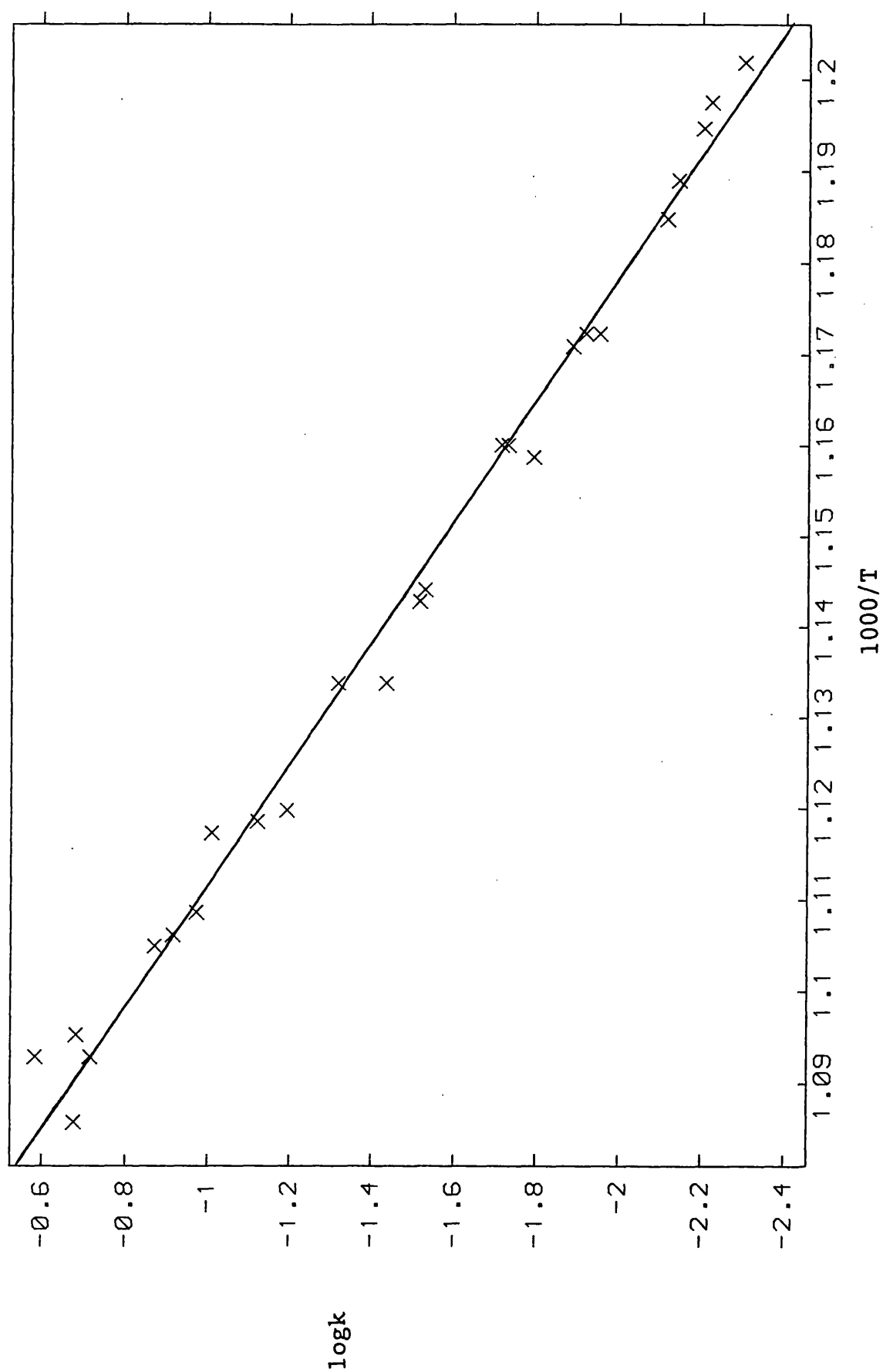
Figure 7.9 : Arrhenius plot for formation of 1,1,3,3-
tetramethyl-1,3-disilacyclobutane from (1).
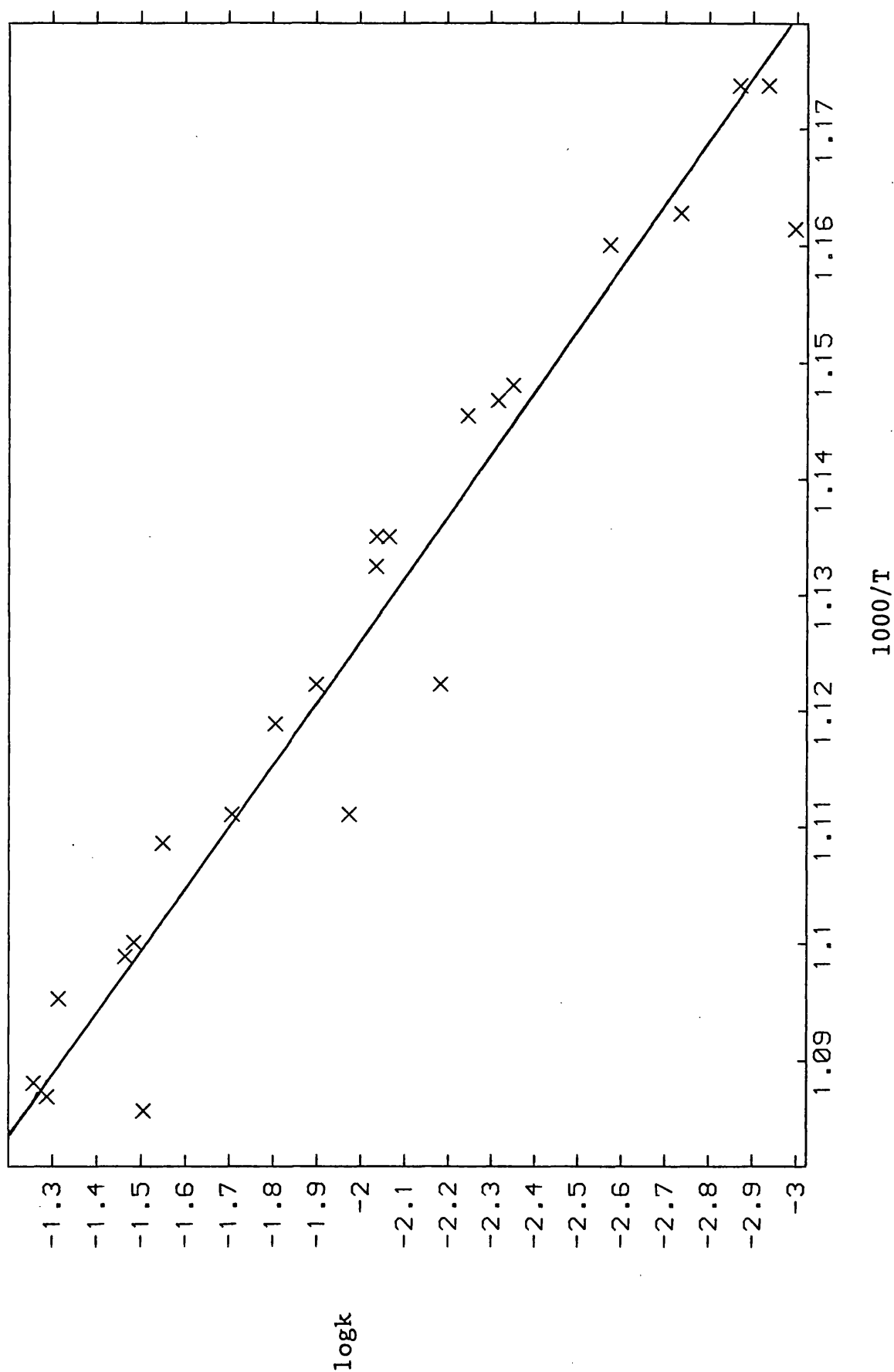
Figure 7.10 : Arrhenius plot for formation of 1,1-dimethyl-
1-silacyclopent-3-ene from (1).
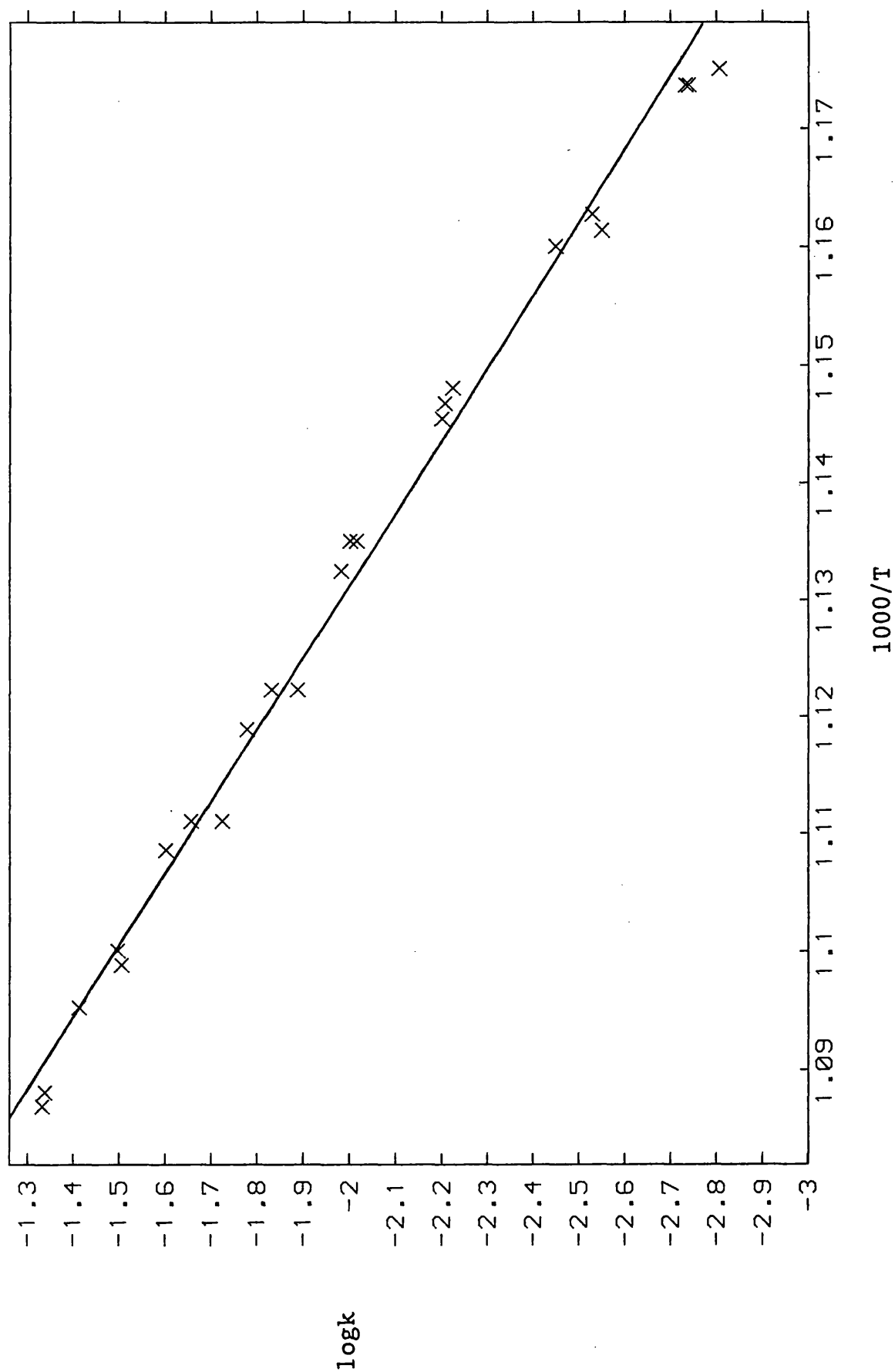
Figure 7.11 : Arrhenius plot for formation of 1,1-dimethyl-
1-silacyclobut-2-ene from (1).
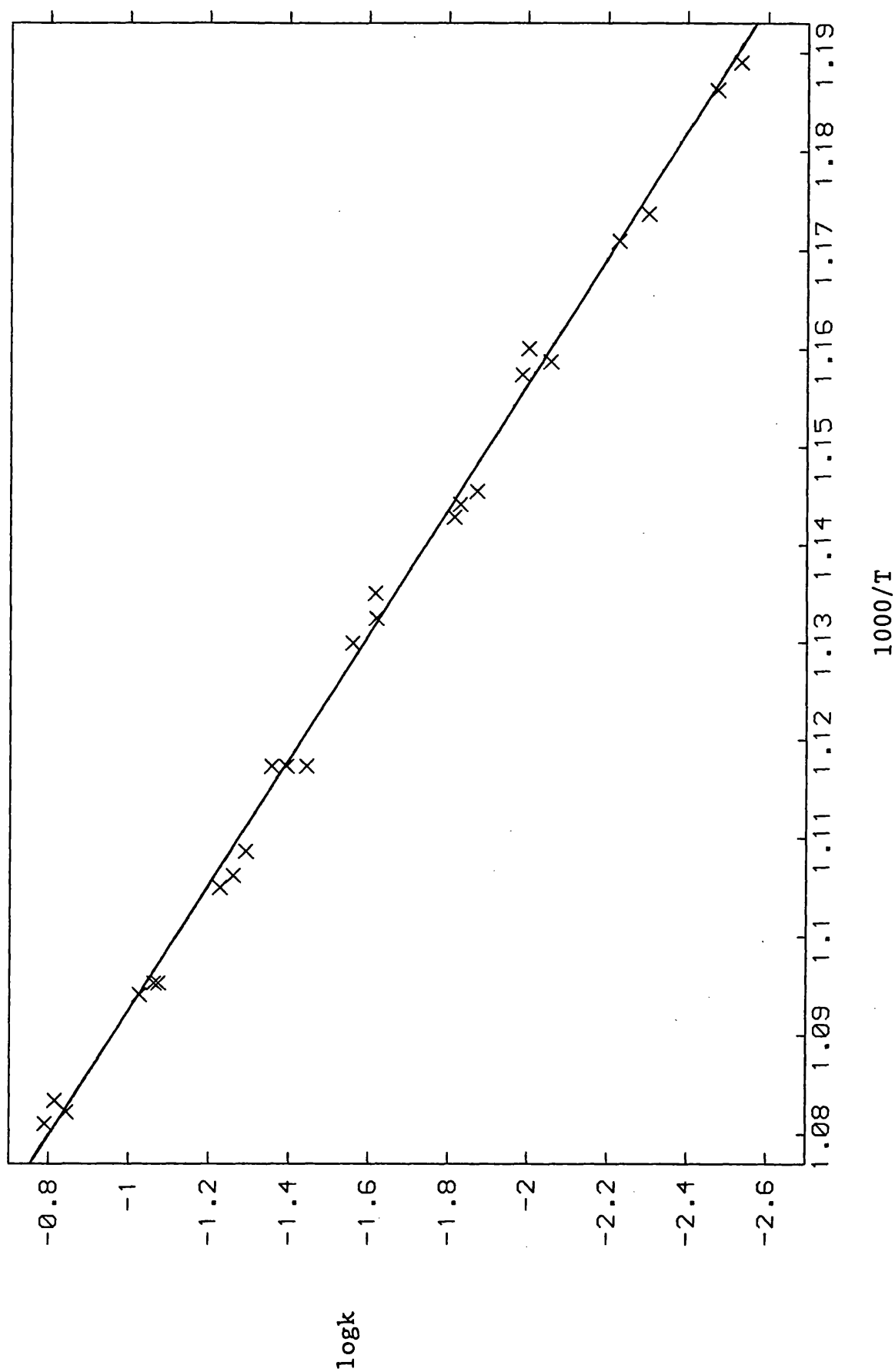
225

Figure 7.12 : Arrhenius plot for formation of 1,1-dimethyl-1-silacyclopenta-2,4-diene from (1).

Figure 7.13 : Arrhenius plot for formation of 1-methyl-1-
silacyclopent-3-ene from (1).

Figure 7.14 : Arrhenius plot for the corrected decay of (1) in excess methanol.

1000/T

logk

Figure 7.15 : Arrhenius plot for formation of butadiene from
(1) + excess methanol.

229

Figure 7.16 : Arrhenius plot for formation of ethene from (3).

Figure 7.17 : Arrhenius plot for formation of propene from (3).

Figure 7.18 : Arrhenius plot for formation of butadiene from (3).

Figure 7.19 : Arrhenius plot for formation of cyclopentadiene from (3).

Figure 7.20 : Arrhenius plot for formation of 1,1-dimethyl-
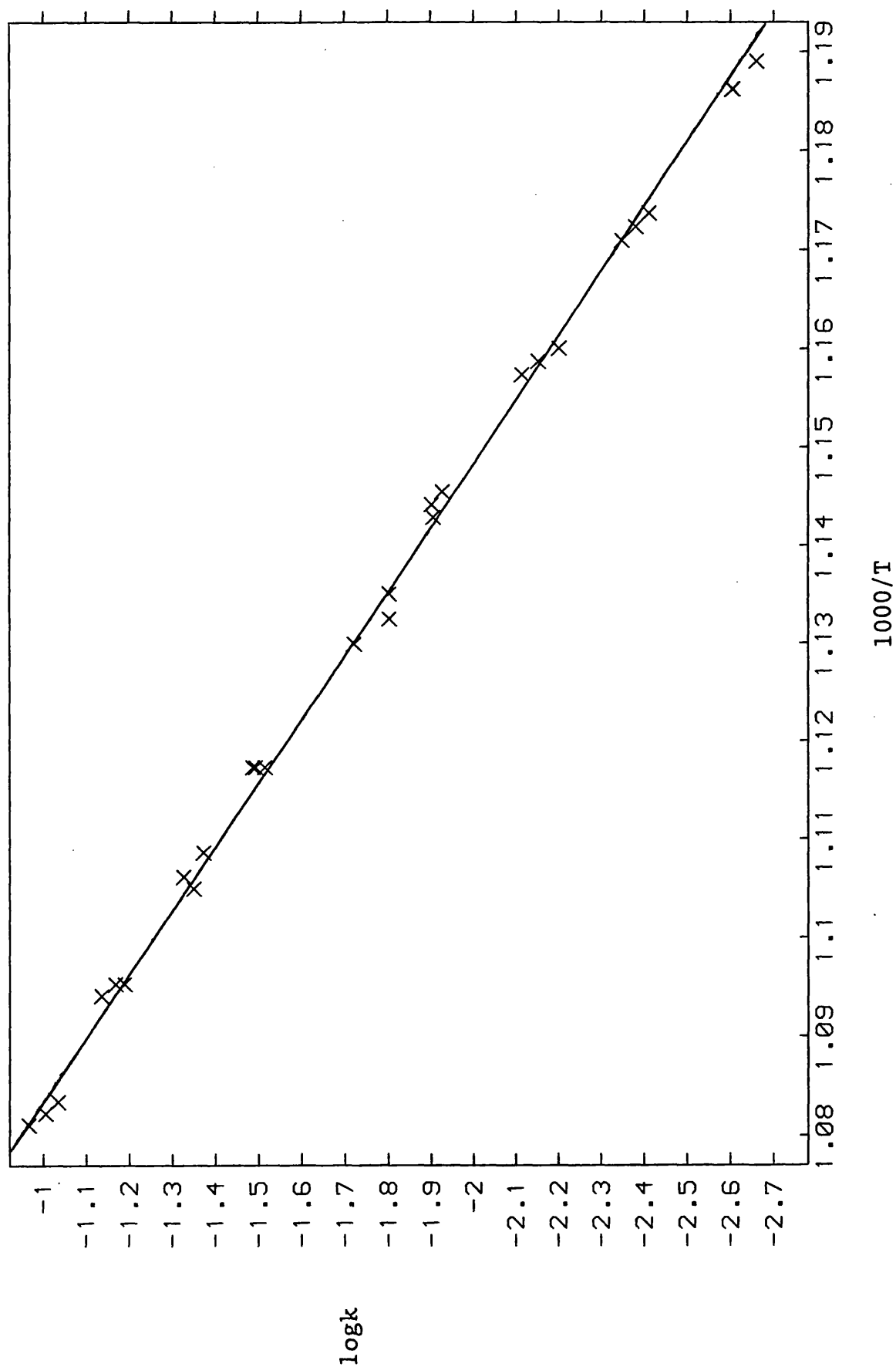1-silacyclopent-3-ene from (3).

1000/T

logk

Figure 7.21 : Arrhenius plot for formation of 1,1-dimethyl-
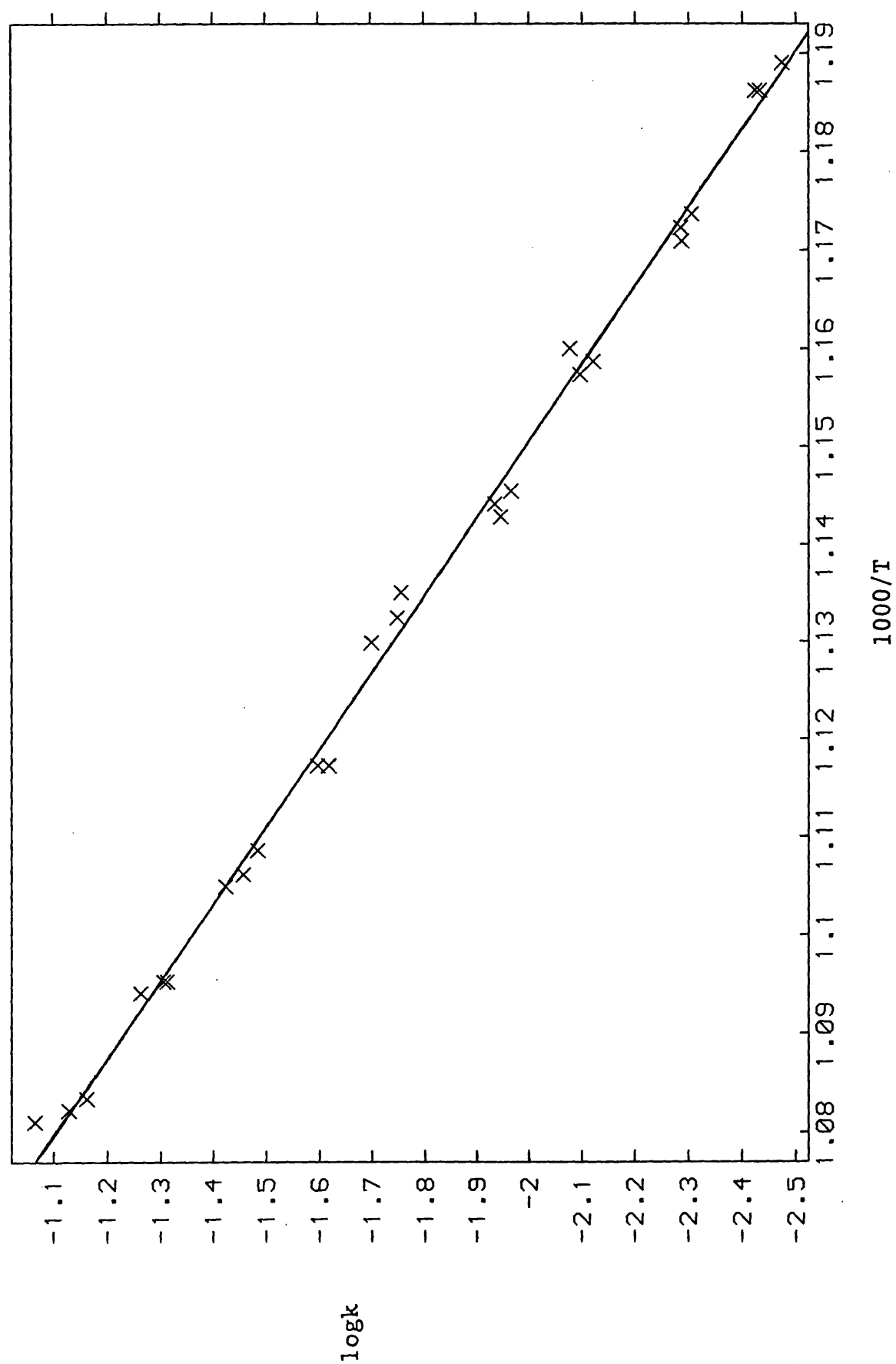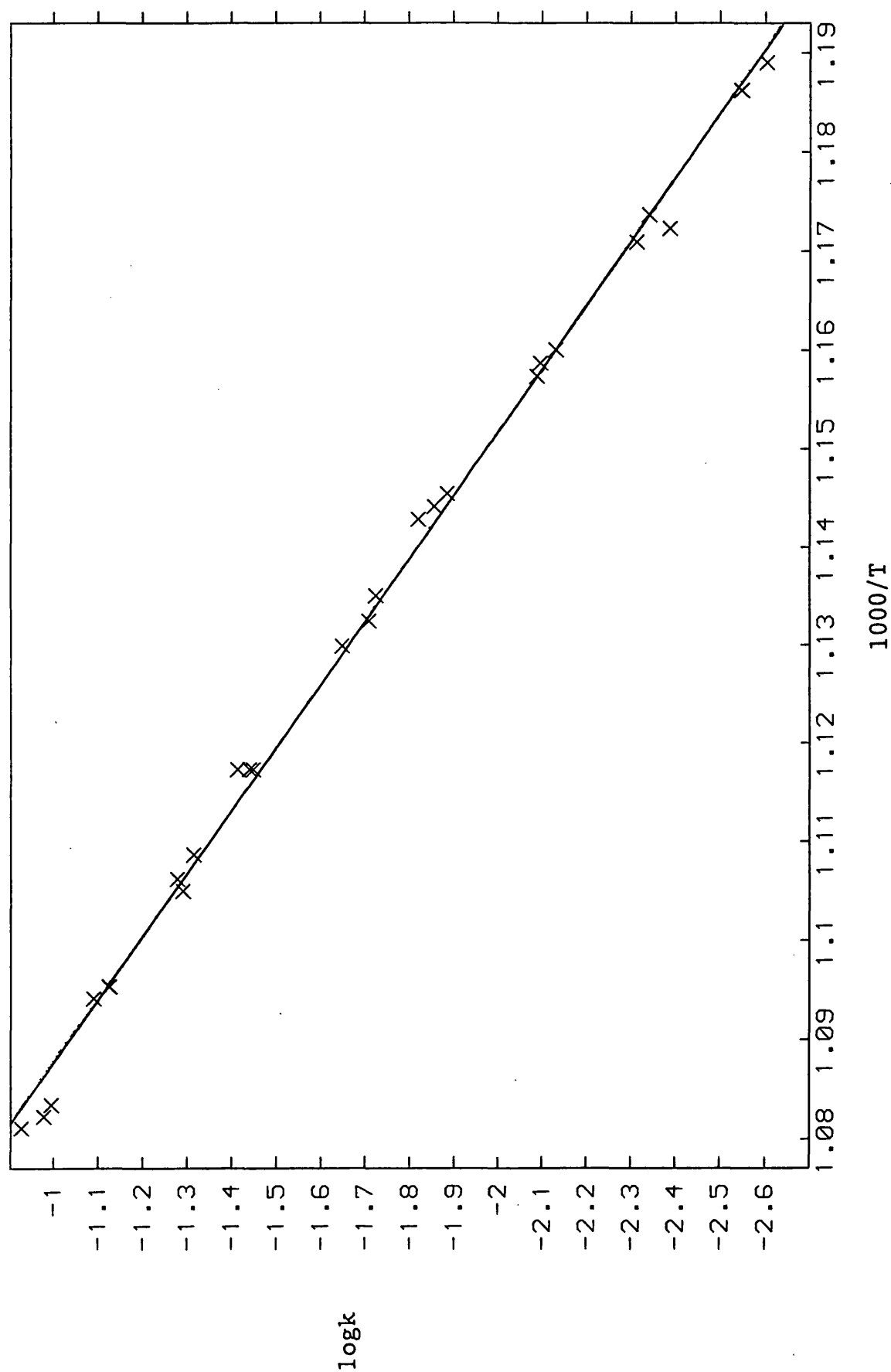1-silacyclopenta-2,4-diene from (3).

235

Figure 7.22 : Arrhenius plot for formation of 1-methyl-1-
silacyclopent-3-ene from (3).

References

1. R. T. Conlin and D. L. Wood, J. Am. Chem. Soc., 1981, 103, 1843.

2. R. T. Conlin and Y. W. Kwak, Organometallics, 1984, 3, 918.

3. R. T. Conlin and R. S. Gill, J. Am. Chem. Soc., 1983, 105, 618.

4. I. M. T. Davidson, S. I.-Maghsoodi, T. J. Barton and N. Tillman, J. C. S. Chem. Comm., 1984, 478.

5. I. M. T. Davidson and R. J. Scampton, J. Organomet. Chem., 1984, 271, 249.

6. R. T. Conlin and Y. W. Kwak, J. Am. Chem. Soc., 1986, 108, 834.

7. See chapter one.

8. R. Walsh, J. C. S. Chem. Comm., 1982, 1415.

9. H. E. O'Neal, personal communication to I. M. T. Davidson.

10. I. M. T. Davidson, A. Fenton, S. I.-Maghsoodi, R. J. Scampton, N. Auner, J. Grobe, N. Tillman and T. J. Barton, Organometallics, 1984, 3, 1593.

11. L. E. Gusel'nikov, K. S. Konobeyevsky, V. M. Vdovin and N. S. Nametkin, Dokl. Akad. Nauk SSSR, 1977, 235, 1086.

12. P. John, personal communication to I. M. T. Davidson.

13. I. M. T. Davidson, C. E. Dean and F. T. Lawrence, J. C. S. Chem. Comm., 1981, 52.

14. I. M. T. Davidson and I. T. Wood, J. C. S. Chem. Comm., 1982, 550.

15. D. Lei, R. J. Hwang and P. P. Gaspar, J. Organomet. Chem., 1984, 271, 1.

16. See chapter one.

17. D. Lei and P. P. Gaspar, J. C. S. Chem. Comm., 1985, 1149.

18. D. Lei and P. P. Gaspar, Organometallics, 1986, 5, 1276.

19. K. Krogh-Jesperson, J. Am. Chem. Soc., 1985, 107, 537.

20. M. S. Gordon, Chem. Phys. Lett., 1985, <u>114</u>, 348.

21. R. Nakao, K. Oka, T. Dohmaru, Y. Nagata and T. Fukumoto, J. C. S. Chem. Comm., 1985, 766.

22. T. N. Bell, K. A. Perkins and P. G. Perkins, J. C. S. Chem. Comm., 1980, 1046.

23. H. M. Frey and R. Pottinger, J. C. S. Faraday Trans. I, 1978, <u>74</u>, 1827.

24. See chapter ten.

25. S. Ijadi-Maghsoodi, unpublished results.

CHAPTER EIGHT

PYROLYSIS OF CIS AND TRANS DIMETHYL(1-PROPENYL)VINYLSILANE

INTRODUCTION

Gaspar and Lei[1] have recently shown that a 1,5-sigmatropic shift is the dominant reaction channel for the silacyclopropane intermediate formed by cis-addition of dimethylsilylene to cis,cis-2,4-hexadiene.
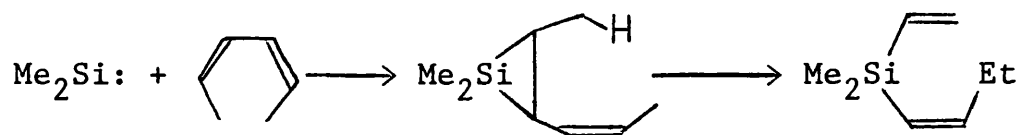

By pyrolysis of the title compounds[2] they have obtained evidence that the process is reversible, and that a sigmatropic hydrogen shift in dimethyl(cis-1-propenyl) vinylsilane gives rise to cis-1,1,2-trimethyl-3-vinylsilacyclopropane.

In the presence of a fivefold excess of 2,3-dimethylbutadiene as a silylene trap, scheme 8.1 was proposed to account for the observed products (see Scheme 8.1 overleaf).

This chapter describes the results of kinetic measurements and computer modelling carried out on the title compounds, in order to investigate the validity of scheme 8.1, and measure Arrhenius parameters for reactions 1, 2 and 3, assuming that under the reaction conditions, the reverse of reaction 3 is negligible.

The pulse stirred-flow (SFR) technique had not been previously applied to such a complex system of reversible and parallel reactions, therefore, the appropriate kinetic equations had to be derived, and are given in appendix 1.

Scheme 8.1
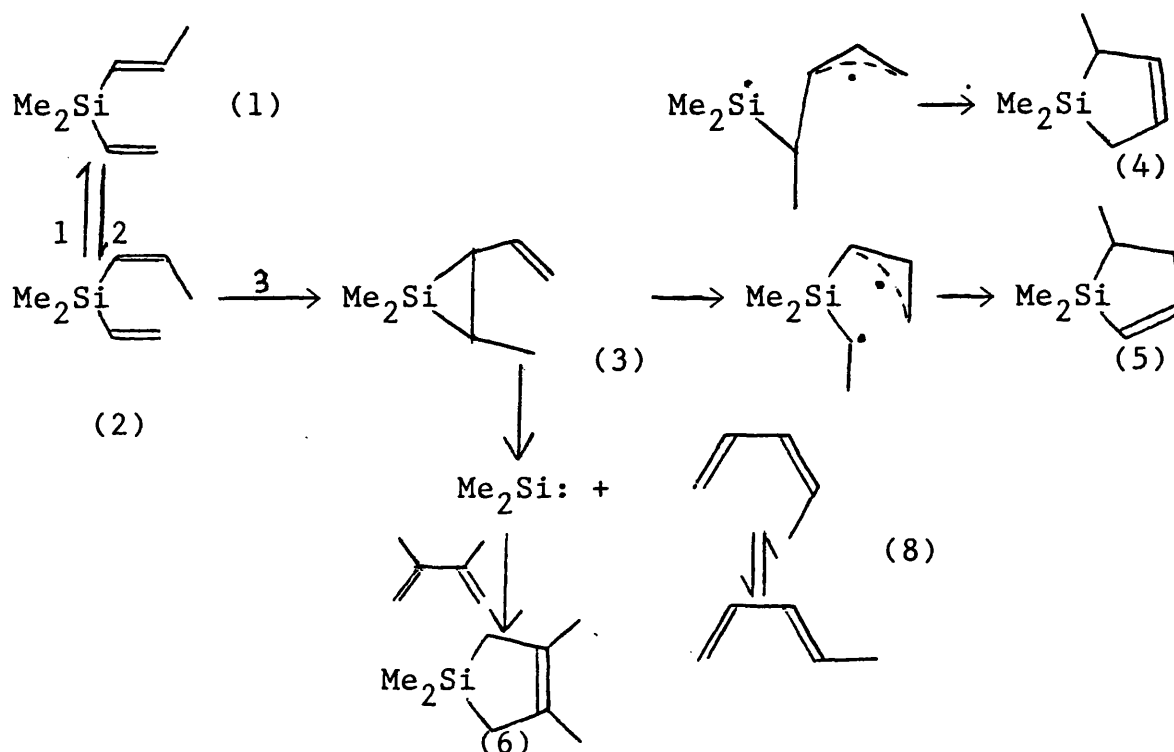
RESULTS AND DISCUSSION

Pyrolysis of dimethyl(cis-1-propenyl)vinylsilane

Approximately 0.2 torr samples of dimethyl(cis-1-propenyl) vinylsilane (2), with a tenfold excess of 2,3-dimethylbutadiene, were pyrolysed using the SFR technique between 501-571°C, giving the same products as observed

originally,[2] and predicted by scheme 8.1.

Rate constants for the formation of products (4), (5), and (6) are given in Table 8.1, a least squares analysis of the resulting Arrhenius plots shown in figures 8.1, 8.2 and 8.3, gave the Arrhenius parameters in Table 8.2.

The most reliable results in Table 8.2 were those for the formation of (6), because there was some difficulty in accurately measuring rate constants for the formation of (4) and (5) due to the relatively small quantities produced. In spite of this, using each as a measure of k_3, as described in appendix 1, gave reasonable agreement for the calculated values of k_3 at 800K, which shows that these results are consistent with scheme 8.1.

Kinetic measurements were also undertaken on the formation of the C_5 hydrocarbons, giving $\log A = 11.2$ and $E = 186$, in fair agreement with the foregoing results, but these measurements were less reliable because of interference from impurities and minor pyrolysis products from the 2,3-dimethylbutadiene.

Pyrolysis of dimethyl(trans-1-propenyl)vinylsilane

SFR pyrolyses of ca. 0.1 torr samples of dimethyl(trans-1-propenyl)vinylsilane, (1), with a tenfold excess of 2,3-dimethylbutadiene, between 501-571°C gave only (2), (6) and (8) as significant products, with very small quantities of

Table 8.1

Rate constants for product formation $/s^{-1}$

T/K	Products (4)	(5)	(6)
844	0.0166	0.0340	0.298
843	0.0166	0.0312	0.285
834	0.0119	0.0227	-
834	0.0104	0.0215	0.195
833	0.0102	0.0213	0.188
824	0.00859	0.0154	0.141
821	0.00813	0.0143	0.128
819	0.00735	0.0133	0.121
814	0.00621	0.0115	0.0995
813	0.00666	0.0117	0.100
813	0.00663	0.0120	0.0990
804	0.00551	0.00981	0.0736
803	0.00476	0.00872	0.0695
801	0.00458	0.00792	0.0650
796	0.00393	0.00748	0.0586
795	0.00359	0.00591	0.0548
795	0.00421	0.00795	0.0578
786	0.00374	0.00616	0.0443
783	-	-	0.0368
782	0.00237	0.00367	0.0352
775	-	-	0.0286
774	-	-	0.0258
774	-	-	0.0275

Table 8.2

product	$E/kJmol^{-1}$	$logA/s^{-1}$	$logA^{*}$	$logA_3/s^{-1}$	$k_3(800K)/s^{-1}$
(4)	157±6	7.91±.39	1.21	9.12	0.074
(5)	170.4±7	9.03±.45	0.93	9.96	0.068
(6)	180.2±2.5	10.59±.16	0.086	10.67	0.081

* : logA=log(1/path factor)

Table 8.3

Rate constants for product formation $/\text{s}^{-1}$

T/K	(6)	(8)
844	0.0188	0.0353
843	0.0202	0.0354
841	0.0196	0.0344
834	0.0164	0.0299
832	0.0151	0.0279
830	0.0143	0.0277
824	0.0120	0.0279
823	0.0118	0.0208
822	0.0119	0.0225
816	0.0107	0.0200
813	0.0100	0.0171
810	0.00928	0.0162
804	0.00773	0.0136
803	0.00716	0.0178
802	0.00767	0.0129
795	0.00636	0.0119
795	0.00613	0.0116
792	0.00585	0.0100
786	0.00508	0.00895
784	0.00487	0.00776
783	0.00478	0.00916
776	0.00376	0.00641
775	0.00388	0.00622
774	0.00369	0.00641
774	0.00361	0.00606

(4) and (5), this was because (1) had a greater thermal stability than (2). Rate constants for the formation of products (6) and (8) are given in Table 8.3.

A least squares analysis of the resulting Arrhenius plots shown in figures 8.4 and 8.5, gave the Arrhenius parameters given in Table 8.4.

Table 8.4

product	$E/kJmol^{-1}$	$logA/s^{-1}$
(6)	131 ± 2	6.4 ± 0.1
(8)	139 ± 2	7.2 ± 0.13

Arrhenius parameters for (6) are preferred, due to some impurities and minor pyrolysis products of 2,3-dimethylbutadiene interfering with (8).

From the results in Table 8.4, it follows that they do not relate to an elementary reaction, which shows that there is not a simple rate determining step in the formation of (6) and (8) from (1).

From the measured yields of (6) and (2) in these experiments, rate constants were obtained for the formation

of (6) from the (2) produced from (1), as shown in Table 8.5.

A least squares fit of the resulting Arrhenius plot (figure 8.6), gave the following Arrhenius parameters for the formation of product (6).

$$\log k/s^{-1} = (10.94 \pm .13) - (184 \pm 2 kJmol^{-1}/2.303RT)$$

in good agreement to the Arrhenius parameters for k_3 obtained from the pyrolysis of (2), as described earlier.

Cis-trans isomerisation

In order to calculate rate constants for the cis-trans isomerisation reactions, the kinetic equations given in appendix 1 had to be used. These require the apparent rate constants k_1' and k_2', obtained by treating the isomerisation as a simple irreversible first-order process, and k_3 as measured experimentally. Since the samples of (1) and (2) were impure, i.e. (1) contained some (2) and (2) contained some (1), it was also necessary to know the ratios $\{1'\}/\{1\}$ and $\{2'\}/\{2\}$ where $\{1'\}$ is the amount of (1) present as an impurity in the sample of (2), and $\{1\}$ is the total amount of (1) after pyrolysis, similarly for $\{2'\}/\{2\}$.

Table 8.6 gives the apparent rate constants k_1', k_2', and the ratios $\{1'\}/\{1\}$ and $\{2'\}/\{2\}$. The ratio $\{1'\}/\{1\}$ was

Table 8.5

Rate constants for product formation/s^{-1}

T/K	(6)
844	0.343
843	0.365
834	0.288
832	0.255
830	0.236
824	0.188
823	0.183
822	0.181
816	0.154
813	0.146
804	0.0968
803	0.0896
802	0.0936
795	0.0715
795	0.0698
792	0.0631
786	0.0525
784	0.0503
783	0.0479
776	0.0363
775	0.0371
774	0.0355
774	0.0341

Table 8.6

T/K	k_1'/s^{-1}	k_2'/s^{-1}	{1'}/{1}	{2'}/{2}
844	0.0942	0.00747	2.576	0.329
843	0.0921	0.00747	2.579	0.326
841	–	0.00723	2.669	–
834	0.0645	0.00767	2.447	0.352
834	0.0633	–	–	–
833	0.0631	–	–	0.352
832	–	0.00790	2.350	–
830	–	0.00813	2.282	–
824	0.0471	0.00855	2.137	0.392
823	–	0.00865	2.109	–
822	–	0.00873	2.083	–
821	0.0431	–	–	0.405
819	0.0411	–	–	0.410
816	–	0.00917	1.968	–
814	0.0334	–	–	0.450
813	0.0340	0.00909	1.974	0.449
813	0.0336	–	–	0.444
810	–	0.00977	1.840	–
804	0.0260	0.0102	1.692	0.506
803	0.0248	0.0105	1.682	0.511
802	–	0.0105	1.651	–
801	0.0223	–	–	0.553
796	0.0239	–	–	0.506
795	0.0196	0.0113	1.532	0.600
795	0.0187	0.0112	1.517	0.594
792	–	0.0117	1.468	–
786	0.0158	0.0122	1.394	0.658
784	–	0.0122	1.389	–
783	0.0159	0.0125	1.351	0.594
782	0.0156	–	–	0.636
776	–	0.0128	1.298	–
775	0.0133	0.0129	1.287	0.678
774	0.0138	0.0130	1.292	0.672
774	0.0132	0.0130	1.269	0.631

calculated by measuring the amount of (1) after pyrolysis. {1'}, the amount of (1) initially present as an impurity in the sample of (2), was calculated from a combination of a knowledge of the ratio of (1)/(2) in the initial sample of (2), and calculation of the total quantity of material initially present, i.e. the combined amount of (1), (2), (4), (5) and (6) observed after pyrolysis.

From the plots of k_1' vs. T, k_2' vs. T, {1'}/{1} vs. T and {2'}/{2} vs. T as shown in figures 8.7, 8.8, 8.9 and 8.10, it was possible to estimate values of k_1', k_2', {1'}/{1} and {2'}/{2} at various temperatures, and calculate k_3 from the experimentally measured Arrhenius parameters. Thus it was possible from the equations in appendix 1 to calculate rate constants for the cis-trans isomerisation, as given in Table 8.7.

Table 8.7

T/K	k_1/s^{-1}	k_2/s^{-1}
785	0.00625	0.00120
795	0.00881	0.00181
805	0.0140	0.0029
815	0.0214	0.00392
825	0.032	0.00619
835	0.0495	0.00977
845	0.077	0.0147

From a least squares analysis of the resulting Arrhenius plots, as shown in figures 8.11 and 8.12, the Arrhenius parameters in Table 8.8 were obtained.

Table 8.8

	E/kJmol^{-1}	$\log A/\text{s}^{-1}$
(2) $\longrightarrow$ (1)	233 ± 5	13.3 ± 0.3
(1) $\longrightarrow$ (2)	230 ± 5	12.3 ± 0.3

Computer modelling

As a further test of the validity of scheme 8.1, it was investigated by numerical integration. Scheme 8.2, equivalent to scheme 8.1 was devised.
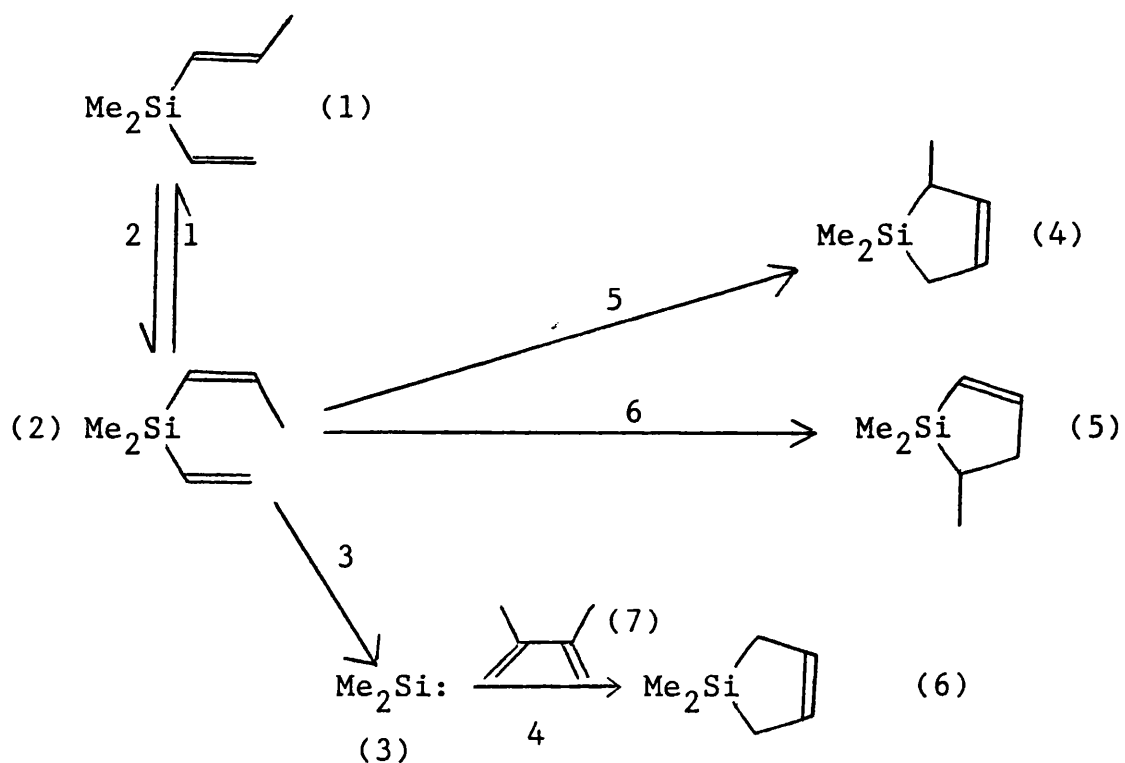
Scheme 8.2

Table 8.9 gives the Arrhenius parameters used for the numerical integration.

Table 8.9

reaction	logA	E/kJmol^{-1}	comments
1	13.3	233	a
2	12.3	230	a
3	10.7	180	a
4	9.2	9.6	see ref.3
5	7.9	157	a
6	9.0	170.4	a

a : this work.

Decomposition of (1)

Numerical integration of scheme 8.2 was used to simulate the decomposition of (1) in the presence of a tenfold excess of 2,3-dimethylbutadiene. From the experimental work, the initial concentration of (1) was estimated to be 2×10^{-6} moldm^{-3}, the initial concentration of (2), present as an impurity in (1) was $2 \times 10^{-6}/7.44 = 2.69 \times 10^{-7}$ moldm^{-3}.

From the calculated species concentrations, rate constants for the formation of (6) from (1) were calculated, and are given in Table 8.10.

Table 8.10

T/K	k/s^{-1}
775	0.00433
790	0.00673
810	0.0110
830	0.0160
845	0.0207

From figure 8.13, it can be seen that there is satisfactory agreement between the Arrhenius plot of the calculated rate constants, and the experimentally observed line, again consistent with scheme 8.1.

Decomposition of (2)

Computer modelling of scheme 8.2 was also undertaken to investigate the decomposition of species (2), in the presence of a tenfold excess of 2,3-dimethylbutadiene. From the experimental work, the initial concentration of (2) was estimated to be $4x10^{-6}$moldm^{-3} and the amount of (1) present as an impurity in each sample of (2) was 1/15th of the initial quantity of (2).

The computed product yields at 800K after 7s were in the ratio of :- (6):(1):(5):(4) = 19:5.54:1.55:1, in good agreement with the experimental product ratios of 19.68:4.96 :1.52:1.

Simulation of Gaspar's experimental results[2] at 610°C with a contact time of 5ms, 0.6 torr of reactant with a fivefold excess of 2,3-dimethylbutadiene gave a computed ratio of (6):(5):(4) = 23.3:1.81:1, in fair agreement with the experimentally measured ratio of 19.3:1.33:1. It was impossible to compare the calculated ratio of (4):(1) with the experimentally observed ratio, due to the quantity of (1) as an impurity in (2) being unspecified. However,

whatever the initial quantity of (1) present, it had no effect on the computed ratio of (6):(5):(4).

CONCLUSION

A series of kinetic experiments have been carried out on (1) and (2), from which Arrhenius parameters for reactions 1,2 and 3 have been obtained.

The results of computer modelling have provided further evidence for the validity of scheme 8.1, by being able to predict with reasonable accuracy various experimentally observed results.
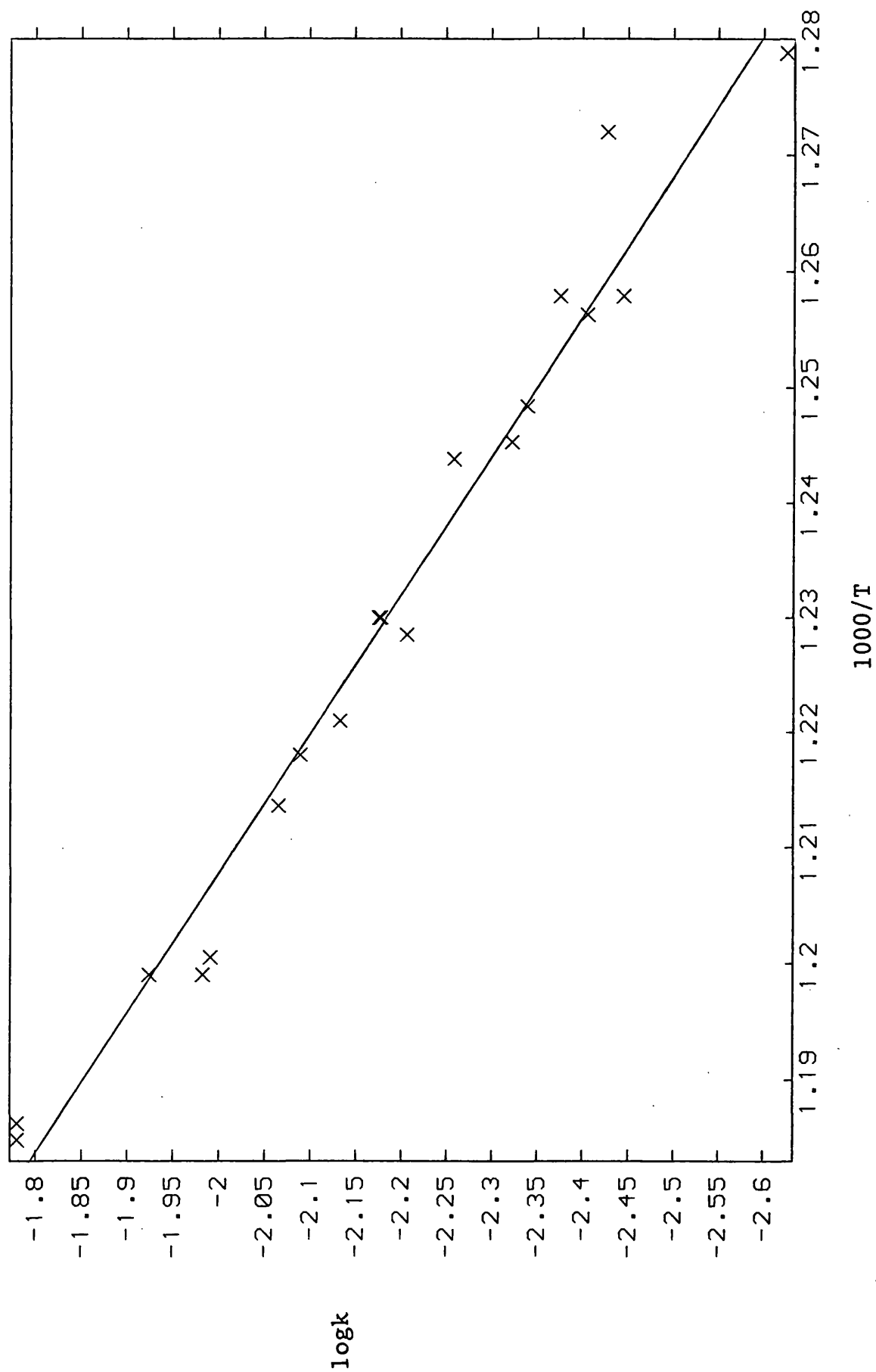
Figure 8.1 : Arrhenius plot for formation of (4) from (2).

Figure 8.2 : Arrhenius plot for formation of (5) from (2).

logk
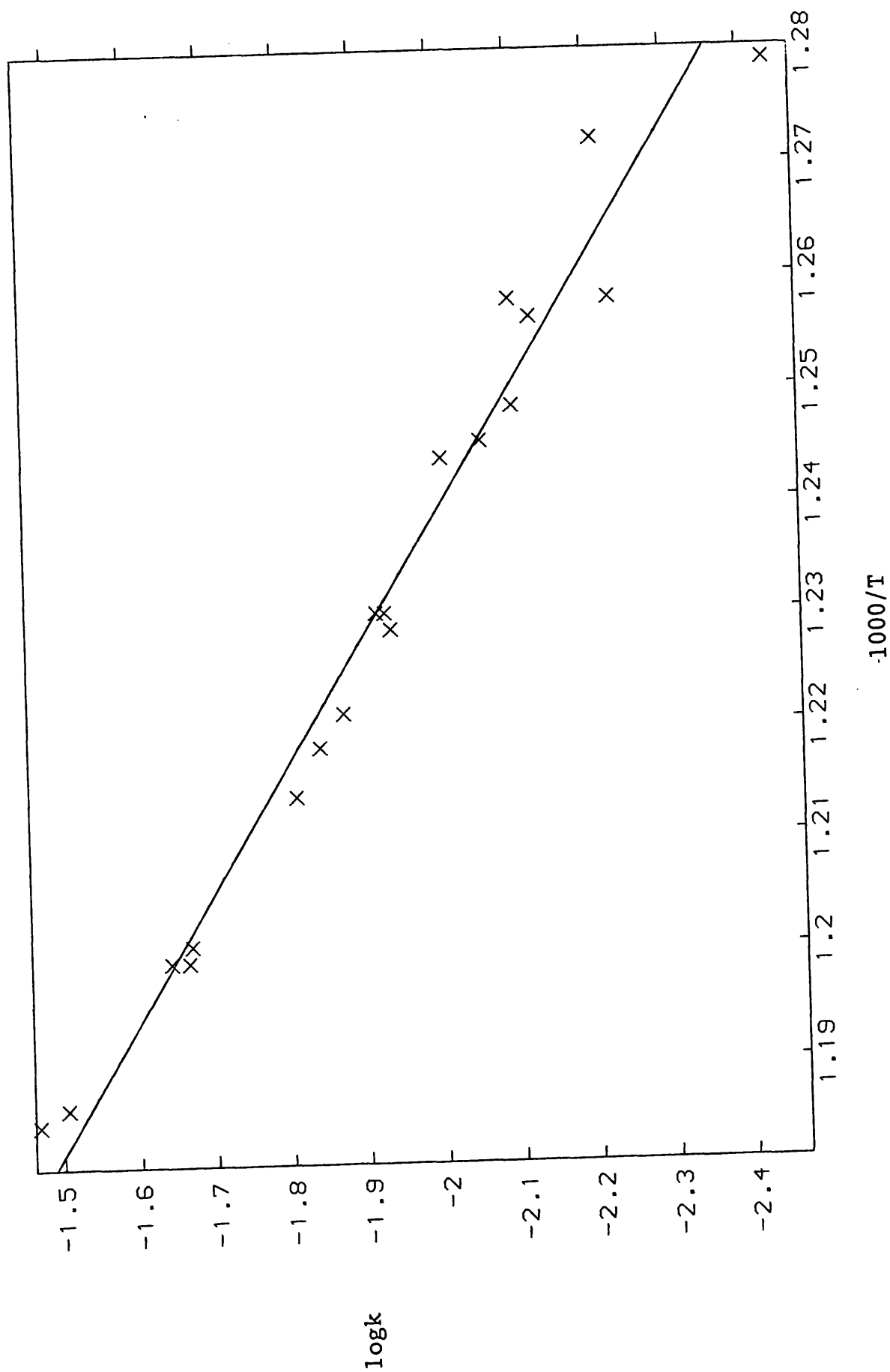
Figure 8.3 : Arrhenius plot for formation of (6) from (2).

logk
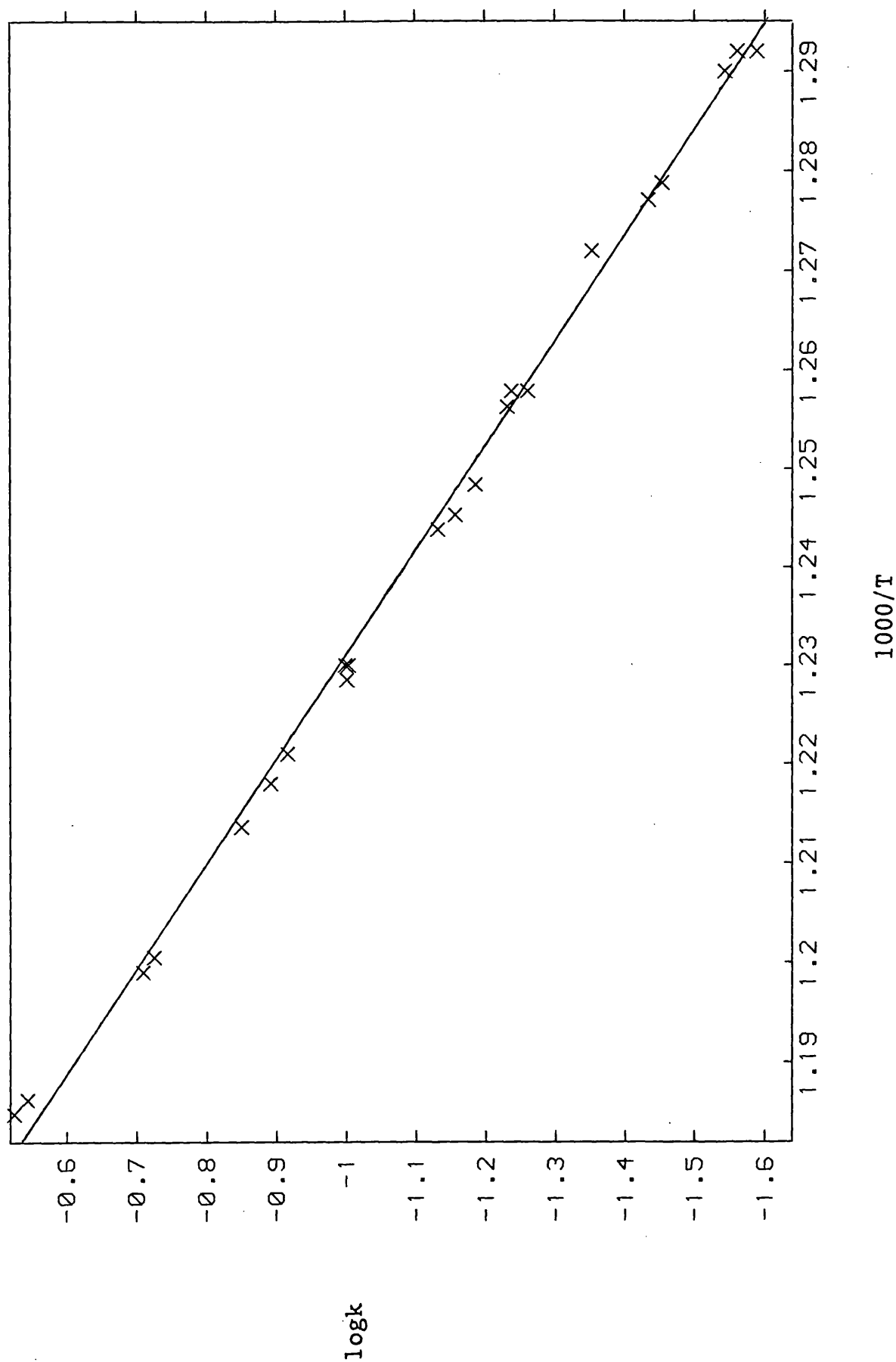
Figure 8.4 : Arrhenius plot for formation of (6) from (1).

256
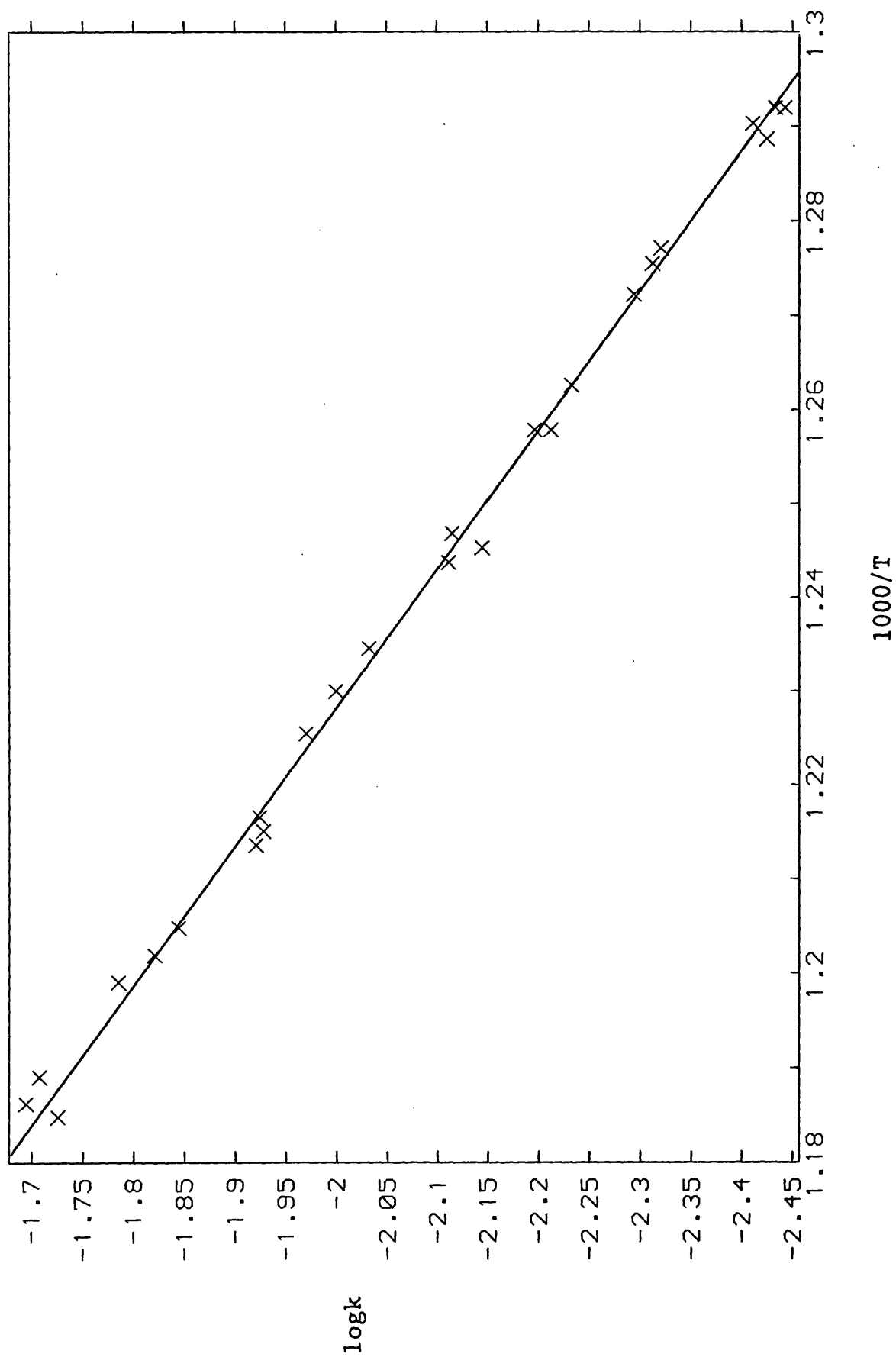
Figure 8.5 : Arrhenius plot for formation of (8) from (1).
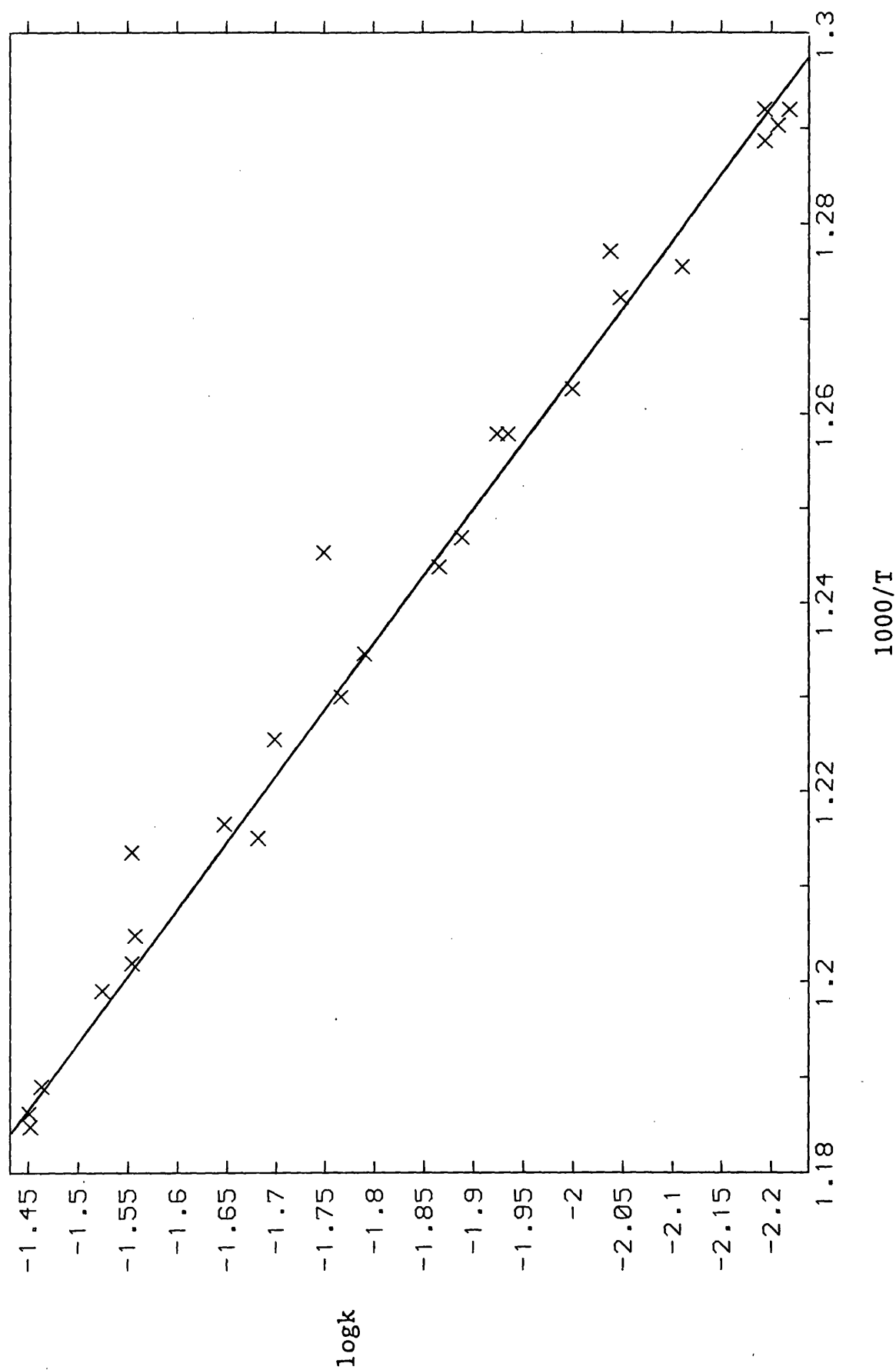
Figure 8.6 : Arrhenius plot for formation of (6) from (2) produced from (1).
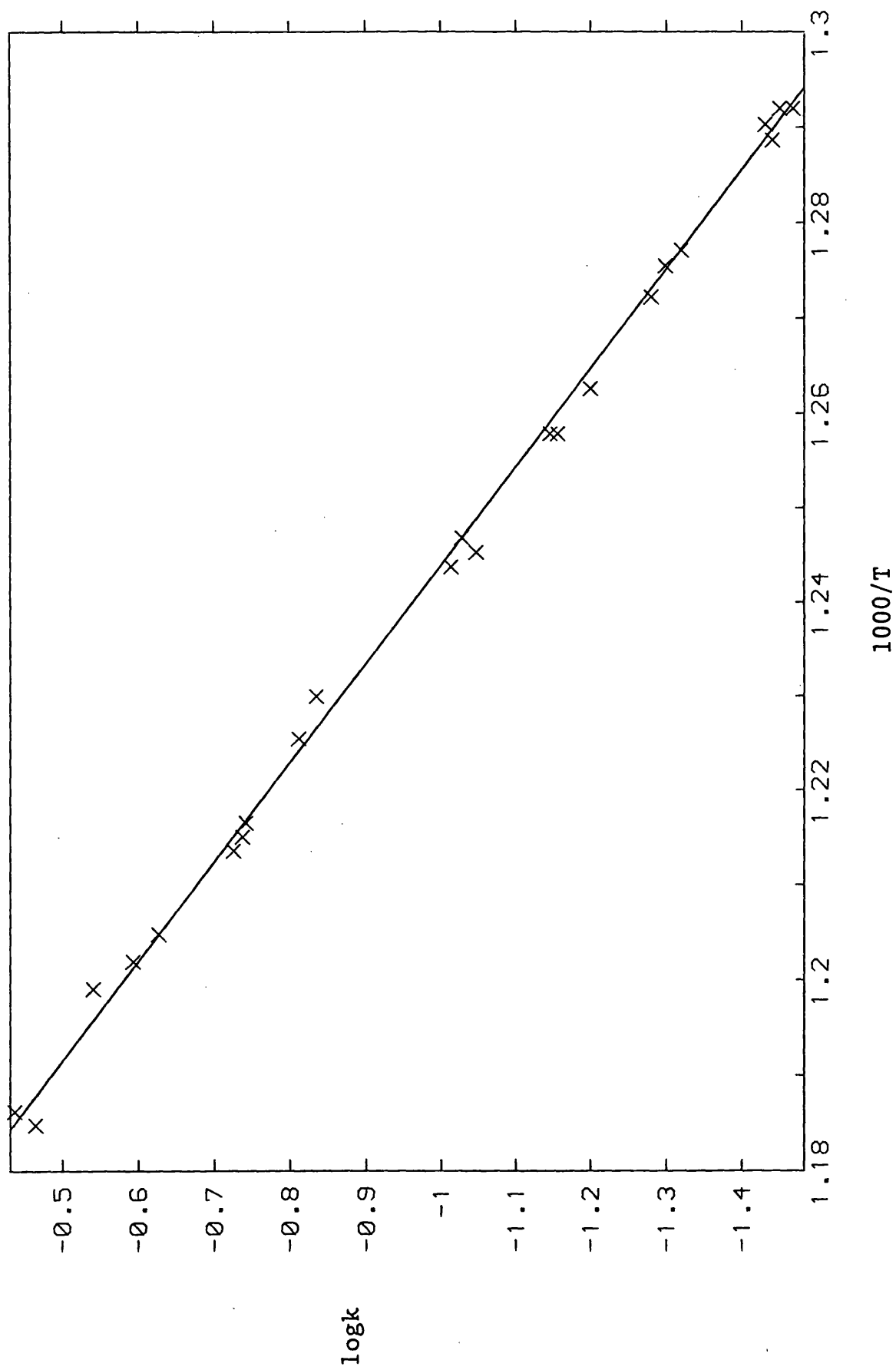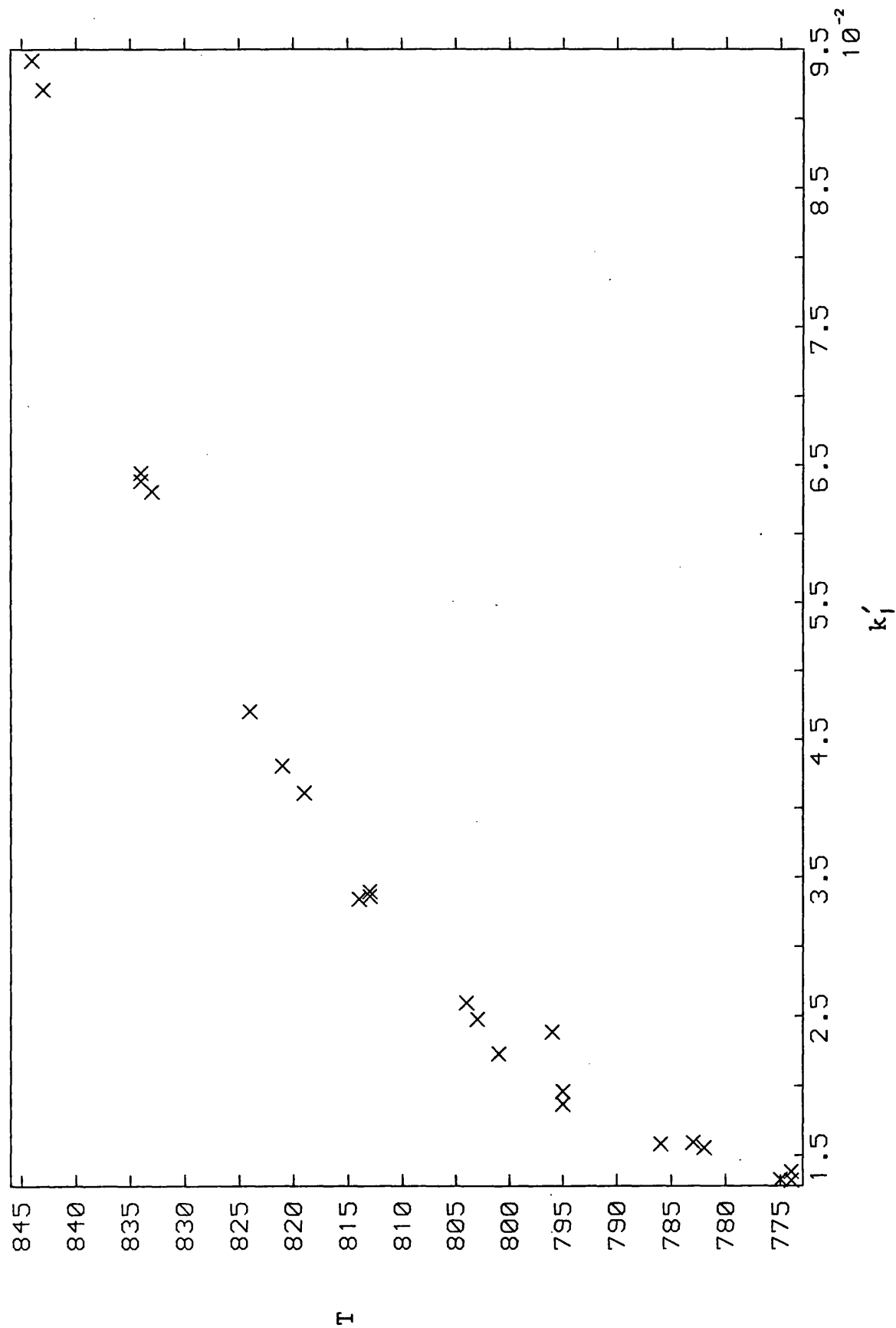
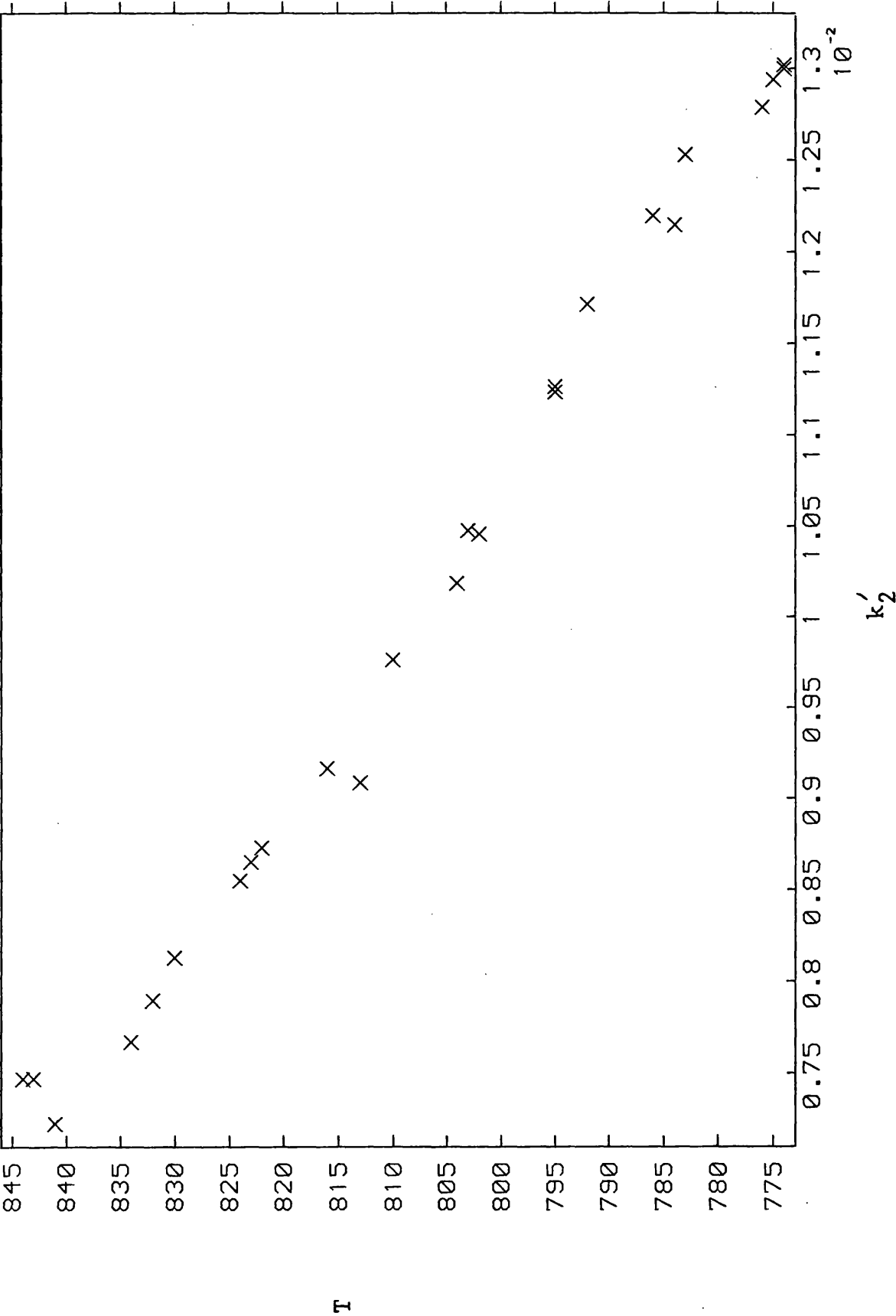Figure 8.7 : Plot of k_1' vs. T.

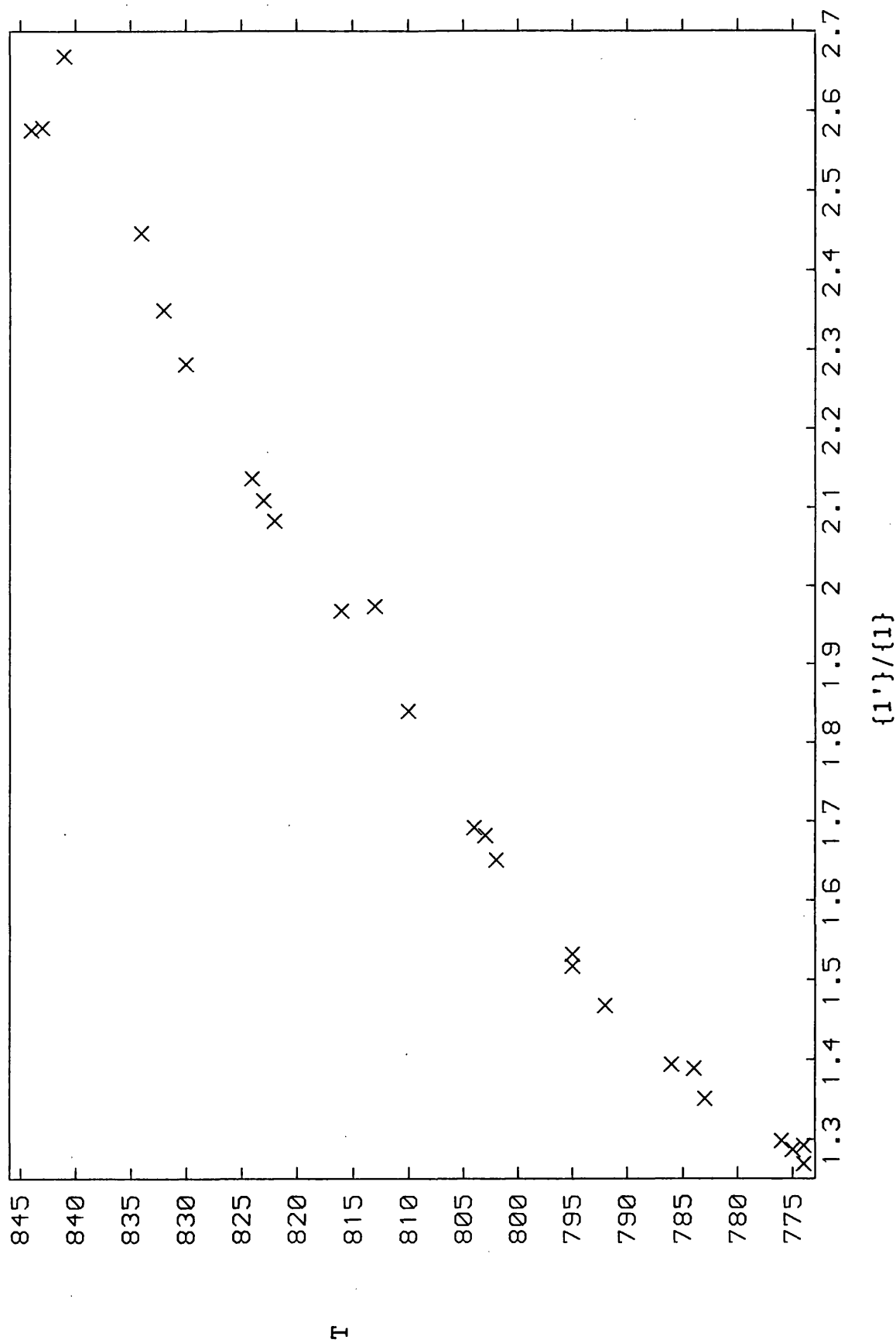Figure 8.8 : Plot of k_2' vs. T.

Figure 8.9 : Plot of {1'}/{1} vs. T
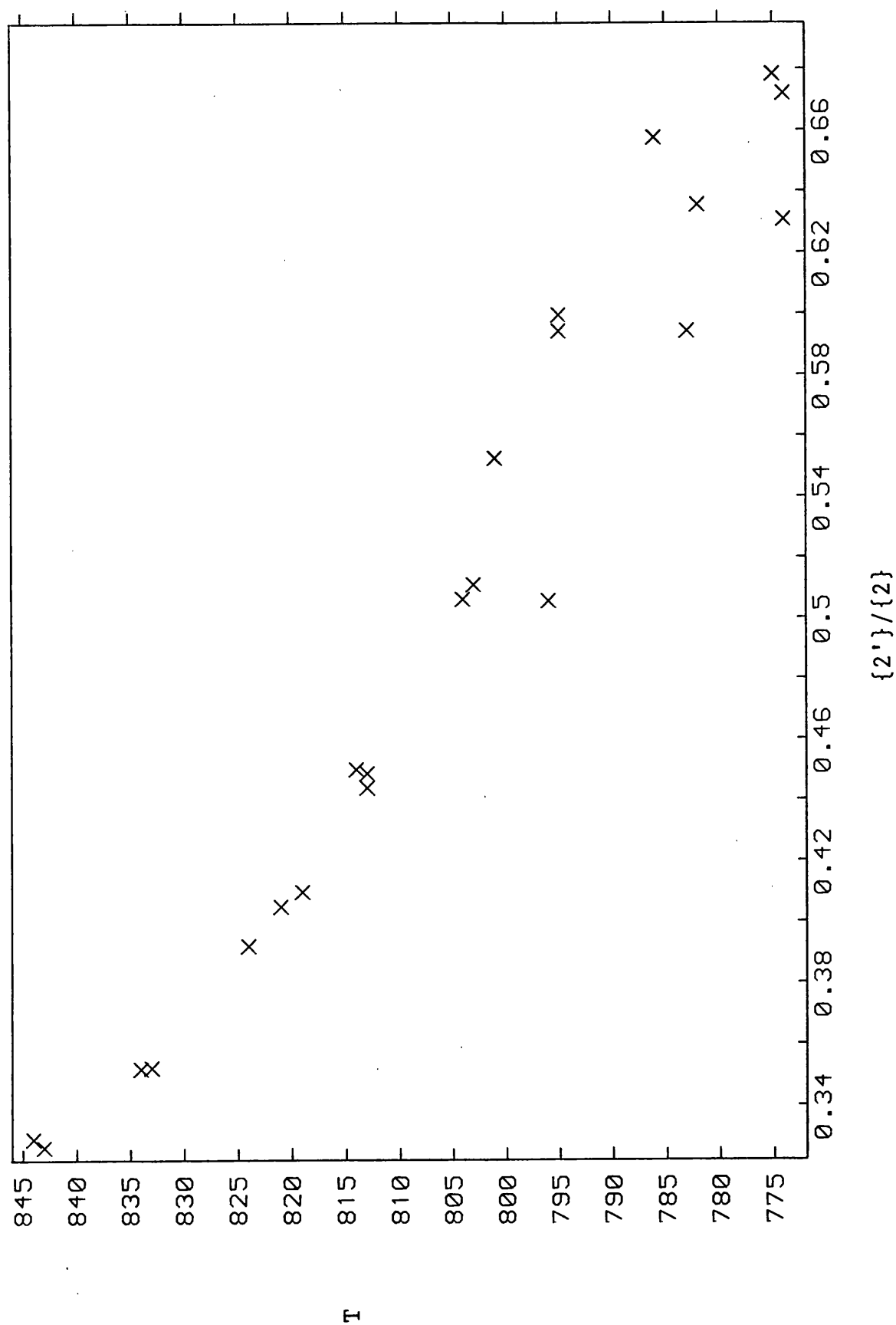
Figure 8.10 : Plot of {2'}/{2} vs. T.

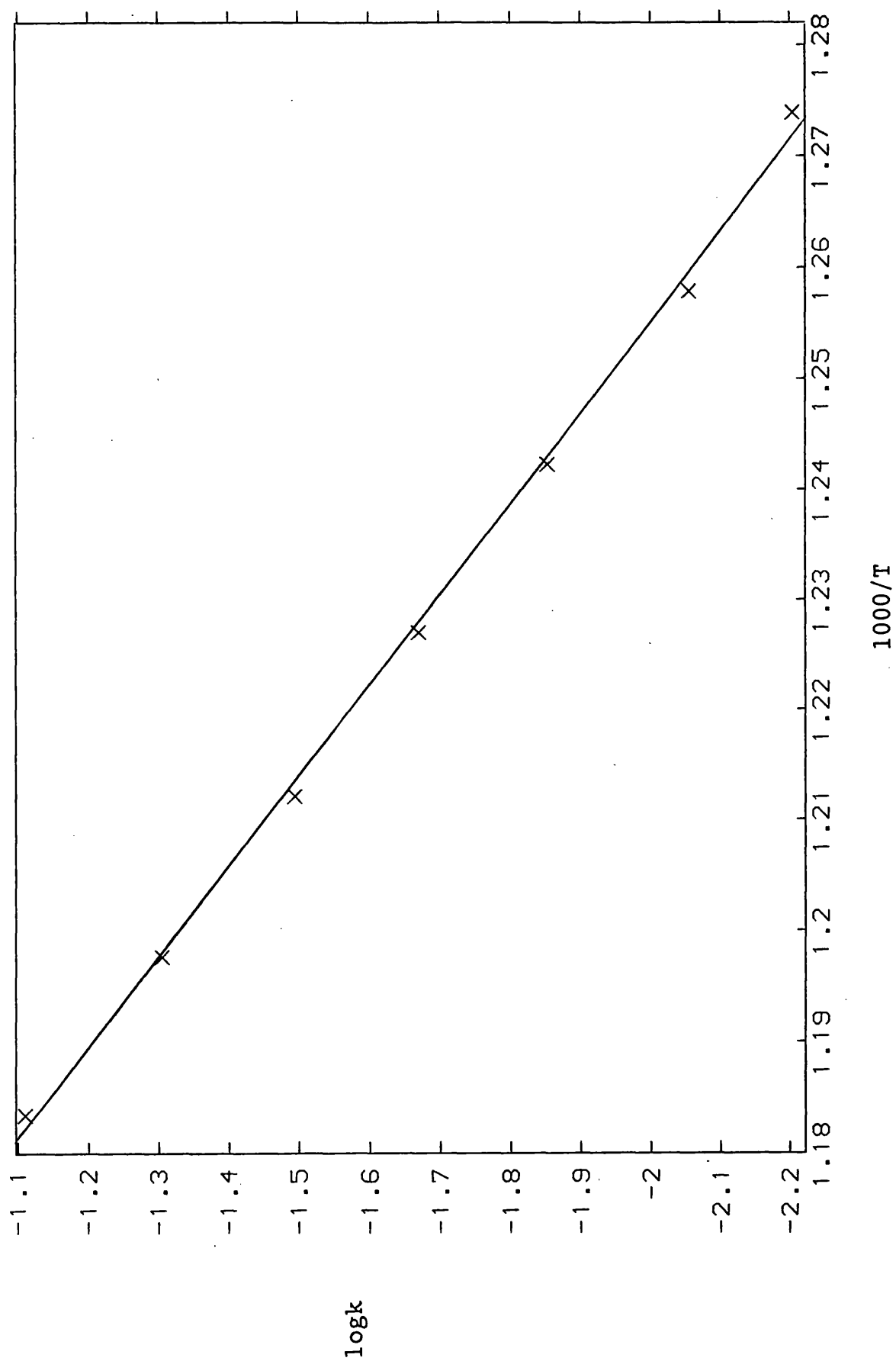Figure 8.11 : Arrhenius plot for formation of (2) from (1).

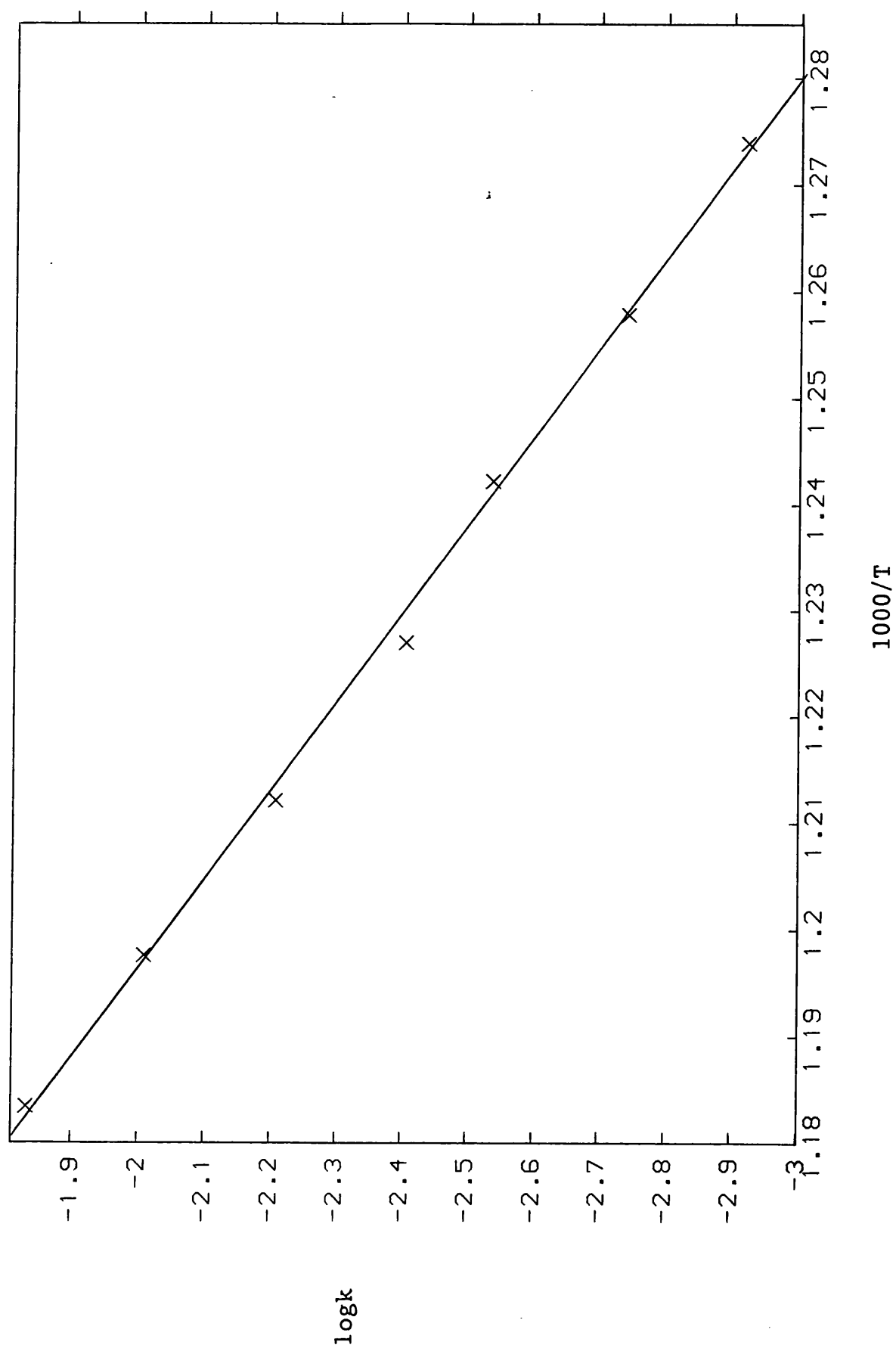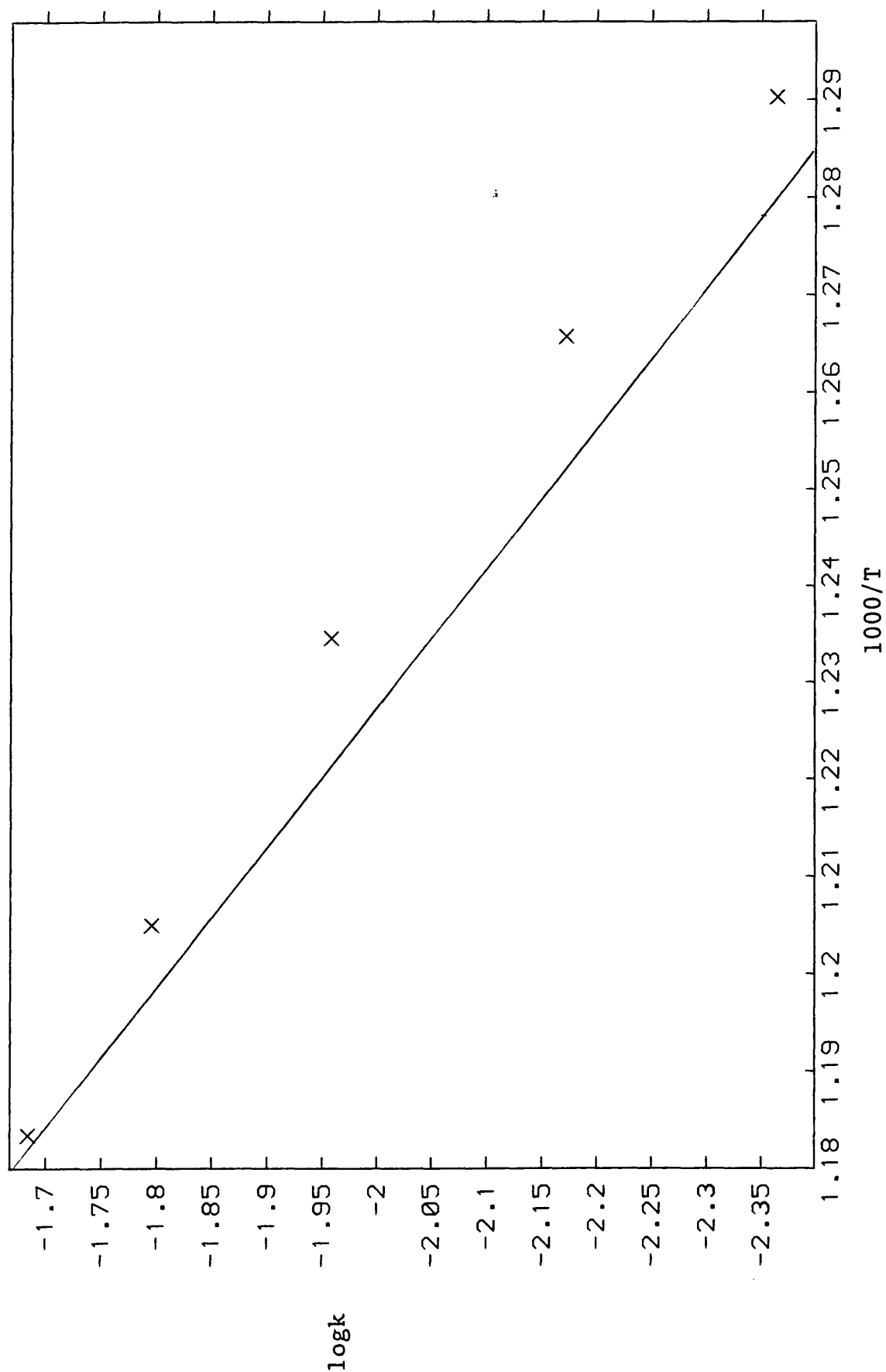Figure 8.12 : Arrhenius plot for formation of (1) from (2).

Figure 8.13 : Calculated (X) and experimental rate constants
for formation of (6) from (1).

References

266

1. D. Lei, P. P. Gaspar, J. C. S. Chem. Comm., 1985, 1149.

2. D. Lei, P. P. Gaspar, Organometallics, 1986, 5, 1276.

3. I. M. T. Davidson, R. J. Scampton, J. Organomet. Chem., 1984, 271, 249.

CHAPTER NINE

PYROLYSIS OF 1,2-DIMETHYLDISILANE

INTRODUCTION

As discussed in chapter one, disilanes containing silicon-hydrogen bonds decompose by a 1,2-hydrogen shift from silicon to silicon producing a silane and a silylene. Thus for 1,2-dimethyldisilane the initial decomposition pathway is as follows:

$$H_2MeSiSiH_2Me \longrightarrow H_3SiMe + HMeSi:$$
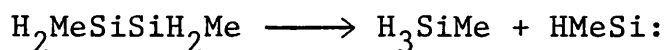
This chapter describes the results of pyrolysis of 1,2-dimethyldisilane, with and without butadiene, in which Arrhenius parameters are obtained for the reaction shown above, and compared with previous results obtained for various disilane decompositions. [1,2] Computer modelling is used to interpret the results of pyrolysis of 1,2-dimethyldisilane in terms of a complex reaction mechanism involving silylene insertions into silicon-hydrogen bonds, and silylene-disilene rearrangements.

RESULTS

Pyrolysis of 1,2-dimethyldisilane with excess butadiene

In the presence of an excess of butadiene, scheme 9.1 describes the mechanism of decomposition of 1,2-dimethyldisilane, in which the butadiene efficiently traps

267

methylsilylene to suppress secondary reactions. Therefore, by measuring rate constants for the formation of methylsilane, 1-methyl-1-silacyclopentene, and decomposition of 1,2-dimethyldisilane, Arrhenius parameters relating to reaction 1 of scheme 9.1 will be obtained.

Scheme 9.1

$$H_2MeSiSiH_2Me \xrightarrow{\;1\;} H_3SiMe + HMeSi:$$
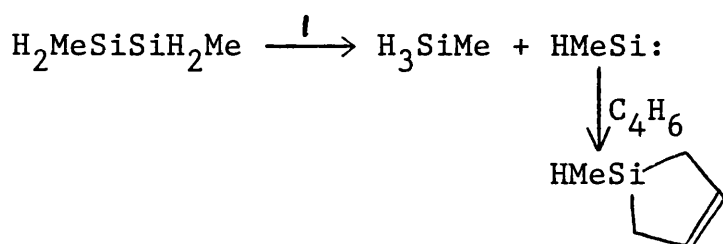
Approximately 2.5torr samples of a 50:1 mixture of butadiene and 1,2-dimethyldisilane were pyrolysed between 644-714K using the SFR technique, giving methylsilane and 1-methyl-1-silacyclopentene as the only products, consistent with scheme 9.1. Table 9.1 gives rate constants for the formation of these products, figures 9.1 and 9.2 give the resulting Arrhenius plots, which were analysed by the method of least squares to give the Arrhenius parameters in table 9.2.

Table 9.2

product	logA	E/kJmol^{-1}
MeSiH$_3$	14.49±.19	202.1±4.5
HMeSi (silacyclopentene)	14.3±.19	200.6±2.5

Table 9.1

Rate constants for product formation $/s^{-1}$
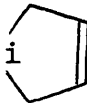
T/K	MeSiH$_3$	HMeSi⬠	T/K	MeSiH$_3$	HMeSi⬠
714	0.568	0.472	673	0.0609	0.0505
714	0.552	0.458	672	0.0666	0.0463
712	0.490	0.407	666	0.0418	0.0344
711	-	0.418	662	0.0339	0.0279
707	-	0.273	660	0.0307	0.0239
706	0.323	0.274	656	0.025	0.0235
704	0.315	0.257	652	0.021	0.0186
703	0.282	0.232	652	0.0184	0.0161
695	0.192	0.168	648	-	0.0128
695	0.179	0.151	647	0.0136	0.0128
694	0.197	0.171	646	0.0153	0.0143
686	0.119	0.0981	645	0.0133	0.0108
686	0.116	0.0978	644	0.0154	0.0121
681	0.0916	0.0734	644	0.0115	0.0104
673	0.064	0.0504			

Table 9.3

Rate constants for the decay of 1,2-dimethyldisilane

T/K	k$/s^{-1}$	T/K	k$/s^{-1}$
717	0.241	674	0.0336
716	0.241	674	0.0309
713	0.224	665	0.0199
704	0.134	665	0.0192
703	0.134	656	0.0116
702	0.130	656	0.0107
697	0.0968	654	0.00916
695	0.0912	647	0.00722
694	0.0923	646	0.00602
687	0.0600	645	0.00532
685	0.0550	636	0.00360
684	0.0539	635	0.00280
677	0.0361		

Approximately 2 torr samples of a 10:1 mixture of butadiene and 1,2-dimethyldisilane were pyrolysed between 635-717K using the LPP technique. Rate constants were obtained for decomposition of 1,2-dimethyldisilane and formation of 1-methyl-1-silacyclopentene by monitoring the mass peaks at $90(M^+)$ and $98(M^+)$ respectively, and are given in Tables 9.3 and 9.4. Figures 9.3 and 9.4 give the resulting Arrhenius plots, which were analysed by the method of least squares to give the Arrhenius parameters in Table 9.5.

<div align="center">Table 9.5</div>

	logA	$E/kJmol^{-1}$
reactant decomposition	14.28±.15	203.9±2
1-methyl-1-silacyclopentene formation	14.34±.14	204.4±1.9

Pyrolysis of 1,2-dimethyldisilane alone

Approximately 0.8 torr samples of 1,2-dimethyldisilane were pyrolysed between 643-726K using the SFR technique. The products, identified by comparison of gas chromatographic retention time with authentic samples and by gc/mass spectrometry were methylsilane, dimethylsilane, which at higher pyrolysis temperatures was the next most abundant product after methylsilane, 1,2,3-trimethyltrisilane and small quantities of other trisilanes, tetrasilanes, and

Table 9.4

Rate constants for the formation of 1-methyl-1-silacyclopentene

T/K	k/s^{-1}	T/K	k/s^{-1}
717	0.297	677	0.038
716	0.269	674	0.0331
713	0.229	674	0.0305
704	0.138	665	0.0199
703	0.146	665	0.0193
702	0.142	664	0.0188
697	0.0962	656	0.0125
695	0.0926	656	0.0111
694	0.0919	654	0.011
687	0.0655	647	0.0074
685	0.0577	645	0.00595
684	0.0492	636	0.00321

Table 9.6

Rate constants for product formation $/s^{-1}$

T/K	$MeSiH_3$	Me_2SiH_2	T/K	$MeSiH_3$	Me_2SiH_2
726	1.412	0.136	685	0.137	0.00737
724	1.281	0.123	674	0.0723	0.00284
715	0.847	0.0718	674	0.0709	0.00238
715	0.821	0.0694	664	0.0409	0.000852
705	0.472	0.037	663	0.0377	0.000597
703	0.434	0.0326	656	0.0239	0.000383
695	0.250	0.0171	654	0.0220	0.000313
695	0.248	0.0154	646	0.0138	-
694	0.248	0.0176	644	0.0121	-
685	0.143	0.00785			

higher polysilanes. Rate constants were obtained for the
formation of methylsilane and dimethylsilane, and are given
in Table 9.6. Figures 9.5 and 9.6 give the resulting
Arrhenius plots, which were analysed by the method of least
squares to give the Arrhenius parameters in Table 9.7.

Table 9.7

product	logA	$E/kJmol^{-1}$
methylsilane	16.65±.12	229.3±1.6
dimethylsilane	23.81±.63	341.2±8.3

DISCUSSION

The results obtained from the decomposition of 1,2-
dimethyldisilane in the presence of butadiene, given in
Tables 9.2 and 9.5 are in excellent agreement and entirely
consistent with scheme 9.1.

From the experiments without butadiene, the Arrhenius
parameters for the formation of methylsilane are a worse
measure of the primary reaction due to curvature in the
Arrhenius plot caused by secondary reactions. Figure 9.7
gives the Arrhenius plot for methylsilane formation, with a
least squares fit through the two lowest temperature data
points, to which there would be a minimal contribution from
secondary reactions, giving Arrhenius parameters for
methylsilane formation of;

$$\log k/s^{-1} = (14.47 \pm .47) - (202.1 \pm 5.8 \text{kJmol}^{-1}/2.303RT)$$

in good agreement with the Arrhenius parameters obtained from the experiments with excess butadiene.

Arrhenius parameters have previously been measured for methylsilylene elimination from two disilanes, and are given in Table 9.8.

<p align="center">Table 9.8</p>

reactant	logA	E/kJmol^{-1}	reference
$HMe_2SiSiMeH_2$	13.66±0.55	193.1±5.9	1
$H_2MeSiSiH_3$	14.14±0.14	208.7±1.5	2

Since the results in Table 9.8 were obtained by monitoring the formation of the appropriate monosilane, and no silylene trap was present to suppress secondary reactions, the results obtained in this experimental work using butadiene as a silylene trap are preferred.

The Arrhenius parameters for dimethylsilane formation clearly indicate that it is a secondary product, consistent with its suppression by excess butadiene. However, it is interesting in that a mechanism for its formation can be devised incorporating ideas developed by Davidson and Scampton,[3] concerning silylene to silene isomerisation and combination; and also silylene to silylene interconversion involving disilene intermediates as proposed

by Gaspar.[4]

It was therefore decided to try and simulate the temperature dependence of dimethylsilane formation by computer modelling, to see what conclusions could be drawn regarding the mechanism of decomposition of 1,2-dimethyldisilane.

Computer Modelling of 1,2-dimethyldisilane decomposition

The aim of this was to see if it was possible to use computer modelling to explain the formation of dimethyldisilane. The experimental data to be simulated were the ratios of methylsilane:dimethylsilane at 655 and 726K, which were 1:0.016 and 1:0.1 respectively.

Scheme 9.2 overleaf shows the main features of the model relevant to the formation of dimethylsilane. Table 9.9 gives the complete list of reactions and Arrhenius parameters for the computer model. The Arrhenius parameters in Table 9.9 were obtained from a combination of experimental results, and the application of 'O'Neal's rules' for the estimation of Arrhenius parameters as discussed in chapter 6, with the modifications given below. The appropriate thermodynamic data were obtained from Table 6.2, modified by the application of Ring and O'Neal's group additivity tables.[7]

The modifications to O'Neal's rules for the estimation of

Scheme 9.2

$H_2MeSiSiH_2Me \overset{1}{\underset{2}{\rightleftharpoons}} (H_3SiMe) + HMeSi: \overset{40}{\underset{41}{\rightleftharpoons}} H_2Si=CH_2 \overset{82}{\longrightarrow} H_2Si\langle\rangle SiH_2$

$HMeSi: \quad \overset{3}{\underset{4}{}} \quad H_2Si=CH_2$

$\overset{42}{\longrightarrow} HMeSi{-}SiH_2$

$H_2MeSiSiHMeSiH_2Me \quad \overset{5}{\underset{6}{}}$

$(H_3SiMe) + Me\ddot{S}iSiMeH_2 \quad \overset{11}{\underset{12}{\rightleftharpoons}} \quad \overset{7}{\underset{8}{}} \quad \overset{9}{\underset{10}{}}$

$H_2Si=SiMe_2 \quad HMeSi=SiHMe$

$\overset{34}{\underset{35}{\rightleftharpoons}} H_2MeSi\langle\rangle SiH$

$\overset{30}{\underset{31}{}} HMe_2Si\ddot{S}iH \quad \overset{36}{\longrightarrow}$

$\overset{15}{\underset{16}{}} \quad \overset{17}{\underset{18}{}}$

$\overset{19}{\underset{20}{\rightleftharpoons}} H_2MeSiSiH_2Me$

$\overset{37}{\underset{38}{}} H_3SiMe$

$HMe_2SiSiH_2SiMeHSiMeH_2 \overset{21}{\longrightarrow} Me_2SiH_2$

$H_2MeSiSiH_2SiHMe_2 \overset{23}{\longrightarrow} Me_2SiH_2$

Table 9.9

reaction number	reaction	logA	E/kcalmol^{-1}	reference
1	A⟶B+C	14.28	48.7	a
2	B+C⟶A	9.2	2.3	b
3	A+C⟶D	9.2	2.3	b
4	D⟶A+C	14.8	49	b
5	D⟶E+B	14.5	49	b
6	E+B⟶D	9.2	2.3	b
7	E⟶F	12.83	31	b
8	F⟶E	13.81	41	b
9	E⟶G	13.13	21	b
10	G⟶E	14.11	28	b
11	E⟶J	12.54	38	b
12	J⟶E	14.03	40.15	b
13	A+E⟶K	9.2	2.3	b
14	K⟶A+E	14.5	49	b
15	F⟶H	13.81	28	b
16	H⟶F	12.83	21	b
17	G⟶H	14.11	41	b
18	H⟶G	13.13	31	b
19	A+H⟶I	9.2	2.3	b
20	I⟶A+H	14.5	49	b
21	I⟶L+M	14.5	49	b
22	I⟶C+N	14.5	49	b
23	N⟶L+O	14.5	49	b
24	K⟶B+P	14.5	49	b
25	B+P⟶K	9.2	2.3	b
26	K⟶C+D	14.8	49	b
27	C+D⟶K	9.2	2.3	b
28	C+L⟶Q	9.2	2.3	b
29	Q⟶C+L	14.5	49	b
30	J⟶H	14.33	29.6	b
31	H⟶J	12.84	33	b
32	J⟶R	13.55	11	b
33	R⟶J	12.52	15	b
34	J⟶S	14.53	11	b
35	S⟶J	12.06	13.5	b
36	S⟶T	11.77	30	b
37	B+H⟶N	9.2	2.3	b
38	N⟶B+H	14.5	49	b
39	C+C⟶G	10	0	b
40	C⟶U	13	43	b
41	U⟶C	13.33	42.2	b
42	C+U⟶J	10	0	b
43	A⟶G+V	14.05	52.9	b, c
44	A⟶E+V	14.65	55.3	b, c
45	A+S⟶W	9.2	2.3	b
46	W⟶A+S	14.5	49	b
47	W⟶E+X	14.5	49	b
48	W⟶B+Y	14.5	49	b
49	W⟶C+Z	14.5	49	b
50	A+R⟶AA	9.2	2.3	b
51	AA⟶A+R	14.5	49	b
52	AA⟶E+X	14.5	49	b

276

reaction number	reaction	logA	E/kcalmol^{-1}	reference
53	AA⟶B+BB	14.5	49	b
54	AA⟶C+CC	14.5	49	b
55	N⟶C+DD	14.5	49	b
56	N⟶EE+FF	14.5	49	b
57	I⟶E+DD	14.5	49	b
58	I⟶B+GG	14.5	49	b
59	I⟶C+HH	14.5	49	b
60	S+B⟶Z	9.2	2.3	b
61	Z⟶B+S	14.5	49	b
62	Z⟶X+C	14.5	49	b
63	R+B⟶CC	9.2	2.3	b
64	CC⟶B+R	14.5	49	b
65	CC⟶X+C	14.5	49	b
66	Q⟶B+EE	14.5	49	b
67	B+EE⟶Q	9.2	2.3	b
68	A+EE⟶II	9.2	2.3	b
69	A+O⟶JJ	9.2	2.3	b
70	A+GG⟶KK	9.2	2.3	b
71	A+M⟶LL	9.2	2.3	b
72	B+O⟶MM	9.2	2.3	b
73	B+GG⟶JJ	9.2	2.3	b
74	B+M⟶NN	9.2	2.3	b
75	D+EE⟶OO	9.2	2.3	b
76	D+O⟶PP	9.2	2.3	b
77	D+GG⟶QQ	9.2	2.3	b
78	D+M⟶RR	9.2	2.3	b
79	D+S⟶SS	9.2	2.3	b
80	D+R⟶TT	9.2	2.3	b
81	C+T⟶UU	9.2	2.3	b
82	U+U⟶T	6.55	0	d

References: a) this work
b) based on application of 'O'Neal's rules' for the estimation of Arrhenius parameters as discussed in chapter 6 and the text
c) see reference 5
d) see reference 6

A,H₂MeSiSiH₂Me; B,H₃SiMe; C,HMeSi:; D,H₂MeSiSiHMeSiH₂Me;

E,H₂MeSiSiMe F,H₂Si=SiMe₂; G,HMeSi=SiHMe; H,HSiSiMe₂H;

I,H₂MeSiSiHMeSiH₂SiHMe₂; J,HMeSi⌒SiH₂;

K,H₂MeSiSiHMeSiHMeSiH₂Me; L,H₂SiMe₂; M,H₂MeSiSiHMeSiH;

N,H₂MeSiSiH₂SiHMe₂; O,H₂MeSiSiH; P,HSiSiHMe₂SiH₂Me;

Q,H₂MeSiSiHMe₂; R,MeSiCH₂SiH₃; S,HSiCH₂SiH₂Me;

T,H₂Si⬡SiH₂; U,H₂Si=CH₂; V,H₂;

W,H₂MeSiSiHMeSiH₂CH₂SiH₂Me; X,H₃SiCH₂SiH₂Me;

Y,MeSiSiH₂CH₂SiH₂Me; Z,H₂MeSiSiH₂CH₂SiH₂Me;

AA,H₂MeSiSiHMeSiHMeCH₂SiH₃; BB,MeSiSiHMeCH₂SiH₃;

CC,H₂MeSiSiHMeCH₂SiH₃; DD,H₃SiSiHMe₂; EE,Me₂Si:;

FF,H₂MeSiSiH₃; GG,MeSiSiH₂SiHMe₂; HH,H₂MeSiSiH₂SiHMe₂;

II,HMe₂SiSiHMeSiH₂Me; JJ,H₂MeSiSiH₂SiHMeSiH₂Me;

KK,H₂MeSiSiHMeSiHMeSiH₂SiHMe₂; LL,H₂MeSiSiHMeSiH₂SiHMeSiH₂Me;

MM,H₂MeSiSiH₂SiH₂Me; NN,H₂MeSiSiH₂SiHMeSiH₂Me;

OO,H₂MeSiSiHMeSiHMeSiHMe₂; PP,H₂MeSiSiH₂SiHMeSiHMeSiH₂Me;

QQ,H₂MeSiSiHMeSiHMeSiHMeSiH₂SiHMe₂;

RR,H₂MeSiSiHMeSiHMeSiH₂SiHMeSiH₂Me;

SS,H₂MeSiSiHMeSiHMeSiH₂CH₂SiH₂Me;

TT,H₂MeSiSiHMeSiHMeSiHMeCH₂SiH₃; UU,H₂Si⬡SiHSiH₂Me

Arrhenius parameters involve the method of calculating ΔS° for unimolecular reactions.[8]   Originally, ΔS° was calculated by estimating S° for each species, but now ΔS° is calculated from the change in the number of internal rotational degrees of freedom. For each internal rotational degree of freedom lost or gained there is a corresponding change of 4.5 e.u.,[8] which gives the intrinsic entropy change for the reaction. The real entropy change is obtained by making a correction to the intrinsic entropy change, due to any alteration in the symmetry number.[9] Therefore, the following formula is used to obtain ΔS° for a unimolecular reaction.

$$\Delta S^\circ = \Delta S^\circ_{intrinsic} - R\ln\sigma_{product} + R\ln\sigma_{reactant}$$

In addition, the change in the number of internal rotors for ring closing reactions involving silylene insertion into a silicon-carbon bond was increased from 2 to 3.[8]

Using the Arrhenius parameters in Table 9.9, with an initial reactant concentration of $2.17 \times 10^{-5} mol\,dm^{-3}$, Table 9.10 gives the calculated ratio of methylsilane:dimethylsilane after 10s.

Table 9.10

Calculated ratio of methylsilane:dimethylsilane

T/K	ratio
655	1:0.0003
726	1:0.137

These results show that at low temperature, dimethylsilane is a negligible product, but becomes important at higher temperature, in good agreement with the experimental results. The model also showed that the major route to dimethylsilane involved reactions 3, 5, and the reactions converting $H_2MeSi\ddot{S}iMe$ to $HMe_2Si\ddot{S}iH$ via disilene intermediates. The disilirane was unimportant, consequently, 1,3-disilacyclobutane which would have been thermally stable under these conditions [9] was computed to be an extremely minor product, with the computed ratio of methylsilane:1,3-disilacyclobutane never exceeding 1: 1.3×10^{-8}, consistent with the failure to detect any 1,3-disilacyclobutane experimentally.

Figure 9.1 : Arrhenius plot for formation of methylsilane.
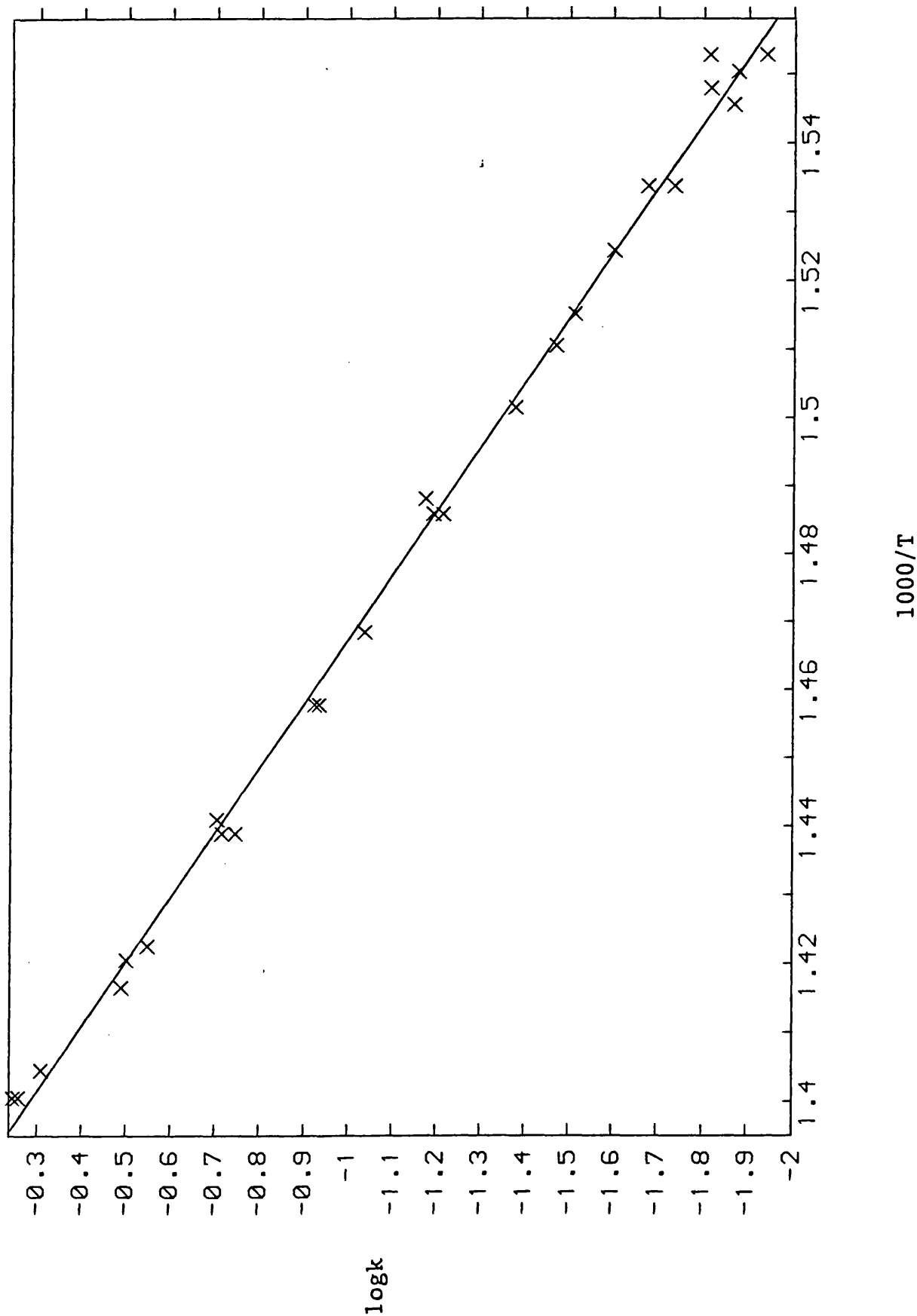
Figure 9.2 : Arrhenius plot for formation of 1-methyl-1-
silacyclopentene.
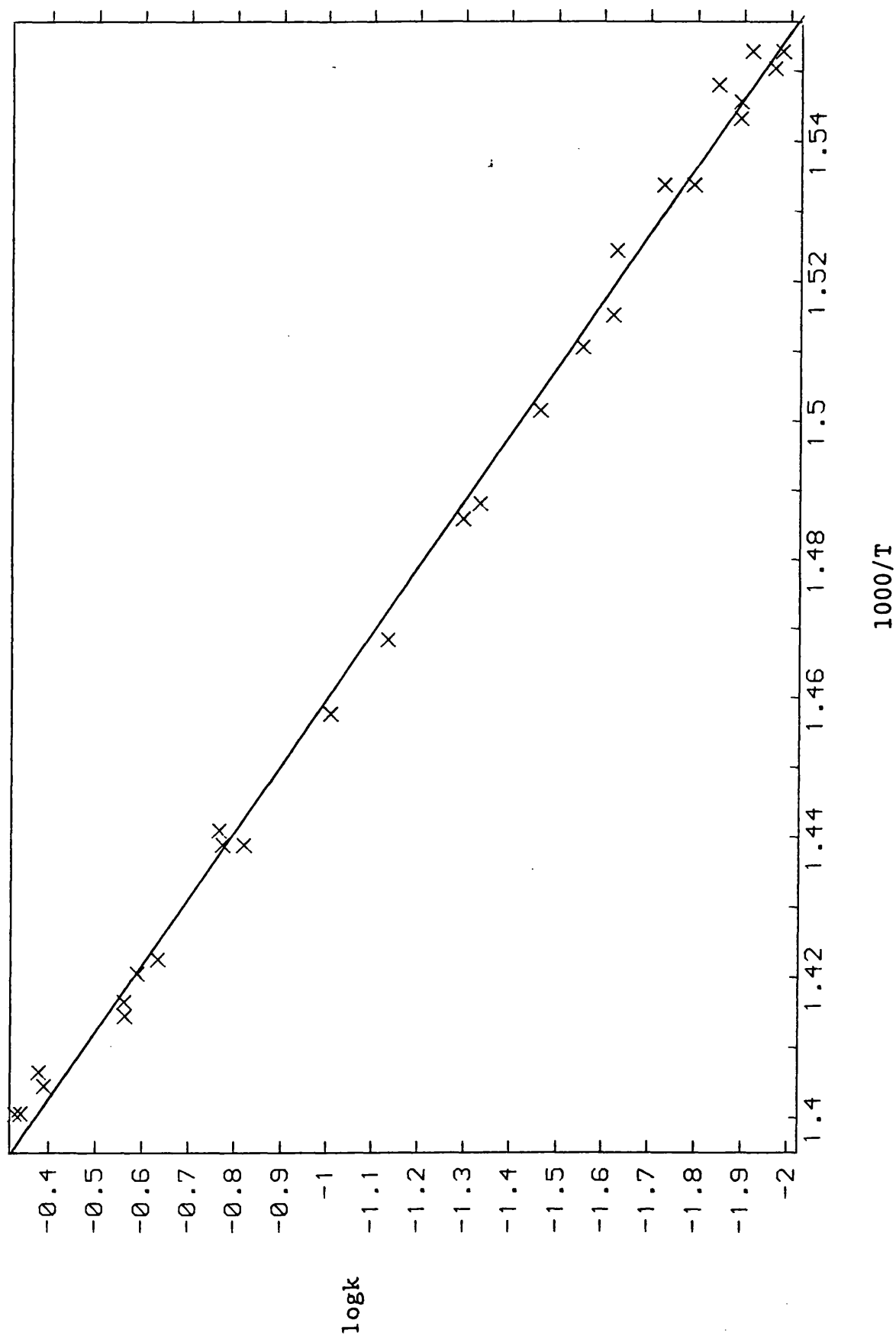
Figure 9.3 : Arrhenius plot for decay of 1,2-dimethyldisilane in excess butadiene.

1000/T

logk
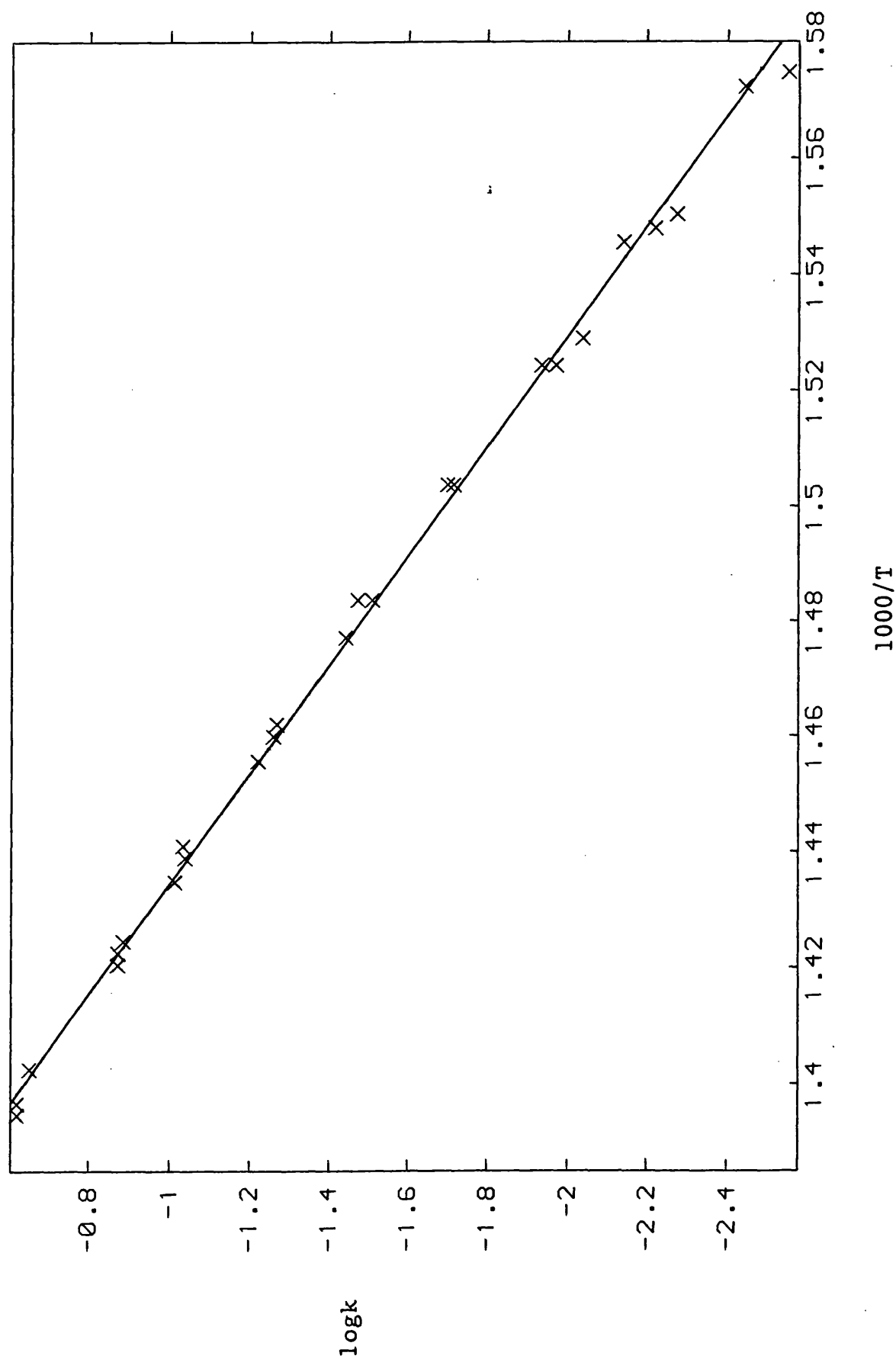
Figure 9.4 : Arrhenius plot for formation of 1-methyl-1-silacyclopentene.
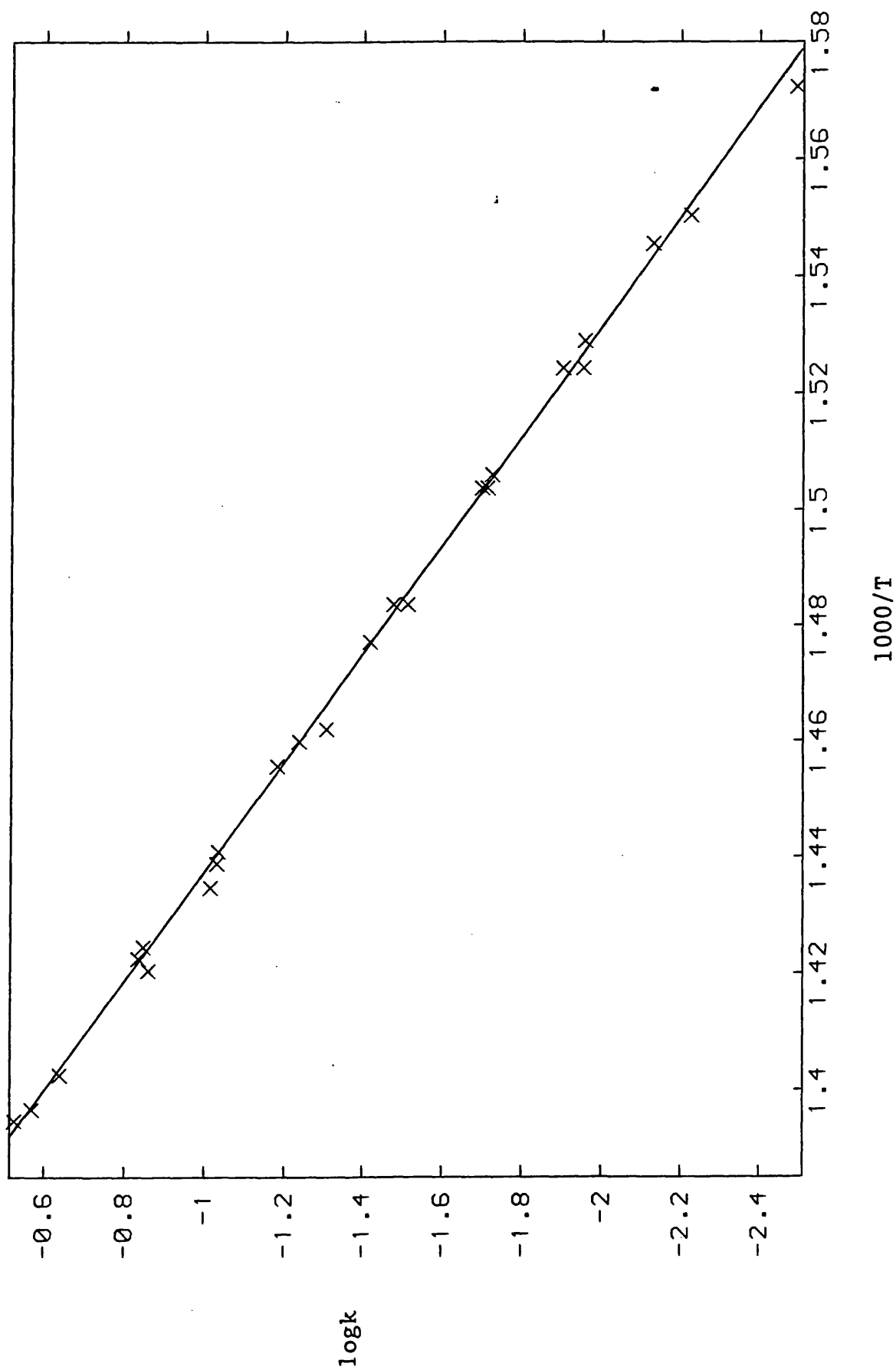
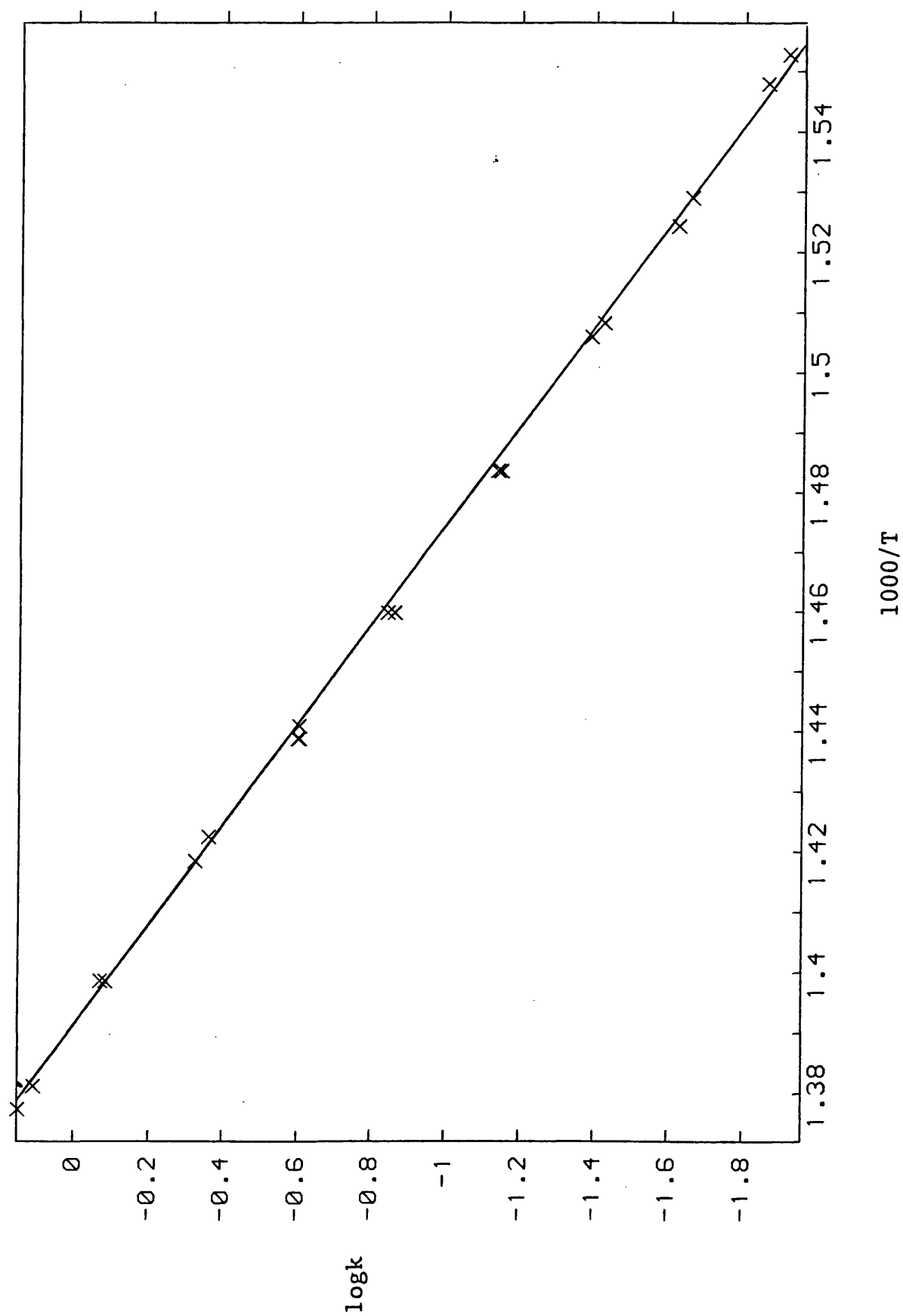Figure 9.5 : Arrhenius plot for formation of methylsilane.

1000/T

logk

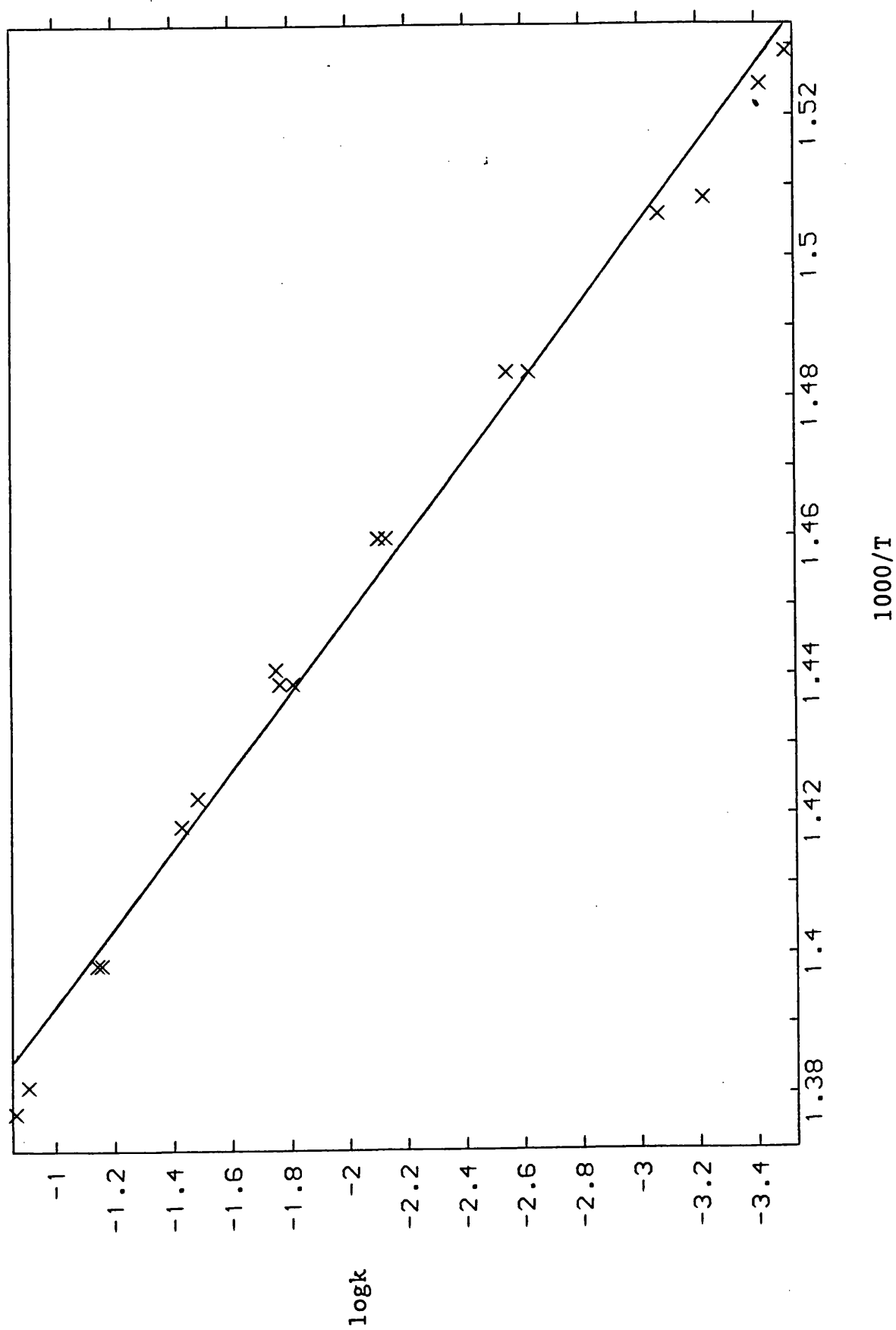Figure 9.6 : Arrhenius plot for formation of dimethylsilane.

Figure 9.7 : Arrhenius plot for formation of methylsilane.
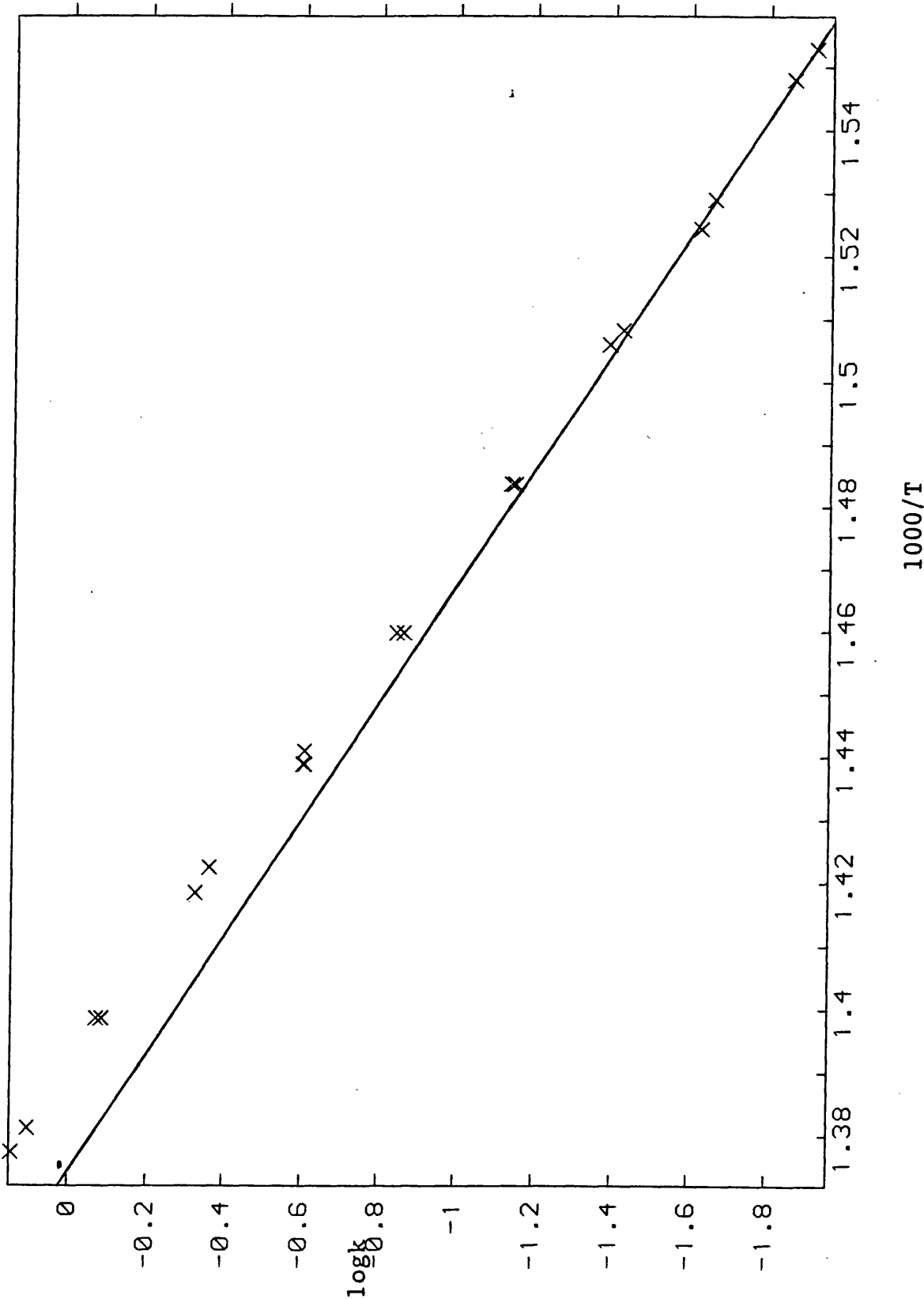
References

1. I. M. T. Davidson and J. I. Matthews, J. C. S. Faraday Trans. I, 1976, 72, 1403.

2. A. J. Vanderwielen, M. A. Ring and H. E. O'Neal, J. Amer. Chem Soc., 1975, 97, 993.

3. I. M. T. Davidson and R. J. Scampton, J. Organomet. Chem., 1984, 271, 249.

4. B. H. Boo and P. P. Gaspar, Organometallics, 1986, 5, 698.

5. G. Olbrich, P. Potzinger, B. Reimann and R. Walsh, Organometallics, 1984, 3, 1267.

6. L. E. Gusel'nikov, K. S. Konobeyevsky, V. M. Vdovin and N. S. Nametkin, Dokl. Akad. Nauk SSSR., 1977, 235, 1086.

7. H. E. O'Neal and M. A. Ring, J. Organomet. Chem., 1981, 213, 419.

8. H. E. O'Neal, personal communication to I. M. T. Davidson.

9. See chapter five.

10. N. Auner, I. M. T. Davidson, S. Ijhadi-Maghsoodi and F. T. Lawrence, Organometallics, 1986, 5, 431.

CHAPTER TEN

PYROLYSIS OF HYDRIDOSILACYCLOBUTANES

INTRODUCTION

The most recent published results concerning the kinetics and mechanism of pyrolysis of hydridosilacyclobutanes [1], in which earlier work is assessed, and Arrhenius parameters obtained for ethene and propene formation, led to the mechanistic suggestions in scheme 10.1 to account for the observed results.
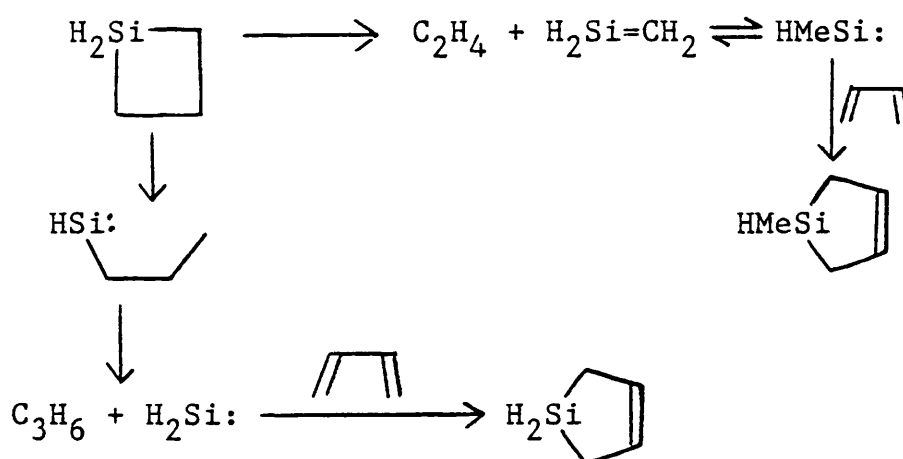
Scheme 10.1

(R = H,Me)
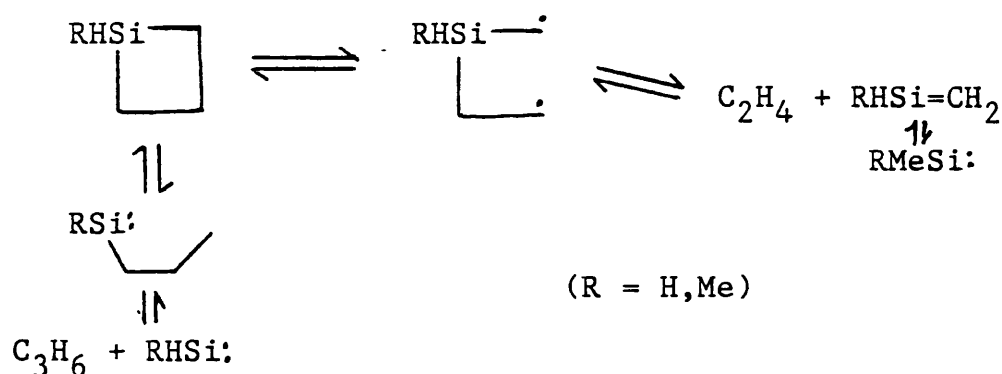
The work in this chapter describes a reinvestigation of the measurement of Arrhenius parameters for ethene and propene formation, using excess butadiene as a silylene trap, thus suppressing secondary reactions, and allowing more accurate Arrhenius parameters to be obtained.

RESULTS AND DISCUSSION

Pyrolysis of silacyclobutane

Scheme 10.2

Scheme 10.2 gives the proposed mechanism of decomposition of silacyclobutane. Approximately 0.6 torr samples of an 8:1 mixture of butadiene and silacyclobutane were pyrolysed using the SFR technique [2], between 728-821K, giving ethene, propene, silacyclopentene and 1-methyl-1-silacyclopentene as the only products. Tables 10.1 and 10.2 give rate constants for the formation of these products.

Figures 10.1 to 10.4 give the resulting Arrhenius plots, which were analysed by the method of least squares to give the Arrhenius parameters in table 10.3.

Table 10.1

Rate constants for product formation $/s^{-1}$

T/K	ethene	propene
804	0.121	0.0276
804	——	0.0252
803	0.121	0.0261
803	0.112	0.0248
802	0.0998	0.0216
801	0.105	0.0236
801	0.0999	0.0219
788	0.047	0.0107
785	0.043	0.00998
781	0.0332	0.00777
769	0.0176	0.0041
768	0.0178	0.00403
765	0.0149	0.00351
757	0.0093	0.00226
755	0.00879	0.002
745	0.00474	0.00115
743	0.00472	0.0011
736	0.00294	0.000766
736	0.0029	0.000772
733	0.00267	0.000615
728	0.00179	0.000523

Table 10.2

Rate constants for product formation $/s^{-1}$

T/K	H$_2$Si	HMeSi
821	0.0538	0.207
815	0.0385	0.168
805	0.0265	0.105
805	0.0256	0.0997
802	0.0239	0.0892
794	0.0148	0.0575
792	0.0148	0.0499
792	——	0.0553
784	0.00905	0.0371
784	0.00911	0.0367
780	0.00751	0.0309
774	0.00511	0.0224
774	——	0.024
773	0.00485	0.0216
773	0.00514	——
769	0.00338	——
768	——	0.018
767	0.00304	0.0169
764	0.00267	0.0134
764	——	0.0139
760	0.00218	0.0115
758	0.00187	0.0103
747	0.000887	0.00487
747	0.00093	0.0063
739	0.00044	0.00385
738	0.00065	0.0028
737	0.000388	0.0024
737	——	0.0025
737	——	0.00244

Table 10.3

Product	logA	E/kJmol^{-1}	k$_{800K}$
ethene	16.12±.16	262.8±2.3	0.091
1-methyl-1-silacyclopentene	15.89±.26	260 ± 3.8	0.082
propene	15.01±.16	255 ± 2.4	0.021
silacyclopentene a	14.90±.38	254 ± 5.9	0.02

a : only includes ten rate constants at the high end of
the temperature range

Pyrolysis of 1-methyl-1-silacyclobutane

Scheme 10.3
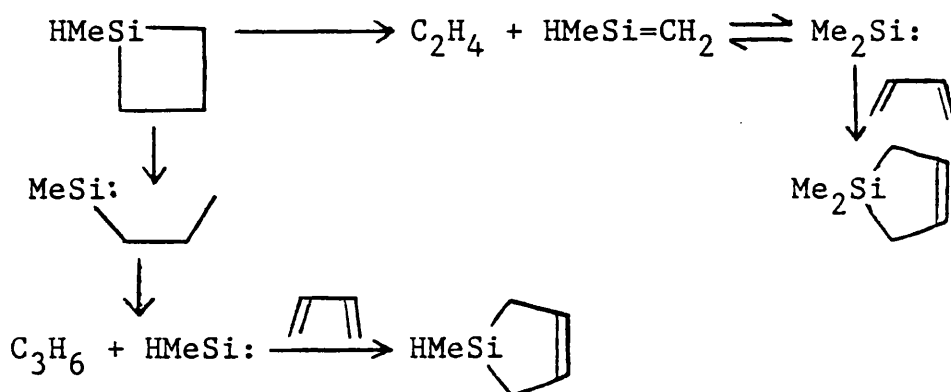
Scheme 10.3 shows the proposed mechanism for the
decomposition of 1-methyl-1-silacyclobutane in the presence
of excess butadiene. Approximately 0.2 torr samples of a
9:1 mixture of butadiene and 1-methyl-1-silacyclobutane were
pyrolysed using the SFR technique [2]   between 763-835K,
giving ethene and dimethylsilacyclopentene as the major
products, with propene and 1-methyl-1-silacyclopentene as

minor products. Tables 10.4 and 10.5 give rate constants for the formation of ethene, propene, and dimethylsilacyclopentene.

Table 10.4

Rate constants for product formation /s^{-1}

T/K	ethene	propene	T/K	ethene	propene
825	0.281	0.0123	807	0.11	0.00567
825	0.29	0.012	805	0.11	0.0047
824	——	0.0125	804	0.0955	0.00448
824	0.277	0.0122	803	0.0921	0.00421
824	0.279	0.012	802	0.085	0.00377
820	0.2	0.0095	792	0.0519	0.00241
819	——	0.009	792	0.0542	0.00256
818	0.195	0.009	791	0.0542	0.00256
811	0.127	0.0058	773	0.021	0.00105
810	0.137	0.00658	772	0.0193	0.001
808	0.125	0.0059	767	0.0152	0.00056
807	0.112	0.0054	766	0.0144	0.000615

Table 10.5

Rate constants for the formation of dimethylsilacyclopentene

T/K	k/s^{-1}	T/K	k/s^{-1}
835	0.329	795	0.051
834	0.311	795	0.048
824	0.193	784	0.0316
822	0.177	784	0.0279
822	0.166	780	0.023
817	0.147	772	0.0148
811	0.115	772	0.0145
811	0.11	772	0.0142
807	0.08	763	0.0091
806	0.082	763	0.0091
797	0.0589	——	——

Figures 10.5 to 10.7 give the resulting Arrhenius plots, which were analysed by the method of least squares to give the Arrhenius parameters in table 10.6.

Table 10.6

Product	logA	E/kJmol^{-1}	k$_{800K}$
ethene	15.86±.28	259.7±4.3	0.08
propene	14.85±.28	264.6±4.3	0.0037
dimethylsilacyclopentene	15.92±.18	262.3±2.7	0.062

As discussed in chapter one, decomposition of dimethylsilacyclobutane proceeds via carbon-carbon bond homolysis to form a diradical intermediate, which falls apart to produce ethene and dimethylsilene. Arrhenius parameters for this process have been measured [3], and are in good agreement with the measured Arrhenius parameters in tables 10.3 and 10.6 for ethene production. This suggests that the mechanism of ethene production in silacyclobutane and 1-methyl-1-silacyclobutane is identical to that described for dimethylsilacyclobutane decomposition. In addition, Arrhenius parameters for the formation of 1-methyl-1-silacyclopentene and dimethylsilacyclopentene are identical to those obtained for ethene formation, as would be expected if schemes 10.2 and 10.3 are correct.

The other decomposition pathway for silacyclobutane and 1-

methyl-1-silacyclobutane, involves a 1,2-hydrogen shift from silicon to carbon with ring opening. Analogous reactions are the molecular elimination of methane from dimethylsilane and trimethylsilane, as shown below:

$$Me_2SiH_2 \longrightarrow HMeSi: + CH_4$$
$$Me_3SiH \longrightarrow Me_2Si: + CH_4$$
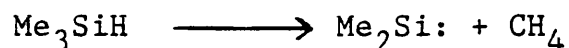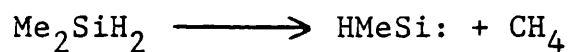
Ring and O'Neal have obtained Arrhenius parameters for both of these reactions [4,5], in each case giving an activation energy of approximately 305kJ/mol. Davidson has obtained a value of ~50kJ/mol for the amount of ring strain released on opening a silacyclobutane ring [6].

Therefore, it would be expected that the activation energy for the 1,2-hydrogen shift with ring opening would be given by E = 305 - ~50 ≈ 255kJ/mol, as was obtained for propene and silacyclopentene formation from silacyclobutane, and in good agreement with the result for propene formation from 1-methyl-1-silacyclobutane.

However, Arrhenius parameters for this process are still uncertain due to some slight curvature in the Arrhenius plots for propene and silacyclopentene formation. In addition, in the pyrolysis of silacyclobutane, the first run of each day gave an abnormally high rate constant for formation of propene, and at the low end of the temperature

range, silacyclopentene was not produced in equivalent amount to propene. These observations suggest a heterogeneous component in the formation of propene, which may not have been totally suppressed in successive runs, especially at lower temperature.

Figure 10.1 : Arrhenius plot for ethene formation from silacyclobutane + excess butadiene.
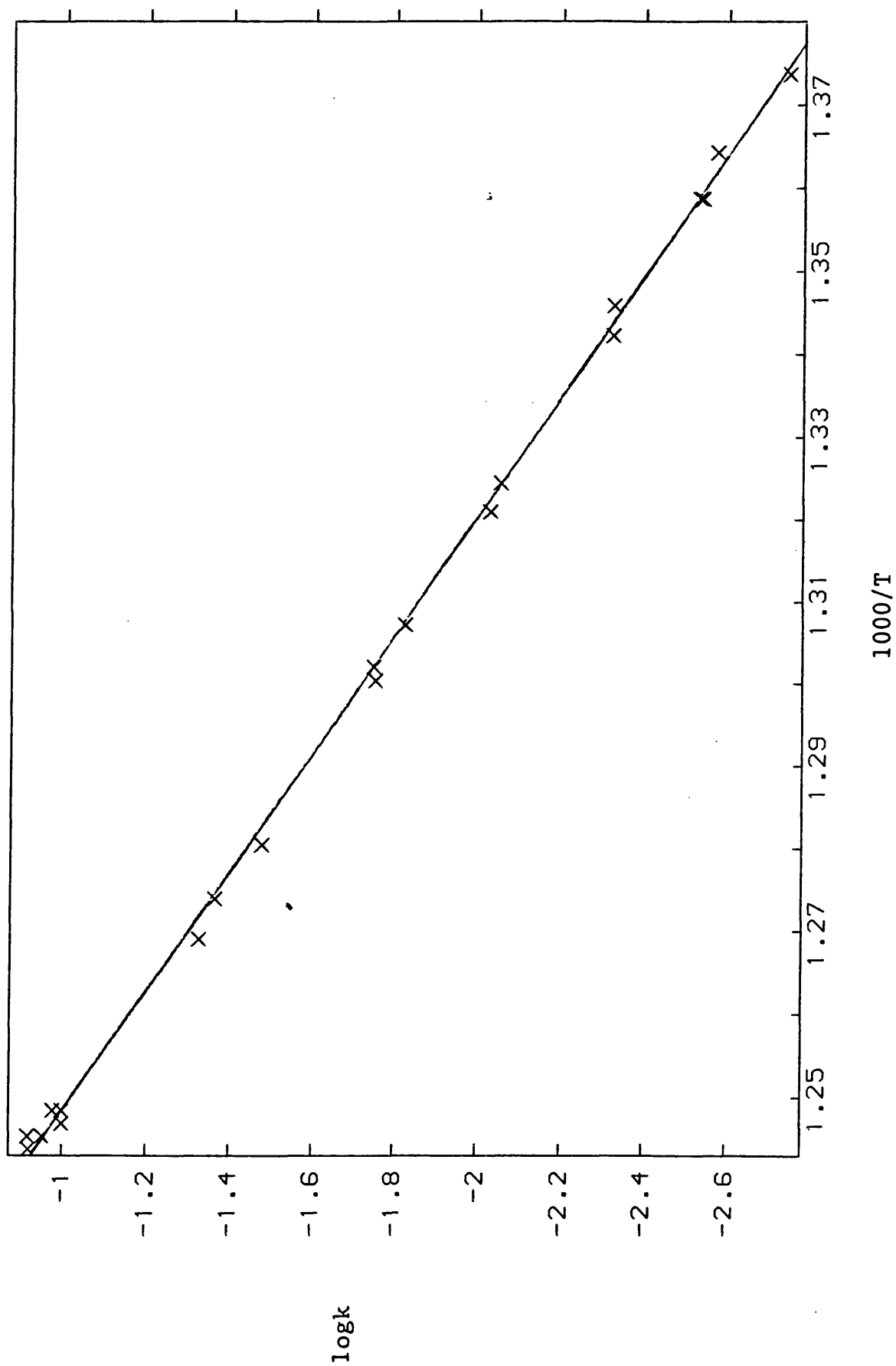

logk

1000/T

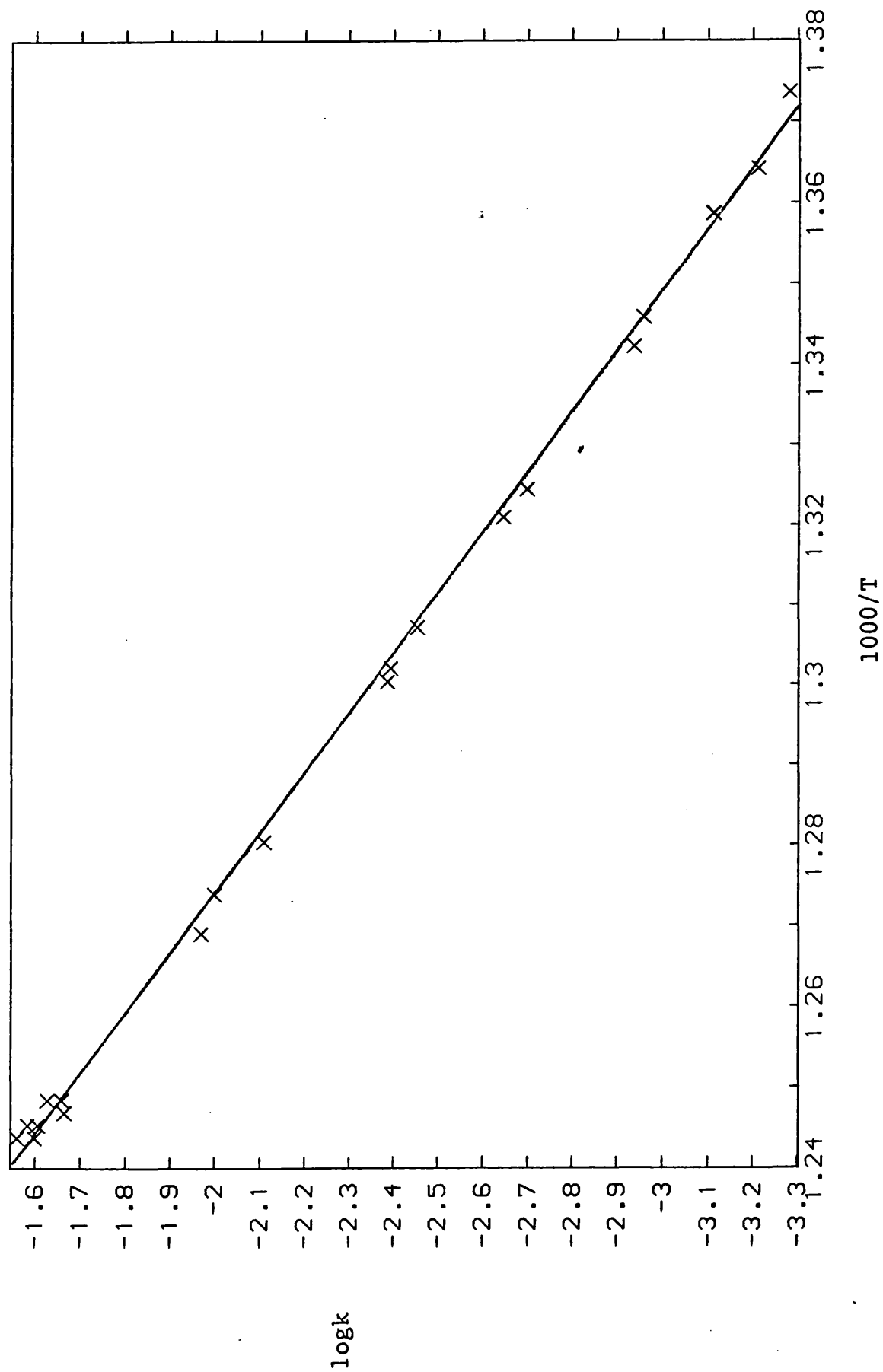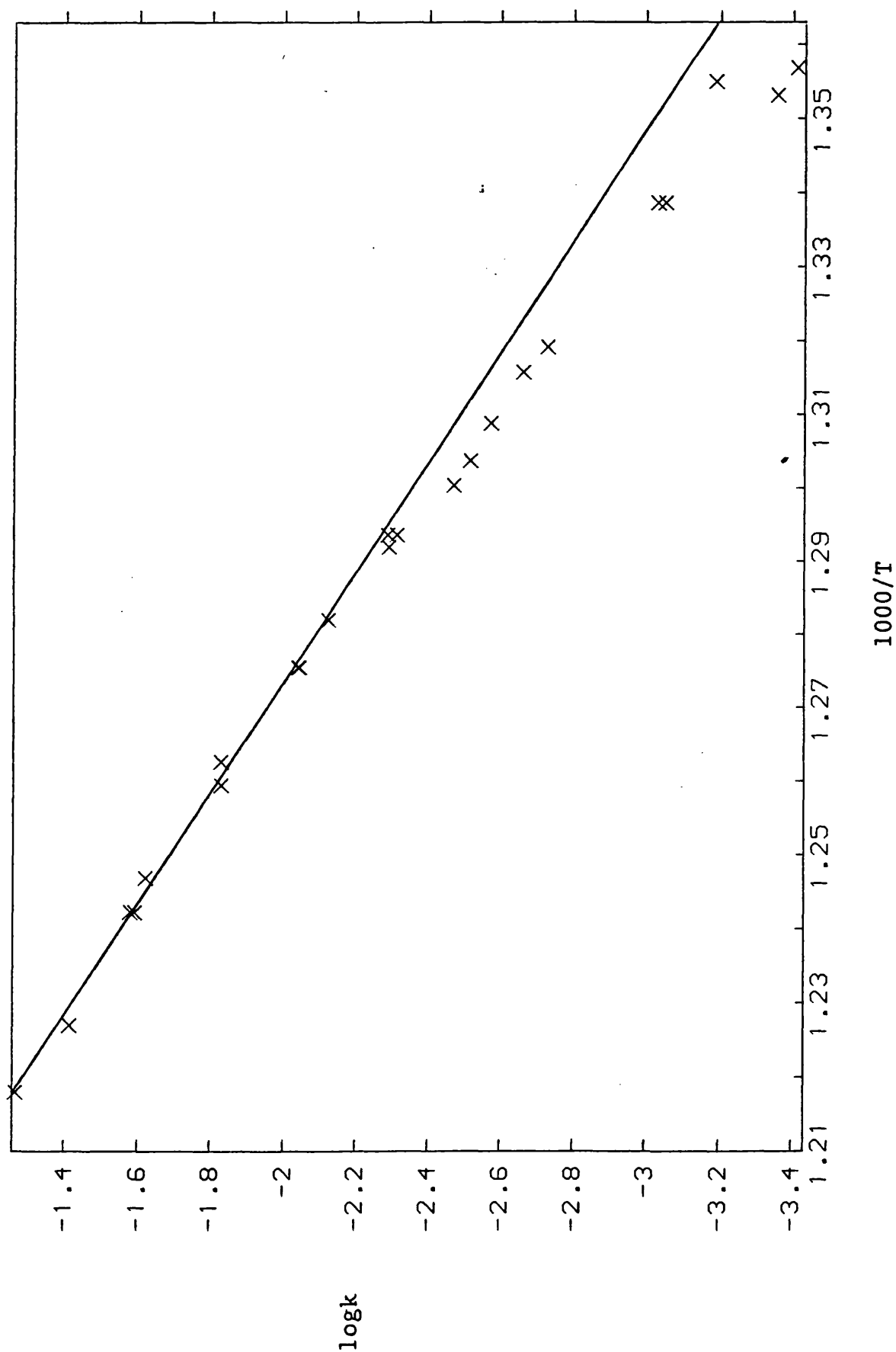Figure 10.2 : Arrhenius plot for propene formation from silacyclobutane + excess butadiene.

Figure 10.3 : Arrhenius plot for silacyclopentene formation
from silacyclobutane + excess butadiene.

Figure 10.4 : Arrhenius plot for 1-methyl-1-silacyclopentene
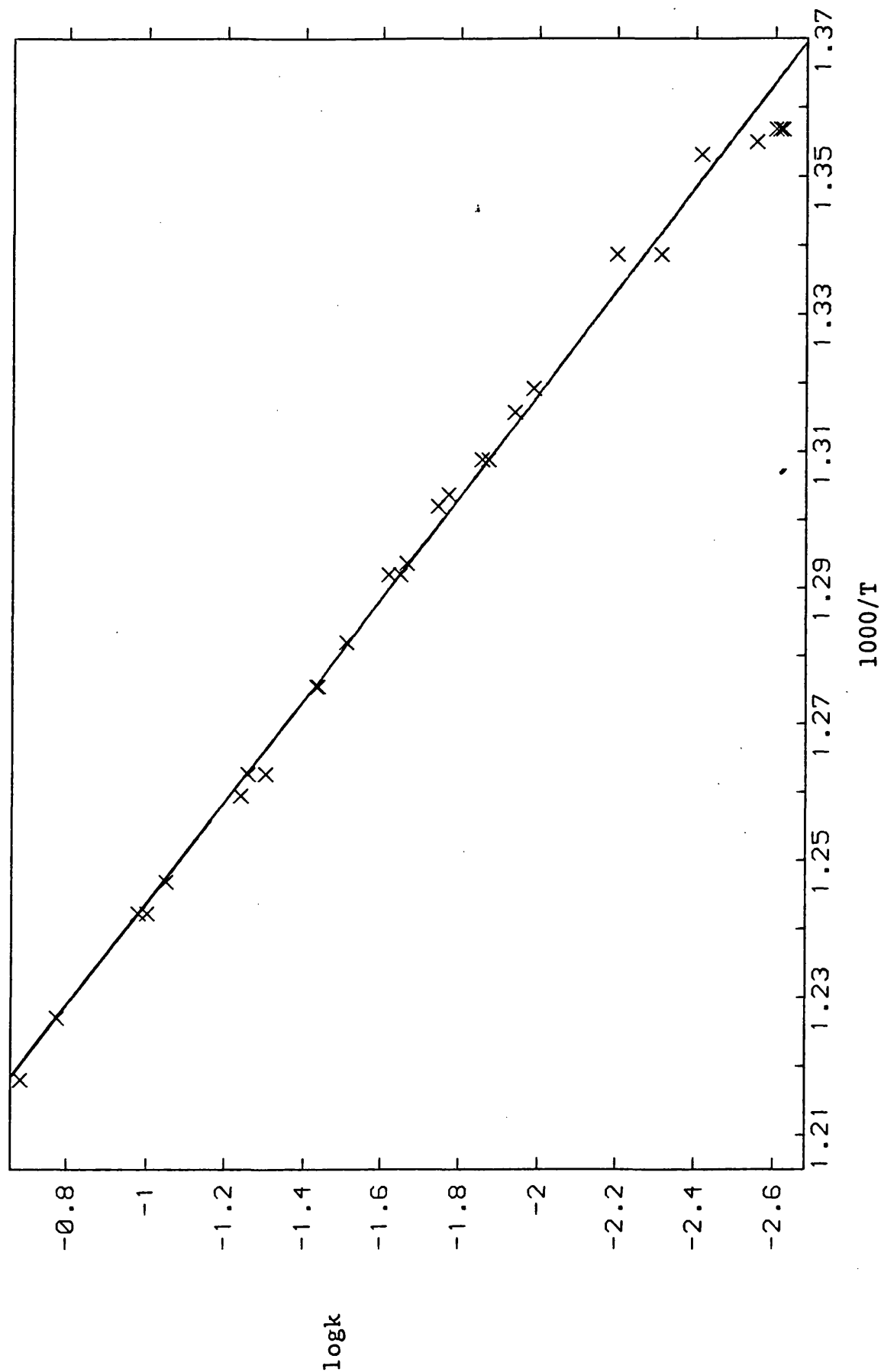formation from silacyclobutane + excess
butadiene.

Figure 10.5 : Arrhenius plot for ethene formation from 1-
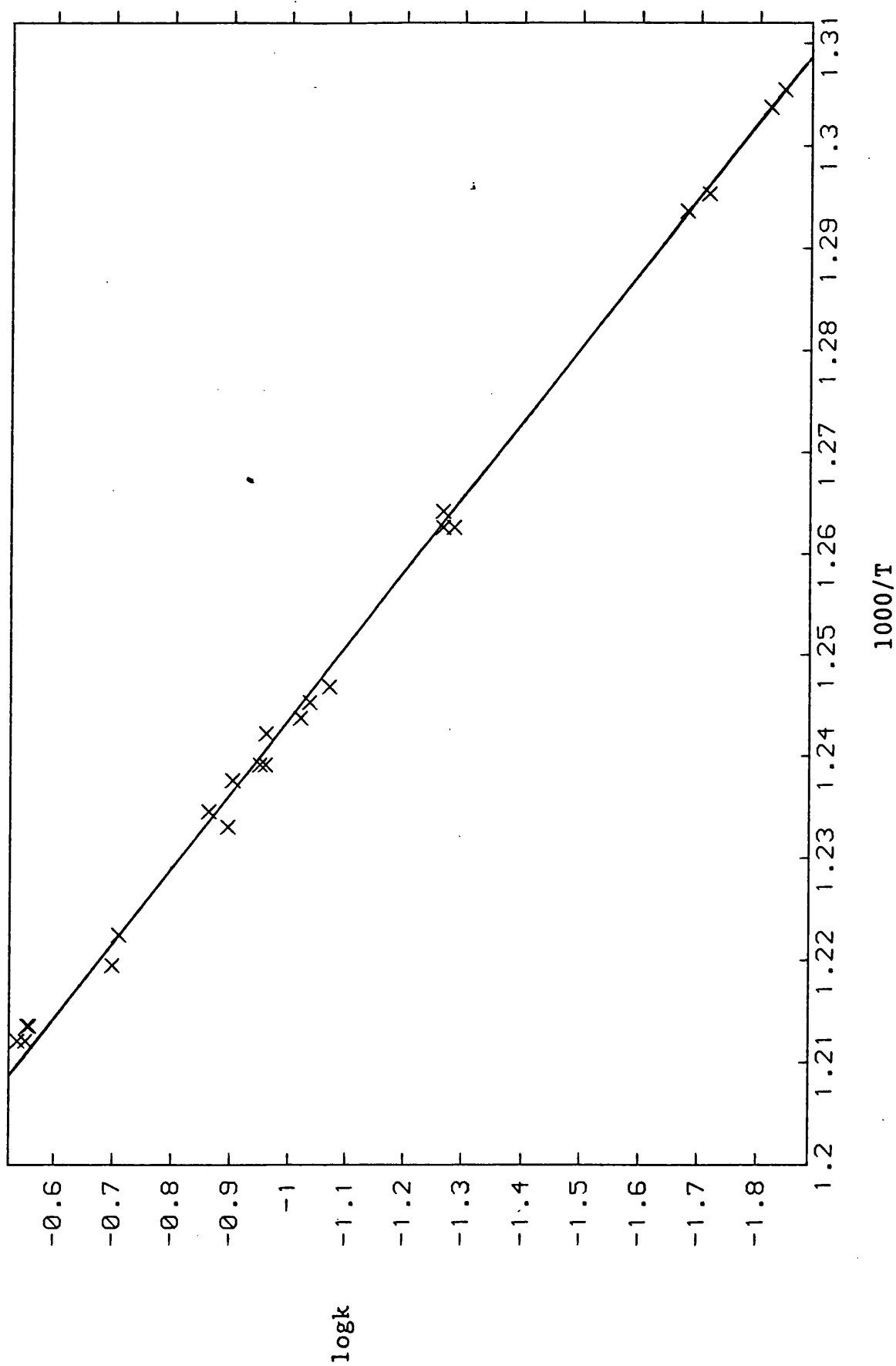methyl-1-silacyclobutane + excess butadiene.

Figure 10.6 : Arrhenius plot for propene formation from 1-methyl-1-silacyclobutane + excess butadiene.
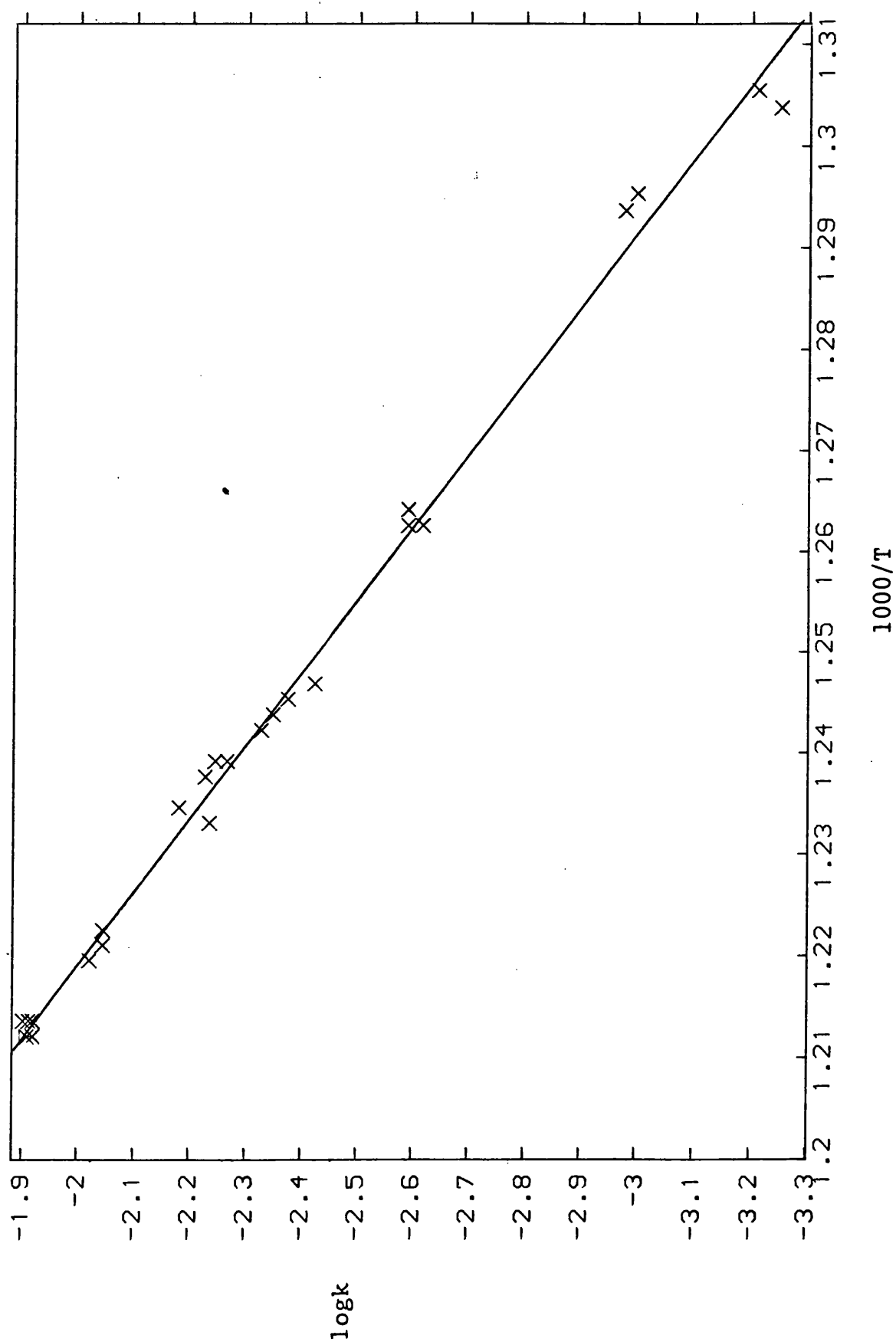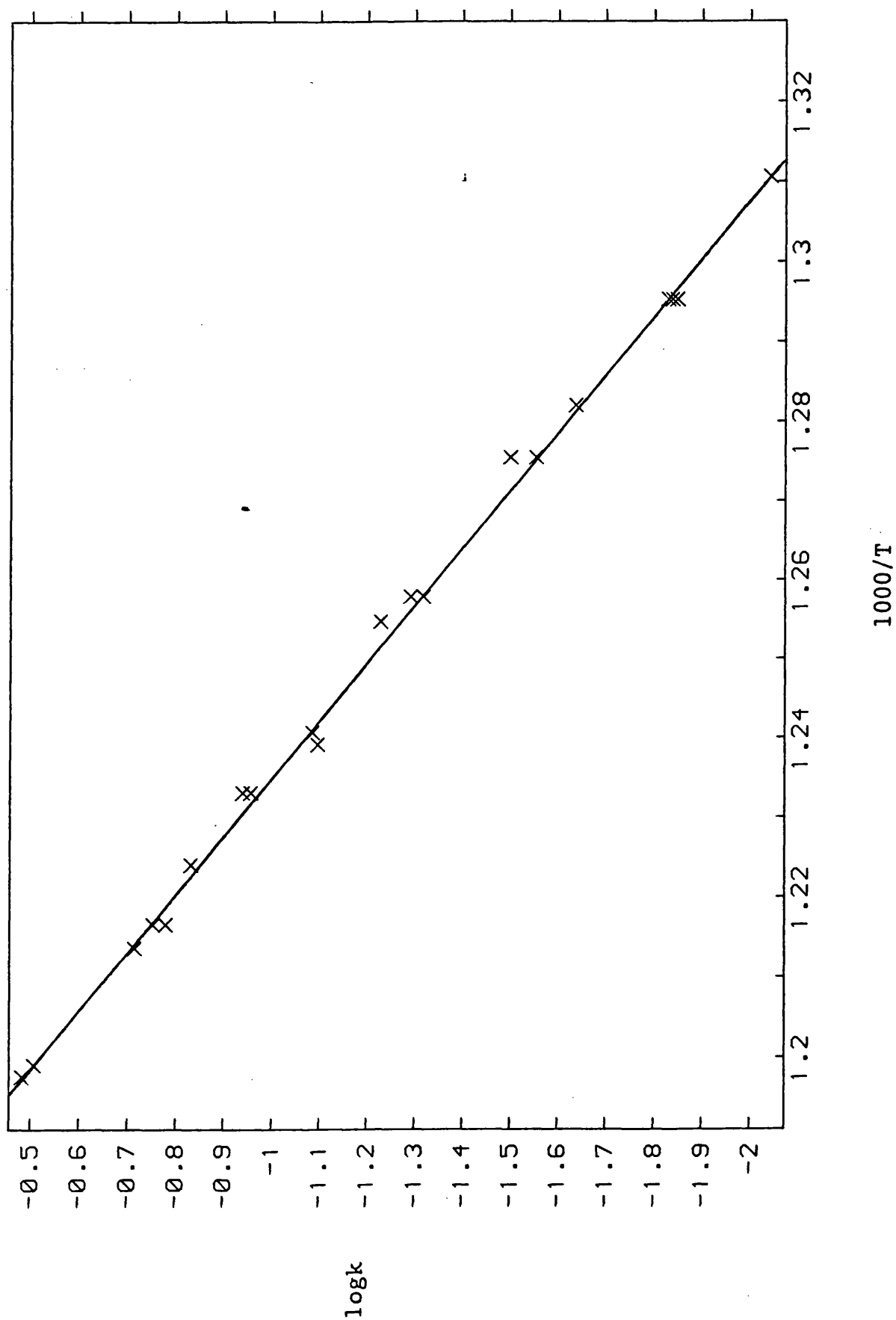
Figure 10.7 : Arrhenius plot for 1,1-dimethyl-1-silacyclopentene formation from 1-methyl-1-silacyclobutane + excess butadiene.

References

1. I. M. T. Davidson, A. Fenton, S. Ijadi-Maghsoodi, R. J. Scampton, N. Auner, J. Grobe, N. Tillman & T. J. Barton, Organometallics, 1984, 3, 1593.

2. A. C. Baldwin, I. M. T. Davidson and A. V. Howard, J.C.S. Faraday Trans. I, 1975, 71, 972.

3. M. C. Flowers & L. E. Gusel'nikov, J. Chem. Soc. (B), 1968, 419.

4. M. A. Ring, H. E. O'Neal, S. F. Rickborn, and B. A. Sawrey, Organometallics, 1983, 2, 1891.

5. S. F. Rickborn, D. S. Rogers, M. A. Ring and H. E. O'Neal, J. Phys. Chem., 1986, 90, 408.

6. I. M. T. Davidson, unpublished work.

APPENDIX

APPENDIX 1

Measurement of Rate Constants for Opposing and Parallel
Reactions in SFR

Rate equations are derived from mass balance, i.e.
Formation - Loss = 0.

(1) Opposing reactions e.g. cis-trans isomerisation $C \overset{1}{\underset{2}{\rightleftharpoons}} T$

(i) Start from C, ignore reverse reaction, apply mass
balance to T:

$$k_1 v[C] - u[T] = 0$$
$$k_1 = u[T]/v[C] = [T]/[C].z \quad - - - (i)$$

v = reactor volume; u = volumetric flow rate; [] = molar
conc. (hence, terms in mass balance are in $mole.s^{-1}$);
v/u = z, the SFR "time constant". Eqn. (1) is the standard
form for a 1st order irreversible reaction.

(ii) Start from C, include reverse reaction, apply mass
balance to T:

$$k_1v[C] - k_2v[T] - u[T] = 0$$

$$k_1v[C] = \{k_2v + u\}[T]$$

$$k_1[C] = \{k_2 + 1/z\}[T]$$

$$[T]/[C] = k_1/\{k_2 + 1/z\} \quad - - - \text{(ii)}$$

Eqn. (ii) simplifies to eqn. (i) only if $k_2 \ll 1/z$; i.e. if $k_2 \lesssim 10^{-3}s^{-1}$, since $1/z \approx 10^{-1}s^{-1}$.

(iii) Start from C, initially containing some T, apply mass balance to T. In this case there is an additional input or "formation" of T from the initial impurity, denoted by $[T']$:

$$u[T'] + k_1v[C] - k_2v[T] - u[T] = 0$$

$$k_1v[C] - k_2v[T] - u\{[T] - [T']\} = 0$$

$$k_1[C] = \{k_2 + 1/z\}[T] - [T']/z$$

$$k_1 = \{k_2 + 1/z\}[T]/[C] - [T']/[C]z$$

Experiments starting from C, treated as if the reaction were a simple irreversible first-order process, give apparent rate constants; $k_1' = [T]/[C].z$, as in eqn. (i).

$$\text{so,} \quad k_1 = \{k_2 + 1/z\}k_1'z - k_1'[T]/[T]$$

$$\underline{\text{i.e.}} \ k_1 = k_1'\{1 + k_2z - [T']/[T]\} \quad - - - \text{(iii)}$$

Experiments starting from T initially containing some C would give a similar expression to eqn. (iii) for k_2. Obviously both sets of experiments would be necessary in

order to evaluate k_1 and k_2.

If isomerisation of C (but not T) is accompanied by a parallel decomposition pathway, with rate constant k_3, then application of mass balance to C for experiments starting from T initially containing some C gives:

$$k_2 = k_2'\{1 + (k_1 + k_3)z - [C']/[C]\} \quad - - - \text{(iv)}$$

Substitution for k_2 in (iii) then gives:

$$k_1 = \frac{k_1'\{1+k_2'z+k_2'k_3z^2-k_2'z[C']/[C]-[T']/[T]\}}{\{1 - k_1'k_2'z^2\}} \quad - - - \text{(v)}$$

Similarly, substitution for k_1 in (iv) gives:

$$k_2 = \frac{k_2'\{1 + k_1'z+k_3z - k_1'z[T']/[T] - [C']/[C]\}}{\{1 - k_1'k_2'z^2\}} \quad - - - \text{(iv)}$$

Once k_3 has been measured (<u>vide infra</u>), eqns. (v) and (vi) may be used to evaluate k_1 and k_2 from experimentally measured quantities, but the complexity of equations (v) and (vi) clearly introduces additional errors compared to eqns. (i) and (ii).

(2) Parallel Reactions

$$B \quad - - - \quad (1)$$

$$\nearrow$$

Consider the special case in which $\quad A \rightarrow I \rightarrow C \quad - - - \quad (2)$
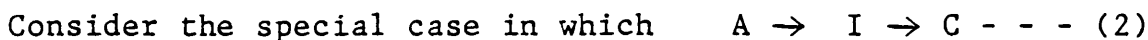
A → I is rate-determining, with $\quad\quad\quad \searrow$

rate constant k, then intermediate $\quad\quad\quad D \quad - - - \quad (3)$

I can decompose by parallel routes

to B, C and D.

Experimentally, we can measure a rate constant k_1 for formation of B from A, k_2 for formation of C from A, and k_3 for formation of D from A. For example: for B, $k_1 v[A]$ − $u[B] = 0$, $k_1 = [B]/[A].z$; similarly for C and D.

Since $k_1 : k_2 : k_3 = [B] : [C] : [D]$, these apparent rate constants give a direct measure of the relative importance of pathways (1), (2), and (3). If the mechanism is as above, $k_1 = f_1 k$, $k_2 = f_2 k$, and $k_3 = f_3 k$, where f_1, f_2, f_3 are "pathway factors". $f_1 = k_1/(k_1 + k_2 + k_3)$, etc., i.e. $\Sigma f_n = 1$. Hence, $k = k_1/f_1 = k_2/f_2 = k_3/f_3$. The major pathway obviously gives the most reliable measure of k.

Chapter one provides a brief history and current state of knowledge of the chemistry of organosilicon reactive intermediates relevant to this thesis. Chapter two outlines the experimental techniques used in the majority of work carried out in this thesis.

Chapter three describes an experimental investigation of the pyrolysis of 4-dimethylsilylbut-1-ene and 5-dimethylsilylpent-1-ene, with and without excess methylchloride as a silyl radical trap. The results of computer modelling of the pyrolysis of 4-dimethylsilylbut-1-ene with excess methylchloride are described, in which information concerning the isomerisation of an alpha-silyl radical to a silyl radical via a hydrogen shift is obtained.

Chapter four describes the results of an experimental investigation of the reactions of dimethylsilene and dimethylsilylene with anions.

Chapters five and six contain the results of computer modelling of three related pyrolysis mechanisms composed of complex series of unimolecular rearrangements of silylenes, silenes, disilenes and disilacyclopropanes.

Chapter seven describes an experimental determination of Arrhenius parameters for the trapping of dimethylsilene by butadiene, together with the results of pyrolysis of butadiene adducts of methylsilene, dimethylsilene and dimethylsilylene.

Chapter eight is an experimental investigation of the pyrolysis of cis and trans dimethyl(1-propenyl)vinylsilane with excess 2,3-dimethylbutadiene as a silylene trap. Interpretation of the results as a cis-trans isomerisation and decomposition of the cis isomer via a silacyclopropane intermediate are reinforced by the results of computer modelling of both systems.

Chapter nine describes an experimental investigation of the pyrolysis of 1,2-dimethyldisilane with and without butadiene as a silylene trap. Computer modelling of the pyrolysis with the absence of butadiene is used to clarify the pyrolysis mechanism.

Chapter ten is an experimental investigation of the pyrolysis of silacyclobutane and methylsilacyclobutane with excess butadiene to trap silylene intermediates and thus suppress secondary decomposition. Arrhenius parameters for the primary decomposition pathways are determined.